frontiers | Research Topics

Non-coding RNA and coronary artery disease

Edited by
En-Zhi Jia, Laiyuan Wang, Xiangming Ding and BuChun Zhang

Published in
Frontiers in Cardiovascular Medicine

ISSN 1664-8714
ISBN 978-2-83251-730-7
DOI 10.3389/978-2-83251-730-7

About Frontiers

Frontiers is more than just an open access publisher of scholarly articles: it is a pioneering approach to the world of academia, radically improving the way scholarly research is managed. The grand vision of Frontiers is a world where all people have an equal opportunity to seek, share and generate knowledge. Frontiers provides immediate and permanent online open access to all its publications, but this alone is not enough to realize our grand goals.

Frontiers journal series

The Frontiers journal series is a multi-tier and interdisciplinary set of open-access, online journals, promising a paradigm shift from the current review, selection and dissemination processes in academic publishing. All Frontiers journals are driven by researchers for researchers; therefore, they constitute a service to the scholarly community. At the same time, the *Frontiers journal series* operates on a revolutionary invention, the tiered publishing system, initially addressing specific communities of scholars, and gradually climbing up to broader public understanding, thus serving the interests of the lay society, too.

Dedication to quality

Each Frontiers article is a landmark of the highest quality, thanks to genuinely collaborative interactions between authors and review editors, who include some of the world's best academicians. Research must be certified by peers before entering a stream of knowledge that may eventually reach the public - and shape society; therefore, Frontiers only applies the most rigorous and unbiased reviews. Frontiers revolutionizes research publishing by freely delivering the most outstanding research, evaluated with no bias from both the academic and social point of view. By applying the most advanced information technologies, Frontiers is catapulting scholarly publishing into a new generation.

What are Frontiers Research Topics?

Frontiers Research Topics are very popular trademarks of the *Frontiers journals series*: they are collections of at least ten articles, all centered on a particular subject. With their unique mix of varied contributions from Original Research to Review Articles, Frontiers Research Topics unify the most influential researchers, the latest key findings and historical advances in a hot research area.

Find out more on how to host your own Frontiers Research Topic or contribute to one as an author by contacting the Frontiers editorial office: frontiersin.org/about/contact

Non-coding RNA and coronary artery disease

Topic editors

En-Zhi Jia — Nanjing Medical University, China

Laiyuan Wang — Fuwai Hospital, Chinese Academy of Medical Sciences and Peking Union Medical College, China

Xiangming Ding — University of Southern California, United States

BuChun Zhang — University of Science and Technology of China, China

Citation

Jia, E.-Z., Wang, L., Ding, X., Zhang, B., eds. (2023). *Non-coding RNA and coronary artery disease*. Lausanne: Frontiers Media SA.

doi: 10.3389/978-2-83251-730-7

Table of contents

frontiers | Frontiers in Cardiovascular Medicine

EDITORIAL
published: 13 May 2022
doi: 10.3389/fcvm.2022.910396

Editorial: Non-coding RNA and Coronary Heart Disease

Shu He[1], *Laiyuan Wang*[2], *Xiangming Ding*[3], *BuChun Zhang*[4] *and En-Zhi Jia*[1]*

[1] Department of Cardiovascular Medicine, The First Affiliated Hospital of Nanjing Medical University, Nanjing, China, [2] Key Laboratory of Cardiovascular Epidemiology & Department of Epidemiology, Fuwai Hospital, National Center for Cardiovascular Diseases, Chinese Academy of Medical Sciences & Peking Union Medical College, Beijing, China, [3] Children's Hospital Los Angeles, University of Southern California, Los Angeles, CA, United States, [4] Department of Cardiology, The First Affiliated Hospital of USTC, Division of Life Sciences and Medicine, University of Science and Technology of China, Hefei, China

Keywords: non-coding RNA, MicroRNAs, lncRNAs, circRNA, coronary heart disease

Editorial on the Research Topic

Non-coding RNA and Coronary Heart Disease

INTRODUCTION

There are only 1.5% of the human genome contains genetic sequences that encode proteins of the human genome, and more than 80% of the genomic sequences are non-coding RNAs (ncRNAs) that are not involved in the protein translation process (1). Regarding their regulatory roles, ncRNA was divided into housekeeping ncRNAs (rRNA, tRNA, snRNA, snoRNA, etc.) and regulatory ncRNAs (miRNA, siRNA, piRNA, lncRNA, circRNA, etc.) (2). Regulatory ncRNAs can function as regulators of gene expression at the epigenetic, transcriptional, and post-transcriptional levels, and miRNAs, lncRNAs, and circRNAs have been continuously investigated in-depth due to their extensive expression and numerous regulatory roles in biological processes. With the development of next-generation sequencing technologies, the research of ncRNA has been greatly advanced. There are plenty of studies that revealed the regulatory role of ncRNA in the occurrence and development of various diseases, predominantly including tumors, neurodegenerative pathologies, autoimmune diseases, cardiovascular diseases, etc. Coronary heart disease (CHD) is a heart condition in which the arteries of the heart do not deliver enough oxygen-rich blood to the heart, resulting in myocardial ischemia, hypoxia, or necrosis. Recent studies have demonstrated that lots of ncRNAs have participated in the occurrence and progression of CHD (3–5). These ncRNAs may act as a new diagnostic basis and therapeutic target for coronary heart disease.

NCRNAS IN CORONARY HEART DISEASE

miRNAs are small fragments of only 21–23nt in length, which are stably identified in body fluids and are resistant to degradation by endogenous RNA enzymes (6). Solingen et al. identified seven novel miRNAs that decrease proprotein convertase subtilisin/kexin type 9 (PCSK9) expression through high-throughput screening of the human microRNA library. These miRNAs will down-regulating PCSK9 secretion and up-regulate hepatic low-density lipoprotein receptor surface expression, which will mark a reduction in the risk of atherosclerotic cardiovascular disease. Matshaz et al. identified 30 dysregulated miRNAs in the whole blood of 48 hypertension females by next-generation sequencing. The differently expressed miRNA was associated with pathways such as platelet activation, calcium signaling, and vascular smooth muscle contraction pathways, which are particularly important in cardiovascular pathogenesis. Moreover, miR-1299 and miR-30a-5p

OPEN ACCESS

Edited and reviewed by:
Pietro Enea Lazzerini, University of Siena, Italy

***Correspondence:**
En-Zhi Jia
enzhijia@njmu.edu.cn

Specialty section:
This article was submitted to General Cardiovascular Medicine, a section of the journal Frontiers in Cardiovascular Medicine

Received: *01 April 2022*
Accepted: *08 April 2022*
Published: *13 May 2022*

Citation:
He S, Wang L, Ding X, Zhang B and Jia E-Z (2022) Editorial: Non-coding RNA and Coronary Heart Disease. Front. Cardiovasc. Med. 9:910396. doi: 10.3389/fcvm.2022.910396

are validated via RT-qPCR in a larger, independent sample in a sub-Saharan population to confirm the miRNA sequencing results. Ghafouri-Fard et al. and Zhang et al. reviewed how miRNAs function in the pathophysiological process in CHD, such as modulation of angiogenesis, lipid metabolism, inflammatory responses. What's more, their diagnostic/prognostic significance as potential biomarkers are also explored.

Available evidence indicates that lncRNAs are widely involved in the pathology of cardiac development, atherosclerosis, myocardial infarction, hypertension, and aneurysms (7–9). Current studies on the involvement mechanisms of lncRNA in CHD are mainly concentrated on constructing lncRNA-miRNA-mRNA regulatory networks based on competing endogenous RNA (ceRNA) theory. Ji et al. constructed 13 ceRNA regulatory pathways and the possible biological functions regulated by these pathways include programmed cell death, ferroptosis, and pyroptosis. Bioinformatics analysis was applied to select hub genes from microarray databases, and online databases including TargetScan, miRanda, and Tarbase were used to predict miRNA-target interactions, as reported by Zheng et al. Furthermore, ncRNA in the ceRNA networks of programmed cell death-related genes was verified in an animal model which makes the consequence credible.

The circRNA, which is highly conserved with a closed circular structure, is stable and insusceptible to RNA exonuclease (10). Its close association with CHD development makes it a potential candidate for biomarkers in the diagnosis and treatment process.

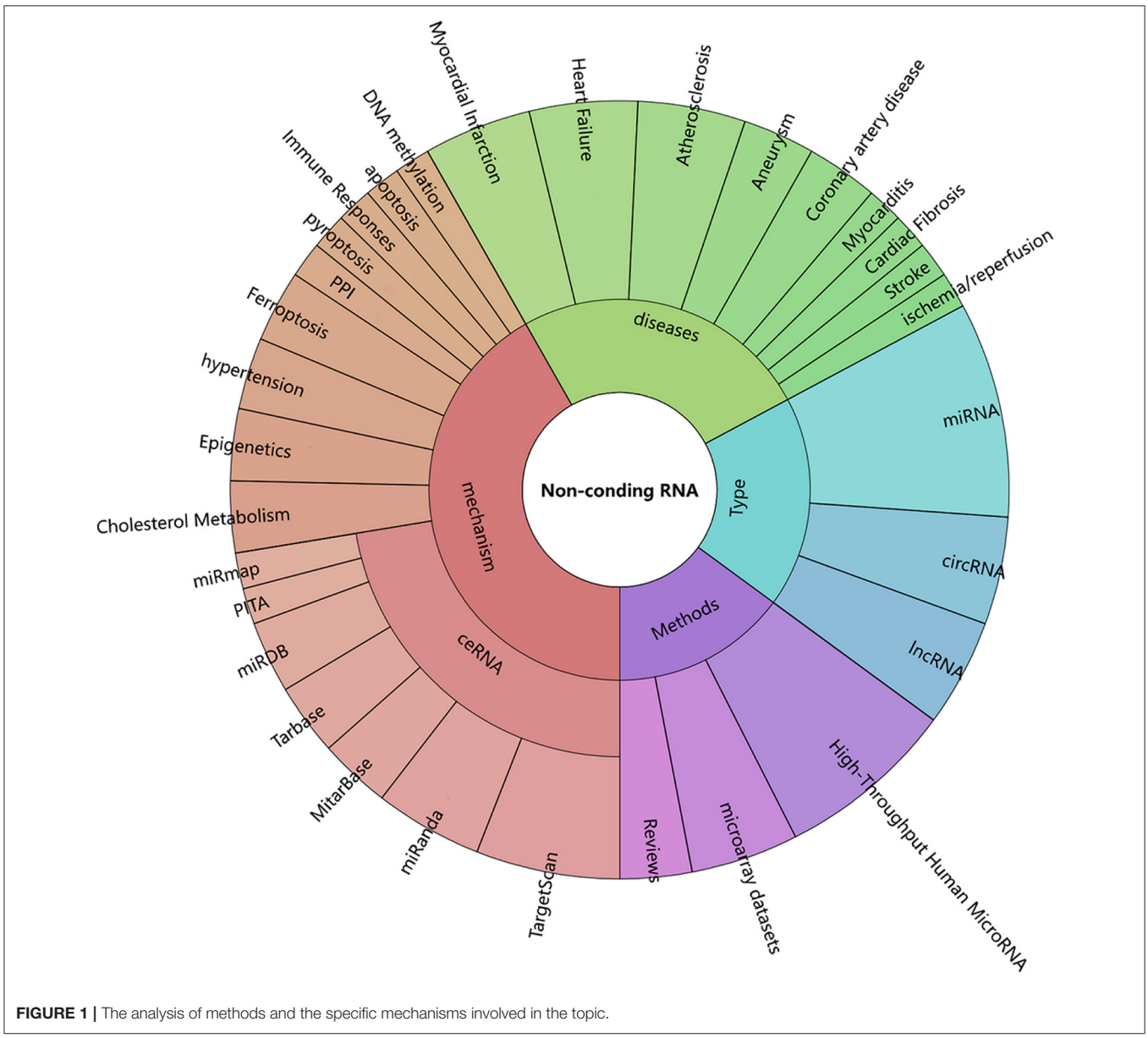

FIGURE 1 | The analysis of methods and the specific mechanisms involved in the topic.

Gain-of-function and loss-of-function of circRNAs hold promise as therapeutic targets. The upregulated expression of circRNA ABCA1 and circRNA KHDRBS1 in atherosclerotic vessels and oxidative-stress damaged endothelial cells were detected by Li et al. In addition, the underlying microRNA and mRNA Target genes were further verified, which provided new ideas for future studies on the biological functions of circRNA in regulating CHD. The review of Min et al. summarizes the current knowledge on molecular mechanisms and clinical implications of circRNAs. They highlight the role of circRNAs as ceRNA in atherosclerosis, myocardial infarction, cardiac fibrosis heart failure, and aneurysm, which will open up new avenues for further CHD research. The clinical application of circRNAs as molecular drugs or targets is also discussed here, and they argue that this remains a huge challenge and awaits extensive investigation.

Programmed cell death includes apoptosis, necrosis, autophagy, and a novel iron-dependent form of ferroptosis (11, 12). In this topic, the researchers observed the function of ncRNA in coordinating ferroptosis during I/R myocardial injury and heart failure. Sun et al. highlight finding from the function of miR-135b-3p in exacerbating cardiomyocyte ferroptosis, providing a new therapeutic target for improving I/R injury. There are numerous mechanisms by which ncRNAs perform the function and impact the development of CHD. The investigation of novel mechanisms including ferroptosis is essential for us to explore the secrets of ncRNA.

Epigenetics is heritable changes gene expression without altering in the nucleotide sequence. Chen et al. pay their attention to DNA methylation and described two hypomethylation gene that that is closely associated with obesity. This study provides evidence of the relationship between DNA methylation and gene expression in obese patients. Matshaz et al. investigated the involvement of DNA methylation on the pathogenesis of hypertension at the same time. They will help us explore the potential relationship between DNA methylation and ncRNA expression on the regulation of CHD.

CONCLUDING REMARKS

In this Research Topic, the reports address in detail the implication of ncRNA in the progress CHD. The analysis of methods and the specific mechanisms involved in these reports can be seen in **Figure 1**. The value of ncRNA in the diagnosis and prognosis of coronary heart disease has also been reported, while its diagnostic sensitivity and specificity remain poorly discussed. It is worth noting that the transformation from research to the clinical application will be a long-drawn-out process, and whether these ncRNAs are influenced by other factors in terms of their role in CHD needs to be verified in larger clinical trials. It is believed that in the near future, a larger amount of ncRNAs will be discovered to be involved in the development of CHD, and ncRNAs will serve as novel biomarkers and therapeutic targets for CHD.

AUTHOR CONTRIBUTIONS

SH and EJ were editors of this Research Topic and wrote this editorial jointly. All authors contributed to the article and approved the submitted version.

ACKNOWLEDGMENTS

We thank all the authors and reviewers for their contribution to the realization of this Research Topic.

REFERENCES

1. Djebali S, Davis CA, Merkel A, Dobin A, Lassmann T, Mortazavi A, et al. Landscape of transcription in human cells. *Nature*. (2012) 489:101–8. doi: 10.1038/nature11233
2. Zhang P, Wu W, Chen Q, Chen M. Non-coding RNAs and their integrated networks. *J Integr Bioinform*. (2019) 16:20190027. doi: 10.1515/jib-2019-0027
3. Ji WF, Chen JX, He S, Zhou YQ, Hua L, Hou C, et al. Characteristics of circular RNAs expression of peripheral blood mononuclear cells in humans with coronary artery disease. *Physiol Genomics*. (2021) 53:349–57. doi: 10.1152/physiolgenomics.00020.2021
4. Peng L, Sang H, Wei S, Li Y, Jin D, Zhu X, et al. circCUL2 regulates gastric cancer malignant transformation and cisplatin resistance by modulating autophagy activation via miR-142-3p/ROCK2. *Mol Cancer*. (2020) 19:156. doi: 10.1186/s12943-020-01270-x
5. Schonrock N, Harvey RP, Mattick JS. Long noncoding RNAs in cardiac development and pathophysiology. *Circ Res*. (2012) 111:1349–62. doi: 10.1161/CIRCRESAHA.112.268953
6. Lee Y, Jeon K, Lee JT, Kim S, Kim VN. MicroRNA maturation: stepwise processing and subcellular localization. *EMBO J*. (2002) 21:4663–70. doi: 10.1093/emboj/cdf476
7. Liu W, Wang Z, Liu L, Yang Z, Liu S, Ma Z, et al. LncRNA Malat1 inhibition of TDP43 cleavage suppresses IRF3-initiated antiviral innate immunity. *Proc Natl Acad Sci U S A*. (2020) 117:23695–706. doi: 10.1073/pnas.2003932117
8. Gast M, Rauch BH, Haghikia A, Nakagawa S, Haas J, Stroux A, et al. Long noncoding RNA NEAT1 modulates immune cell functions and is suppressed in early onset myocardial infarction patients. *Cardiovasc Res*. (2019) 115:1886–906. doi: 10.1093/cvr/cvz085
9. Cho H, Shen GQ, Wang X, Wang F, Archacki S, Li Y, et al. Long noncoding RNA ANRIL regulates endothelial cell activities associated with coronary artery disease by up-regulating CLIP1, EZR, and LYVE1 genes. *J Biol Chem*. (2019) 294:3881–98. doi: 10.1074/jbc.RA118.005050
10. Kristensen LS, Andersen MS, Stagsted LVW, Ebbesen KK, Hansen TB, Kjems J. The biogenesis, biology and characterization of circular RNAs. *Nat Rev Genet*. (2019) 20:675–91. doi: 10.1038/s41576-019-0158-7
11. Zhaolin Z, Guohua L, Shiyuan W, Zuo W. Role of pyroptosis in cardiovascular disease. *Cell Prolif*. (2019) 52:e12563. doi: 10.1111/cpr.12563
12. Dixon SJ, Lemberg KM, Lamprecht MR, Skouta R, Zaitsev EM, Gleason CE, et al. Ferroptosis: an iron-dependent form of nonapoptotic

cell death. *Cell.* (2012) 149:1060–72. doi: 10.1016/j.cell.2012.03.042

Conflict of Interest: The authors declare that the research was conducted in the absence of any commercial or financial relationships that could be construed as a potential conflict of interest.

Publisher's Note: All claims expressed in this article are solely those of the authors and do not necessarily represent those of their affiliated organizations, or those of the publisher, the editors and the reviewers. Any product that may be evaluated in this article, or claim that may be made by its manufacturer, is not guaranteed or endorsed by the publisher.

frontiers in Cardiovascular Medicine

REVIEW
published: 20 January 2021
doi: 10.3389/fcvm.2020.610561

MiR-223-3p in Cardiovascular Diseases: A Biomarker and Potential Therapeutic Target

*Meng-Wan Zhang, Yun-Jie Shen, Jing Shi and Jian-Guang Yu**

Department of Pharmacy, Shanghai Chest Hospital, Shanghai Jiao Tong University, Shanghai, China

Cardiovascular diseases, involving vasculopathy, cardiac dysfunction, or circulatory disturbance, have become the major cause of death globally and brought heavy social burdens. The complexity and diversity of the pathogenic factors add difficulties to diagnosis and treatment, as well as lead to poor prognosis of these diseases. MicroRNAs are short non-coding RNAs to modulate gene expression through directly binding to the 3′-untranslated regions of mRNAs of target genes and thereby to downregulate the protein levels post-transcriptionally. The multiple regulatory effects of microRNAs have been investigated extensively in cardiovascular diseases. MiR-223-3p, expressed in multiple cells such as macrophages, platelets, hepatocytes, and cardiomyocytes to modulate their cellular activities through targeting a variety of genes, is involved in the pathological progression of many cardiovascular diseases. It participates in regulation of several crucial signaling pathways such as phosphatidylinositol 3-kinase/protein kinase B, insulin-like growth factor 1, nuclear factor kappa B, mitogen-activated protein kinase, NOD-like receptor family pyrin domain containing 3 inflammasome, and ribosomal protein S6 kinase B1/hypoxia inducible factor 1 α pathways to affect cell proliferation, migration, apoptosis, hypertrophy, and polarization, as well as electrophysiology, resulting in dysfunction of cardiovascular system. Here, in this review, we will discuss the role of miR-223-3p in cardiovascular diseases, involving its verified targets, influenced signaling pathways, and regulation of cell function. In addition, the potential of miR-223-3p as therapeutic target and biomarker for diagnosis and prediction of cardiovascular diseases will be further discussed, providing clues for clinicians.

Keywords: cardiovascular diseases, miR-223-3p, signaling pathway, cardiomyocyte, biomarker

OPEN ACCESS

Edited by:
BuChun Zhang,
University of Science and Technology of China, China

Reviewed by:
Ronald J. Vagnozzi,
Cincinnati Children's Hospital Medical Center, United States
Tao Li Chan,
Nanjing Medical University, China

****Correspondence:***
Jian-Guang Yu
yueqingqiu@163.com
orcid.org/0000-0001-5596-5406

Specialty section:
This article was submitted to General Cardiovascular Medicine, a section of the journal Frontiers in Cardiovascular Medicine

Received: *26 September 2020*
Accepted: *23 December 2020*
Published: *20 January 2021*

Citation:
Zhang M-W, Shen Y-J, Shi J and Yu J-G (2021) MiR-223-3p in Cardiovascular Diseases: A Biomarker and Potential Therapeutic Target. Front. Cardiovasc. Med. 7:610561. doi: 10.3389/fcvm.2020.610561

INTRODUCTION

Cardiovascular diseases (CVDs), as the first leading cause of death from non-communicable diseases worldwide, include atherosclerosis, coronary artery disease, heart failure, hypertension, arrhythmia, etc (1–3). Deaths from CVDs are increasing in recent years, mainly resulting from the global aging and population growth (2–5). The driving causes of cardiovascular system dysfunction refer to multiple factors such as aging, hyperlipidemia or atherosclerosis, hypertension, inflammatory response or infection, and genetic influence. Although medical advances in diagnosis and treatments of CVDs, as well as methods to improve prognosis of these diseases, have made benefits for patients, the burden of CVDs remains huge in all regions of the world, as one of the

vital obstacles of sustainable development of human (2, 3, 6). Current techniques and drugs to treat CVDs are still limited and the diagnostic methods are often complex and invasive, therefore convenient and effective biomarkers and therapeutic targets for CVDs are urgently needed.

MicroRNAs (miRNAs/miRs), as a kind of non-coding RNA, have been proved to participate in multiple cardiovascular disorders and varieties of pathological processes of CVDs, such as atherosclerosis, coronary artery disease, heart failure, cardiac hypertrophy, cardiac remodeling, arrhythmia, and myocardium ischemia (7–10). For example, miR-208, which is cardiac-specifically expressed, is the first miRNA to be found affecting cardiac hypertrophy. MiRNAs have been increasingly recognized as the potential therapeutic target for CVDs and the miRNA-based therapeutic approaches to perform in clinical applications are challenging but promising (11). MiRNAs are synthesized firstly in the nucleus through transcribing the genes from DNA to primary miRNAs and then processing them to precursor miRNAs (12–15). The precursor miRNAs, which are transferred from nucleus to cytoplasm, are cleaved to become the mature miRNAs duplex (16). In most cases, one of two strands (5p/3p) of mature miRNAs duplex are degraded or less active and is called the passenger strand, while the reserved strand is often identified as the guide strand to form miRNA-induced silencing complex and executes the active regulatory function, although sometimes the passenger strand is also functional (17–19). The canonical mechanisms underlying the post-transcriptional gene silencing by miRNAs are directly binding to the 3′-untranslated regions of the target mRNAs, which lead to the degradation of mRNAs and the reduction of protein levels (20, 21). Besides intracellular gene regulation, miRNAs can be also transported by microparticles, exosomes, or binding to proteins in body fluids, as well as in the free form in blood, to play a part in intercellular signaling (20, 22–24). These diverse and powerful functions of miRNAs lay the foundation for their potential use in clinical diagnosis and treatments of many diseases such as CVDs.

MiR-223-3p is recognized as the guide strand of the miR-223 duplex and used to be called miR-223 (25). Although the other strand named miR-223-5p or miR-223* has been recognized functional in some cases recently (26, 27), most studies have been focused on the regulatory effects of miR-223-3p. MiR-223-3p is initially thought to be a myeloid-specific miRNA affecting hematopoiesis, immune response, and inflammatory diseases (28–31), but currently has been reported to express in many other types of cells such as hepatocytes and cardiomyocytes (32, 33). It has been demonstrated that miR-223-3p is related to multiple pathological processes or features of CVDs including atherosclerosis, vascular or myocardium remodeling, abnormal platelet reactivity, and myocardium ischemia (33–37), which draws our attention to the potential role of miR-223-3p in the diagnosis and treatments of CVDs. In this review, we will systemically elaborate the role of miR-223-3p in different pathophysiological activities causing CVDs and highlight the function of miR-223-3p as therapeutic target, as well as diagnostic or predictive biomarker in these diseases.

MiR-223-3p IN LIPID METABOLISM DYSFUNCTION AND ATHEROSCLEROSIS

Lipid metabolism dysfunction, represented by disturbed triglyceride and cholesterol homeostasis, as well as abnormal level and function of lipoproteins, may lead to severe lipid-associated diseases, including atherosclerosis, non-alcoholic fatty liver disease, and diabetes. Atherosclerosis is thought to be a driving force for coronary artery disease and ischemic cerebral stroke, mediated by complex mechanisms including lipid metabolism disorder, vascular cellular dysfunction, chronic inflammation, and plaque development (8). Cholesterol biosynthesis, transport, and efflux are essential for maintaining systemic lipid homeostasis and a high level of plasma cholesterol has been considered a risk factor for atherosclerosis development (38). Lipoproteins, especially the atheroprotective high-density lipoproteins (HDLs) and the atherogenic low-density lipoproteins, carry on different roles in cholesterol metabolism and atherosclerosis (39, 40). MiR-223-3p has been involved in modulating cholesterol homeostasis and transport function of lipoproteins and also has been proved to regulate cellular activities contributing to the pathogenesis of atherosclerosis.

Effect of MiR-223-3p on Lipoprotein Function and Cholesterol Metabolism

Lipoproteins can combine with nucleic acids to form complex and transport nucleic acids systemically or specifically (41–43). HDLs are responsible for reversing the transport of cholesterol from periphery back to liver and finally excreting cholesterol out of the body (39). As an important member of lipoproteins especially in atherosclerosis, HDLs are capable of delivering endogenous miRNAs including miR-223-3p to neighbor cells for intercellular communication and cellular target genes regulation, and this delivery ability may present differently in pathological situations such as hypercholesterolemia (24, 44, 45). MiR-223-3p was demonstrated as one of the most abundant plasma HDL-miRNAs in familial hypercholesterolemia patients or atherosclerotic mice, and also quite abundant in HDLs of healthy subjects (24). HDL-carried miR-223-3p which generated from polymorphonuclear neutrophils (PMNs) and macrophages was upregulated by native HDLs through increasing the expression of Dicer, and the export of miR-223-3p from PMNs and macrophages to HDLs was increased by HDLs and PMNs activation through promoting the activity of protein kinase C (PKC) and production of reactive oxygen species (ROS) (45). Excessive dietary intake of trans-fatty acids, as one of the risk factors of CVDs, also has been reported to have an impact on HDL-carried miR-223-3p through affecting the plasma HDL-C levels and inflammatory markers (44).

Both native and reconstituted HDLs are capable of acquiring endogenous or exogenous miR-223-3p and delivering it to recipient cells including hepatic and endothelial cells through combination with scavenger receptor class B type I (SR-BI) (24, 46). SR-BI, which is found expressed in hepatocytes, endothelial cells or macrophages, is the primary and high-affinity HDL receptor, and thus plays an important role in regulating

cholesterol homeostasis (47, 48). There is an interaction between SR-BI and miR-223-3p. It was demonstrated that SR-BI could facilitate the selective uptake of HDL-cholesterol (HDL-C) and HDL-carried miR-223-3p by cells, as well as might affect miR-223-3p levels in PMNs and macrophages (45), while miR-223-3p, in turn, decreased the expression of SR-BI in hepatocytes, resulting in reduced HDL-C uptake (32, 49). Besides, miR-223-3p also regulates other proteins involved in cholesterol metabolism to reduce cholesterol biosynthesis and promote cholesterol efflux.

MiR-223-3p is abundant in human liver and primary hepatocytes (50). Hepatic miR-223-3p is either delivered from plasma into the liver or natively expressed in hepatocytes. The abundance and functional activity of miR-223-3p increased with elevation of cholesterol levels in hepatocytes and circulation (32). Hepatic miR-223-3p decreased the mRNA and protein level of SR-BI through directly targeting the binding sites of 3′-untranslated region in SR-BI mRNA of human while inhibition of endogenous miR-223-3p abrogated these effects, proving that SR-BI was a downstream target of miR-223-3p in human. This posttranscriptional regulation of SR-BI markedly reduced the uptake of HDL-C and lipid accumulation in hepatic cells (32, 49). The similar regulatory effects of miR-223-3p on SR-BI were also found in human coronary arterial endothelial cells, suggesting the endothelial protection by miR-223-3p. In addition to SR-BI, two cholesterol biosynthetic enzymes 3-hydroxy-3-methylglutaryl-CoA synthase 1 (HMGCS1) and methylsterol monooxygenase 1 (SC4MOL) were found to be direct targets of miR-223-3p, resulting in cholesterol biosynthesis repression by miR-223-3p. Moreover, miR-223-3p also increased efflux of cholesterol by upregulating ATP-binding cassette transporter A1 (ABCA1) through directly targeting transcription factor Sp3 (32). Thus, the reduced uptake of HDL-C and biosynthesis of cholesterol, as well as the promoted efflux of cholesterol, are likely to decrease the liver cholesterol levels. These regulatory mechanisms involved in human cholesterol metabolism by miR-223-3p imply that miR-223-3p may influence plasma lipid levels and lipid-related diseases such as hypercholesterolemia or atherosclerosis in a diverse manner. Based on the experiments conducted in miR-223(-3p/5p) knockout mice, the depletion of miR-223(-3p/5p) contributed to hypercholesterolemia and the elevation of plasma cholesterol levels were associated with HDL-C. However, the elevated HDL-C levels caused by miR-223(-3p/5p) deficiency were thought to be the results of different regulation of target genes in rodents such as SR-BI, which was found inhibited in miR-223(-3p/5p) deficient mice (32). Therefore, the role of miR-223-3p on plasma lipid levels and lipid-related diseases in human still needs further researches.

Taken together, miR-223-3p modulates cholesterol metabolism through directly or indirectly targeting genes related to cholesterol transport, biosynthesis, and efflux (**Figure 1**). Both HDL-carried miR-223-3p and hepatocyte-expressed miR-223-3p could execute the regulatory function. MiR-223-3p could inhibit the expression of SR-BI, while the inhibition could lead to reduced uptake of HDL-carried miR-223-3p from plasma, so this loop regulation may be one of the mechanisms helping to maintain the cholesterol homeostasis in cellular or systemic level.

Effect of MiR-223-3p on Vascular Cells, Platelets, and Macrophages

Vascular endothelial cells (VECs) and vascular smooth muscle cells (VSMCs), as well as platelets and macrophages, are involved in all stages of atherosclerosis and play vital roles in plaque development (8). Endothelial dysfunction contributes to cellular inflammatory phenotypes through activating multiple signaling pathways and increasing the excretion of pro-inflammatory factors, consequently prompting monocytes recruitment and differentiation into macrophages which could form inflammatory foam cells in the lesions of vessel walls (51, 52). Aberrant proliferation, differentiation, and migration of VSMCs promote atherosclerosis progression through the formation of neointima and plaque (53). MiR-223-3p is firstly described in hematopoietic cells and blood cells and recent studies have shown that miR-223-3p is a pleiotropic miRNA in several tissues (28, 34). Although some studies consider that miR-223-3p may be barely expressed in VECs or VSMCs, a considerable amount of miR-223-3p which probably derived and excreted from platelets, monocytes, or macrophages has been found in these two types of cells, executing anti-inflammatory and anti-atherosclerotic effects (35, 46, 54). In addition, miR-223-3p impacts atherosclerosis also via regulating cytopoiesis, cell survival, and the function of platelets and macrophages (55–57).

VECs can ingest HDL-carried miR-223-3p or miR-223-3p from activated-platelet-derived exosomes in plasma (46, 54). Platelet activation displays pro-atherosclerotic effects, resulting from its role in endothelial damages and thrombus formation, however, activated-platelet-derived exosomes are found to be protective for atherosclerosis and endothelial inflammation (54, 58). The components contained in activated-platelet-derived exosomes included a high level of miR-223-3p, which was found upregulated in exosomes of atherosclerotic models (54). MiR-223-3p ingested by VECs contributed to the downregulation of intercellular adhesion molecule 1 (ICAM1), which could be upregulated by tumor necrosis factor α (TNF-α) or thrombosis (46, 54). Given that miR-223-3p was thought to be barely expressed in VECs and mostly from extracellular sources, it indicates that extracellular miR-223-3p is capable of regulating gene expression in cells. MiR-223-3p can suppress the inflammation and endothelial activation through directly or indirectly regulating ICAM1 in VECs. MiR-223-3p downregulated the expression of ICAM1 through directly targeting or depending on the suppression of nuclear factor kappa B (NFκB) and mitogen-activated protein kinase (MAPK) signaling pathways, with inhibiting cytoplasm-to-nucleus translocation of NFκB p65 and phosphorylation of p38, c-Jun N-terminal kinase (JNK), and extracellular signal-regulated kinase (ERK) (46, 54). MiR-223-3p could also be transcribed and secreted from platelets and leukocytes to serum, and then entered VSMCs and vascular walls, resulting in elevation of miR-223-3p levels in serum and vascular walls of atherosclerotic animals and patients. MiR-223-3p reduced VSMCs proliferation and migration, as well as increased cell apoptosis, through directly targeting insulin-like growth factor 1 receptor (IGF1R) to inhibit its downstream phosphatidylinositol

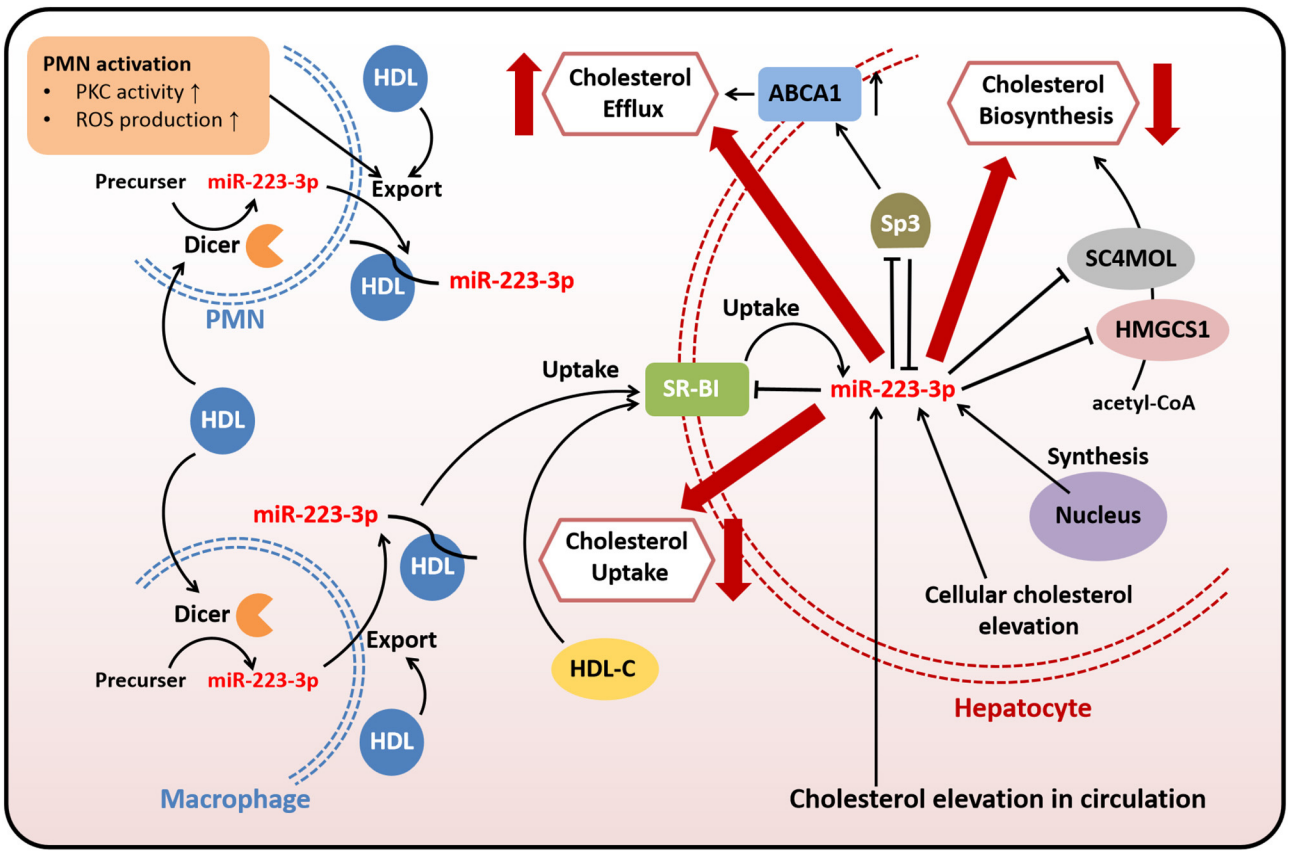

FIGURE 1 | MiR-223-3p is involved in cholesterol transport, biosynthesis, and efflux. Both endogenous and exogenous miR-223-3p in hepatocytes contribute to maintaining cholesterol homeostasis through targeting multiple genes related to cholesterol transport, biosynthesis, and efflux. Exogenous miR-223-3p is mostly originated from PMNs or macrophages and transported by HDLs. The uptake of HDL-carried miR-223-3p depends on SR-BI which is identified as one of the targets of miR-223-3p. Other targets involved in cholesterol metabolism include HMGCS1, SC4MOL and Sp3. MiR-223-3p directly inhibits the expression of these proteins to reduce the cholesterol uptake and biosynthesis, as well as to increase the cholesterol efflux. MiR-223-3p levels in hepatocytes can be upregulated with the elevation of cellular or circulating cholesterol.

3-kinase (PI3K)/protein kinase B (AKT) pathway with reduced phosphorylation of AKT. The regulation on these signaling pathways affected cellular activities of VSMCs, and ultimately suppressed vascular neointimal formation and atherosclerosis (35). Although these findings have been argued by other studies of miR-223-3p on VSMCs function, which indicated that overexpression of miR-223-3p promoted the proliferation and migration of VSMCs (59) and thus downregulation of miR-223-3p might decrease neointimal hyperplasia and prevent restenosis after angioplasty through augmenting expression of genes implicated in VSMCs differentiation and contractility (60), it is quite evident that miR-223-3p can help to prevent pathological changes in atherosclerosis.

Platelets and macrophages play vital roles in the development of plaque and thrombosis during the atherosclerotic progression. As one of the most abundant miRNAs in platelets (61–63), miR-223-3p showed a mild acceleration on platelets production but with no influence on platelets function (55). It suggests that platelet function may not depend on regulation pathways mediated by miR-223-3p. Contrast to effects on platelets, miR-223-3p plays significant roles in macrophages differentiation, survival, and function during inflammatory stimulation and atherosclerosis. As the same as activated platelets, macrophages generate microvesicles containing miRNAs (64). Although miR-223-3p contained in activated macrophage-derived microvesicles could be transported to monocytes and induce the differentiation from monocytes to macrophage, as well as macrophages survival, suggesting the pro-inflammatory effects of microvesicles containing miR-223-3p (56), the upregulation of miR-223-3p in macrophages presented protective effects against atherosclerosis through decreasing macrophage foam cells, macrophage-mediated lipid deposition, and excretion of pro-inflammatory factors. The anti-atherosclerotic effects of miR-223-3p in macrophages were performed through activating the PI3K/AKT pathway with upregulation of p-AKT to inhibit the toll-like receptor 4 (TLR4)/NFκB pathway with suppression of phosphor-p65. The expression of miR-223-3p was reduced in lipopolysaccharide-induced macrophages, while in lesions

of atherosclerotic animals it was upregulated, probably in a feedback way (57).

To summarize, miR-223-3p can function as an endocrine genetic signal for intercellular communication among blood cells, immune cells, and vascular cells, mediated by HDLs, platelet-derived exosomes, or macrophage-derived microparticles. It also plays essential roles against atherosclerotic progression primarily through anti-inflammation, endothelial protection, reducing vascular remodeling, and decreasing lipid deposition (**Figure 2**), indicating its therapeutic role for atherosclerosis and related CVDs.

MiR-223-3p as a Potential Biomarker for Atherosclerosis

The characteristics of miRNAs, which can be easily acquired from plasma or serum in patients and conveniently detected by commonly used techniques, make it an important potential biomarker in multiple diseases (8, 65). Circulating levels of miR-223-3p have been associated with atherosclerotic diseases and hyperlipidemia (35, 66–68). It was found that miR-223-3p levels were elevated in serum and atherosclerotic vessels of patients with atherosclerosis, as well as atherosclerotic models established in apolipoprotein E deficient mice (35). Hypertension associated with hyperlipidemia, as the major risk factor leading to atherosclerotic diseases, could mimic the atherosclerotic situation and increase the plasma and platelet levels of miR-223-3p but reduced the levels in platelet-derived microvesicles in hamsters (68). However, other research indicated that plasma miR-223-3p levels were reduced in patients with abdominal aortic aneurysm, an atherosclerosis-related disease (66). The lower level of plasma miR-223-3p was correlated with increased atherosclerotic manifestations including coronary artery disease, peripheral arterial disease and stroke in heart failure patients, and elevated levels of atherosclerosis-related indicators such as growth differentiation factor 15, as well as augmented risk of cardiovascular-related rehospitalization (67). Thus, patients or animal models with only atherosclerosis or atherosclerotic situation seem to manifest a higher level of circulating miR-223-3p, while in patients combined with other diseases, atherosclerosis is associated with reduced circulating miR-223-3p. Although miR-223-3p has the potential to protect against atherosclerosis based on its regulation of lipid metabolism and cellular activities involved in atherosclerosis, its role to function as a biomarker of atherosclerosis diagnosis or risk prediction remains indeterminate. Further researches to investigate the explicit role of miR-223-3p as a diagnostic or prognostic biomarker for atherosclerosis and atherosclerosis-related diseases based on large cohorts and rigorous designs are needed.

MiR-223-3p IN CORONARY ARTERY DISEASE

Coronary artery disease is usually originated from atherosclerotic pathological alterations which lead to coronary artery narrow or block and ultimately ischemia of myocardium (69). Therefore, it is also known as coronary heart disease or ischemic heart disease, including multiple clinical manifestations such as stable angina pectoris and acute coronary syndrome (ACS), and affects lots of people worldwide (69, 70). There have been many researches uncovering the effects of miR-223-3p in coronary artery disease, mostly in regard to its adverse impacts on myocardial infarction and potential regulatory mechanisms involved in antiplatelet therapy, as well as its role in diagnosis and risk prediction of coronary artery disease.

MiR-223-3p in Myocardial Infarction

Myocardial infarction, as a main category of ACS, is a worldwide devastating coronary artery disease with high morbidity and mortality, usually caused by a severe reduction of blood flow to the cardiac tissues and the accompanying myocardial ischemia or hypoxia (7). Cardiac damages induced by these conditions are closely related to processes such as cardiomyocytes apoptosis, oxidative stress, and inflammation, so therapies to alleviate these processes, as well as angiogenic factors, are conducive to recover cardiac function (7, 71). Pathological conditions present during or after myocardial infarction include myocardial fibrosis, arrhythmia, and ischemic/reperfusion (I/R) injury, etc (7, 72–74). Some researches have indicated that miR-223-3p can protect cardiomyocytes from myocardial I/R-induced inflammation and necroptosis, while others have proved that miR-223-3p displays pro-apoptosis and anti-angiogenesis effects, as well as promotes myocardial fibrosis and arrhythmia induced by myocardial infarction.

I/R injury, commonly induced by interventional therapies such as percutaneous coronary intervention or thrombolytic therapy, which are necessary when myocardial infarction occurred, could result in cardiomyocytes apoptosis and necrosis and has been demonstrated to be manipulated by gene regulation (26, 75, 76). MiR-223-3p has been reported upregulated in I/R hearts and involved in mechanisms underlying I/R-induced cardiomyocytes necroptosis in myocardial infarction (26, 77). MiR-223-3p cooperative with miR-223-5p inhibited cell necroptosis involved in I/R-induced myocardium injuries through regulating inflammatory response and necrotic signaling pathway respectively, which together promoted the necroptosis (26, 78–80). MiR-223-3p could attenuate I/R-triggered inflammation through suppressing the NOD-like receptor family pyrin domain containing 3 (NLRP3) inflammasome signaling pathway. MiR-223-3p directly targeted IkB kinase α (IKKα) and NLRP3 to abrogate the activation of NLRP3 inflammasome and downregulate the expression of TNF-α and interleukin 1 β (IL-1β), the inflammatory cytokines involved in I/R-triggered inflammation. While miR-223-5p repressed the necrotic signaling pathway through the inhibition of the necrosome containing receptor-interacting protein 3 (RIP3) with its partners receptor-interacting protein 1 (RIP1) and mixed lineage kinase domain-like (MLKL) (26). Taken together, miR-223-3p may exert beneficial effects on I/R-induced inflammatory response and cardiomyocytes necroptosis following myocardial infarction and other ischemic heart diseases.

Despite the protective effects on I/R-induced damages, more studies have regarded miR-223-3p as a potential therapeutic

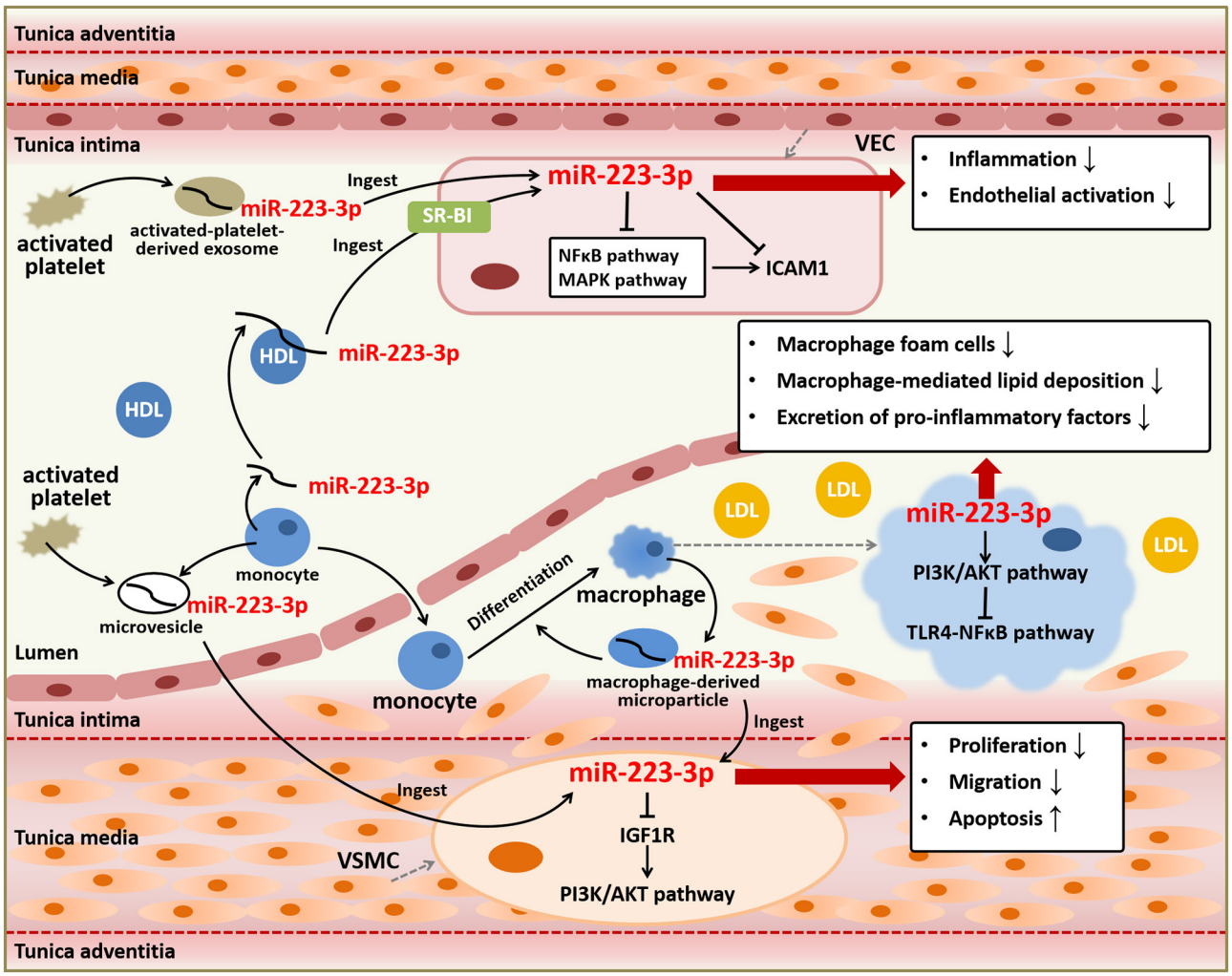

FIGURE 2 | Anti-atherosclerotic role of miR-223-3p. MiR-223-3p plays important roles in atherosclerotic progression based on its effects on various types of cells involved in atherosclerosis including VECs, VSMCs, and macrophages. MiR-223-3p can suppress endothelial inflammation and activation through targeting ICAM1 and regulating NFκB and MAPK signaling pathways. MiR-223-3p also alleviates vascular remodeling mediated by proliferation and migration of VSMCs and lipid deposition and inflammation mediated by macrophages through PI3K/AKT or TLR4/NFκB signaling pathways. Besides, MiR-223-3p is an important endocrine signal factor for communication between platelets, monocytes, and vascular cells.

target that should be suppressed in myocardial infarction due to its effects of pro-apoptosis in cardiomyocytes and antiangiogenesis. Angiogenesis, which is normally restricted by the physiological activity of VECs, is essential for the recovery of myocardial ischemia and myocardial infarction. It was demonstrated that miR-223-3p was highly expressed in natively quiescent VECs which were freshly isolated from human vessels, while in VECs that were cultured for angiogenesis with stimulation of growth factors the miR-223-3p were downregulated to very low levels (81). This sharp downregulation of miR-223-3p is in accordance with previous studies that suggested nearly undetectable expression of miR-223-3p in cultured VECs and may result from the epigenetic silencing mechanisms or a lack of exogenous miR-223-3p delivered by other cells from plasma *in vivo* as we mentioned in the former parts (46, 54, 81). MiR-223-3p in VECs reduced cellular proliferation and migration to inhibit angiogenesis through targeting integrin β 1 (ITGB1). Downregulation of ITGB1 suppressed the phosphorylation of vascular endothelial growth factor receptor 2 (VEGFR2) and fibroblast growth factor receptor 1 (FGFR1) of growth factor (GF) signaling pathway, leading to inhibition of AKT signaling pathway, while the antagonist of miR-223-3p reversed these antiangiogenic effects (81). Another study revealed that miR-223-3p was upregulated in ischemia cardiac microvascular endothelial cells from a myocardial infarction model and also played antiangiogenic roles. MiR-223-3p inhibited endothelial cells proliferation and migration through targeting ribosomal protein S6 kinase B1 (RPS6KB1) to inhibit hypoxia inducible factor 1 α (HIF-1α) signaling pathway, an important pathway for angiogenesis, and

affect the downstream proteins including vascular endothelial growth factor (VEGF), MAPK, PI3K, and AKT (37).

Furthermore, miR-223-3p was found to be concerned with the hypoxia-induced cardiomyocytes apoptosis. Hypoxia is a common condition during myocardial ischemia and acts as a promoting factor of apoptosis, contributing to ischemic heart diseases such as myocardial infarction (82, 83). It was proved that miR-223-3p in cultured cardiomyocytes was increased under 1% O_2 hypoxia and directly suppressed Kruppel-like factor 15 (KLF15), a regulator of cardiomyocyte structure and function to repress cardiac hypertrophy, to promote hypoxia-induced apoptosis and oxidative stress of cardiomyocytes (82), although others reported that 10% O_2 alveolar hypoxia induced reduction of miR-223-3p expression in ventricular myocardium of mice (84). Inhibition of miR-223-3p reduced hypoxia-induced cardiomyocytes apoptosis with the induction of anti-apoptotic protein B cell lymphoma 2 (BCL2) and reduction of pro-apoptotic protein B cell lymphoma 2-associated X (BAX), as well as decrease of cleaved caspase 3. Besides, inhibition of miR-223-3p also repressed the production of ROS and decreased peroxidation activities under hypoxia with reducing the malondialdehyde (MDA) contents and enhancing antioxidant enzymes such as superoxide dismutase (SOD), catalase (CAT), and glutathione peroxidase 1 (GPX1), to alleviate hypoxia-induced oxidative stress (82).

Myocardial fibrosis is a pathological change that could occur after myocardial infarction to obstruct the renewal of myocardium, mainly resulting from abnormal proliferation and differentiation of cardiac fibroblasts which take place of dead cardiomyocytes, and finally leads to myocardial remodeling and stiffness, as well as other complications related to myocardial infarction (85–88). MiR-223-3p has been shown to participate in fibrosis, including the cardiac fibrosis after myocardial infarction (85, 89). MiR-223-3p, which could be regulated by transforming growth factor β (TGF-β), was abundant in activated cardiac fibroblasts than cardiomyocytes and could stimulate cardiac fibroblasts proliferation, migration, differentiation, collagen synthesis, and α-smooth muscle actin (ACTA2) expression. The pro-fibrosis effects mediated by miR-223-3p were through targeting RAS p21 protein activator (RASA1), a RAS signal negative regulator, to upregulate the downstream MAPK and PI3K/AKT signaling pathways with increasing the phosphorylation of MAPK kinase 1/2 (MEK1/2), ERK1/2, and AKT, leading to myocardial fibrosis and deterioration of ventricular function (85).

Arrhythmia is another severe disorder following myocardial infarction and caused by electrophysiological dysfunction, especially characterized by extended action potential due to the reduction of transient outward K^+ current (I_{to}) (90–92). MiR-223-3p was thought to have the potential to regulate potassium voltage-gated channel subfamily D member 2 (KCND2), a subunit of voltage-gated transient outward K^+ channel carrying I_{to}, probably leading to a reduction of I_{to} (93). A recent study verified this and proved the role of miR-223-3p suppressing arrhythmia in myocardial infarction. In the ventricular cardiomyocytes of a myocardial infarction animal model, it was found that miR-223-3p levels were elevated, while expression of KCND2 and I_{to} were diminished resulting from the direct inhibition of KCND2 by miR-223-3p, and the upregulation of miR-223-3p promoted arrhythmia following myocardial infarction (94). Therefore, blocking the endogenous miR-223-3p is possible to develop into a therapeutic method for the prevention of myocardial fibrosis and arrhythmia after myocardial infarction or other ischemia situations, consequently improving the prognosis of these diseases.

Therefore, on the one hand, miR-223-3p may act as an inducer of myocardial infarction due to its promotion of hypoxia-induced cardiomyocytes apoptosis, antagonism to angiogenesis, and induction of complications following myocardial infarction including fibrosis and arrhythmia. On the other hand, miR-223-3p may improve I/R injury after myocardial infarction based on its inhibition of inflammatory response and necroptosis in cardiomyocytes (**Figure 3**). Although the expression of miR-223-3p was found increased in cardiomyocytes of myocardial infarction models and heart tissues of patients with myocardial infarction (94, 95), the study investigating the potential of circulating miR-223-3p as a biomarker related to myocardial infarction remains scarce.

MiR-223-3p as a Potential Biomarker and Therapeutic Target for Coronary Artery Disease

Although at present there exist some efficient medical interventions for the treatment of coronary artery disease such as percutaneous coronary intervention, clinical non-invasive biomarkers, which could accurately and conveniently be used for assisting diagnosis, assessing the severity, evaluating the efficacy of treatment, and predicting prognosis of coronary artery disease, are still in need. Based on the multiple functions of miR-223-3p associated with the pathophysiological processes of coronary artery disease, it is expected to become a biomarker for the disease.

Role of MiR-223-3p in Antiplatelet Therapy

Platelet activity contributes to the pathophysiological process in coronary artery disease, especially the formation of thrombosis (96). Antiplatelet therapy plays a significant role in pharmacological prevention of cardiovascular events and markedly impacts the prognosis of coronary artery disease, including the classic dual antiplatelet therapy (DAPT) with aspirin and clopidogrel, combination of aspirin and other P2Y12 antagonists, or monotherapy with one single antiplatelet drug (97). Responsiveness to the antiplatelet drugs and the platelet activity in patients with ischemic CVDs determine the benefits from antiplatelet therapy, while poor responsiveness or high platelet activity, known as high on-treatment platelet reactivity, is related to the risk of adverse cardiovascular outcomes (98–101). MiR-223-3p is quite abundant in both platelets and plasma, and directly targets P2Y12 in platelets, making it important for antiplatelet drugs, especially the P2Y12 antagonists used in antiplatelet therapy such as clopidogrel and ticagrelor (35, 62, 102, 103).

In patients with non-ST elevation ACS who received a regular DAPT with aspirin and clopidogrel, it was indicated that both the

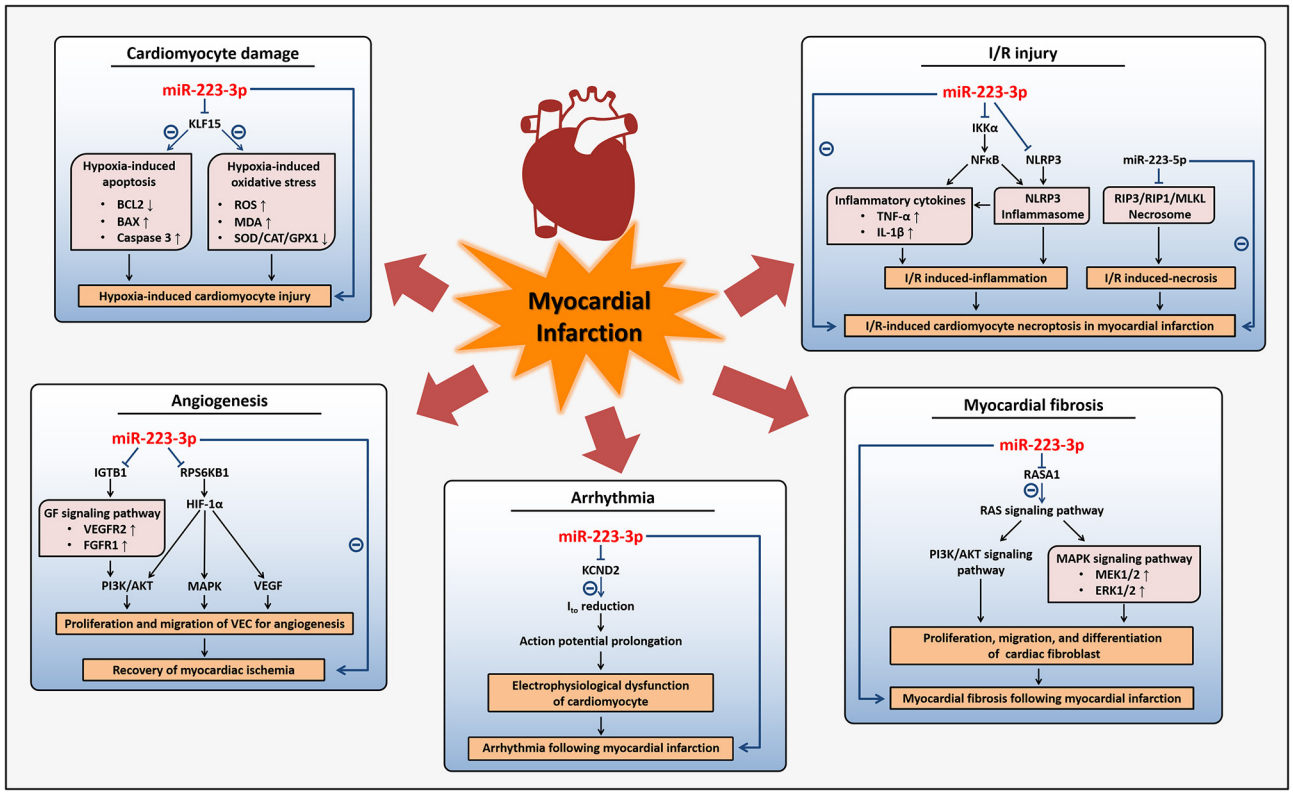

FIGURE 3 | Regulatory mechanisms of miR-223-3p in myocardial infarction. MiR-223-3p participates in different pathophysiological activities affecting myocardial infarction through regulation on multiple genes and diverse signaling pathways. MiR-223-3p promotes hypoxia-induced cardiomyocyte injury and inhibits the recovery of myocardial ischemia with its anti-angiogenesis effects during myocardial infarction. Myocardial fibrosis and arrhythmia can be induced by miR-223-3p to impact the prognosis of myocardial infarction. Besides, miR-223-3p is helpful for alleviation of I/R injury which often occurs after myocardial infarction.

levels of miR-223-3p in plasma and platelets were downregulated in low clopidogrel response patients (104, 105), characterized by the high platelet reactivity index (PRI) of patients based on the measurement of vasodilator-stimulated phosphoprotein phosphorylation (106–108). MiR-223-3p levels were negatively correlated with PRI and the reduced miR-223-3p in plasma or platelets was demonstrated to be the only independent predictive factor of low responders to clopidogrel determined by PRI, compared with other factors that could potentially affect platelet reactivity, such as age, genotypes, use of calcium channel blockers or proton-pump inhibitors, and diabetes (104, 105). Therefore, low levels of circulating miR-223-3p may be a promising biomarker to predict the poor responsiveness to clopidogrel in ACS patients and the decrease of miR-223-3p in platelets is probably involved in the mechanism of clopidogrel resistance based on its inhibition of P2Y12 in platelets.

While downregulation of miR-223-3p might increase the platelet reactivity to reduce the efficacy of DAPT containing clopidogrel, the enhanced inhibition of platelet reactivity by more potent P2Y12 antagonists ticagrelor or prasugrel instead of clopidogrel of DAPT in patients with non-ST elevation ACS was associated with the elevation of plasma miR-223-3p (109). Therefore, miR-223-3p levels seem to be positively correlated with the effectiveness of antiplatelet therapy with P2Y12 antagonists. Besides, it was reported that in patients with ACS, plasma miR-223-3p level decreased 24 h after switching the DAPT from clopidogrel to ticagrelor in order to further inhibit platelet reactivity (96). Another study also showed that inhibition of platelet reactivity in healthy volunteers with prasugrel or DAPT containing prasugrel decreased the circulating miR-223-3p (62). In patients with coronary artery disease who received antiplatelet treatment for 24 h, the severity of coronary artery disease based on SYNTAX score was positively correlated with the platelet level of miR-223-3p, which might indirectly reflect the relation between platelet reactivity and miR-223-3p (110). Thus, although miR-223-3p can inhibit P2Y12 in platelets to affect the platelet reactivity, the circulating miR-223-3p levels may also be influenced by degree of P2Y12 inhibition and associated with platelet reactivity, and as a result, the definite correlation between circulating miR-223-3p levels and platelet reactivity might depend on status of patients, categories of drugs, or administration time. Even so, circulating miR-223-3p is helpful to predict the efficacy of antiplatelet therapy, especially the responsiveness to clopidogrel in ACS patients. Thus, circulating miR-223-3p may be useful for identifying patients suitable to receive clopidogrel as one of the antiplatelet

drugs, thus saving the time and cost of switching therapeutic strategy for these patients.

Role of MiR-223-3p in Diagnosis, Severity Assessment, and Risk Prediction of Coronary Artery Disease

So far, the effective and convenient biomarker for coronary artery disease is still lacking. It was reported that in patients with coronary artery disease, the circulating miR-223-3p levels were elevated and positively associated with the severity of coronary atherosclerotic lesions evaluating by Gensini scores (111). The increased circulating miR-223-3p in coronary artery disease also could be used to predict cardiovascular death risk for patients, in particular for patients with ACS (112). Besides, compared with patients with stable coronary artery disease, the plasma HDL-carried miR-223-3p in ACS patients decreased during the transcoronary passage, indicating that in ACS patients the uptake of HDL-carried miR-223-3p by the coronary vascular wall was promoted, which suggested the positive correlation between uptake of plasma HDL-carried miR-223-3p and severity of coronary artery disease (113). Thus, miR-223-3p may probably be developed into a biomarker for assessing the severity and predicting the death risk of coronary artery disease. The levels of serum miR-223-3p were upregulated in myocardial infarction patients, compared with healthy controls and angina pectoris patients (114). While another study showed that circulating miR-223-3p levels were negatively correlated to the risk of myocardial infarction (102). More researches are needed to confirm the role of miR-223-3p as a diagnostic or predictive biomarker of myocardial infarction. Furthermore, the expression of miR-223-3p in peripheral blood mononuclear cells was downregulated in patients who were diagnosed as coronary artery disease with significant or insignificant stenosis compared with healthy controls, which was most prominent in patients with insignificant stenosis, indicating that miR-223-3p in peripheral blood mononuclear cells might be positively related to severity of coronary artery disease and could be used for discriminate patients with significant or insignificant stenosis (115).

Taken together, owing to the complex mechanisms and diverse symptoms of coronary artery disease, miR-223-3p may play multiple roles in these diseases, depending on its regulatory effects on the development of atherosclerosis, myocardial ischemia or hypoxia, and platelet function. The circulating miR-223-3p can be developed into both a therapeutic target and a biomarker to evaluate the treatment effects in coronary artery disease because it is capable of regulating the platelet aggregation and predicting the responsiveness to antiplatelet drugs of patients. MiR-223-3p is a promising biomarker that can be used for evaluating the severity of coronary artery disease such as stenotic degree of coronary atherosclerosis and predicting the prognosis of coronary artery disease, for its convenient detection, lower cost, and less damage to human body. Future studies should be more focused on the specific diagnostic or predictive function of miR-223-3p in coronary artery disease of different categories, or with different pathogenic mechanisms and inducing factors.

MiR-223-3p IN HEART FAILURE

Heart failure is one of the most serious CVDs because of its high morbidity and mortality, mainly characterized by exhausted cardiac function of systole and diastole, and threatens worldwide people for a lack of effective treatments (116, 117). Cardiac hypertrophy, especially pathological cardiac hypertrophy, which acts as a cardiac compensatory mechanism in response to multiple pathophysiological stress, leads to cardiac ventricle remodeling and is an important pathogenic factor for heart failure (118). Other cardiac ventricle remodeling processes including fibrosis and malignant arrhythmia also contribute to the development of heart failure (119–121). Besides, pro-inflammatory conditions in myocardium that may result from systemic inflammation, such as activation and polarization of macrophages infiltrating into the myocardium, also promote heart failure progression (122, 123). Researchers have found numerous heart failure-related miRNAs such as miR-223-3p which prominently plays a part in heart failure through regulating cardiomyocytes hypertrophy and inflammation. In addition, miR-223-3p levels have been proved closely related to complications or combined symptoms of heart failure.

Effect of MiR-223-3p on Pathophysiological Processes in Heart Failure

Current researches have demonstrated that miR-223-3p has biphasic effects on heart failure through bidirectional regulation of cardiac hypertrophy and promotion of inflammatory response. Both in the rat model of cardiac hypertrophy induced by transverse aorta constriction and in hypertrophic cardiomyocyte models treated with different inducing reagents endothelin-1 or phenylephrine, the expression of miR-223-3p in myocardium and cardiomyocytes were downregulated (124, 125). The mechanism underlying the phenylephrine-induced downregulation of miR-223-3p in cardiomyocytes was suppressing glycogen synthase kinase 3 β activity to reduce β-catenin degradation and increase its activation (125). This modulation upregulated SRY-box transcription factor 2, which could promote cardiomyocytes proliferation and increase heart size, to inhibit the transcription of primary miR-223 (125, 126). Inhibition of primary miR-223 increased the stromal interaction molecule 1 (STIM1), a target of miR-223-3p, to induce cardiomyocyte hypertrophy through elevating the cytosolic Ca^{2+} levels of cardiomyocytes (125, 127–129). When overexpressing miR-223-3p or miR-223(-3p/5p) in cardiomyocytes, the hypertrophy was ameliorated mainly manifesting as smaller cellular surface area, downregulation of classic pathological hypertrophy marker genes encoding atrial natriuretic peptide (ANP), B type natriuretic peptide (BNP), α-actinin, and myosin heavy chain 6/7 (MYH6/7) (124, 125). The protective effects of miR-223-3p against cardiomyocytes hypertrophy might also depend on direct inhibition of troponin I3 interacting kinase (TNNI3K), a cardiac kinase that was upregulated in hypertrophic cardiomyocytes and induced cardiomyocytes hypertrophy through regulating cardiac remodeling process

(124, 130, 131). Overexpression of miR-223-3p decreased the phosphorylation of cardiac troponin I, the downstream target of TNNI3K, and reversed the increased intracellular Ca^{2+} concentration and contractility of cardiomyocytes that were induced by TNNI3K, thus resulting in amelioration of cardiomyocytes hypertrophy (124). Notably, TNNI3K is also thought to be a promoter of physiological cardiac hypertrophy (132), so miR-223-3p may target TNNI3K to suppress either physiological or pathological cardiac hypertrophy.

Similar to the findings in models of cardiac hypertrophy, miR-223-3p was also downregulated in the myocardium of patients with non-end stage heart failure, more prominently in non-diabetic heart failure patients compared with diabetic heart failure patients or healthy controls (133). Among the advanced heart failure patients who received heart transplantation directly or after a period of left ventricular assist devices support, the expression of miR-223-3p in failing hearts before transplantation was significantly higher in patients with a period of left ventricular assist devices support and positively correlated with the cardiac index values, which reflect the cardiac output and function. This suggested that miR-223-3p might be involved in cardiac reverse remodeling and heart recovery (134). Therefore, miR-223-3p can be downregulated in models of cardiac hypertrophy or heart failure and might make a beneficial contribution to heart failure primarily through alleviating the ventricle remodeling processes concerned in cardiac hypertrophy, promoting the heart recovery process, and improving the cardiac function.

However, others have reported that overexpressed miR-223-3p could induce both pathological and physiological cardiac hypertrophy, as well as regulate the inflammatory response in hearts, probably resulting in the development of heart failure. MiR-223-3p was found upregulated in hearts of end stage heart failure patients and mouse models of cardiac hypertrophy induced by isoproterenol treatment or transverse aorta constriction (33, 135, 136), suggesting the detrimental roles of miR-223-3p in cardiac hypertrophy and heart failure, which was opposite to the above-mentioned studies (124, 125, 133). Both pathological and physiological cardiac hypertrophy have been found in transgenic mouse models with cardiac-specifically overexpression of miR-223(-3p/5p) (33, 137). These transgenic mice could develop pathological cardiac hypertrophy at the age of 8–12 weeks, characterized by higher heart/body weights, larger size of cardiomyocytes, interstitial fibrosis, upregulation of pathological cardiac hypertrophy marker genes in hearts, and impaired cardiac function which could lead to heart failure. Furthermore, in miR-223(-3p/5p) knockout mice, isoproterenol-induced pathological cardiac hypertrophy and heart failure were alleviated, also indicating the harmful role of miR-223(-3p/5p) in heart failure (33). MiR-223-3p directly targeted apoptosis repressor with CARD (ARC), which was reduced in human failing hearts and involved in cardiomyocytes hypertrophy and apoptosis, to induce pathological cardiac hypertrophy in animals and cardiomyocytes (33, 138, 139). Aiming to block the inductive effects of miR-223-3p for cardiac hypertrophy and heart failure, researchers screened a heart-related circular RNA to directly bind miR-223-3p and increase the expression of ARC of cardiomyocytes, resulting in alleviation of cardiac hypertrophy and heart failure induced by isoproterenol (33). This throws light on the development of the promising therapeutic target for heart failure.

The opposite effects of miR-223-3p in cardiac hypertrophy progression and heart failure may result from different stimuli and species to establish models of cardiac hypertrophy, considering different mechanisms of cardiac hypertrophy inducers such as endothelin-1, phenylephrine, or isoproterenol, and the species variation such as rats, mice, and human. The different expressions of miR-223-3p among patients may be due to diverse progression of disease such as non-end stage or end stage of heart failure. Besides, in experiments overexpressing miR-223-3p *in vitro* or *in vivo*, different regulatory effects on cardiac hypertrophy were observed, as *in vitro* studies showed inhibition on cardiac hypertrophy while *in vivo* studies showed induction on cardiac hypertrophy (33, 124, 125, 137). It is believed that *in vivo* studies are closer to real pathophysiological processes in cardiac hypertrophy and heart failure in human. Therefore, it is reasoned that miR-223-3p may display an inductive effect on cardiac hypertrophy and heart failure in human body, although more studies are needed.

Physiological cardiac hypertrophy is an adaptive response of hearts which is often caused by exercise training and characterized by relatively normal cardiac structure and function without fibrosis or abnormal expression of pathological cardiac hypertrophy gene markers such as ANP, BNP, and MYH7 (140, 141). Physiological cardiac hypertrophy was found in 3, 6, or 12-months aged transgenic mice overexpressing miR-223(-3p/5p), only manifesting larger hearts and thicker left ventricular walls with enhanced cardiac function (137). The inductive effects of miR-223(-3p/5p) on physiological cardiac hypertrophy were mediated by activation of the AKT signal pathway which played significant roles in the promotion of physiological cardiac hypertrophy (137, 142, 143). MiR-223-3p repressed the degradation of HIF-1α through directly inhibiting F-Box and WD repeat domain containing 7 (FBXW7) or targeting activin A receptor type 2A (ACVR2A) to downregulate egl-9 family hypoxia inducible factor 3 (EGLN3). The activated HIF-1α signaling pathway could increase phosphorylation of AKT directly or through upregulating periostin. Meanwhile, miR-223-3p in cardiomycytes was found to directly target two upstream positive regulators of AKT pathway, IGF1R and ITGB1, tending to inhibit the phosphorylation of AKT. Although both positive and negative regulators of AKT were influenced, the overexpression of miR-223(-3p/5p) led to the activation of AKT signaling pathway and induced physiological cardiac hypertrophy in models (137). Dual contribution of miR-223-3p overexpression to both pathological and physiological cardiac hypertrophy might result from the difference of transgenic models construction, as the length of DNA fragments containing primary miR-223 and the sequences of the primers used to generate transgenic models were different (33, 137), possibly leading to the diverse abundance of miR-223-3p overexpression and effects on cardiac hypertrophy.

In addition, miR-223-3p could also accelerate heart failure depending on its pro-inflammatory effects in macrophages

including activation and polarization of macrophage toward a pro-inflammatory (M1) phenotype, as well as induction of inflammation markers and secretion of cytokines, probably contributing to the development of heart failure (122, 123, 144).

Conclusively, miR-223-3p regulates pathophysiological processes that drive heart failure, including hypertrophy of cardiomyocytes and myocardium, as well as the inflammatory response. Although the specific role of miR-223-3p in cardiac hypertrophy and heart failure remains controversial, the therapeutic method to repress miR-223-3p with a heart-related circular RNA and thus to alleviate cardiac hypertrophy and heart failure has been identified (33). Therefore, miR-223-3p seems to be a promising therapeutic target in clinical treatments of heart failure.

MiR-223-3p as a Potential Biomarker for Heart Failure

Circulating biomarkers can facilitate the diagnosis, therapy, and prognostic assessment of heart failure. Currently, the classic and recommended biomarkers for heart failure evaluation only refer to BNP or N terminal pro BNP (NT-proBNP) (145). However, BNP or NT-proBNP is not a specific biomarker for heart failure because some other diseases also display an elevation of BNP or NT-proBNP, such as cardiopulmonary disease and renal failure. Thus, to screen more effective and specific biomarkers for heart failure is still in need. Based on the stability and functional diversity, miRNAs could be potential and powerful biomarkers for heart failure (146, 147). The relationship between circulating miR-223-3p and heart failure has been investigated both in human and animal models.

There are evidences that in acute heart failure patients, plasma miR-223-3p decreased significantly compared with healthy controls or chronic heart failure patients, and its further decline was associated with the increased risk of 180-day mortality in these patients (148, 149). In addition, the plasma miR-223-3p level decreased 48 h after hospitalization, and its level was negatively correlated with circulating growth differentiation factor 15 that was identified as one of the parameters for worse clinical outcomes in acute heart failure. The correlation was more obvious in the severest group of patients, while not observed at the time of admission (150). The circulating levels of miR-223-3p in heart failure patients were also negatively related to rehospitalization caused by CVDs (67). Both atherosclerotic diseases and renal injuries are common in heart failure (67, 151). It was reported that in heart failure patients the reduced circulating miR-223-3p was associated with increased manifestations of atherosclerosis and elevation of atherosclerosis-related indicators (67). Circulating levels of miR-223-3p were also negatively associated with the tubular damage biomarker neutrophil gelatinase associated lipocalin, which could signify early worsening of renal function in heart failure (152–154). These concomitant situations often aggravate the severity of heart failure and lead to adverse prognosis in patients, so looking for biomarkers, including the candidate miR-223-3p, to precisely predict the progression and risk, even comorbidities or complications of the disease is of great value in the treatment of heart failure.

Whereas, in muscular dystrophy patients combined with advanced heart failure and a hypertension-induced congestive heart failure rat model, plasma miR-223-3p levels were elevated and positively correlated with circulating level of heart failure marker BNP and cardiac MYH7 expression in the animal model, which were upregulated in heart failure (155–159). It is noteworthy that there exist differences in circulating miRNAs signature between rodent heart failure models and human. The observed alteration of circulating miR-223-3p levels in heart failure patients did not occur in multiple rodent models with well-established heart failure (160). MiR-223-3p was identified to have similar sequences between human and mice, but different in rats. The diversity of miRNAs signature of different species may also due to the limitation of experimental animal models that could usually only mimic the heart failure symptoms caused by one stimulus but not accurately and roundly replicate the diverse pathogenesis of clinical human heart failure, and heart failure animal models are more likely to approximate the state of chronic heart failure in human. Furthermore, etiological factors in heart failure, such as hypertension, ischemia, and myocardial dystrophy, should also be considered when investigating the role of biomarkers related to heart failure.

Taken together, circulating levels of miR-223-3p are associated with the severity, current biomarkers for worse clinical outcomes, and the mortality of heart failure, as well as the risk of rehospitalization and concomitant diseases. Thus, circulating miR-223-3p level might not only evaluate the progression of heart failure but also act as a prognostic indicator or a predictor for comorbidities and complications of heart failure. Also, based on the regulatory networks of miR-223-3p in processes involved in heart failure, it is more likely to be a potential therapeutic target and serve as a biomarker to evaluate the treatment effects of heart failure.

MiR-223-3p IN OTHER CVDs

MiR-223-3p in Pulmonary Arterial Hypertension

Pulmonary arterial hypertension (PAH) is a serious and progressive disease commonly characterized by pulmonary arterial obstruction and elevated pulmonary arterial pressure (161). These conditions are commonly caused by excessive pulmonary vasoconstriction, inflammation, and pulmonary vascular remodeling, and are usually accompanied by hypoxic condition and dysfunction of pulmonary vasculature, leading to right ventricular failure or even death (161–163). As one of the most significant mechanisms involved in vascular remodeling of PAH, aberrant proliferation, migration, and apoptosis of pulmonary arterial endothelial cells and pulmonary arterial smooth muscle cells (PASMCs) affect the progression of PAH (164–166). Recent studies have verified the regulatory effects of miR-223-3p on PAH and PAH-related dysfunction of PASMCs.

MiR-223-3p was downregulated in lung, pulmonary arteries and PASMCs of both PAH patients and PAH models (167–169). In serum of female PAH patients associated with congenital heart disease, miR-223-3p levels were reduced compared with healthy females while there was no difference in males, suggesting the potential of miR-223-3p as a biomarker for PAH associated with congenital heart disease in females (168). Researchers have explored the specific mechanisms underlying the regulatory effects of miR-223-3p on PAH. HIF-1α, which is usually upregulated under hypoxia, was activated in PAH and led to the inhibition of miR-223-3p in PASMCs of PAH patients, resulting in upregulation of multiple miR-223-3p targets and the development of PAH (167–169). MiR-223-3p directly targeted integrin β 3 (ITGB3), IGF1R, poly (ADP-ribose) polymerase 1 (PARP1), ras homolog family member B (RHOB), and myosin light chain 2 (MYL2) in PASMCs to repress the proliferation and migration, and to promote the differentiation and DNA damage-induced apoptosis (167–172). Besides, the downregulation of miR-223-3p and upregulation of ITGB3 both increased the expression of IGF1R and PARP1, indicating that miR-223-3p could suppress IGF1R and PARP1 through direct regulation or by targeting ITGB3 (169). Therefore, both overexpression of miR-223-3p or suppression of ITGB3 regulated PASMCs activities to alleviate the pathological features of PAH animals including pulmonary vascular remodeling, pulmonary or myocardial hemorrhage, fibrosis of lung or myocardium, and right ventricular hypertrophy. The reverse of PAH phenotypes reduced the pulmonary resistance, improved the cardiac function, and finally prolonged the survival time of animals (167–169). Taken together, miR-223-3p inhibits PAH through directly targeting multiple genes and signaling pathways involved in abnormal activities of PASMCs and pulmonary vascular remodeling, so it might be a promising therapeutic target for PAH.

TABLE 1 | Verified target genes of miR-223-3p in CVDs.

Gene	Gene function	Cell/Tissue type	Species	References
SR-BI	Cholesterol transport	Hepatocyte	Human	(32, 49)
		VEC		(32)
*HMGCS1**	Cholesterol biosynthesis	Hepatocyte	Human	(49)
*SC4MOL**	Cholesterol biosynthesis	Hepatocyte	Human	(49)
*Sp3**	Cholesterol efflux	Hepatocyte	Human	(49)
*ICAM1**	Inflammation	VEC	Human	(46)
IGF1R	Proliferation, migration, apoptosis	VSMC	Rat, mouse	(35)
	Proliferation, differentiation	PASMC	Human, rat, mouse	(169, 170)
	Hypertrophy	Cardiomyocyte	Rat, mouse	(137)
NLRP3	Inflammation, necroptosis	Cardiomycyte	Rat, mouse	(26)
	Inflammation	Dendritic cell	Mouse	(178)
*IKKα**	Inflammation, necroptosis	Cardiomycyte	Rat, mouse	(26)
ITGB1	Proliferation, migration	VEC	Human, mouse	(81)
	Hypertrophy	Cardiomyocyte	Rat, mouse	(137)
*RPS6KB1**	Proliferation, migration	VEC	Rat	(37)
*KLF15**	Hypoxia-induced apoptosis, oxidative stress	Cardiomycyte	Rat	(82)
*RASA1**	Proliferation, migration, differentiation	Cardiac fibroblast	Rat	(85)
*KCND2**	Electrophysiology	Cardiomyocyte	Rat	(94)
P2Y12	Platelet aggregation, thrombus growth/stability	Platelet	Human	(103)
		Megakaryocyte		
*STIM1**	Hypertrophy	Cardiomyocyte	Rat	(125)
*TNNI3K**	Hypertrophy	Cardiomyocyte	Rat	(124)
*ARC**	Hypertrophy	Cardiomyocyte	Mouse	(33)
*FBXW7**	Hypertrophy	Cardiomyocyte	Rat, mouse	(137)
*ACVR2A**	Hypertrophy	Cardiomyocyte	Rat, mouse	(137)
*ITGB3**	Proliferation, differentiation, DNA damage-induced apoptosis	PASMC	Rat	(169)
*PARP1**	DNA damage-induced apoptosis	PASMC	Human, rat	(167, 169)
*RHOB**	Proliferation, migration	PASMC	Human, rat	(168)
*MYL2**	Proliferation, migration	PASMC	Human, rat	(168)
*PKNOX1**	Activation, polarization	Macrophage	Mouse	(177)
STAT3	Inflammation	Heart	Mouse	(27)
IL-6	Inflammation	Heart	Mouse	(27)

**The target genes marked with an asterisk are cell-specific targets of miR-223-3p corresponding to the certain cell types in the table according to the current research.*

MiR-223-3p in Inflammation-Related Myocardial Disease

MiR-223-3p is considered to play a key role in inflammatory or immune responses during varieties of diseases through targeting different genes involved in monocytes differentiation, macrophages activation, and polarization, as well as regulation of eosinophil cells, resulting in modulation of both pro-inflammatory and anti-inflammatory signaling pathways (25, 30, 173). Myocarditis is a kind of inflammatory heart disease usually caused by infectious factors including virus and bacteria while non-infectious factors may also trigger the immune response in myocardium, such as autoimmune myocarditis (174, 175). Myocarditis has become one of the most common reasons for sudden death in children and young people (174, 176). It was reported that miR-223-3p displayed a protective function on both coxsackievirus B3 (CVB3)-induced viral myocarditis and autoimmune myocarditis, as well as on inflammation-related myocardial depression in polymicrobial sepsis (27, 177, 178).

In heart tissues and macrophages that infiltrated in hearts of CVB3-infected mice, the expression of miR-223-3p was downregulated, accompanied by elevation of PBX/knotted 1 homeobox 1 (PKNOX1). Upregulation of miR-223-3p altered the polarization phenotypes of macrophages from classical pro-inflammatory M1 type to alternative anti-inflammatory M2 type, partly depending on directly targeting PKNOX1 (177). This transition manifested as the inhibition of M1 markers such as nitric oxide synthase 2 and TNF-α, as well as the increase of M2 markers such as arginase-1 and fizz-1 (177, 179). These effects of miR-223-3p on macrophage activation and polarization made contributions to alleviating CVB3-induced inflammation and myocarditis with reducing pro-inflammatory and myocardial injury markers including interferon-γ, interleukin 6 (IL-6), creatine kinase MB, lactate dehydrogenase, and aspartate transaminase, as well as increasing the anti-inflammatory factor interleukin 10. As a result, miR-223-3p improved the indexes of cardiac function, body weights, and survival of CVB3-infected animals, indicating the alleviation of CVB3-induced myocarditis (177, 180, 181).

The protective role of miR-223-3p in autoimmune myocarditis lies in the regulation of another kind of immune cells, dendritic cells (DCs) which have been recognized as essential regulators to balance immunity and tolerance depending on their activation status (178, 182, 183). The tolerogenic DCs (tDCs) can be induced by immunosuppressive factors including interleukin 10 and TGF-β, leading to the unresponsiveness of T cells and tolerance of inflammatory stimulation, which is helpful in autoimmune diseases (184, 185). MiR-223-3p levels were reduced in serum and DCs of experimental autoimmune myocarditis mice while upregulating miR-223-3p in DCs prompted their transition to tDCs with reduced cellular surface markers of mature DCs and increased anti-inflammatory cytokines. MiR-223-3p also alleviated autoimmune myocarditis *in vivo* through reducing pericardial inflammation, increasing immunosuppressive response, and improving cardiac function. MiR-223-3p induced the transition of DCs to tDCs through directly targeting NLRP3, an important regulator to maintain immune homeostasis and tolerance, resulting in reduced production of NLRP3

TABLE 2 | Signaling pathways regulated by miR-223-3p in CVDs.

Signaling pathway	Cell function	Disease/Process	References
NFκB	Inflammation of VEC	Atherosclerosis	(54)
	Lipid accumulation and inflammation of macrophage	Atherosclerosis	(57)
	Inflammation and necroptosis of cardiomycyte	Myocardial I/R injury	(26)
TLR4	Lipid accumulation and inflammation of macrophage	Atherosclerosis	(57)
MAPK	Proliferation, migration, and inflammation of VEC	Atherosclerosis, cardiac angiogenesis	(37, 54)
	Proliferation, migration, and differentiation of cardiac fibroblast	Myocardial fibrosis following myocardial infarction	(85)
PI3K/AKT	Proliferation, migration, and apoptosis of VSMC	Atherosclerosis	(35)
	Inflammation of macrophage	Atherosclerosis	(57)
	Proliferation and migration of VEC	Cardiac angiogenesis	(37, 81)
	Hypertrophy of cardiomyocyte	Cardiac hypertrophy	(137)
	Proliferation, migration, and differentiation of cardiac fibroblast	Myocardial fibrosis following myocardial infarction	(85)
IGF1	Proliferation, migration, and apoptosis of VSMC	Atherosclerosis	(35)
	Hypertrophy of cardiomyocyte	Cardiac hypertrophy	(137)
	Proliferation and differentiation of PASMC	PAH	(169, 170)
NLRP3 inflammasome	Inflammation and necroptosis of cardiomycyte	Myocardial I/R injury	(26)
	Inflammation of dendritic cell	Autoimmune myocarditis	(178)
HIF-1α	Hypertrophy of cardiomyocyte	Cardiac hypertrophy	(137)
	Proliferation and migration of VEC	Cardiac angiogenesis	(37)
GF	Proliferation and migration of VEC	Cardiac angiogenesis	(37, 81)
BCL2 family-mediated apoptosis	Hypoxia-induced apoptosis of cardiomyocyte	Myocardial hypoxia	(82)
IL-6/STAT3	Inflammation of myocardium	Septic cardiomyopathy	(27)
RAS	Proliferation, migration, and differentiation of cardiac fibroblast	Myocardial fibrosis following myocardial infarction	(85)

inflammasome and its downstream signaling molecules such as caspase-1 and IL-1β (178).

In addition to myocarditis, miR-223-3p could also alleviate the myocardial depression in polymicrobial sepsis cooperated with miR-223-5p (27). Myocardial depression induced by sepsis is a major cause of cardiac dysfunction and septic cardiomyopathy, as well as increases the mortality in sepsis (186, 187). Both miR-223-3p and miR-223-5p were found downregulated in the polymicrobial sepsis model, and deficiency of miR-223(-3p/5p) weakened cardiac systolic function and reduced survival rate of animals in sepsis model. MiR-223(-3p/5p) deficiency also aggravated the inflammation induced by severe sepsis in myocardium, peritoneal fluid, and blood, with elevation of pro-inflammatory factors including TNF-α, IL-6, and IL-1β, increased bacterial load in body fluids, and neutrophil infiltration in hearts (27). The sepsis-induced myocardial depression can be inhibited via different pathways by miR-223-3p and miR-223-5p. MiR-223-3p targeted both signal transducer and activator of transcription 3 (STAT3) and IL-6 to inhibit the pro-inflammatory signaling pathway while miR-223-5p targeted semaphorin 3A to improve the autonomic control of cardiac function (27, 188). These effects of miR-223(-3p/5p) reduced the inflammation of heart and alleviated cardiac dysfunction, resulting in amelioration of myocardial depression and reduction of sudden death in severe sepsis (27, 189–191).

MiR-223-3p in Hypertension

Hypertension is one of the most common diseases and has become a major risk factor for many other diseases, such as myocardial infarction, stroke, and chronic renal failure (192–195). To overcome the clinical challenges of adverse effects of drugs and failure to achieve the optimum blood pressure control in hypertension, it requires earlier detection and accurate therapy to manage blood pressure and reduce its complications (196, 197). MiRNAs have been considered as useful biomarkers or indicators in many diseases depending on their properties such as high stability, easy detection, and low cost, to predict and evaluate the progression or risk of diseases as above-mentioned. Studies have illuminated the role of miRNAs in diagnosis and treatment of hypertension (198–200). A few researches have indicated that miR-223-3p might also be a promising biomarker for the diagnosis of hypertension and prediction of CVDs risk in hypertensive patients (201, 202).

Circulating miR-223-3p levels were downregulated in hypertensive patients, and the reduced serum miR-223-3p along with miR-199a-3p, miR-208a-3p, and miR-122-5p exhibited better diagnostic effects on hypertension than other miRNAs, with the highest sensitivity (202). Another research attempt to uncover the role of platelet miR-223-3p in hypertension and its related risk of CVDs. Platelets, which are abundant with miRNAs, are involved in the progression of hypertension-related pro-thrombotic status and blood pressure elevation during thrombogenesis (201, 203, 204). To explore the miRNAs in platelets could be helpful to screen biomarkers for hypertension. Platelet miR-223-3p levels decreased in hypertensive patients and the levels were negatively correlated with the systolic blood pressure of patients. Besides, the platelet levels of miR-223-3p in hypertensive patients were lower in patients with other CVDs, so platelet miR-223-3p could be a prognostic biomarker for hypertension (201). Therefore, both the circulating and platelet miR-223-3p might be developed into biomarkers for diagnosis and prognosis estimation of hypertension.

MiR-223-3p in Arrhythmia

Arrhythmia is an important category of CVDs and may occur alone or with other diseases. Severe or frequent arrhythmia attack could lead to hemodynamic disorder, heart failure, and sudden death. MiR-223-3p expression was increased in atrial tissues of atrial fibrillation (AF) patients with rheumatic heart disease, as well as in animal models of AF, suggesting the possible role of miR-223-3p involved in pathogenesis of AF (205). As we mentioned in previous parts, miR-223-3p induced arrhythmia following myocardial infarction through decreasing KCND2 and I_{to}, indicating the potential of miR-223-3p to regulate electrophysiological functions of myocardium (94). More effects of miR-223-3p in arrhythmia are worth investigating.

CONCLUSION

CVDs remain a major public health problem and result in heavy burden for human society. We have summarized the role of miR-223-3p in CVDs and recent developments in its potential as biomarker and therapeutic target for CVDs. MiR-223-3p is widely expressed in varieties of cell types that link to CVDs including monocytes, macrophages, platelets, hepatocytes, endothelial cells (resting state), cardiomyocytes, and cardiac fibroblasts to influence their cellular activities. These regulatory effects primarily depend on suppressing the mRNAs of target genes involved in lipid metabolism, inflammation, cell proliferation or apoptosis, electrophysiology, cell hypertrophy, and cell polarization (**Table 1**). Besides, MiR-223-3p participates in regulatory networks of multiple signaling pathways such as NFκB, MAPK, PI3K/AKT, RPS6KB1/HIF-1α, and NLRP3 inflammasome pathways to play diverse roles in CVDs (**Table 2**). Nevertheless, there still exist controversies about the effects of miR-223-3p in some CVDs. Studies to determine the specific role of circulating miR-223-3p for diagnosis and prediction of various CVDs are further needed. Future works to modulate the local level of miR-223-3p may lead to more effective treatment of CVDs.

AUTHOR CONTRIBUTIONS

M-WZ: conceptualization and writing—original draft. Y-JS: literature collection. JS: visualization. J-GY: conceptualization and writing—review and editing. All authors contributed to the article and approved the submitted version.

FUNDING

This work was supported by grants from the Nurture projects for basic research of Shanghai Chest Hospital (2020YNJCM08 and 2020YNJCQ01).

REFERENCES

1. *World Health Statistics 2020: Monitoring Health for the SDGs, Sustainable Development Goals*. Geneva: World Health Organization (2020).
2. Thomas H, Diamond J, Vieco A, Chaudhuri S, Shinnar E, Cromer S, et al. Global atlas of cardiovascular disease 2000-2016: the path to prevention and control. *Glob Heart*. (2018) 13:143–63. doi: 10.1016/j.gheart.2018.09.511
3. Roth GA, Johnson C, Abajobir A, Abd-Allah F, Abera SF, Abyu G, et al. Global, regional, and national burden of cardiovascular diseases for 10 causes, 1990 to 2015. *J Am Coll Cardiol*. (2017) 70:1–25. doi: 10.1016/j.jacc.2017.04.052
4. Lozano R, Naghavi M, Foreman K, Lim S, Shibuya K, Aboyans V, et al. Global and regional mortality from 235 causes of death for 20 age groups in 1990 and 2010: a systematic analysis for the Global Burden of Disease Study 2010. *Lancet*. (2012) 380:2095–128. doi: 10.1016/S0140-6736(12)61728-0
5. Roth GA, Forouzanfar MH, Moran AE, Barber R, Nguyen G, Feigin VL, et al. Demographic and epidemiologic drivers of global cardiovascular mortality. *N Engl J Med*. (2015) 372:1333–41. doi: 10.1056/NEJMoa1406656
6. Clark H. NCDs: a challenge to sustainable human development. *Lancet*. (2013) 381:510–1. doi: 10.1016/S0140-6736(13)60058-6
7. Mirzadeh Azad F, Arabian M, Maleki M, Malakootian M. Small molecules with big impacts on cardiovascular diseases. *Biochem Genet*. (2020) 58:359–83. doi: 10.1007/s10528-020-09948-z
8. Solly EL, Dimasi CG, Bursill CA, Psaltis PJ, Tan JTM. MicroRNAs as therapeutic targets and clinical biomarkers in atherosclerosis. *J Clin Med*. (2019) 8:2199. doi: 10.3390/jcm8122199
9. Barraclough JY, Joan M, Joglekar MV, Hardikar AA, Patel S. MicroRNAs as prognostic markers in acute coronary syndrome patients-a systematic review. *Cells*. (2019) 8.:1572. doi: 10.3390/cells8121572
10. Barwari T, Joshi A, Mayr M. MicroRNAs in cardiovascular disease. *J Am Coll Cardiol*. (2016) 68:2577–84. doi: 10.1016/j.jacc.2016.09.945
11. Mellis D, Caporali A. MicroRNA-based therapeutics in cardiovascular disease: screening and delivery to the target. *Biochem Soc Trans*. (2018) 46:11–21. doi: 10.1042/BST20170037
12. Lee Y, Kim M, Han J, Yeom KH, Lee S, Baek SH, et al. MicroRNA genes are transcribed by RNA polymerase II. *EMBO J*. (2004) 23:4051–60. doi: 10.1038/sj.emboj.7600385
13. Lee Y, Ahn C, Han J, Choi H, Kim J, Yim J, et al. The nuclear RNase III Drosha initiates microRNA processing. *Nature*. (2003) 425:415–9. doi: 10.1038/nature01957
14. Gregory RI, Yan KP, Amuthan G, Chendrimada T, Doratotaj B, Cooch N, et al. The Microprocessor complex mediates the genesis of microRNAs. *Nature*. (2004) 432:235–40. doi: 10.1038/nature03120
15. Lee Y, Jeon K, Lee JT, Kim S, Kim VN. MicroRNA maturation: stepwise processing and subcellular localization. *EMBO J*. (2002) 21:4663–70. doi: 10.1093/emboj/cdf476
16. Yi R, Qin Y, Macara IG, Cullen BR. Exportin-5 mediates the nuclear export of pre-microRNAs and short hairpin RNAs. *Genes Dev*. (2003) 17:3011–6. doi: 10.1101/gad.1158803
17. Noland CL, Doudna JA. Multiple sensors ensure guide strand selection in human RNAi pathways. *RNA*. (2013) 19:639–48. doi: 10.1261/rna.037424.112
18. Khvorova A, Reynolds A, Jayasena SD. Functional siRNAs and miRNAs exhibit strand bias. *Cell*. (2003) 115:209–16. doi: 10.1016/S0092-8674(03)00801-8
19. Meijer HA, Smith EM, Bushell M. Regulation of miRNA strand selection: follow the leader? *Biochem Soc Trans*. (2014) 42:1135–40. doi: 10.1042/BST20140142
20. Condrat CE, Thompson DC, Barbu MG, Bugnar OL, Boboc A, Cretoiu D, et al. miRNAs as biomarkers in disease: latest findings regarding their role in diagnosis and prognosis. *Cells*. (2020) 9:276. doi: 10.3390/cells9020276
21. O'Brien J, Hayder H, Zayed Y, Peng C. Overview of MicroRNA biogenesis, mechanisms of actions, and circulation. *Front Endocrinol*. (2018) 9:402. doi: 10.3389/fendo.2018.00402
22. Weber JA, Baxter DH, Zhang S, Huang DY, Huang KH, Lee MJ, et al. The microRNA spectrum in 12 body fluids. *Clin Chem*. (2010) 56:1733–41. doi: 10.1373/clinchem.2010.147405
23. Raposo G, Stoorvogel W. Extracellular vesicles: exosomes, microvesicles, and friends. *J Cell Biol*. (2013) 200:373–83. doi: 10.1083/jcb.201211138
24. Vickers KC, Palmisano BT, Shoucri BM, Shamburek RD, Remaley AT. MicroRNAs are transported in plasma and delivered to recipient cells by high-density lipoproteins. *Nat Cell Biol*. (2011) 13:423–33. doi: 10.1038/ncb2210
25. Essandoh K, Li Y, Huo J, Fan GC. MiRNA-mediated macrophage polarization and its potential role in the regulation of inflammatory response. *Shock*. (2016) 46:122–31. doi: 10.1097/SHK.0000000000000604
26. Qin D, Wang X, Li Y, Yang L, Wang R, Peng J, et al. MicroRNA-223-5p and−3p cooperatively suppress necroptosis in ischemic/reperfused hearts. *J Biol Chem*. (2016) 291:20247–59. doi: 10.1074/jbc.M116.732735
27. Wang X, Huang W, Yang Y, Wang Y, Peng T, Chang J, et al. Loss of duplexmiR-223 (5p and 3p) aggravates myocardial depression and mortality in polymicrobial sepsis. *Biochim Biophys Acta*. (2014) 1842:701–11. doi: 10.1016/j.bbadis.2014.01.012
28. Chen CZ, Li L, Lodish HF, Bartel DP. MicroRNAs modulate hematopoietic lineage differentiation. *Science*. (2004) 303:83–6. doi: 10.1126/science.1091903
29. Johnnidis JB, Harris MH, Wheeler RT, Stehling-Sun S, Lam MH, Kirak O, et al. Regulation of progenitor cell proliferation and granulocyte function by microRNA-223. *Nature*. (2008) 451:1125–9. doi: 10.1038/nature06607
30. Aziz F. The emerging role of miR-223 as novel potential diagnostic and therapeutic target for inflammatory disorders. *Cell Immunol*. (2016) 303:1–6. doi: 10.1016/j.cellimm.2016.04.003
31. Haneklaus M, Gerlic M, O'Neill LA, Masters SL. miR-223: infection, inflammation and cancer. *J Intern Med*. (2013) 274:215–26. doi: 10.1111/joim.12099
32. Vickers KC, Landstreet SR, Levin MG, Shoucri BM, Toth CL, Taylor RC, et al. MicroRNA-223 coordinates cholesterol homeostasis. *Proc Natl Acad Sci USA*. (2014) 111:14518–23. doi: 10.1073/pnas.1215767111
33. Wang K, Long B, Liu F, Wang JX, Liu CY, Zhao B, et al. A circular RNA protects the heart from pathological hypertrophy and heart failure by targeting miR-223. *Eur Heart J*. (2016) 37:2602–11. doi: 10.1093/eurheartj/ehv713
34. Taibi F, Metzinger-Le Meuth V, Massy ZA, Metzinger L. miR-223: an inflammatory oncomiR enters the cardiovascular field. *Biochim Biophys Acta*. (2014) 1842:1001–9. doi: 10.1016/j.bbadis.2014.03.005
35. Shan Z, Qin S, Li W, Wu W, Yang J, Chu M, et al. An Endocrine genetic signal between blood cells and vascular smooth muscle cells: role of MicroRNA-223 in smooth muscle function and atherogenesis. *J Am Coll Cardiol*. (2015) 65:2526–37. doi: 10.1016/j.jacc.2015.03.570
36. Shi R, Zhou X, Ji WJ, Zhang YY, Ma YQ, Zhang JQ, et al. The emerging role of miR-223 in platelet reactivity: implications in antiplatelet therapy. *Biomed Res Int*. (2015) 2015:981841. doi: 10.1155/2015/981841
37. Dai GH, Ma PZ, Song XB, Liu N, Zhang T, Wu B. MicroRNA-223-3p inhibits the angiogenesis of ischemic cardiac microvascular endothelial cells via affecting RPS6KB1/hif-1a signal pathway. *PLoS ONE*. (2014) 9:e108468. doi: 10.1371/journal.pone.0108468
38. Glass CK, Witztum JL. Atherosclerosis. the road ahead. *Cell*. (2001) 104:503–16. doi: 10.1016/S0092-8674(01)00238-0
39. Rosenson RS, Brewer HB Jr, Davidson WS, Fayad ZA, Fuster V, Goldstein J, et al. Cholesterol efflux and atheroprotection: advancing the concept of reverse cholesterol transport. *Circulation*. (2012) 125:1905–19. doi: 10.1161/CIRCULATIONAHA.111.066589
40. Pentikainen MO, Oorni K, Ala-Korpela M, Kovanen PT. Modified LDL - trigger of atherosclerosis and inflammation in the arterial intima. *J Intern Med*. (2000) 247:359–70. doi: 10.1046/j.1365-2796.2000.00655.x
41. Janas T, Janas T, Yarus M. Specific RNA binding to ordered phospholipid bilayers. *Nucleic Acids Res*. (2006) 34:2128–36. doi: 10.1093/nar/gkl220
42. Manavbasi Y, Suleymanoglu E. Nucleic acid-phospholipid recognition: fourier transform infrared spectrometric characterization of ternary phospholipid-inorganic cation-DNA complex and its relevance to chemicopharmaceutical design of nanometric liposome based gene delivery formulations. *Arch Pharm Res*. (2007) 30:1027–40. doi: 10.1007/BF02993973
43. Kim SI, Shin D, Choi TH, Lee JC, Cheon GJ, Kim KY, et al. Systemic and specific delivery of small interfering RNAs to the liver mediated by apolipoprotein A-I. *Mol Ther*. (2007) 15:1145–52. doi: 10.1038/sj.mt.6300168

44. Desgagne V, Guay SP, Guerin R, Corbin F, Couture P, Lamarche B, et al. Variations in HDL-carried miR-223 and miR-135a concentrations after consumption of dietary trans fat are associated with changes in blood lipid and inflammatory markers in healthy men - an exploratory study. *Epigenetics*. (2016) 11:438–48. doi: 10.1080/15592294.2016.1176816
45. Cuesta Torres LF, Zhu W, Ohrling G, Larsson R, Patel M, Wiese CB, et al. High-density lipoproteins induce miR-223-3p biogenesis and export from myeloid cells: role of scavenger receptor BI-mediated lipid transfer. *Atherosclerosis*. (2019) 286:20–9. doi: 10.1016/j.atherosclerosis.2019.04.227
46. Tabet F, Vickers KC, Cuesta Torres LF, Wiese CB, Shoucri BM, Lambert G, et al. HDL-transferred microRNA-223 regulates ICAM-1 expression in endothelial cells. *Nat Commun*. (2014) 5:3292. doi: 10.1038/ncomms4292
47. Acton S, Rigotti A, Landschulz KT, Xu S, Hobbs HH, Krieger M. Identification of scavenger receptor SR-BI as a high density lipoprotein receptor. *Science*. (1996) 271:518–20. doi: 10.1126/science.271.5248.518
48. Krieger M. Charting the fate of the "good cholesterol": identification and characterization of the high-density lipoprotein receptor SR-BI. *Annu Rev Biochem*. (1999) 68:523–58. doi: 10.1146/annurev.biochem.68.1.523
49. Wang L, Jia XJ, Jiang HJ, Du Y, Yang F, Si SY, et al. MicroRNAs 185, 96, and 223 repress selective high-density lipoprotein cholesterol uptake through posttranscriptional inhibition. *Mol Cell Biol*. (2013) 33:1956–64. doi: 10.1128/MCB.01580-12
50. Hou J, Lin L, Zhou W, Wang Z, Ding G, Dong Q, et al. Identification of miRNomes in human liver and hepatocellular carcinoma reveals miR-199a/b-3p as therapeutic target for hepatocellular carcinoma. *Cancer Cell*. (2011) 19:232–43. doi: 10.1016/j.ccr.2011.01.001
51. Sun X, Belkin N, Feinberg MW. Endothelial microRNAs and atherosclerosis. *Curr Atheroscler Rep*. (2013) 15:372. doi: 10.1007/s11883-013-0372-2
52. Libby P. Inflammation in atherosclerosis. *Arterioscler Thromb Vasc Biol*. (2012) 32:2045–51. doi: 10.1161/ATVBAHA.108.179705
53. Schachter M. Vascular smooth muscle cell migration, atherosclerosis, and calcium channel blockers. *Int J Cardiol*. (1997) 62(Suppl. 2):S85–90. doi: 10.1016/S0167-5273(97)00245-3
54. Li J, Tan M, Xiang Q, Zhou Z, Yan H. Thrombin-activated platelet-derived exosomes regulate endothelial cell expression of ICAM-1 via microRNA-223 during the thrombosis-inflammation response. *Thromb Res*. (2017) 154:96–105. doi: 10.1016/j.thromres.2017.04.016
55. Leierseder S, Petzold T, Zhang L, Loyer X, Massberg S, Engelhardt S. MiR-223 is dispensable for platelet production and function in mice. *Thromb Haemost*. (2013) 110:1207–14. doi: 10.1160/TH13-07-0623
56. Ismail N, Wang Y, Dakhlallah D, Moldovan L, Agarwal K, Batte K, et al. Macrophage microvesicles induce macrophage differentiation and miR-223 transfer. *Blood*. (2013) 121:984–95. doi: 10.1182/blood-2011-08-374793
57. Wang J, Bai X, Song Q, Fan F, Hu Z, Cheng G, et al. miR-223 inhibits lipid deposition and inflammation by suppressing toll-like receptor 4 signaling in macrophages. *Int J Mol Sci*. (2015) 16:24965–82. doi: 10.3390/ijms161024965
58. Wolfs IM, Donners MM, de Winther MP. Differentiation factors and cytokines in the atherosclerotic plaque micro-environment as a trigger for macrophage polarisation. *Thromb Haemost*. (2011) 106:763–71. doi: 10.1160/TH11-05-0320
59. Rangrez AY, M'Baya-Moutoula E, Metzinger-Le Meuth V, Henaut L, Djelouat MS, Benchitrit J, et al. Inorganic phosphate accelerates the migration of vascular smooth muscle cells: evidence for the involvement of miR-223. *PLoS ONE*. (2012) 7:e47807. doi: 10.1371/journal.pone.0047807
60. M'Baya-Moutoula E, Marchand A, Six I, Bahrar N, Celic T, Mougenot N, et al. Inhibition of miR-223 expression using a sponge strategy decreases restenosis in rat injured carotids. *Curr Vasc Pharmacol*. (2019) 18:507–16. doi: 10.2174/1570161117666190705141152
61. Nagalla S, Shaw C, Kong X, Kondkar AA, Edelstein LC, Ma L, et al. Platelet microRNA-mRNA coexpression profiles correlate with platelet reactivity. *Blood*. (2011) 117:5189–97. doi: 10.1182/blood-2010-09-299719
62. Willeit P, Zampetaki A, Dudek K, Kaudewitz D, King A, Kirkby NS, et al. Circulating microRNAs as novel biomarkers for platelet activation. *Circ Res*. (2013) 112:595–600. doi: 10.1161/CIRCRESAHA.111.300539
63. Osman A, Falker K. Characterization of human platelet microRNA by quantitative PCR coupled with an annotation network for predicted target genes. *Platelets*. (2011) 22:433–41. doi: 10.3109/09537104.2011.560305
64. Hunter MP, Ismail N, Zhang X, Aguda BD, Lee EJ, Yu L, et al. Detection of microRNA expression in human peripheral blood microvesicles. *PLoS ONE*. (2008) 3:e3694. doi: 10.1371/journal.pone.0003694
65. Chen X, Ba Y, Ma L, Cai X, Yin Y, Wang K, et al. Characterization of microRNAs in serum: a novel class of biomarkers for diagnosis of cancer and other diseases. *Cell Res*. (2008) 18:997–1006. doi: 10.1038/cr.2008.282
66. Kin K, Miyagawa S, Fukushima S, Shirakawa Y, Torikai K, Shimamura K, et al. Tissue- and plasma-specific MicroRNA signatures for atherosclerotic abdominal aortic aneurysm. *J Am Heart Assoc*. (2012) 1:e000745. doi: 10.1161/JAHA.112.000745
67. Vegter EL, Ovchinnikova ES, van Veldhuisen DJ, Jaarsma T, Berezikov E, van der Meer P, et al. Low circulating microRNA levels in heart failure patients are associated with atherosclerotic disease and cardiovascular-related rehospitalizations. *Clin Res Cardiol*. (2017) 106:598–609. doi: 10.1007/s00392-017-1096-z
68. Alexandru N, Constantin A, Nemecz M, Comarita IK, Vilcu A, Procopciuc A, et al. Hypertension associated with hyperlipidemia induced different MicroRNA expression profiles in plasma, platelets, and platelet-derived microvesicles; effects of endothelial progenitor cell therapy. *Front Med*. (2019) 6:280. doi: 10.3389/fmed.2019.00280
69. Wu MY, Li CJ, Hou MF, Chu PY. New insights into the role of inflammation in the pathogenesis of atherosclerosis. *Int J Mol Sci*. (2017) 18:2034. doi: 10.3390/ijms18102034
70. Thomas MR, Lip GY. Novel risk markers and risk assessments for cardiovascular disease. *Circ Res*. (2017) 120:133–49. doi: 10.1161/CIRCRESAHA.116.309955
71. Teringova E, Tousek P. Apoptosis in ischemic heart disease. *J Transl Med*. (2017) 15:87. doi: 10.1186/s12967-017-1191-y
72. Swynghedauw B. Molecular mechanisms of myocardial remodeling. *Physiol Rev*. (1999) 79:215–62. doi: 10.1152/physrev.1999.79.1.215
73. Bouzeghrane F, Reinhardt DP, Reudelhuber TL, Thibault G. Enhanced expression of fibrillin-1, a constituent of the myocardial extracellular matrix in fibrosis. *Am J Physiol Heart Circ Physiol*. (2005) 289:H982–91. doi: 10.1152/ajpheart.00151.2005
74. Powell DW, Mifflin RC, Valentich JD, Crowe SE, Saada JI, West AB. Myofibroblasts. I. Paracrine cells important in health and disease. *Am J Physiol*. (1999) 277:C1–9. doi: 10.1152/ajpcell.1999.277.1.C1
75. Gershlick AH, Banning AP, Myat A, Verheugt FW, Gersh BJ. Reperfusion therapy for STEMI: is there still a role for thrombolysis in the era of primary percutaneous coronary intervention? *Lancet*. (2013) 382:624–32. doi: 10.1016/S0140-6736(13)61454-3
76. Frohlich GM, Meier P, White SK, Yellon DM, Hausenloy DJ. Myocardial reperfusion injury: looking beyond primary PCI. *Eur Heart J*. (2013) 34:1714–22. doi: 10.1093/eurheartj/eht090
77. Zhu H, Fan GC. Role of microRNAs in the reperfused myocardium towards post-infarct remodelling. *Cardiovasc Res*. (2012) 94:284–92. doi: 10.1093/cvr/cvr291
78. Kang TB, Yang SH, Toth B, Kovalenko A, Wallach D. Activation of the NLRP3 inflammasome by proteins that signal for necroptosis. *Methods Enzymol*. (2014) 545:67–81. doi: 10.1016/B978-0-12-801430-1.00003-2
79. Cullen SP, Kearney CJ, Clancy DM, Martin SJ. Diverse activators of the NLRP3 inflammasome promote IL-1beta secretion by triggering necrosis. *Cell Rep*. (2015) 11:1535–48. doi: 10.1016/j.celrep.2015.05.003
80. Silke J, Rickard JA, Gerlic M. The diverse role of RIP kinases in necroptosis and inflammation. *Nat Immunol*. (2015) 16:689–97. doi: 10.1038/ni.3206
81. Shi L, Fisslthaler B, Zippel N, Fromel T, Hu J, Elgheznawy A, et al. MicroRNA-223 antagonizes angiogenesis by targeting beta1 integrin and preventing growth factor signaling in endothelial cells. *Circ Res*. (2013) 113:1320–30. doi: 10.1161/CIRCRESAHA.113.301824
82. Tang Q, Li MY, Su YF, Fu J, Zou ZY, Wang Y, et al. Absence of miR-223-3p ameliorates hypoxia-induced injury through repressing cardiomyocyte apoptosis and oxidative stress by targeting KLF15. *Eur J Pharmacol*. (2018) 841:67–74. doi: 10.1016/j.ejphar.2018.10.014
83. Zhang J, He Z, Xiao W, Na Q, Wu T, Su K, et al. Overexpression of BAG3 attenuates hypoxia-induced cardiomyocyte apoptosis by inducing autophagy. *Cell Physiol Biochem*. (2016) 39:491–500. doi: 10.1159/000445641

84. Chouvarine P, Legchenko E, Geldner J, Riehle C, Hansmann G. Hypoxia drives cardiac miRNAs and inflammation in the right and left ventricle. *J Mol Med*. (2019) 97:1427–38. doi: 10.1007/s00109-019-01817-6
85. Liu X, Xu Y, Deng Y, Li H. MicroRNA-223 regulates cardiac fibrosis after myocardial infarction by targeting RASA1. *Cell Physiol Biochem*. (2018) 46:1439–54. doi: 10.1159/000489185
86. Zamilpa R, Lindsey ML. Extracellular matrix turnover and signaling during cardiac remodeling following MI: causes and consequences. *J Mol Cell Cardiol*. (2010) 48:558–63. doi: 10.1016/j.yjmcc.2009.06.012
87. Tomasek JJ, Gabbiani G, Hinz B, Chaponnier C, Brown RA. Myofibroblasts and mechano-regulation of connective tissue remodelling. *Nat Rev Mol Cell Biol*. (2002) 3:349–63. doi: 10.1038/nrm809
88. van den Borne SW, Diez J, Blankesteijn WM, Verjans J, Hofstra L, Narula J. Myocardial remodeling after infarction: the role of myofibroblasts. *Nat Rev Cardiol*. (2010) 7:30–7. doi: 10.1038/nrcardio.2009.199
89. Morishita Y, Yoshizawa H, Watanabe M, Imai R, Imai T, Hirahara I, et al. MicroRNA expression profiling in peritoneal fibrosis. *Transl Res*. (2016) 169:47–66. doi: 10.1016/j.trsl.2015.10.009
90. Kaprielian R, Wickenden AD, Kassiri Z, Parker TG, Liu PP, Backx PH. Relationship between K+ channel down-regulation and [Ca2+]i in rat ventricular myocytes following myocardial infarction. *J Physiol*. (1999) 517 (Pt 1):229–45. doi: 10.1111/j.1469-7793.1999.0229z.x
91. Kaprielian R, Sah R, Nguyen T, Wickenden AD, Backx PH. Myocardial infarction in rat eliminates regional heterogeneity of AP profiles, I(to) K(+) currents, and [Ca(2+)](i) transients. *Am J Physiol Heart Circ Physiol*. (2002) 283:H1157–68. doi: 10.1152/ajpheart.00518.2001
92. Volk T, Nguyen TH, Schultz JH, Faulhaber J, Ehmke H. Regional alterations of repolarizing K+ currents among the left ventricular free wall of rats with ascending aortic stenosis. *J Physiol*. (2001) 530(Pt 3):443–55. doi: 10.1111/j.1469-7793.2001.0443k.x
93. Wang Z, Feng J, Shi H, Pond A, Nerbonne JM, Nattel S. Potential molecular basis of different physiological properties of the transient outward K+ current in rabbit and human atrial myocytes. *Circ Res*. (1999) 84:551–61. doi: 10.1161/01.RES.84.5.551
94. Liu X, Zhang Y, Du W, Liang H, He H, Zhang L, et al. MiR-223-3p as a novel MicroRNA regulator of expression of voltage-gated K+ channel Kv4.2 in acute myocardial infarction. *Cell Physiol Biochem*. (2016) 39:102–14. doi: 10.1159/000445609
95. van Rooij E, Sutherland LB, Thatcher JE, DiMaio JM, Naseem RH, Marshall WS, et al. Dysregulation of microRNAs after myocardial infarction reveals a role of miR-29 in cardiac fibrosis. *Proc Natl Acad Sci USA*. (2008) 105:13027–32. doi: 10.1073/pnas.0805038105
96. Carino A, De Rosa S, Sorrentino S, Polimeni A, Sabatino J, Caiazzo G, et al. Modulation of circulating MicroRNAs levels during the switch from clopidogrel to ticagrelor. *Biomed Res Int*. (2016) 2016:3968206. doi: 10.1155/2016/3968206
97. Jneid H, Anderson JL, Wright RS, Adams CD, Bridges CR, Casey DE Jr, et al. 2012 ACCF/AHA focused update of the guideline for the management of patients with unstable angina/non-ST-elevation myocardial infarction (updating the 2007 guideline and replacing the 2011 focused update): a report of the American College of Cardiology Foundation/American Heart Association Task Force on Practice Guidelines. *J Am Coll Cardiol*. (2012) 60:645–81. doi: 10.1161/CIR.0b013e318256f1e0
98. Aradi D, Komocsi A, Vorobcsuk A, Rideg O, Tokes-Fuzesi M, Magyarlaki T, et al. Prognostic significance of high on-clopidogrel platelet reactivity after percutaneous coronary intervention: systematic review and meta-analysis. *Am Heart J*. (2010) 160:543–51. doi: 10.1016/j.ahj.2010.06.004
99. Breet NJ, van Werkum JW, Bouman HJ, Kelder JC, Harmsze AM, Hackeng CM, et al. High on-treatment platelet reactivity to both aspirin and clopidogrel is associated with the highest risk of adverse events following percutaneous coronary intervention. *Heart*. (2011) 97:983–90. doi: 10.1136/hrt.2010.220491
100. Holmes DR Jr, Dehmer GJ, Kaul S, Leifer D, O'Gara PT, Stein CM. ACCF/AHA clopidogrel clinical alert: approaches to the FDA "boxed warning": a report of the American College of Cardiology Foundation Task Force on clinical expert consensus documents and the American Heart Association endorsed by the Society for Cardiovascular Angiography and Interventions and the Society of Thoracic Surgeons. *J Am Coll Cardiol*. (2010) 56:321–41. doi: 10.1016/j.jacc.2010.05.013
101. Matetzky S, Shenkman B, Guetta V, Shechter M, Beinart R, Goldenberg I, et al. Clopidogrel resistance is associated with increased risk of recurrent atherothrombotic events in patients with acute myocardial infarction. *Circulation*. (2004) 109:3171–5. doi: 10.1161/01.CIR.0000130846.46168.03
102. Zampetaki A, Willeit P, Tilling L, Drozdov I, Prokopi M, Renard JM, et al. Prospective study on circulating MicroRNAs and risk of myocardial infarction. *J Am Coll Cardiol*. (2012) 60:290–9. doi: 10.1016/j.jacc.2012.03.056
103. Landry P, Plante I, Ouellet DL, Perron MP, Rousseau G, Provost P. Existence of a microRNA pathway in anucleate platelets. *Nat Struct Mol Biol*. (2009) 16:961–6. doi: 10.1038/nsmb.1651
104. Zhang YY, Zhou X, Ji WJ, Shi R, Lu RY, Li JL, et al. Decreased circulating microRNA-223 level predicts high on-treatment platelet reactivity in patients with troponin-negative non-ST elevation acute coronary syndrome. *J Thromb Thrombolysis*. (2014) 38:65–72. doi: 10.1007/s11239-013-1022-9
105. Shi R, Ge L, Zhou X, Ji WJ, Lu RY, Zhang YY, et al. Decreased platelet miR-223 expression is associated with high on-clopidogrel platelet reactivity. *Thromb Res*. (2013) 131:508–13. doi: 10.1016/j.thromres.2013.02.015
106. Aleil B, Ravanat C, Cazenave JP, Rochoux G, Heitz A, Gachet C. Flow cytometric analysis of intraplatelet VASP phosphorylation for the detection of clopidogrel resistance in patients with ischemic cardiovascular diseases. *J Thromb Haemost*. (2005) 3:85–92. doi: 10.1111/j.1538-7836.2004.01063.x
107. Cuisset T, Frere C, Quilici J, Barbou F, Morange PE, Hovasse T, et al. High post-treatment platelet reactivity identified low-responders to dual antiplatelet therapy at increased risk of recurrent cardiovascular events after stenting for acute coronary syndrome. *J Thromb Haemost*. (2006) 4:542–9. doi: 10.1111/j.1538-7836.2005.01751.x
108. Cuisset T, Cayla G, Frere C, Quilici J, Poyet R, Gaborit B, et al. Predictive value of post-treatment platelet reactivity for occurrence of post-discharge bleeding after non-ST elevation acute coronary syndrome. Shifting from antiplatelet resistance to bleeding risk assessment? *EuroIntervention*. (2009) 5:325–9. doi: 10.4244/51
109. Chyrchel B, Toton-Zuranska J, Kruszelnicka O, Chyrchel M, Mielecki W, Kolton-Wroz M, et al. Association of plasma miR-223 and platelet reactivity in patients with coronary artery disease on dual antiplatelet therapy: a preliminary report. *Platelets*. (2015) 26:593–7. doi: 10.3109/09537104.2014.974527
110. Chen YC, Lin FY, Lin YW, Cheng SM, Chang CC, Lin RH, et al. Platelet MicroRNA 365-3p expression correlates with high on-treatment platelet reactivity in coronary artery disease patients. *Cardiovasc Drugs Ther*. (2019) 33:129–37. doi: 10.1007/s10557-019-06855-3
111. Guo JF, Zhang Y, Zheng QX, Zhang Y, Zhou HH, Cui LM. Association between elevated plasma microRNA-223 content and severity of coronary heart disease. *Scand J Clin Lab Invest*. (2018) 78:373–8. doi: 10.1080/00365513.2018.1480059
112. Schulte C, Molz S, Appelbaum S, Karakas M, Ojeda F, Lau DM, et al. miRNA-197 and miRNA-223 predict cardiovascular death in a cohort of patients with symptomatic coronary artery disease. *PLoS ONE*. (2015) 10:e0145930. doi: 10.1371/journal.pone.0145930
113. Choteau SA, Cuesta Torres LF, Barraclough JY, Elder AMM, Martinez GJ, Chen Fan WY, et al. Transcoronary gradients of HDL-associated MicroRNAs in unstable coronary artery disease. *Int J Cardiol*. (2018) 253:138–44. doi: 10.1016/j.ijcard.2017.09.190
114. Li C, Fang Z, Jiang T, Zhang Q, Liu C, Zhang C, et al. Serum microRNAs profile from genome-wide serves as a fingerprint for diagnosis of acute myocardial infarction and angina pectoris. *BMC Med Genomics*. (2013) 6:16. doi: 10.1186/1755-8794-6-16
115. Saadatian Z, Nariman-Saleh-Fam Z, Bastami M, Mansoori Y, Khaheshi I, Parsa SA, et al. Dysregulated expression of STAT1, miR-150, and miR-223 in peripheral blood mononuclear cells of coronary artery disease patients with significant or insignificant stenosis. *J Cell Biochem*. (2019) 120:19810–24. doi: 10.1002/jcb.29286
116. Burchfield JS, Xie M, Hill JA. Pathological ventricular remodeling: mechanisms: part 1 of 2. *Circulation*. (2013) 128:388–400. doi: 10.1161/CIRCULATIONAHA.113.001878

117. Lloyd-Jones D, Adams RJ, Brown TM, Carnethon M, Dai S, De Simone G, et al. Executive summary: heart disease and stroke statistics—2010 update: a report from the American Heart Association. *Circulation*. (2010) 121:948–54. doi: 10.1161/CIRCULATIONAHA.109.192666
118. Samak M, Fatullayev J, Sabashnikov A, Zeriouh M, Schmack B, Farag M, et al. Cardiac hypertrophy: an introduction to molecular and cellular basis. *Med Sci Monit Basic Res*. (2016) 22:75–9. doi: 10.12659/MSMBR.900437
119. Assomull RG, Prasad SK, Lyne J, Smith G, Burman ED, Khan M, et al. Cardiovascular magnetic resonance, fibrosis, and prognosis in dilated cardiomyopathy. *J Am Coll Cardiol*. (2006) 48:1977–85. doi: 10.1016/j.jacc.2006.07.049
120. Bisping E, Wakula P, Poteser M, Heinzel FR. Targeting cardiac hypertrophy: toward a causal heart failure therapy. *J Cardiovasc Pharmacol*. (2014) 64:293–305. doi: 10.1097/FJC.0000000000000126
121. Orenes-Pinero E, Montoro-Garcia S, Patel JV, Valdes M, Marin F, Lip GY. Role of microRNAs in cardiac remodelling: new insights and future perspectives. *Int J Cardiol*. (2013) 167:1651–9. doi: 10.1016/j.ijcard.2012.09.120
122. Frieler RA, Mortensen RM. Immune cell and other noncardiomyocyte regulation of cardiac hypertrophy and remodeling. *Circulation*. (2015) 131:1019–30. doi: 10.1161/CIRCULATIONAHA.114.008788
123. Heymans S, Hirsch E, Anker SD, Aukrust P, Balligand JL, Cohen-Tervaert JW, et al. Inflammation as a therapeutic target in heart failure? A scientific statement from the Translational Research Committee of the Heart Failure Association of the European Society of Cardiology. *Eur J Heart Fail*. (2009) 11:119–29. doi: 10.1093/eurjhf/hfn043
124. Wang YS, Zhou J, Hong K, Cheng XS, Li YG. MicroRNA-223 displays a protective role against cardiomyocyte hypertrophy by targeting cardiac troponin I-interacting kinase. *Cell Physiol Biochem*. (2015) 35:1546–56. doi: 10.1159/000373970
125. Zhao ZH, Luo J, Li HX, Wang SH, Li XM. SOX2-mediated inhibition of miR-223 contributes to STIM1 activation in phenylephrine-induced hypertrophic cardiomyocytes. *Mol Cell Biochem*. (2018) 443:47–56. doi: 10.1007/s11010-017-3209-4
126. Heallen T, Zhang M, Wang J, Bonilla-Claudio M, Klysik E, Johnson RL, et al. Hippo pathway inhibits Wnt signaling to restrain cardiomyocyte proliferation and heart size. *Science*. (2011) 332:458–61. doi: 10.1126/science.1199010
127. Pan Z, Brotto M, Ma J. Store-operated Ca2+ entry in muscle physiology and diseases. *BMB Rep*. (2014) 47:69–79. doi: 10.5483/BMBRep.2014.47.2.015
128. Luo X, Hojayev B, Jiang N, Wang ZV, Tandan S, Rakalin A, et al. STIM1-dependent store-operated Ca(2)(+) entry is required for pathological cardiac hypertrophy. *J Mol Cell Cardiol*. (2012) 52:136–47. doi: 10.1016/j.yjmcc.2011.11.003
129. Ohba T, Watanabe H, Murakami M, Sato T, Ono K, Ito H. Essential role of STIM1 in the development of cardiomyocyte hypertrophy. *Biochem Biophys Res Commun*. (2009) 389:172–6. doi: 10.1016/j.bbrc.2009.08.117
130. Tang H, Xiao K, Mao L, Rockman HA, Marchuk DA. Overexpression of TNNI3K, a cardiac-specific MAPKKK, promotes cardiac dysfunction. *J Mol Cell Cardiol*. (2013) 54:101–11. doi: 10.1016/j.yjmcc.2012.10.004
131. Wang L, Wang H, Ye J, Xu RX, Song L, Shi N, et al. Adenovirus-mediated overexpression of cardiac troponin I-interacting kinase promotes cardiomyocyte hypertrophy. *Clin Exp Pharmacol Physiol*. (2011) 38:278–84. doi: 10.1111/j.1440-1681.2011.05499.x
132. Wang X, Wang J, Su M, Wang C, Chen J, Wang H, et al. TNNI3K, a cardiac-specific kinase, promotes physiological cardiac hypertrophy in transgenic mice. *PLoS ONE*. (2013) 8:e58570. doi: 10.1371/journal.pone.0058570
133. Greco S, Fasanaro P, Castelvecchio S, D'Alessandra Y, Arcelli D, Di Donato M, et al. MicroRNA dysregulation in diabetic ischemic heart failure patients. *Diabetes*. (2012) 61:1633–41. doi: 10.2337/db11-0952
134. Barsanti C, Trivella MG, D'Aurizio R, El Baroudi M, Baumgart M, Groth M, et al. Differential regulation of microRNAs in end-stage failing hearts is associated with left ventricular assist device unloading. *Biomed Res Int*. (2015) 2015:592512. doi: 10.1155/2015/592512
135. Verma SK, Krishnamurthy P, Barefield D, Singh N, Gupta R, Lambers E, et al. Interleukin-10 treatment attenuates pressure overload-induced hypertrophic remodeling and improves heart function via signal transducers and activators of transcription 3-dependent inhibition of nuclear factor-kappaB. *Circulation*. (2012) 126:418–29. doi: 10.1161/CIRCULATIONAHA.112.112185
136. Kashihara T, Nakada T, Shimojo H, Horiuchi-Hirose M, Gomi S, Shibazaki T, et al. Chronic receptor-mediated activation of Gi/o proteins alters basal t-tubular and sarcolemmal L-type Ca(2)(+) channel activity through phosphatases in heart failure. *Am J Physiol Heart Circ Physiol*. (2012) 302:H1645–54. doi: 10.1152/ajpheart.00589.2011
137. Yang L, Li Y, Wang X, Mu X, Qin D, Huang W, et al. Overexpression of miR-223 tips the balance of pro- and anti-hypertrophic signaling cascades toward physiologic cardiac hypertrophy. *J Biol Chem*. (2016) 291:15700–13. doi: 10.1074/jbc.M116.715805
138. Donath S, Li P, Willenbockel C, Al-Saadi N, Gross V, Willnow T, et al. Apoptosis repressor with caspase recruitment domain is required for cardioprotection in response to biomechanical and ischemic stress. *Circulation*. (2006) 113:1203–12. doi: 10.1161/CIRCULATIONAHA.105.576785
139. Murtaza I, Wang HX, Feng X, Alenina N, Bader M, Prabhakar BS, et al. Down-regulation of catalase and oxidative modification of protein kinase CK2 lead to the failure of apoptosis repressor with caspase recruitment domain to inhibit cardiomyocyte hypertrophy. *J Biol Chem*. (2008) 283:5996–6004. doi: 10.1074/jbc.M706466200
140. Maillet M, van Berlo JH, Molkentin JD. Molecular basis of physiological heart growth: fundamental concepts and new players. *Nat Rev Mol Cell Biol*. (2013) 14:38–48. doi: 10.1038/nrm3495
141. Bernardo BC, Weeks KL, Pretorius L, McMullen JR. Molecular distinction between physiological and pathological cardiac hypertrophy: experimental findings and therapeutic strategies. *Pharmacol Ther*. (2010) 128:191–227. doi: 10.1016/j.pharmthera.2010.04.005
142. Yeves AM, Villa-Abrille MC, Perez NG, Medina AJ, Escudero EM, Ennis IL. Physiological cardiac hypertrophy: critical role of AKT in the prevention of NHE-1 hyperactivity. *J Mol Cell Cardiol*. (2014) 76:186–95. doi: 10.1016/j.yjmcc.2014.09.004
143. Moc C, Taylor AE, Chesini GP, Zambrano CM, Barlow MS, Zhang X, et al. Physiological activation of Akt by PHLPP1 deletion protects against pathological hypertrophy. *Cardiovasc Res*. (2015) 105:160–70. doi: 10.1093/cvr/cvu243
144. Verjans R, Derks WJA, Korn K, Sonnichsen B, van Leeuwen REW, Schroen B, et al. Functional screening identifies MicroRNAs as multi-cellular regulators of heart failure. *Sci Rep*. (2019) 9:6055. doi: 10.1038/s41598-019-41491-9
145. McMurray JJ, Adamopoulos S, Anker SD, Auricchio A, Bohm M, Dickstein K, et al. ESC guidelines for the diagnosis and treatment of acute and chronic heart failure 2012: The Task Force for the Diagnosis and Treatment of Acute and Chronic Heart Failure 2012 of the European Society of Cardiology. Developed in collaboration with the Heart Failure Association (HFA) of the ESC. *Eur J Heart Fail*. (2012) 14:803–69. doi: 10.1093/eurheartj/ehs104
146. Derda AA, Thum S, Lorenzen JM, Bavendiek U, Heineke J, Keyser B, et al. Blood-based microRNA signatures differentiate various forms of cardiac hypertrophy. *Int J Cardiol*. (2015) 196:115–22. doi: 10.1016/j.ijcard.2015.05.185
147. Vegter EL, van der Meer P, de Windt LJ, Pinto YM, Voors AA. MicroRNAs in heart failure: from biomarker to target for therapy. *Eur J Heart Fail*. (2016) 18:457–68. doi: 10.1002/ejhf.495
148. Marfella R, Di Filippo C, Potenza N, Sardu C, Rizzo MR, Siniscalchi M, et al. Circulating microRNA changes in heart failure patients treated with cardiac resynchronization therapy: responders vs. non-responders. *Eur J Heart Fail*. (2013) 15:1277–88. doi: 10.1093/eurjhf/hft088
149. Ovchinnikova ES, Schmitter D, Vegter EL, Ter Maaten JM, Valente MA, Liu LC, et al. Signature of circulating microRNAs in patients with acute heart failure. *Eur J Heart Fail*. (2016) 18:414–23. doi: 10.1002/ejhf.332
150. Vegter EL, Schmitter D, Hagemeijer Y, Ovchinnikova ES, van der Harst P, Teerlink JR, et al. Use of biomarkers to establish potential role and function of circulating microRNAs in acute heart failure. *Int J Cardiol*. (2016) 224:231–9. doi: 10.1016/j.ijcard.2016.09.010
151. Damman K, Valente MA, Voors AA, O'Connor CM, van Veldhuisen DJ, Hillege HL. Renal impairment, worsening renal function, and outcome in

patients with heart failure: an updated meta-analysis. *Eur Heart J*. (2014) 35:455–69. doi: 10.1093/eurheartj/eht386
152. Bruno N, ter Maaten JM, Ovchinnikova ES, Vegter EL, Valente MA, van der Meer P, et al. MicroRNAs relate to early worsening of renal function in patients with acute heart failure. *Int J Cardiol*. (2016) 203:564–69. doi: 10.1016/j.ijcard.2015.10.217
153. Saikumar J, Hoffmann D, Kim TM, Gonzalez VR, Zhang Q, Goering PL, et al. Expression, circulation, and excretion profile of microRNA-21,−155, and−18a following acute kidney injury. *Toxicol Sci*. (2012) 129:256–67. doi: 10.1093/toxsci/kfs210
154. Kaucsar T, Revesz C, Godo M, Krenacs T, Albert M, Szalay CI, et al. Activation of the miR-17 family and miR-21 during murine kidney ischemia-reperfusion injury. *Nucleic Acid Ther*. (2013) 23:344–54. doi: 10.1089/nat.2013.0438
155. Matsumura T, Matsui M, Iwata Y, Asakura M, Saito T, Fujimura H, et al. A pilot study of tranilast for cardiomyopathy of muscular dystrophy. *Intern Med*. (2018) 57:311–8. doi: 10.2169/internalmedicine.8651-16
156. Dickinson BA, Semus HM, Montgomery RL, Stack C, Latimer PA, Lewton SM, et al. Plasma microRNAs serve as biomarkers of therapeutic efficacy and disease progression in hypertension-induced heart failure. *Eur J Heart Fail*. (2013) 15:650–9. doi: 10.1093/eurjhf/hft018
157. Dahl LK, Knudsen KD, Heine MA, Leitl GJ. Effects of chronic excess salt ingestion. Modification of experimental hypertension in the rat by variations in the diet. *Circ Res*. (1968) 22:11–8. doi: 10.1161/01.RES.22.1.11
158. Pfeffer MA, Pfeffer J, Mirsky I, Iwai J. Cardiac hypertrophy and performance of Dahl hypertensive rats on graded salt diets. *Hypertension*. (1984) 6:475–81. doi: 10.1161/01.HYP.6.4.475
159. Gupta MP. Factors controlling cardiac myosin-isoform shift during hypertrophy and heart failure. *J Mol Cell Cardiol*. (2007) 43:388–403. doi: 10.1016/j.yjmcc.2007.07.045
160. Vegter EL, Ovchinnikova ES, Sillje HHW, Meems LMG, van der Pol A, van der Velde AR, et al. Rodent heart failure models do not reflect the human circulating microRNA signature in heart failure. *PLoS ONE*. (2017) 12:e0177242. doi: 10.1371/journal.pone.0177242
161. Humbert M, Sitbon O, Yaici A, Montani D, O'Callaghan DS, Jais X, et al. Survival in incident and prevalent cohorts of patients with pulmonary arterial hypertension. *Eur Respir J*. (2010) 36:549–55. doi: 10.1183/09031936.00057010
162. Archer SL, Weir EK, Wilkins MR. Basic science of pulmonary arterial hypertension for clinicians: new concepts and experimental therapies. *Circulation*. (2010) 121:2045–66. doi: 10.1161/CIRCULATIONAHA.108.847707
163. Negi V, Chan SY. Discerning functional hierarchies of microRNAs in pulmonary hypertension. *JCI Insight*. (2017) 2:e91327. doi: 10.1172/jci.insight.91327
164. Humbert M, Morrell NW, Archer SL, Stenmark KR, MacLean MR, Lang IM, et al. Cellular and molecular pathobiology of pulmonary arterial hypertension. *J Am Coll Cardiol*. (2004) 43(12 Suppl S):13S−24S. doi: 10.1016/j.jacc.2004.02.029
165. Crosswhite P, Sun Z. Molecular mechanisms of pulmonary arterial remodeling. *Mol Med*. (2014) 20:191–201. doi: 10.2119/molmed.2013.00165
166. Li L, Kim IK, Chiasson V, Chatterjee P, Gupta S. NF-kappaB mediated miR-130a modulation in lung microvascular cell remodeling: Implication in pulmonary hypertension. *Exp Cell Res*. (2017) 359:235–42. doi: 10.1016/j.yexcr.2017.07.024
167. Meloche J, Le Guen M, Potus F, Vinck J, Ranchoux B, Johnson I, et al. miR-223 reverses experimental pulmonary arterial hypertension. *Am J Physiol Cell Physiol*. (2015) 309:C363–72. doi: 10.1152/ajpcell.00149.2015
168. Zeng Y, Zhang X, Kang K, Chen J, Wu Z, Huang J, et al. MicroRNA-223 attenuates hypoxia-induced vascular remodeling by targeting RhoB/MLC2 in pulmonary arterial smooth muscle cells. *Sci Rep*. (2016) 6:24900. doi: 10.1038/srep24900
169. Liu A, Liu Y, Li B, Yang M, Liu Y, Su J. Role of miR-223-3p in pulmonary arterial hypertension via targeting ITGB3 in the ECM pathway. *Cell Prolif*. (2019) 52:e12550. doi: 10.1111/cpr.12550
170. Shi L, Kojonazarov B, Elgheznawy A, Popp R, Dahal BK, Bohm M, et al. miR-223-IGF-IR signalling in hypoxia- and load-induced right-ventricular failure: a novel therapeutic approach. *Cardiovasc Res*. (2016) 111:184–93. doi: 10.1093/cvr/cvw065
171. Liu X, Deng Y, Xu Y, Jin W, Li H. MicroRNA-223 protects neonatal rat cardiomyocytes and H9c2 cells from hypoxia-induced apoptosis and excessive autophagy via the Akt/mTOR pathway by targeting PARP-1. *J Mol Cell Cardiol*. (2018) 118:133–46. doi: 10.1016/j.yjmcc.2018.03.018
172. Meloche J, Pflieger A, Vaillancourt M, Paulin R, Potus F, Zervopoulos S, et al. Role for DNA damage signaling in pulmonary arterial hypertension. *Circulation*. (2014) 129:786–97. doi: 10.1161/CIRCULATIONAHA.113.006167
173. Zhuang G, Meng C, Guo X, Cheruku PS, Shi L, Xu H, et al. A novel regulator of macrophage activation: miR-223 in obesity-associated adipose tissue inflammation. *Circulation*. (2012) 125:2892–903. doi: 10.1161/CIRCULATIONAHA.111.087817
174. Sagar S, Liu PP, Cooper LT Jr. Myocarditis. *Lancet*. (2012) 379:738–47. doi: 10.1016/S0140-6736(11)60648-X
175. Rose NR. Myocarditis: infection versus autoimmunity. *J Clin Immunol*. (2009) 29:730–7. doi: 10.1007/s10875-009-9339-z
176. Steinberger J, Lucas RV, Jr, Edwards JE, Titus JL. Causes of sudden unexpected cardiac death in the first two decades of life. *Am J Cardiol*. (1996) 77:992–5. doi: 10.1016/S0002-9149(96)00035-5
177. Gou W, Zhang Z, Yang C, Li Y. MiR-223/Pknox1 axis protects mice from CVB3-induced viral myocarditis by modulating macrophage polarization. *Exp Cell Res*. (2018) 366:41–8. doi: 10.1016/j.yexcr.2018.03.004
178. Chen L, Hou X, Zhang M, Zheng Y, Zheng X, Yang Q, et al. MicroRNA-223-3p modulates dendritic cell function and ameliorates experimental autoimmune myocarditis by targeting the NLRP3 inflammasome. *Mol Immunol*. (2020) 117:73–83. doi: 10.1016/j.molimm.2019.10.027
179. Sica A, Mantovani A. Macrophage plasticity and polarization: *in vivo* veritas. *J Clin Invest*. (2012) 122:787–95. doi: 10.1172/JCI59643
180. Wang C, Dong C, Xiong S. IL-33 enhances macrophage M2 polarization and protects mice from CVB3-induced viral myocarditis. *J Mol Cell Cardiol*. (2017) 103:22–30. doi: 10.1016/j.yjmcc.2016.12.010
181. He J, Yue Y, Dong C, Xiong S. MiR-21 confers resistance against CVB3-induced myocarditis by inhibiting PDCD4-mediated apoptosis. *Clin Invest Med*. (2013) 36:E103–11. doi: 10.25011/cim.v36i2.19573
182. Steinman RM, Cohn ZA. Identification of a novel cell type in peripheral lymphoid organs of mice. I. Morphology, quantitation, tissue distribution. *J Exp Med*. (1973) 137:1142–62. doi: 10.1084/jem.137.5.1142
183. Svajger U, Rozman P. Induction of tolerogenic dendritic cells by endogenous biomolecules: an update. *Front Immunol*. (2018) 9:2482. doi: 10.3389/fimmu.2018.02482
184. Osorio F, Fuentes C, Lopez MN, Salazar-Onfray F, Gonzalez FE. Role of dendritic cells in the induction of lymphocyte tolerance. *Front Immunol*. (2015) 6:535. doi: 10.3389/fimmu.2015.00535
185. Hongo D, Tang X, Zhang X, Engleman EG, Strober S. Tolerogenic interactions between CD8(+) dendritic cells and NKT cells prevent rejection of bone marrow and organ grafts. *Blood*. (2017) 129:1718–28. doi: 10.1182/blood-2016-07-723015
186. Romero-Bermejo FJ, Ruiz-Bailen M, Gil-Cebrian J, Huertos-Ranchal MJ. Sepsis-induced cardiomyopathy. *Curr Cardiol Rev*. (2011) 7:163–83. doi: 10.2174/157340311798220494
187. Hochstadt A, Meroz Y, Landesberg G. Myocardial dysfunction in severe sepsis and septic shock: more questions than answers? *J Cardiothorac Vasc Anesth*. (2011) 25:526–35. doi: 10.1053/j.jvca.2010.11.026
188. Ieda M, Kanazawa H, Kimura K, Hattori F, Ieda Y, Taniguchi M, et al. Sema3a maintains normal heart rhythm through sympathetic innervation patterning. *Nat Med*. (2007) 13:604–12. doi: 10.1038/nm1570
189. Zhang H, Wang HY, Bassel-Duby R, Maass DL, Johnston WE, Horton JW, et al. Role of interleukin-6 in cardiac inflammation and dysfunction after burn complicated by sepsis. *Am J Physiol Heart Circ Physiol*. (2007) 292:H2408–16. doi: 10.1152/ajpheart.01150.2006
190. Joulin O, Petillot P, Labalette M, Lancel S, Neviere R. Cytokine profile of human septic shock serum inducing cardiomyocyte contractile dysfunction. *Physiol Res*. (2007) 56:291–7.
191. Wen H, Lei Y, Eun SY, Ting JP. Plexin-A4-semaphorin 3A signaling is required for Toll-like receptor- and sepsis-induced cytokine storm. *J Exp Med*. (2010) 207:2943–57. doi: 10.1084/jem.20101138

192. Lawes CM, Vander Hoorn S, Rodgers A, International Society of H. Global burden of blood-pressure-related disease, 2001. *Lancet*. (2008) 371:1513–8. doi: 10.1016/S0140-6736(08)60655-8
193. Conen D, Bamberg F. Noninvasive 24-h ambulatory blood pressure and cardiovascular disease: a systematic review and meta-analysis. *J Hypertens*. (2008) 26:1290–9. doi: 10.1097/HJH.0b013e3282f97854
194. Harjutsalo V, Groop PH. Epidemiology and risk factors for diabetic kidney disease. *Adv Chronic Kidney Dis*. (2014) 21:260–6. doi: 10.1053/j.ackd.2014.03.009
195. Lewington S, Clarke R, Qizilbash N, Peto R, Collins R, Prospective Studies C. Age-specific relevance of usual blood pressure to vascular mortality: a meta-analysis of individual data for one million adults in 61 prospective studies. *Lancet*. (2002) 360:1903–13. doi: 10.1016/S0140-6736(02)11911-8
196. Mills KT, Bundy JD, Kelly TN, Reed JE, Kearney PM, Reynolds K, et al. Global disparities of hypertension prevalence and control: a systematic analysis of population-based studies from 90 countries. *Circulation*. (2016) 134:441–50. doi: 10.1161/CIRCULATIONAHA.115.018912
197. Whelton PK, Carey RM, Aronow WS, Casey DE Jr, Collins KJ, Dennison Himmelfarb C, et al. 2017 ACC/AHA/AAPA/ABC/ACPM/AGS/APhA/ASH/ASPC/NMA/PCNA Guideline for the Prevention, Detection, Evaluation, and Management of High Blood Pressure in Adults: Executive Summary: A Report of the American College of Cardiology/American Heart Association Task Force on Clinical Practice Guidelines. *Hypertension*. (2018) 71:1269–324. doi: 10.1161/HYP.0000000000000075
198. Small EM, Olson EN. Pervasive roles of microRNAs in cardiovascular biology. *Nature*. (2011) 469:336–42. doi: 10.1038/nature09783
199. Heggermont WA, Heymans S. MicroRNAs are involved in end-organ damage during hypertension. *Hypertension*. (2012) 60:1088–93. doi: 10.1161/HYPERTENSIONAHA.111.187104
200. Caruso P, Dunmore BJ, Schlosser K, Schoors S, Dos Santos C, Perez-Iratxeta C, et al. Identification of MicroRNA-124 as a major regulator of enhanced endothelial cell glycolysis in pulmonary arterial hypertension via PTBP1 (Polypyrimidine Tract Binding Protein) and pyruvate kinase M2. *Circulation*. (2017) 136:2451–67. doi: 10.1161/CIRCULATIONAHA.117.028034
201. Marketou M, Kontaraki J, Papadakis J, Kochiadakis G, Vrentzos G, Maragkoudakis S, et al. Platelet microRNAs in hypertensive patients with and without cardiovascular disease. *J Hum Hypertens*. (2019) 33:149–56. doi: 10.1038/s41371-018-0123-5
202. Zhang X, Wang X, Wu J, Peng J, Deng X, Shen Y, et al. The diagnostic values of circulating miRNAs for hypertension and bioinformatics analysis. *Biosci Rep*. (2018) 38:BSR20180525. doi: 10.1042/BSR20180525
203. Poli KA, Tofler GH, Larson MG, Evans JC, Sutherland PA, Lipinska I, et al. Association of blood pressure with fibrinolytic potential in the Framingham offspring population. *Circulation*. (2000) 101:264–9. doi: 10.1161/01.CIR.101.3.264
204. Spencer CG, Gurney D, Blann AD, Beevers DG, Lip GY, Ascot Steering Committee A-SCOT. Von Willebrand factor, soluble P-selectin, and target organ damage in hypertension: a substudy of the Anglo-Scandinavian Cardiac Outcomes Trial (ASCOT). *Hypertension*. (2002) 40:61–6. doi: 10.1161/01.HYP.0000022061.12297.2E
205. Lu Y, Zhang Y, Wang N, Pan Z, Gao X, Zhang F, et al. MicroRNA-328 contributes to adverse electrical remodeling in atrial fibrillation. *Circulation*. (2010) 122:2378–87. doi: 10.1161/CIRCULATIONAHA.110.958967

Conflict of Interest: The authors declare that the research was conducted in the absence of any commercial or financial relationships that could be construed as a potential conflict of interest.

frontiers in Cardiovascular Medicine

REVIEW
published: 23 February 2021
doi: 10.3389/fcvm.2021.632393

The Emerging Role of Long Non-coding RNAs and Circular RNAs in Coronary Artery Disease

Soudeh Ghafouri-Fard[1], *Mahdi Gholipour*[2] *and Mohammad Taheri*[3]*

[1] Urogenital Stem Cell Research Center, Shahid Beheshti University of Medical Sciences, Tehran, Iran, [2] Department of Medical Genetics, Shahid Beheshti University of Medical Sciences, Tehran, Iran, [3] Urology and Nephrology Research Center, Shahid Beheshti University of Medical Sciences, Tehran, Iran

Coronary artery disease (CAD) is a common disorder caused by atherosclerotic processes in the coronary arteries. This condition results from abnormal interactions between numerous cell types in the artery walls. The main participating factors in this process are accumulation of lipid deposits, endothelial cell dysfunction, macrophage induction, and changes in smooth muscle cells. Several lines of evidence underscore participation of long non-coding RNAs (lncRNAs) and circular RNAs (circRNAs) in the pathogenesis of CAD. Several lncRNAs such as H19, ANRIL, MIAT, lnc-DC, IFNG-AS1, and LEF1-AS1 have been shown to be up-regulated in the biological materials obtained from CAD patients. On the other hand, Gas5, Chast, HULC, DICER1-AS1, and MEG3 have been down-regulated in CAD patients. Meanwhile, a number of circRNAs have been demonstrated to influence function of endothelial cells or vascular smooth muscle cells, thus contributing to the pathogenesis of CAD. In the current review, we summarize the function of lncRNAs and circRNAs in the development and progression of CAD.

Keywords: long non-coding RNA, circRNA, coronary artery disorder, expression, biomarkers

OPEN ACCESS

Edited by:
En-Zhi Jia,
Nanjing Medical University, China

Reviewed by:
Mingxian Chen,
Central South University, China
Shujie Guo,
Shanghai Institute of Hypertension, China

***Correspondence:**
Mohammad Taheri
mohammad_823@yahoo.com

Specialty section:
This article was submitted to General Cardiovascular Medicine, a section of the journal Frontiers in Cardiovascular Medicine

Received: *23 November 2020*
Accepted: *15 January 2021*
Published: *23 February 2021*

Citation:
Ghafouri-Fard S, Gholipour M and Taheri M (2021) The Emerging Role of Long Non-coding RNAs and Circular RNAs in Coronary Artery Disease. Front. Cardiovasc. Med. 8:632393. doi: 10.3389/fcvm.2021.632393

INTRODUCTION

Coronary artery disease (CAD) is a common disorder caused by atherosclerotic processes in the coronary arteries. This condition can be asymptomatic or can result in fatal situations. In fact, CAD is the main cause of the mortality associated with coronary heart disorders (1). Atherosclerosis is regarded as a progressive inflammatory condition during which oxidative, hemodynamic, and biochemical factors destruct the function of endothelial cells (2). Subsequent alterations in the permeability of endothelial cells, accumulation of macrophages, production of inflammatory substances, and activation of smooth muscle cells are additional steps in the development of atherosclerosis (3, 4). Two classes of regulatory non-coding RNAs, namely, long non-coding RNAs (lncRNAs) and circular RNAs (circRNAs), have been shown to affect the process of atherosclerosis and CAD development (5, 6). Although both having regulatory effects on the expression of genes, they vary in terms of biogenesis and mechanism of action. LncRNAs have sizes of more than 200 nucleotides (7) and can function as signal, sequester, scaffold, guide, or enhancer RNAs to influence genomic organization or gene expression (8). They share several features with mRNAs such as the presence of RNA polymerase II binding sites, 3′ poly A tails and 5′ caps (9). On the other hand, circRNAs are single-stranded covalently enclosed molecules made via back-splicing of linear precursor transcripts (10). Both classes of transcript can influence function of endothelial cells or

smooth muscle cells in the process of atherosclerosis. In the current review, we summarize the function of lncRNAs and circRNAs in the development and progression of CAD.

LncRNAs AND CAD

Role of LncRNAs in CAD

LncRNAs can affect CAD pathogenesis through regulation of immune responses, modulation of function of endothelial cells and vascular smooth muscles, and changing lipid metabolism. In some cases, a certain lncRNA can affect more than one route.

LncRNAs Regulate Immune Responses

H19 is a transcript encoded by a conserved imprinted gene cluster containing the insulin-like growth factor 2 gene (11). H19 has been shown to function as a molecular sponge for let-7. Expression of this lncRNA has been shown to be reduced in the muscle of patients with type-2 diabetes, as well as animal model of this disorder. The consequent up-regulation of let-7 decreases expression levels let-7 targets (12). This lncRNA has been overexpressed in patients with CAD despite its normal expression in other forms of cardiovascular disorders and therefore has been suggested as a marker for prediction of CAD. Notably, its expression levels have been associated with duration of CAD and serum concentrations of transforming growth factor β1 (TGF-β1). *In vitro* studies verified the effects of H19 overexpression in enhancement of TGF-β1 secretion (13). The lncRNA CoroMarker has been shown to be functionally clustered with genes, which are related with signal transduction, transmembrane transport, synaptic communication, and innate immune responses, while having negative correlation with inflammation-related genes. Small interfering RNA–mediated silencing of CoroMarker has reduced the production of proinflammatory cytokines (14). IFNG-AS1 is another overexpressed lncRNA in CAD patients whose expression has been considerably associated with Gensini

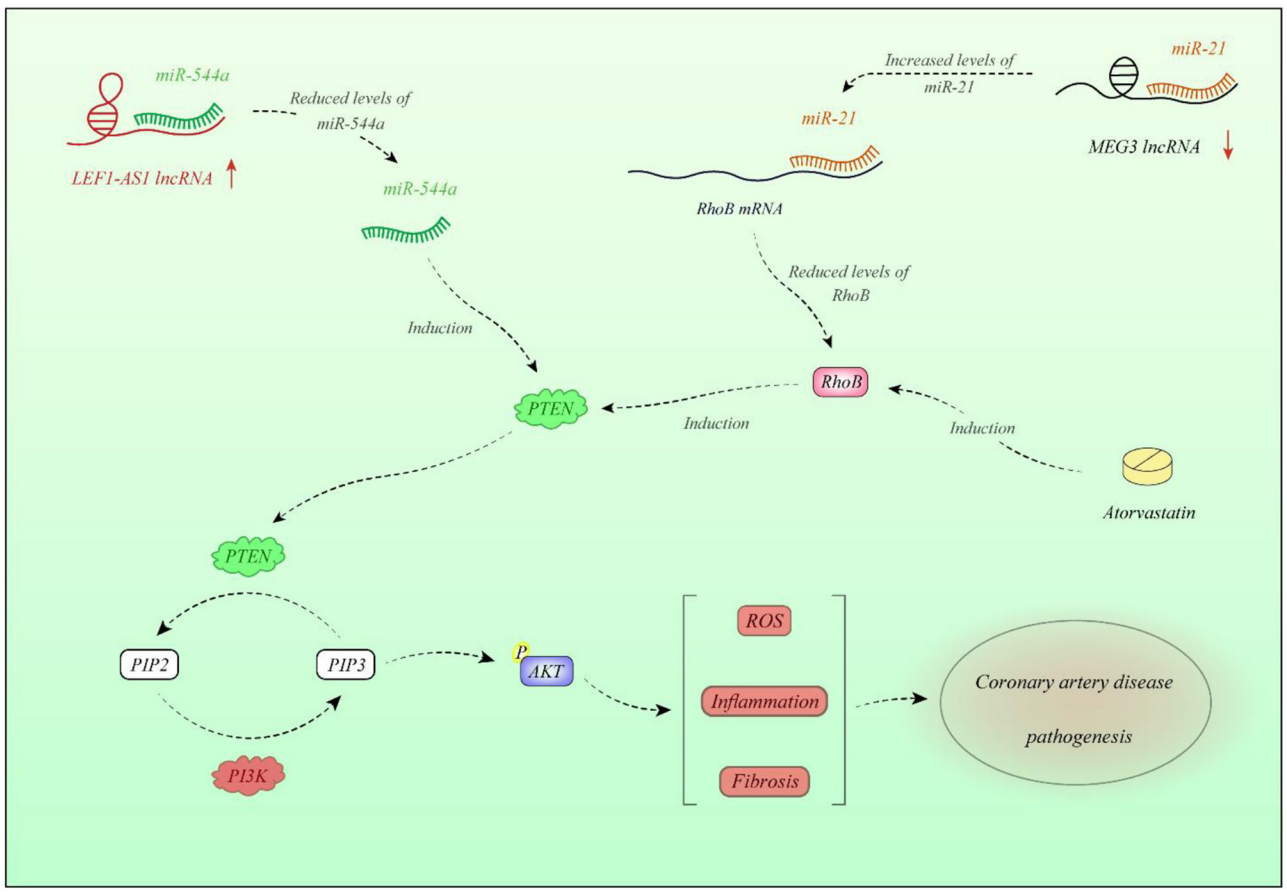

FIGURE 1 | Expression of LEF1-AS1 is increased in plasma and tissues of CAD patients. LEF1-AS1 inhibits miR-544a, thus decreasing PTEN. This is because miR-544a increases PTEN levels. PTEN diminishes AKT activity. LEF1-AS1 contributes in enhancement of reactive oxygen species (ROS) formation, elevation of inflammatory responses, and fibrosis through miR-544a/PTEN axis (28). On the other hand, expression of MEG3 is decreased in CAD tissues compared with normal tissues. Down-regulation of MEG3 is associated with up-regulation of miR-21. miR-21 binds with 3′-UTR of RhoB and decreases its expression. RhoB has a role in activation of PTEN; therefore, MEG3 down-regulation is associated with the lower activity of PTEN (29). Atorvastatin has a regulatory role on PTEN through modulation of RhoB (30).

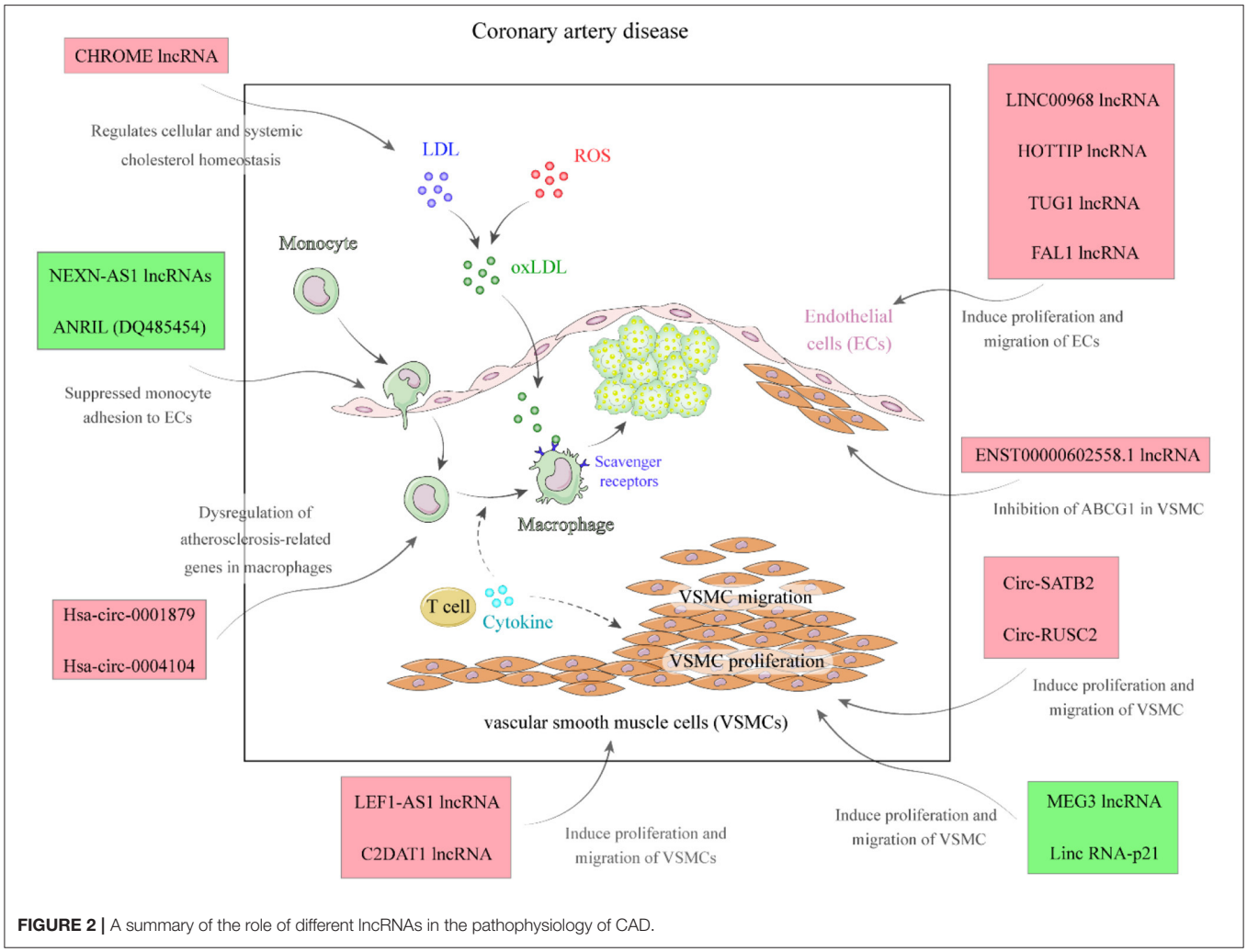

FIGURE 2 | A summary of the role of different lncRNAs in the pathophysiology of CAD.

score, as well as levels of inflammatory markers high sensitivity C-reactive protein (hs-CRP), tumor necrosis factor α (TNF-α), and interleukin 6 (IL-6). On the other hand, IFNG-AS1 levels have been inversely associated with the levels of anti-inflammatory cytokine IL-10 level (15). Cho et al. (16) have demonstrated DQ485454 as the main ANRIL transcript in the endothelial cells. Expression of this transcript has been significantly higher in endothelial cells compared with THP-1 monocytes. Notably, they reported down-regulation of DQ485454 in CAD coronary arteries as compared with samples obtained from non-CAD arteries. Forced up-regulation of this transcript has attenuated cellular processes participating in CAD initiation as it decreased monocyte adhesion to endothelial cells, transendothelial monocyte migration, and endothelial cell migration. Moreover, expression of several CAD-related genes were altered after DQ485454 silencing (16). A microarray-based study has demonstrated down-regulation of NEXN-AS1 in human atherosclerotic plaques. This lncRNA interacts with the chromatin modifier BAZ1A and the 5′ part of the NEXN gene. Overexpression of NEXN-AS1 suppressed TLR4 oligomerization and nuclear factor κB (NF-κB) function, decreased endothelial production of adhesion proteins and inflammatory cytokines, and repressed adhesion of monocyte to endothelial cells (17). Another study in CAD patients demonstrated down-regulation of Chast, HULC, and DICER1-AS1 in the peripheral blood samples (18). Expression of CASC11 has also been decreased in patients with CAD parallel with overexpression of TGF-β1. Functional studies revealed the impact of this lncRNA in the suppression of TGF-β1 expression in endothelial cells (19).

LncRNAs Alter Function of Endothelial Cells and Vascular Smooth Muscle Cells

ANRIL is another up-regulated lncRNA in CAD patients as well as animal model of this disorder. Overexpression of ANRIL decreases expression of miR-181b and is associated with risk of CAD in the subpopulations of elderly patients with history of smoking, hypertension, and hyperlipidemia. Overexpression of ANRIL in human coronary endothelial cells has down-regulated miR-181b, increased p50/p65 expressions, enhanced viability of human coronary endothelial cells, and promoted release of inflammatory molecules and vascular-protecting proteins (20). Another study has revealed overexpression of

TABLE 1 | List of up-regulated lncRNAs in CAD (HCAECs, human coronary endothelial cells; HUVECs, human umbilical vein endothelial cells; VSMCs, vascular smooth muscle cells).

LncRNA	Samples	Assessed cell lines	Interactions	Signaling pathway	Association with clinical properties	Function	References
ANRIL	327 patients with CAD, SD rats	HCAECs HUVECs	miR-181b, NF-κB	NF-κB signaling pathway	Age >60 years, smoking history, hyperlipidemia, hypertension, cholesterol level, triglyceride (TG) level	Regulates viability and survival of HCAECs and modulates secretion of inflammatory agents from HCAECs through targeting miR-181b and regulating expression of NF-κB	(20)
ANRIL	111 CAD patients and 20 healthy controls	HUVECs	let-7b, TGF-βR1	TGF-βR1/Smad signaling pathway	–	Regulates HUVEC function by targeting let-7b and regulation of TGF-βR1/Smad signaling pathway activation	(21)
ANRIL, *MIAT*	Atherosclerotic coronary tissue specimens from 20 patients	–	–	–	–	Are up-regulated and may participate in pathogenesis of CAD	(22)
lnc-DC	37 patients with CAD and 36 patients without CAD	–	SOCS1, STAT3	JAK/STAT pathway	–	My be implicated in pathogenesis of CAD	(25)
IFNG-AS1	Plasma samples from 102 patients with CAD and 89 control subjects	–	–	–	Gensini score, hs-CRP, TNF-α, IL-6, and IL-10 levels	Its expression was associated with augmented risk of CAD, enhanced severity of disease, and increased inflammation	(15)
LEF1-AS1	Tissue specimens from 70 patients with coronary artery atherosclerosis and 30 healthy controls	VSMCs	miR-544a, PTEN	PTEN pathway	Patients survival	Promotes proliferation, invasion, and migration of smooth muscle cells through regulating miR-544a/PTEN axis	(28)
H19	Serum samples from 30 CAD patients and 30 healthy subjects	HCAEC	TGF-β1	–	–	Contributes to CAD pathogenesis through increasing expression TGF-β1	(13)
FAL1	15 CAD tissues and 15 normal arterial tissues	HUVECs	–	PTEN/AKT pathway	–	Enhances proliferation, migration, and cell cycle progression through activating PTEN/AKT pathway	(26)
OTTHUMT00000 387022	246 CAD patients and 206 control subjects	THP-1	–	–	–	Its knockdown in THP-1 cells reduces release of proinflammatory cytokines from these cells	(34)
LncPPARδ	246 patients with CAD and 206 healthy subjects	THP-1	PPARδ, ADRP, ANGPTL4	–	–	Its knockdown influenced expression of PPARδ, ADRP and ANGPTL4	(14)
C2dat1	20 CAD tissues and 20	VSMC	miR-34a, SIRT1	–	–	Its overexpression enhances proliferation and migration of VSMC by regulating miR-34a/SIRT1 axis	(35)
CHROME (ENSG0000 0223960)	Plasma samples from 14 CAD patients and 33 healthy volunteers as controls, 127 atherosclerotic plaques from CAD patients and 10 normal arteries, male African green monkeys	THP-1, HEK293T, HepG2	miR-33b, miR-27b, miR-128, miR-33a, ABCA1	–	–	Its knockdown inhibits HDL biogenesis and cholesterol efflux through modulating expression of miR-33b, miR-27b, miR-128, miR-33a, and ABCA1	(32)

(Continued)

TABLE 1 | Continued

LncRNA	Samples	Assessed cell lines	Interactions	Signaling pathway	Association with clinical properties	Function	References
THRIL	Plasma samples from 220 patients with coronary heart disease and 200 control individuals	–	–	–	Gensini score, diabetes mellitus, fasting blood glucose, CRP, TNF-α, MACE accumulating rate	Can be a potential risk factor for prediction of coronary heart disease	(36)
HOTTIP	15 CAD tissues and 15 normal arterial tissues	HU-VECs	β-catenin, c-Myc	Wnt/β-catenin pathway	–	Its up-regulation enhances proliferation and migration of endothelial cells by regulating β-catenin expression and activation of Wnt/β-catenin pathway	(37)
ENST00000602558.1		VSMCs	ABCG1	–	–	Its overexpression decreases expression of ABCG1 and thus lower cholesterol efflux and HDL biogenesis	(38)
LINC00968	20 CAD tissues and 20 normal arterial tissues	Endothelial cell	miR-9-3p	–	–	Its overexpression promotes migration and proliferation of endothelial cells through targeting miR-9-3p	(39)
TUG1	15 CAD tissues and normal arterial tissues	HUVECs	β-catenin, c-Myc	Wnt pathway	–	Enhances migration, proliferation, and cell cycle progression in HUVECs	(40)

ANRIL in patients with acute coronary syndrome in association with levels of monocyte chemoattractant protein-1 and IL-10. Notably, these proinflammatory cytokines are produced in reaction to dysfunction of endothelial cells. ANRIL silencing has enhanced cell proliferation and tubule development and suppressed induction of inflammatory responses and apoptosis of endothelial cells. Such effects were linked to ANRIL-mediated suppression of let-7b and its impacts on the TGF-βR1/Smad signaling (21). Another study has demonstrated higher levels of ANRIL and MIAT in the atherosclerotic arteries when compared to the non-atherosclerotic ones (22). ANRIL can also regulate growth of vascular smooth muscle cells via modulation of CDKN2A/B locus, which has a direct effect on the pathobiology of atherosclerosis (23). H19 in addition to its role in the regulation of immune responses can influence vascular smooth muscle cells. Expression of this lncRNA has been increased in the injured neointima and in human atherosclerotic plaques but is scarcely deceted in normal vessels. H19 sequesters let-7 family microRNAs (miRNAs), which are known to shield vascular smooth muscle cells from oxidative damage (12, 24). Expression of lnc-DC has been higher in patients with type 2 diabetes and CAD compared with diabetic patients without CAD. Such up-regulation has been accompanied by overexpression of STAT3. Yet, expression of these genes was not associated with the severity of CAD. Based on the observed correlations between expression of genes, authors have suggested the importance of JAK/STAT-related-lncRNAs in the pathogenesis of CAD (25). Expression of FAL1 has been shown to be elevated in CAD tissues and TNF-α-stimulated endothelial cells compared with normal and unstimulated cells. Up-regulation of FAL1 in endothelial cells has enhanced cell cycle progression, proliferation, and migration via modulation of PTEN/AKT pathway (26). In addition, HIF1a-AS1 partakes in the pathology of atherosclerosis via modulating apoptosis of vascular smooth muscle cells and endothelial cells (27). Expression of CASC11 has also been decreased in patients with CAD parallel with overexpression of TGF-β1. Functional studies revealed the impact of this lncRNA in the suppression of TGF-β1 expression in endothelial cells (19). Expression of LEF1-AS1 has been elevated in plasma and tissue samples of CAD patients, whereas expression of its target miRNA, i.e., miR-544a, has been decreased. LEF1-AS1 modulates proliferation and migration of smooth muscle cells via the miR-544a/PTEN route (28). **Figure 1** shows the molecular cascade of contribution of LEF1-AS1 and MEG3 in CAD.

LncRNAs Regulate Lipid Metabolism

LincRNA-DYNLRB2-2 is an lncRNA whose expression is stimulated by Ox-LDL. This transcript enhances ABCA1-associated cholesterol efflux and suppresses inflammatory responses via GPR119 in macrophage originated foam cells (31). CHROME is another up-regulated lncRNA in CAD patients whose expression is altered by nutritional and cellular cholesterol levels via the sterol-activated liver X receptor transcription factors. This lncRNA enhances cholesterol secretion and HDL synthesis through suppression of the activity of a number of miRNAs. CHROME silencing in human hepatocytes and macrophages enhances expressions of miR-27b, miR-33a, miR-33b, and miR-128, thus decreasing the levels of their shared target genes, particularly ABCA1, which controls *de novo* synthesis of HDL (**Figure 2**) (32). Expression of FAL1 has been shown to be

TABLE 2 | List of down-regulated lncRNAs in CAD (HCAEC, human coronary endothelial cells; HUVEC, human umbilical vein endothelial cells).

LncRNA	Samples	Cell lines	Interactions	Signaling pathway	Association with clinical properties	Function	References
GAS5	Plasma samples from 30 CAD patients and 30 healthy controls	HCAECs	p-mTOR	mTOR pathway	–	Its down-regulation increases phosphorylated mTOR levels, but its up-regulation has reverse effects	(41)
GAS5	Serum samples from 102 CAD patients and 98 control subjects, 72 y Sprague–Dawley rats established as CAD model	–	–	Wnt/β-catenin signaling pathway	CK-MB, Troponin I, Gensini score	Inhibits apoptosis of cardiomyocyte, oxidative stress, and inflammatory damage in CAD rat models; reduces myocardial damages in these rats	(33)
NEXN-AS1	Atherosclerotic arterial samples from patients and normal individuals, blood samples from 113 CAD patients, 69 myocardial infarction, 40 heart failure, and 40 healthy subjects, ApoE$^{-/-}$ mice, NEXN$^{+/-}$ mice	THP-1, HUVECs, VSMCs	NEXN, BAZ1A	–	–	Interacts with BAZ1A and contributes to elevation of NEXN expression	(17)
ANRIL (DQ485454)		HCAECs, HUVECs	CLIP1, EZR, LYVE1	–	–	Its overexpression suppresses TEM process in monocyte migration of endothelial cells and adhesion of monocytes to endothelial cells	(16)
Chast	Blood samples from 50 premature CAD patients and 50 age- and gender-matched healthy volunteers as controls	–	–	–	FBS levels	May be implicated in CAD development	(18)
HULC	Blood samples from 50 premature CAD patients and 50 age- and gender-matched healthy volunteers as controls	–	–	–	Age, FBS, TG	Has diagnostic value for distinguishing CAD patients from healthy individuals	(18)
DICER1-AS1	Blood samples from 50 premature CAD patients and 50 age- and gender-matched healthy volunteers as controls	–	–	–	FBS levels, TG, TG/HDL ratio	Has diagnostic value for distinguishing CAD patients from healthy individuals	(18)
MEG3	40 CAD tissues and 35 control tissues	VSMC	miR-26a, Smad1	–	–	Its overexpression represses proliferation and induces apoptosis in VSMCs by targeting miR-26a and increasing expression of Smad1	(42)
MEG3	15 CAD tissues and 15 normal arterial tissues	HUVECs	miR-21, RhoB, PTEN	–	–	Its overexpression suppressed proliferation and migration through targeting miR-21 and regulation of RhoB and PTEN expression	(29)
lincRNA-p21	Blood samples from 12 CAD patients and 8 control subjects, ApoE$^{-/-}$ mice	HA-VSMC, RAW264.7	MDM2, p53	–	–	Regulates proliferation and apoptosis in vascular smooth muscle cell by interacting with MDM2 and modulation of p53 activity	(43)
CASC11	Plasma samples from 82 CAD patients and 82 age- and gender-matched healthy individuals	HCAECs	TGF-β1	–	Patients survival	Its overexpression reduces expression of TGF-β1 in HCAECs	(19)

TABLE 3 | Prognostic role of lncRNAs in CAD (OS, overall survival).

LncRNA	Samples	Kaplan–Meier analysis	Univariate analysis	Multivariate analysis	References
CASC11	Plasma samples from 82 CAD patients and 82 age- and gender-matched healthy individuals	Its low expression was associated with decreased overall survival in CAD patients	–	–	(19)
ANRIL	327 patients with CAD	–	Its expression was correlated with CAD patients survival	Its expression can be an independent predictor of CAD patients' survival	(20)
LEF1-AS1	Tissue specimens from 70 patients with coronary artery atherosclerosis and 30 healthy controls	High expression of *LEF1-AS1* was associated with poor OS.	–	–	(28)
ANRIL	Plasma samples from 125 CAD patients and 105 control individuals	High expression of *ANRIL* was associated with shorter OS in CAD patients.	–	–	(44)

elevated in CAD tissues and TNF-α-stimulated endothelial cells compared with normal and unstimulated cells. Up-regulation of FAL1 in endothelial cells has enhanced cell cycle progression, proliferation, and migration via modulation of PTEN/AKT pathway (26). GAS5 is another down-regulated lncRNA in CAD. Enforced up-regulation of GAS5 in animal models of CAD has improved hyperlipidemia, reduced myocardial damage, suppressed apoptosis of cardiac cells, and diminished oxidative stress, inflammatory damage, and aberrant induction of the Wnt/β-catenin pathway in cardiac tissue (33). The function of up-regulated and down-regulated lncRNAs in CAD is summarized in **Tables 1**, **2**, respectively.

Prognostic Value of LncRNAs in CAD

LncRNAs can be used for evaluation of prognosis of CAD patients. For instance, a long-term follow-up study has demonstrated correlation between down-regulation of CASC11 and poor survival of patients with CAD (19). On the other hand, overexpression of LEF1-AS1 and ANRIL has been shown to be correlated with poor clinical outcome of patients with CAD (28, 44). Kaplan–Meier analysis has also demonstrated association between ANRIL and LEF1-AS1 overexpression and short overall survival in CAD patients (28, 44). **Table 3** reviews the studies that appraised the prognostic role of lncRNAs in CAD.

Diagnostic Value of LncRNAs in CAD

Blood or serum levels of some lncRNAs can be used as diagnostic markers in CAD. The best diagnostic value has been reported for H19 where the receiver operating characteristic (ROC) curves showed the diagnostic power of 0.9367, signifying H19 as a suitable marker for CAD (13). Cai et al. (14) have profiled lncRNAs in circulating peripheral blood monocytes and plasma samples of CAD patients and healthy subjects. Their preliminary results demonstrated possible biomarker role for CoroMarker, BAT5, and IL21R-AS1 lncRNAs. The verification step in the larger cohort of CAD patients supported the biomarker role of CoroMarker. This lncRNA could differentiate CAD patients from healthy subjects with accuracy of 0.920 and in an independent manner from identified CAD risk factors and other cardiovascular disorders (14). Another study demonstrated the accuracy of 0.90 and 0.87 for HULC and DICER1-AS1, respectively, in differentiation between CAD patients and healthy individuals (18). In addition, up-regulation of IFNG-AS1 in CAD patients could be used to forecast the risk of CAD with accuracy of 0.755 (15). **Table 4** summarizes the points regarding the diagnostic significance of lncRNAs in CAD.

LncRNAs Polymorphisms and CAD

A number of functional single-nucleotide polymorphisms (SNPs) in lncRNAs have been associated with susceptibility to CAD. ANRIL has been the mostly assessed lncRNA in this regard. For instance, rs1330049, rs2383206, rs10757278, and rs10757274 SNPs have been associated with risk of CAD in Asians (52). On the other hand, rs2383207 and rs1333049 SNPs of ANRIL have not been associated with CAD risk in Han Chinese (53). In addition, rs1333040 and rs1004638 SNPs of ANRIL have not been associated with this disorder in Iranian population (54). H19 is another lncRNA whose association with risk of CAD has been assessed in some populations. Hu et al. (55) have reported an association between H19 rs2735971 and rs3024270 SNPs and susceptibility to CAD in a Chinese population, suggesting the significance of these SNPs as markers for prediction of risk of CAD in this population. Other SNPs within LINC00841, MALAT1, and lincRNA-p21 have been associated with risk of CAD in some ethnic groups (**Table 5**).

CIRCRNAS AND CAD

Role of CircRNAs in CAD

A comprehensive circRNA profiling in CAD patients has shown up-regulation of 624 circRNAs and down-regulation of 171 circRNAs in these patients compared with healthy subjects. Subsequent validation in a larger cohort of patients supported up-regulation of hsa_circ_0001879 and hsa_circ_0004104 in CAD patients. Remarkably, up-regulation of hsa_circ_0004104 has led to aberrant expression of atherosclerosis-associated genes in macrophages (63). Another high-throughput study of circRNAs expression in CAD patients has shown up-regulation of 18

TABLE 4 | Diagnostic role of lncRNAs in CAD.

LncRNA	Expression pattern	Sample	Type of marker	ROC curve analysis			References
				Sensitivity	Specificity	Area under the curve (AUC)	
GAS5	Down-regulated	Serum samples from 102 CAD patients and 98 control subjects	Diagnostic marker	86.7%	86.5%	0.889	(33)
HULC	Down-regulated	Blood samples from 50 premature CAD patients and 50 age- and gender-matched healthy volunteers as controls	Diagnostic marker	–	–	0.90	(18)
DICER1-AS1	Down-regulated	Blood samples from 50 premature CAD patients and 50 age- and gender-matched healthy volunteers as controls	Diagnostic marker	–	–	0.87	(18)
CASC11	Down-regulated	Plasma samples from 82 CAD patients and 82 age- and gender-matched healthy individuals	Diagnostic marker	–	–	0.90	(19)
ANRIL (EU741058)	Down-regulated	Blood samples from 50 CAD patients and 50 healthy volunteers	Diagnostic marker	82%	69%	–	(45)
IFNG-AS1	Up-regulated	Plasma samples from 102 patients with CAD and 89 control subjects	Diagnostic marker (for prediction of CAD risk)	–	–	0.755	(15)
H19	Up-regulated	Serum samples from 30 CAD patients and 30 healthy subjects	Diagnostic marker	–	–	0.9367	(13)
OTTHUMT00000387022	Up-regulated	246 CAD patients and 206 control subjects	Diagnostic marker	–	–	0.920	(34)
LncPPARδ	Up-regulated	246 patients with CAD and 206 healthy subjects	Diagnostic marker	–	–	0.727	(14)
LncPPARδ along with CAD risk factors	Up-regulated	246 patients with CAD and 206 healthy subjects	Diagnostic marker	–	–	0.785	
THRIL	Up-regulated	Plasma samples from 220 patients with coronary heart disease and 200 control individuals	Diagnostic marker	–	–	0.869	(36)
ANRIL	Up-regulated	Plasma samples from 125 CAD patients and 105 control individuals	Diagnostic marker	–	–	0.789	(44)
AC100865.1	Up-regulated	Plasma samples from 256 patients with CAD and 222 healthy individuals	Diagnostic marker	–	–	0.795	(46)
ENST00000444488.1	–	Blood samples [peripheral blood mononuclear cells (PBMCs)] from 505 CAD patients and 343 male individuals as controls	Diagnostic marker [distinguishing patients with acute myocardial infarction (AMI) form non-AMI patients]	–	–	0.758	(47)

(Continued)

TABLE 4 | Continued

LncRNA	Expression pattern	Sample	Type of marker	ROC curve analysis			References
				Sensitivity	Specificity	Area under the curve (AUC)	
ENST00000444488.1	–	Blood samples (PBMCs) from 505 CAD patients and 343 male individuals as controls	Diagnostic marker (distinguishing patients with CAD from controls)	–	–	0.799	
uc010yfd.1	–	Blood samples (PBMCs) from 505 CAD patients and 343 male individuals as controls	Diagnostic marker (distinguishing patients with CAD from controls)	–	–	0.779	
ENST00000444488.1 uc010yfd.1	–	Blood samples (PBMCs) from 505 CAD patients and 343 male individuals as controls	Diagnostic marker (distinguishing patients with CAD from controls)	–	–	0.851	
ENST00000444488.1 uc010yfd.1 along with age, BMI, glucose, and HDL	–	Blood samples (PBMCs) from 505 CAD patients and 343 male individuals as controls	Diagnostic marker (distinguishing patients with CAD from controls)	–	–	0.902	
H19	Up-regulated	Plasma samples from 300 CAD patients and 180 control individuals	Diagnostic marker	–	–	0.631	(48)
LIPCAR	Up-regulated	Plasma samples from 300 CAD patients and 180 control individuals	Diagnostic marker	–	–	0.722	
KCNQ1OT1	Up-regulated	Blood samples (PBMCs) from 20 patients with CAD and 20 individuals without CAD	Diagnostic marker	–	–	0.865	(49)
HIF1A-AS2	Up-regulated	Blood samples (PBMCs) from 20 patients with CAD and 20 individuals without CAD	Diagnostic marker	–	–	0.852	
APOA1-AS	Up-regulated	Blood samples (PBMCs) from 20 patients with CAD and 20 individuals without CAD	Diagnostic marker	–	–	0.967	
KCNQ1OT1 HIF1A-AS2 APOA1-AS	Up-regulated Up-regulated Up-regulated	Blood samples (PBMCs) from 20 patients with CAD and 20 individuals without CAD	Diagnostic marker	–	–	0.990	
ENST00000512246.1	Up-regulated	Blood samples from 173 CAD patients and 151 healthy controls	Diagnostic marker	0.833	0.7	0.804	(50)
TCONS_00023843	Up-regulated	Blood samples from 173 CAD patients and 151 healthy controls	Diagnostic marker	0.767	0.567	0.69	
NR_028044.1	Up-regulated	Blood samples from 173 CAD patients and 151 healthy controls	Diagnostic marker	0.6	0.833	0.739	

(Continued)

TABLE 4 | Continued

LncRNA	Expression pattern	Sample	Type of marker	ROC curve analysis			References
				Sensitivity	Specificity	Area under the curve (AUC)	
TCONS_00029157	Up-regulated	Blood samples from 173 CAD patients and 151 healthy controls	Diagnostic marker	0.667	0.833	0.769	
MIAT	Up-regulated	Blood samples from 110 CAD patients and 117 volunteers as controls	Diagnostic marker	95.5%	72.7%	0.888	(51)

circRNAs, whereas down-regulation has been shown in six circRNAs. Subsequently, authors have reported the role of nine circRNAs in the enhancement of TRPM3 expression through suppression of hsa-miR-130a-3p (64). Expression of circ-SATB2 has been shown to be increased in proliferative vascular smooth muscle cells in association with down-regulation of miR-939. Circ-SATB2 was able to augment expression of a target of miR-939, namely, STIM1. Up-regulation of circ-SATB2 decreases expression of SM22-α, a marker of contractile vascular smooth muscle cells. Functional studies verified the role of this circRNA in the regulation of differentiation, proliferation, apoptosis, and migration of vascular smooth muscle cells through enhancing STIM1 expression (65). Expression of circZNF609 has been shown to be reduced in peripheral blood leukocytes of CAD patients in correlation with levels of CRP and lymphocyte counts. Forced overexpression of circZNF609 has enhanced production of inflammatory cytokines IL-6 and TNF-α, while enhancing expression of IL-10. These effects are possibly mediated through sponging miRNAs (66). In an eminent study, Guo et al. (67) have assessed levels of hsa_circ_0002984, hsa_circ_0010283, and hsa_circ_0029589 in human peripheral blood mononuclear cell–originated macrophages from CAD patients and evaluated the consequences of overexpression or silencing of these circRNAs. Authors have reported down-regulation of hsa_circ_0029589 in macrophages, whereas up-regulation of the N6-methyladenosine levels of hsa_circ_0029589 in macrophages of patients with acute coronary syndrome has been shown. Notably, up-regulation of IRF-1 has diminished the expression of hsa_circ_0029589, but surged its m6A levels. Therefore, IRF-1 has been shown to enhance macrophage pyroptosis and inflammatory responses in acute coronary syndrome and atherosclerotic patients by obstructing circ_0029589 via increasing its m6A modifications (67). **Tables 6**, **7** show the list and function of up-regulated and down-regulated circRNAs in CAD, respectively.

Diagnostic Value of CircRNAs in CAD

ROC curve analysis has shown that hsa_circ_0001879 and hsa_circ_0004104 could differentiate CAD patients from healthy subjects with diagnostic values of 0.703 and 0.700, respectively. Notably, combination of expression levels of these circRNAs, in conjunction with CAD risk factors, could enhance the diagnostic power (63). Expression of circZNF609 has been shown to be reduced in peripheral blood leukocytes of CAD patients in correlation with levels of CRP and lymphocyte counts. In addition, down-regulation of circZNF609 has been associated with higher risks of CAD with accuracy of 0.761 (66). In a high-throughput circRNA profiling, Zhang et al. have demonstrated differential expression of 22 circRNAs between CAD patients and healthy subjects. Among these circRNAs, hsa_circ_0124644 has been shown to have the highest AUC value. Validation of their results in a larger cohort of CAD patients showed the diagnostic power of 0.769 for this circRNA (69). Combination of expression profile of certain circRNAs with conventional CAD risk factors has enhanced the diagnostic power (**Table 8**).

CircRNA Polymorphisms and CAD

Finally, SNPs within circRNAs can alter the risk of CAD. Zhou et al. (73) have appraised the impact of two SNPs at the circFOXO3 flanking introns in the development of CAD in a Chinese population. They reported the association between the rs12196996 G allele and elevated susceptibility to CAD. Moreover, such association was more remarkable among younger individuals and non-smokers. The haplotype rs12196996G-rs9398171C has also been associated with susceptibility to CAD. Functionally, the rs12196996 GG genotype conferred lower amounts of circFOXO3 expression (73).

DISCUSSION

CAD is a pathogenic condition in which several cell types and molecules are involved. In fact, this condition results from abnormal interactions between numerous cell types in the artery walls. The main participating factors in this process are accumulation of lipid deposits, endothelial cell dysfunction, macrophage induction, and changes in smooth muscle cells (5). Non-coding RNAs can influence almost every aspect of this pathogenic process. Dysregulation of several lncRNAs and circRNAs has been noted in CAD. ANRIL has been among the most assessed lncRNAs in CAD. Whereas, most studies have demonstrated up-regulation of ANRIL in patients with CAD or animal models of CAD (20, 22), a single study has reported down-regulation of certain transcript of ANRIL in CAD coronary arteries as compared with samples obtained from non-CAD arteries (16). Therefore, transcript variants of lncRNAs might

TABLE 5 | LncRNAs polymorphisms and CAD.

LncRNA	Polymorphism	Samples	Population	Assay method	Association	References
ANRIL	rs1330049, rs2383206, rs10757278, rs10757274	Blood samples from 1,034 CAD patients and 1,034 healthy subjects	Asian Indians	TaqMan allelic discrimination assay	All of these SNPs were associated with CAD risk	(52)
ANRIL	rs2383207, rs1333049	Blood samples from 550 CAD patients, 550 patients with ischemic stroke, and 550 healthy individuals	Han Chinese	Sequenom MassARRAY on an Agena platform	There was no association between theses SNPs and CAD predisposition	(56)
ANRIL	rs496892, rs7865618	Blood samples from 100 patients with periodontitis (PD) and CAD and 100 healthy volunteers as controls	South Indian population	ARMS-PCR, PCR-RFLP	Both of these polymorphisms were associated with elevated risk of PD and CAD Also rs496892-rs7865618 A-G and rs496892-rs7865618 G-G haplotypes were associated with increased risk of PD and CAD	(53)
ANRIL	rs564398, rs4977574, rs2891168, rs1333042	Blood samples from 250 patients with CAD and 252 age-matched control subjects	Saudi Population	TaqMan assay	Distribution of these SNPs were different in CAD group and control group	(57)
ANRIL	rs1333040, rs1004638	Blood samples from 200 patients with CAD 110 healthy subjects	Iranian	PCR-RFLP	There was no association between these SNPs and CAD susceptibility	(54)
H19	rs2735971, rs3024270, rs2839698	Blood samples from 366 CAD patients and 366 matched control individuals	Chinese	KASP platform	Genotypes of rs2735971 and rs3024270 were associated with reduced risk of CAD Also rs2735971-rs2839698-rs3024270 A-C-C haplotype was associated with decreased risk of CAD.	(55)
H19	rs217727, rs2067051	Blood samples from 701 patients with CAD and 873 age- and gender-matched control individuals	Chinese	TaqMan real time PCR	A allele of rs2067051 was associated with reduced risk of CAD, but T allele of rs217727 was correlated with elevated CAD risk.	(58)
LINC00841	rs1870634	Blood samples from 155 patients with CAD and 112 age- and sex-matched subjects without CAD	Iranian	real-time PCR-HRM	GG genotype of rs1870634 was correlated with augmented risk of CAD	(59)
MALAT1	rs619586	Blood samples from 508 patients with CAD and 562 age-, sex-, and ethnicity-matched control individuals	Chinese	TaqMan allelic discrimination assay	G allele and AG/GG genotypes of rs619586 were associated with decreased risk of CAD	(60)
lincRNA-p21	rs9380586, rs4713998, rs6930083, rs6931097	Blood samples from 615 CAD patients and 655 control subjects	Han Chinese	PCR-LDR	rs9380586-rs4713998-rs6930083-rs6931097 G-A-A-G haplotype was associated with decreased CAD risk	(61)
SENCR	rs555172	Blood samples from 150 CAD patients and 149 healthy controls	Iranian	ARMS-PCR	There was no association between rs555172 polymorphism and CAD predisposition	(62)

TABLE 6 | List of up-regulated circRNAs in CAD.

CircRNAs	Samples	Assessed cell line	Gene/protein interaction	Association with clinical features	Function	References
Hsa_circ_0004104	Blood samples from 436 male patients with CAD 297 male control subjects	THP-1	–	HDL-C levels	Its up-regulation was implicated in CAD pathogenesis and dysregulates proatherosclerotic and antiatherosclerotic genes expression	(63)
circ-SATB2	–	VSMCs	STIM1	–	Regulates proliferation, migration, and apoptosis in VSMCs by up-regulating expression of STIM1	(65)
hsa_circ_0089378 *hsa_circ_0083357* *hsa_circ_0082824* *hsa_circ_0068942* *hsa_circ_0057576* *hsa_circ_0054537* *hsa_circ_0051172* *hsa_circ_0032970* *hsa_circ_0006323*	651 CAD patients and 287 control subjects	–	hsa-miR-130a-3p	–	Theses circRNAs suppress expression of hsa-miR-130a-3p and thus up-regulate expression of TRPM3 in CAD patients	(64)
circ_RUSC2	–	VSMCs	SYK	–	Promotes migration and invasion of VSMCs by up-regulating SYK expression	(68)

TABLE 7 | List of down-regulated circRNAs in CAD.

CircRNAs	Samples	Assessed cell line	Association with clinical features	Function	References
circZNF609	Blood samples from (peripheral blood leukocytes) 330 patients with CAD and 209 control individuals	RAW264.7	C-reactive protein levels, lymphocyte counts	Its overexpression contributes to decreased expression of IL-6 and TNF-α and increased expression of IL-10	(66)
hsa_circ_0029589	Blood samples (PBMCs) from 24 patients with clinical presentation of chest pain, 16 patients with stable angina, and 28 patients with acute coronary syndrome	–	–	Its overexpression decreased pyroptosis of macrophages	(67)

have different tissue specificity and diverse functional roles. Such detailed analysis of transcript variants has not been performed for other lncRNAs in the context of CAD.

Dysregulated lncRNAs in CAD patients have functional interactions with Wnt/β-catenin, NF-κB, TGF-βR1/Smad, JAK/STAT, PTEN/AKT, and mTOR signaling pathways. Therefore, these signaling pathways are putative targets for therapeutic manipulations in CAD. Comprehensive studies are needed to explore the interactions between all mentioned lncRNAs and these pathways to find the most appropriate lncRNA for therapeutic interventions. The lncRNAs with the most robust interactions with higher numbers of these pathways are probably the most suitable targets. Moreover, CAD-related lncRNAs have interactions with a number of miRNAs such as miR-181b, let-7b, miR-544a, miR-34a, miR-33b, miR-26a, miR-27b, miR-21, miR-128, and miR-33a, suggesting the complicated interactions between diverse non-coding RNAs in the context of CAD. Identification of this multifaceted interaction network is

TABLE 8 | Diagnostic Role of circRNAs in CAD.

CircRNAs	Expression pattern	Samples	ROC curve analysis			References
			Sensitivity	Specificity	AUC	
Hsa_circ_0004104	Up-regulated	Blood samples from (PBMCs) 436 male patients with CAD 297 male control subjects	–	–	0.700	(70)
Hsa_circ_0001879	Up-regulated	Blood samples from (PBMCs) 436 male patients with CAD 297 male control subjects	–	–	0.703	
Hsa_circ_0004104 *Hsa_circ_0001879*	Up-regulated Up-regulated	Blood samples from (PBMCs) 436 male patients with CAD 297 male control subjects	–	–	0.742	
Hsa_circ_0004104 *Hsa_circ_0001879* together with smoking, TC and serum creatinine	Up-regulated Up-regulated	Blood samples from (PBMCs) 436 male patients with CAD 297 male control subjects	–	–	0.832	
Hsa_circ_0124644	Up-regulated	Blood samples from 179 CAD patients and 157 control individuals	0.861	0.626	0.769	(69)
Hsa_circ_0124644 along with smoking, hypertension, DM, LDL, and TC	Up-regulated	Blood samples from 179 CAD patients and 157 control individuals	0.759	0.704	0.804	
Hsa_circ_0124644 *Hsa_circ_0098964*	Up-regulated Up-regulated	Blood samples from 179 CAD patients and 157 control individuals	0.825	0.730	0.811	
Hsa_circ_0124644 *Hsa_circ_0098964* along with smoking, hypertension, DM, LDL, and TC	Up-regulated Up-regulated	Blood samples from 179 CAD patients and 157 control individuals	0.832	0.696	0.843	
hsa_circ_0005540	Up-regulated	Plasma exosomes 108 patients with CAD and 89 subjects without CAD	–	–	0.853	(71)
circ-YOD1	Up-regulated	Analysis of 7 CAD-related microarray datasets	–	–	0.824	(72)
circZNF609	Down-regulated	Blood samples from (peripheral blood leukocytes) 330 patients with CAD and 209 control individuals	–	–	0.761	(66)

a prerequisite for the development of anti-CAD strategies. Such network has a practical significance in the design of prognostic or diagnostic panels.

Functional studies have confirmed the causal effects of lncRNAs/circRNAs in the pathogenesis of CAD, as the ectopic expression of these transcripts in human endothelial cells has led to dysregulation of proliferation, cell cycle transition, and migration in the favor of CAD development. Moreover, altered expression of these transcripts in immune cells has provoked immune responses and suppressed anti-inflammatory cytokines. A number of additional lncRNAs/circRNAs have functional impact on deposition of lipid in the vessels as demonstrated by *in vivo* experiments. The synergic effects of these transcripts in the pathobiology of CAD should also be evaluated in functional studies through establishment of double-knockout models.

Some SNPs within lncRNAs have been related with risk of CAD in certain populations. However, the results of these studies have not been replicated in other populations. Therefore, these data are not sufficient to propose these SNPs as markers for CAD in a pan-ethnic scale. Moreover, assessment of haplotypes of these SNPs and their association with risk of CAD would provide more reliable results in this regard.

In addition, circRNAs could partake in the development of CAD via modulation of proliferation, differentiation, or

apoptosis in CAD-related cells such as vascular smooth muscle cells. Such roles may be mediated through modulation of expression of several target genes, particularly miRNAs. Similar to lncRNAs, circRNAs can serve as molecular sponges for miRNAs. Expression levels of some circRNAs can be used as diagnostic markers in CAD.

In brief, CAD has been associated with dysregulation of numerous lncRNAs and circRNAs. Moreover, these kinds of non-coding transcripts can be used as markers for prediction of risk of CAD and disease course. The potential of these transcripts as therapeutic targets should be appraised in upcoming investigations. The most important limitation of studies that assessed the functional role of lncRNAs/circRNAs in the pathogenesis of CAD is that they are mostly dependent on cell line studies or animal studies whose generalization to human subjects is not easy. Moreover, the consequences of the observed altered expression of lncRNAs/circRNAs in human subjects should be assessed in follow-up studies. Finally, the association between lncRNAs/circRNAs signature and response to the therapeutic option in CAD patients including coronary artery bypass graft, percutaneous coronary intervention, and medical therapies should be assessed in upcoming studies.

AUTHOR CONTRIBUTIONS

MT and SG-F wrote the draft and revised it. MG collected the data and designed the tables. MT designed the figures. All the authors approved the submitted version.

REFERENCES

1. Sanchis-Gomar F, Perez-Quilis C, Leischik R, Lucia A. Epidemiology of coronary heart disease and acute coronary syndrome. *Ann Transl Med.* (2016) 4:256. doi: 10.21037/atm.2016.06.33
2. Matsuzawa Y, Lerman A. Endothelial dysfunction and coronary artery disease: assessment, prognosis, and treatment. *Coron Artery Dis.* (2014) 25:713–24. doi: 10.1097/MCA.0000000000000178
3. Ding L, Su XX, Zhang WH, Xu YX, Pan XF. Gene expressions underlying mishandled calcium clearance and elevated generation of reactive oxygen species in the coronary artery smooth muscle cells of chronic heart failure rats. *Chin Med J.* (2017) 130:460–9. doi: 10.4103/0366-6999.199825
4. Nurnberg ST, Cheng K, Raiesdana A, Kundu R, Miller CL, Kim JB, et al. Coronary artery disease associated transcription factor TCF21 regulates smooth muscle precursor cells that contribute to the fibrous cap. *PLoS Genet.* (2015) 11:e1005155. doi: 10.1371/journal.pgen.1005155
5. Zhang Y, Zhang L, Wang Y, Ding H, Xue S, Qi H, et al. MicroRNAs or long noncoding RNAs in diagnosis and prognosis of coronary artery disease. *Aging Dis.* (2019) 10:353–66. doi: 10.14336/AD.2018.0617
6. Pan RY, Zhao CH, Yuan JX, Zhang YJ, Jin JL, Gu MF, et al. Circular RNA profile in coronary artery disease. *Am J Transl Res.* (2019) 11:7115–25. doi: 10.2139/ssrn.3398517
7. Esteller M. Non-coding RNAs in human disease. *Nat Rev Genet.* (2011) 12:861–74. doi: 10.1038/nrg3074
8. Fang Y, Fullwood MJ. Roles, functions, and mechanisms of long non-coding RNAs in cancer. *Genom Proteom Bioinform.* (2016) 14:42–54. doi: 10.1016/j.gpb.2015.09.006
9. Kashi K, Henderson L, Bonetti A, Carninci P. Discovery and functional analysis of lncRNAs: methodologies to investigate an uncharacterized transcriptome. *Biochim Biophys Acta Gene Regul Mechan.* (2016) 1859:3–15. doi: 10.1016/j.bbagrm.2015.10.010
10. Lasda E, Parker R. Circular RNAs: diversity of form and function. *RNA.* (2014) 20:1829–42. doi: 10.1261/rna.047126.114
11. Gabory A, Jammes H, Dandolo L. The H19 locus: role of an imprinted non-coding RNA in growth and development. *Bioessays.* (2010) 32:473–80. doi: 10.1002/bies.200900170
12. Gao Y, Wu F, Zhou J, Yan L, Jurczak MJ, Lee HY, et al. The H19/let-7 double-negative feedback loop contributes to glucose metabolism in muscle cells. *Nucleic Acids Res.* (2014) 42:13799–81. doi: 10.1093/nar/gku1160
13. Yao Y, Xiong G, Jiang X, Song T. The overexpression of lncRNA H19 as a diagnostic marker for coronary artery disease. *Rev Assoc Méd Bras.* (2019) 65:110–7. doi: 10.1590/1806-9282.65.2.110
14. Cai Y, Yang Y, Chen X, He D, Zhang X, Wen X, et al. Circulating "LncPPARδ" from monocytes as a novel biomarker for coronary artery diseases. *Medicine.* (2016) 95:e2360. doi: 10.1097/MD.0000000000002360
15. Xu Y, Shao B. Circulating lncRNA IFNG-AS1 expression correlates with increased disease risk, higher disease severity and elevated inflammation in patients with coronary artery disease. *J Clin Lab Anal.* (2018) 32:e22452. doi: 10.1002/jcla.22452
16. Cho H, Shen GQ, Wang X, Wang F, Archacki S, Li Y, et al. Long noncoding RNA ANRIL regulates endothelial cell activities associated with coronary artery disease by up-regulating CLIP1, EZR, and LYVE1 genes. *J Biol Chem.* (2019) 294:3881–98. doi: 10.1074/jbc.RA118.005050
17. Hu YW, Guo FX, Xu YJ, Li P, Lu ZF, McVey DG, et al. Long noncoding RNA NEXN-AS1 mitigates atherosclerosis by regulating the actin-binding protein NEXN. *J Clin Invest.* (2019) 129:1115–28. doi: 10.1172/JCI98230
18. Ebadi N, Ghafouri-Fard S, Taheri M, Arsang-Jang S, Parsa SA, Omrani MD. Dysregulation of autophagy-related lncRNAs in peripheral blood of coronary artery disease patients. *Eur J Pharmacol.* (2020) 867:172852. doi: 10.1016/j.ejphar.2019.172852
19. Chen J, Dang J. LncRNA CASC11 was downregulated in coronary artery disease and inhibits transforming growth factor-β 1. *J Int Med Res.* (2020) 48:300060519889187. doi: 10.1177/0300060519889187
20. Guo F, Tang C, Li Y, Liu Y, Lv P, Wang W, et al. The interplay of Lnc RNA ANRIL and miR-181b on the inflammation-relevant coronary artery disease through mediating NF-κB signalling pathway. *J Cell Mol Med.* (2018) 22:5062–75. doi: 10.1111/jcmm.13790
21. Liu X, Li S, Yang Y, Sun Y, Yang Q, Gu N, et al. The lncRNA ANRIL regulates endothelial dysfunction by targeting the let-7b/TGF-βR1 signalling pathway. *J Cell Physiol.* (2020) 236:2058–69. doi: 10.1002/jcp.29993
22. Arslan S, Berkan Ö, Lalem T, Özbilüm N, Göksel S, Korkmaz Ö, et al. Long non-coding RNAs in the atherosclerotic plaque. *Atherosclerosis.* (2017) 266:176–81. doi: 10.1016/j.atherosclerosis.2017.10.012
23. Zhuang J, Peng W, Li H, Wang W, Wei Y, Li W, et al. Methylation of p15 INK4b and expression of ANRIL on chromosome 9p21 are associated with coronary artery disease. *PLoS ONE.* (2012) 7:e47193. doi: 10.1371/journal.pone.0047193
24. Kallen AN, Zhou XB, Xu J, Qiao C, Ma J, Yan L, et al. The imprinted H19 lncRNA antagonizes let-7 microRNAs. *Mol Cell.* (2013) 52:101–12. doi: 10.1016/j.molcel.2013.08.027
25. Alikhah A, Kakhki MP, Ahmadi A, Dehghanzad R, Boroumand MA, Behmanesh M. The role of lnc-DC long non-coding RNA and SOCS1 in the regulation of STAT3 in coronary artery disease and type 2 diabetes mellitus. *J. Diabetes Complicat.* (2018) 32:258–65. doi: 10.1016/j.jdiacomp.2017.12.001
26. Shang J, Li Q, Zhang J, Yuan H. FAL1 regulates endothelial cell proliferation in diabetic arteriosclerosis through PTEN/AKT pathway. *Eur Rev Med Pharmacol Sci.* (2018) 22:6492–9. doi: 10.26355/eurrev_201810_16063
27. Zhao Y, Feng G, Wang Y, Yue Y, Zhao W. Regulation of apoptosis by long non-coding RNA HIF1A-AS1 in VSMCs: implications for TAA pathogenesis. *Int J Clin Exp Pathol.* (2014) 7:7643–52.
28. Zhang L, Zhou C, Qin Q, Liu Z, Li P. LncRNA LEF1-AS1 regulates the migration and proliferation of vascular smooth muscle cells by targeting miR-544a/PTEN axis. *J Cell Biochem.* (2019) 120:14670–8. doi: 10.1002/jcb.28728

29. Wu Z, He Y, Li D, Fang X, Shang T, Zhang H, et al. Long noncoding RNA MEG3 suppressed endothelial cell proliferation and migration through regulating miR-21. *Am J Transl Res.* (2017) 9:3326–35.
30. Ma Q, Gao Y, Xu P, Li K, Xu X, Gao J, et al. Atorvastatin inhibits breast cancer cells by downregulating PTEN/AKT pathway via promoting ras homolog family member B (RhoB). *Biomed Res Int.* (2019) 2019:3235021. doi: 10.1155/2019/3235021
31. Hu YW, Yang JY, Ma X, Chen ZP, Hu YR, Zhao JY, et al. A lincRNA-DYNLRB2-2/GPR119/GLP-1R/ABCA1-dependent signal transduction pathway is essential for the regulation of cholesterol homeostasis. *J Lipid Res.* (2014) 55:681–97. doi: 10.1194/jlr.M044669
32. Hennessy EJ, van Solingen C, Scacalossi KR, Ouimet M, Afonso MS, Prins J, et al. The long noncoding RNA CHROME regulates cholesterol homeostasis in primates. *Nat Metab.* (2019) 1:98–110. doi: 10.1038/s42255-018-0004-9
33. Li X, Hou L, Cheng Z, Zhou S, Qi J, Cheng J. Overexpression of GAS5 inhibits abnormal activation of Wnt/β-catenin signaling pathway in myocardial tissues of rats with coronary artery disease. *J Cell Physiol.* (2019) 234:11348–59. doi: 10.1002/jcp.27792
34. Cai Y, Yang Y, Chen X, Wu G, Zhang X, Liu Y, et al. Circulating 'lncRNA OTTHUMT00000387022'from monocytes as a novel biomarker for coronary artery disease. *Cardiovasc Res.* (2016) 112:714–24. doi: 10.1093/cvr/cvw022
35. Wang H, Jin Z, Pei T, Song W, Gong Y, Chen D, et al. Long noncoding RNAs C2dat1 enhances vascular smooth muscle cell proliferation and migration by targeting MiR-34a-5p. *J Cell Biochem.* (2019) 120:3001–8. doi: 10.1002/jcb.27070
36. Qi H, Shen J, Zhou W. Up-regulation of long non-coding RNA THRIL in coronary heart disease: prediction for disease risk, correlation with inflammation, coronary artery stenosis, and major adverse cardiovascular events. *J Clin Lab Anal.* (2020) 34:e23196. doi: 10.1002/jcla.23196
37. Liao B, Chen R, Lin F, Mai A, Chen J, Li H, et al. Long noncoding RNA HOTTIP promotes endothelial cell proliferation and migration via activation of the Wnt/β-catenin pathway. *J Cell Biochem.* (2018) 119:2797–805. doi: 10.1002/jcb.27284
38. Cai C, Zhu H, Ning X, Li L, Yang B, Chen S, et al. LncRNA ENST00000602558.1 regulates ABCG1 expression and cholesterol efflux from vascular smooth muscle cells through a p65-dependent pathway. *Atherosclerosis.* (2019) 285:31–9. doi: 10.1016/j.atherosclerosis.2019.04.204
39. Wang X, Zhao Z, Zhang W, Wang Y. Long noncoding RNA LINC00968 promotes endothelial cell proliferation and migration via regulating miR-9-3p expression. *J Cell Biochem.* (2019) 120:8214–21. doi: 10.1002/jcb.28103
40. Yan H, Bu S, Zhou W, Mai Y. TUG1 promotes diabetic atherosclerosis by regulating proliferation of endothelial cells via Wnt pathway. *Eur Rev Med Pharmacol Sci.* (2018) 22:6922–9. doi: 10.26355/eurrev_201810_16162
41. Yin Q, Wu A, Liu M. Plasma long non-coding RNA (lncRNA) GAS5 is a new biomarker for coronary artery disease. *Med Sci Monit.* (2017) 23:6042–8. doi: 10.12659/MSM.907118
42. Bai Y, Zhang Q, Su Y, Pu Z, Li K. Modulation of the proliferation/apoptosis balance of vascular smooth muscle cells in atherosclerosis by lncRNA-MEG3 via regulation of miR-26a/Smad1 axis. *Int Heart J.* (2019) 60:444–50. doi: 10.1536/ihj.18-195
43. Wu G, Cai J, Han Y, Chen J, Huang ZP, Chen C, et al. LincRNA-p21 regulates neointima formation, vascular smooth muscle cell proliferation, apoptosis, and atherosclerosis by enhancing p53 activity. *Circulation.* (2014) 130:1452–65. doi: 10.1161/CIRCULATIONAHA.114.011675
44. Hu Y, Hu J. Diagnostic value of circulating lncRNA ANRIL and its correlation with coronary artery disease parameters. *Braz J Med Biol Res.* (2019) 52:e8309. doi: 10.1590/1414-431x20198309
45. Yari M, Bitarafan S, Broumand MA, Fazeli Z, Rahimi M, Ghaderian SMH, et al. Association between long noncoding RNA ANRIL expression variants and susceptibility to coronary artery disease. *Int J Mol Cell Med.* (2018) 7:1. doi: 10.1590/1414-431X20198309
46. Yang Y, Cai Y, Wu G, Chen X, Liu Y, Wang X, et al. Plasma long non-coding RNA, CoroMarker, a novel biomarker for diagnosis of coronary artery disease. *Clin Sci.* (2015) 129:675–85. doi: 10.1042/CS20150121
47. Lai Z, Lin P, Weng X, Su J, Chen Y, He Y, et al. MicroRNA-574-5p promotes cell growth of vascular smooth muscle cells in the progression of coronary artery disease. *Biomed Pharmacother.* (2018) 97:162–7. doi: 10.1016/j.biopha.2017.10.062
48. Zhang Z, Gao W, Long QQ, Zhang J, Li YF, Yan JJ, et al. Increased plasma levels of lncRNA H19 and LIPCAR are associated with increased risk of coronary artery disease in a Chinese population. *Sci Rep.* (2017) 7:7491. doi: 10.1038/s41598-017-07611-z
49. Zhang Y, Zhang L, Wang Y, Ding H, Xue S, Yu H, et al. KCNQ 1 OT 1, HIF 1A-AS 2 and APOA 1-AS are promising novel biomarkers for diagnosis of coronary artery disease. *Clin Exp Pharmacol Physiol.* (2019) 46:635–42. doi: 10.1111/1440-1681.13094
50. Li X, Zhao Z, Gao C, Rao L, Hao P, Jian D, et al. Identification of a peripheral blood Long non-coding RNA (Upperhand) as a potential diagnostic marker of coronary artery disease. *Cardiol J.* (2018) 25:393–402. doi: 10.5603/CJ.a2017.0133
51. Toraih EA, El-Wazir A, Alghamdi SA, Alhazmi AS, El-Wazir M, Abdel-Daim MM, et al. Association of long non-coding RNA MIAT and MALAT1 expression profiles in peripheral blood of coronary artery disease patients with previous cardiac events. *Genet Mol Biol.* (2019) 42:509–18. doi: 10.1590/1678-4685-gmb-2018-0185
52. Shanker J, Arvind P, Jambunathan S, Nair J, Kakkar VV. Genetic analysis of the 9p21. 3 CAD risk locus in Asian Indians. *Thromb Haemost.* (2014) 112:960–9. doi: 10.1160/TH13-08-0706
53. Mangalarapu M, Vinukonda S, Komaravalli PL, Nagula P, Koduganti RR, Korripally P, et al. Association of CDKN2BAS gene polymorphism with periodontitis and coronary artery disease from south Indian population. *Gene.* (2019) 710:324–32. doi: 10.1016/j.gene.2019.06.002
54. Khademi KG, Foroughmand AM, Galehdari H, Yazdankhah S, Borujeni MP, Shahbazi Z, et al. Association study of rs1333040 and rs1004638 polymorphisms in the 9p21 locus with coronary artery disease in Southwest of Iran. *Iran Biomed J.* (2016) 20:122–7. doi: 10.7508/ibj.2016.02.008
55. Hu WN, Ding HX, Xu Q, Zhang XY, Yang DT, Jin YZ. Relationship between long noncoding RNA H19 Polymorphisms and risk of coronary artery disease in a chinese population: a case-control study. *Dis Markers.* (2020) 2020:9839612. doi: 10.1155/2020/9839612
56. Yang J, Gu L, Guo X, Huang J, Chen Z, Huang G, et al. LncRNA ANRIL expression and ANRIL gene polymorphisms contribute to the risk of ischemic stroke in the Chinese han population. *Cell Mol Neurobiol.* (2018) 38:1253–69. doi: 10.1007/s10571-018-0593-6
57. AbdulAzeez S, Al-Nafie AN, Al-Shehri A, Borgio JF, Baranova EV, Al-Madan MS, et al. Intronic polymorphisms in the CDKN2B-AS1 gene are strongly associated with the risk of myocardial infarction and coronary artery disease in the Saudi population. *Int J Mol Sci.* (2016) 17:395. doi: 10.3390/ijms17030395
58. Gao W, Zhu M, Wang H, Zhao S, Zhao D, Yang Y, et al. Association of polymorphisms in long non-coding RNA H19 with coronary artery disease risk in a Chinese population. *Mutat Res.* (2015) 772:15–22. doi: 10.1016/j.mrfmmm.2014.12.009
59. Tarighi S, Alipoor B, Zare A, Ghaedi H, Shanaki M. Association of the rs1870634 variant in long intergenic non-protein coding RNA 841 with coronary artery disease: a GWAS-replication study in an Iranian population. *Biochem Genet.* (2018) 56:522–32. doi: 10.1007/s10528-018-9859-4
60. Wang G, Li Y, Peng Y, Tang J, Li H. Association of polymorphisms in MALAT1 with risk of coronary atherosclerotic heart disease in a Chinese population. *Lipids Health Dis.* (2018) 17:75. doi: 10.1007/978-981-13-0620-4
61. Tang SS, Cheng J, Cai MY, Yang XL, Liu XG, Zheng BY, et al. Association of lincRNA-p21 haplotype with coronary artery disease in a Chinese Han population. *Dis Markers.* (2016) 2016:9109743. doi: 10.1155/2016/9109743
62. Shahmoradi N, Nasiri M, Kamfiroozi H, Kheiry MA. Association of the rs555172 polymorphism in SENCR long non-coding RNA and atherosclerotic coronary artery disease. *J Cardiovasc Thorac Res.* (2017) 9:170–4. doi: 10.15171/jcvtr.2017.29
63. Wang L, Shen C, Wang Y, Zou T, Zhu H, Lu X, et al. Identification of circular RNA Hsa_circ_0001879 and Hsa_circ_0004104 as novel biomarkers for coronary artery disease. *Atherosclerosis.* (2019) 286:88–96. doi: 10.1016/j.atherosclerosis.2019.05.006
64. Pan RY, Liu P, Zhou HT, Sun WX, Song J, Shu J, et al. Circular RNAs promote TRPM3 expression by inhibiting hsa-miR-130a-3p in coronary artery disease patients. *Oncotarget.* (2017) 8:60280–90. doi: 10.18632/oncotarget.19941
65. Mao YY, Wang JQ, Guo XX, Bi Y, Wang CX. Circ-SATB2 upregulates STIM1 expression and regulates vascular smooth muscle cell proliferation

and differentiation through miR-939. *Biochem Biophys Res Commun*. (2018) 505:119–25. doi: 10.1016/j.bbrc.2018.09.069
66. Wang M, Li J, Cai J, Cheng L, Wang X, Xu P, et al. Overexpression of microRNA-16 alleviates atherosclerosis by inhibition of inflammatory pathways. *Biomed Res Int.* (2020) 2020:8504238. doi: 10.1155/2020/8504238
67. Guo M, Yan R, Ji Q, Yao H, Sun M, Duan L, et al. IFN regulatory Factor-1 induced macrophage pyroptosis by modulating m6A modification of circ_0029589 in patients with acute coronary syndrome. *Int Immunopharmacol.* (2020) 86:106800. doi: 10.1016/j.intimp.2020.106800
68. Sun J, Zhang Z, Yang S. Circ_RUSC2 upregulates the expression of miR-661 target gene SYK and regulates the function of vascular smooth muscle cells. *Biochem Cell Biol.* (2019) 97:709–14. doi: 10.1139/bcb-2019-0031
69. Zhao Z, Li X, Gao C, Jian D, Hao P, Rao L, et al. Peripheral blood circular RNA hsa_circ_0124644 can be used as a diagnostic biomarker of coronary artery disease. *Sci Rep.* (2017) 7:39918. doi: 10.1038/srep39918
70. Gao L, Zeng H, Zhang T, Mao C, Wang Y, Han Z, et al. MicroRNA-21 deficiency attenuated atherogenesis and decreased macrophage infiltration by targeting Dusp-8. *Atherosclerosis.* (2019) 291:78–86. doi: 10.1016/j.atherosclerosis.2019.10.003
71. Wu WZ, Pan YH, Cai MY, Cen JM, Chen C, Zheng L, et al. Plasma-derived exosomal circular RNA hsa_circ_0005540 as a novel diagnostic biomarker for coronary artery disease. *Dis Markers.* (2020) 2020:3178642. doi: 10.1155/2020/3178642
72. Miao L, Yin RX, Zhang QH, Liao PJ, Wang Y, Nie RJ, et al. A novel circRNA-miRNA-mRNA network identifies circ-YOD1 as a biomarker for coronary artery disease. *Sci Rep.* (2019) 9:18314. doi: 10.1038/s41598-019-54603-2
73. Zhou YL, Wu WP, Cheng J, Liang LL, Cen JM, Chen C, et al. CircFOXO3 rs12196996, a polymorphism at the gene flanking intron, is associated with circFOXO3 levels and the risk of coronary artery disease. *Aging.* (2020) 12:13076–89. doi: 10.18632/aging.103398

Conflict of Interest: The authors declare that the research was conducted in the absence of any commercial or financial relationships that could be construed as a potential conflict of interest.

frontiers in Cardiovascular Medicine

REVIEW
published: 12 April 2021
doi: 10.3389/fcvm.2021.632392

Role of MicroRNAs in the Pathogenesis of Coronary Artery Disease

Soudeh Ghafouri-Fard[1], *Mahdi Gholipour*[1] *and Mohammad Taheri*[2]*

[1] Department of Medical Genetics, Shahid Beheshti University of Medical Sciences, Tehran, Iran, [2] Urology and Nephrology Research Center, Shahid Beheshti University of Medical Sciences, Tehran, Iran

Coronary artery disease (CAD) is the main reason of cardiovascular mortalities worldwide. This condition is resulted from atherosclerotic occlusion of coronary arteries. MicroRNAs (miRNAs) are implicated in the regulation of proliferation and apoptosis of endothelial cells, induction of immune responses and different stages of plaque formation. Up-regulation of miR-92a-3p, miR-206, miR-216a, miR-574-5p, miR-23a, miR-499, miR-451, miR-21, miR-146a, and a number of other miRNAs has been reported in CAD patients. In contrast, miR-20, miR-107, miR-330, miR-383-3p, miR-939, miR-4306, miR-181a-5p, miR-218, miR-376a-3p, and miR-3614 are among down-regulated miRNAs in CAD. Differential expression of miRNAs in CAD patients has been exploited to design diagnostic or prognostic panels for evaluation of CAD patients. We appraise the recent knowledge about the role of miRNAs in the development of diverse clinical subtypes of CAD.

Keywords: coronary artery disease, miRNA, expression, biomarkers, myocardial infarction

OPEN ACCESS

Edited by:
Laiyuan Wang,
Chinese Academy of Medical Sciences and Peking Union Medical College, China

Reviewed by:
Zhi Xin Shan,
Guangdong Provincial People's Hospital, China
Chen Gao,
UCLA, United States

***Correspondence:**
Mohammad Taheri
mohammad_823@yahoo.com

Specialty section:
This article was submitted to General Cardiovascular Medicine, a section of the journal Frontiers in Cardiovascular Medicine

Received: *23 November 2020*
Accepted: *18 March 2021*
Published: *12 April 2021*

Citation:
Ghafouri-Fard S, Gholipour M and Taheri M (2021) Role of MicroRNAs in the Pathogenesis of Coronary Artery Disease. Front. Cardiovasc. Med. 8:632392. doi: 10.3389/fcvm.2021.632392

INTRODUCTION

Coronary artery disease (CAD) is the principal source of cardiovascular mortalities worldwide (1). In 2020, it is expected that 11.1 million patients die as a results of CAD related complications (2). Clinically, CAD has different categories ranging from stable angina pectoris to acute coronary syndromes which comprises unstable angina (UA) and myocardial infarction (MI) (3). The majority of MI cases are resulted from the establishment of acute intraluminal coronary thrombus inside an epicardial coronary artery and the subsequent occlusion of the coronary artery (4, 5). The acute coronary thrombosis results in a sudden decrease in the blood flow and induction of necrosis in the myocardial region which is takes the blood supply from this coronary artery (6). Some other cardiovascular pathologies might be associated with CAD. For instance, acute MI might lead to defects in functioning myocytes resulting in myocardial fibrosis and left ventricle dilatation. Subsequent induction of neurohormonal responses and left ventricle remodeling results in progressive weakening of the residual viable myocardium (7). Moreover, ischemic conditions leads to upsurge of endogenous catecholamines in the myocardial interstitial fluid which in turn increases myocardial apoptosis and fibrosis (8). Dysregulation of several microRNAs (miRNAs) has been displayed in different categories of CAD, potentiating these transcripts as biomarkers of this devastating condition (9). miRNAs have been shown to modulate gene expression at post transcriptional level via destroying mRNA targets or by obstructing their translation (10). Since each miRNA is capable of regulating expression of several transcripts, it is estimated that more than half of protein-coding genes in the human genome are influenced by miRNAs (11). Therefore,

miRNAs can affect numerous important biological and cellular function such as cell differentiation, proliferation, and cell death in the cardiovascular system (12). Understanding the role of miRNAs in the pathogenesis of CAD would lead to identification of appropriate therapies for this global health problem. We appraise the recent knowledge about the role of miRNAs in the development of diverse clinical subtypes of CAD.

miRNAs IN CAD

Function of miRNAs in CAD has been assessed in different cell types. Endothelial cells have been the mostly assessed cell type in this regard. Liu et al. have extracted circulating microvesicles (MVs) from plasma samples of CAD patients to assess signature of their miRNA constituents. Among miRNAs which were reported to regulate vascular performance, miR-92a-3p has been shown to be up-regulated in CAD cases compared with non-CAD individuals. MVs enclosing miR-92a-3p have been demonstrated to be mostly originated from endothelial cells. Treatment of these cells with oxidized LDL and IL-6 has resulted in up-regulation of miR-92a-3p levels in these cells and higher incorporation of this miRNA in MVs. Transport of these MVs to other endothelial cells has enhanced their migration and proliferation. miR-92a-3p exerts these functions through inhibition of expression of THBS1, the inhibitor of angiogenesis. Taken together, atherosclerosis enhances the incorporation of endothelial miR-92a-3p into MVs, which controls angiogenesis in recipient endothelial cells through a THBS1-associated route (13). Wang et al. have demonstrated up-regulation of miR-206 in endothelial progenitor cells as well as plasma samples gathered from CAD patients. However, expression levels of miR-206 have not been associated with clinicopathological characteristics of CAD patients. Functionally, miR-206 has been shown to inhibit the viability and invasion of endothelial progenitor cells in CAD patients, while enhancing apoptosis in these cells. miR-206 can also suppress expression of vascular endothelial growth factor (VEGF) (14). Moreover, this miRNA modulates endothelial progenitor cell functions through targeting the protein kinase PIK3C2α. This protein kinase has been shown to be down-regulated in endothelial progenitor cells of CAD patients. miR-206 silencing in these cells enhanced their angiogenic and vasculogenic capacities both *in vitro* and in an animal model of ischemia. Besides, miR-206 silencing enhanced activities of PIK3C2α, Akt, and endothelial nitric oxide synthase (15). miR-216a is another miRNA which is involved in endothelial aging and dysfunction through modulating expression of Smad3. Over-expression of miR-216a in human umbilical vein endothelial cells (HUVECs) has activated an untimely senescence-like feature in these cells which was accompanied by defects in proliferation and migration. The consequent suppression of Smad3 has resulted in enhancement of adhesion of these cells to monocytes, modulation of the destruction of NF-κB inhibitor alpha (IκBα) and stimulation of adhesion proteins. Levels of miR-216a has been shown to be elevated in the plasma samples of old CAD patients in association with higher susceptibility to CAD (16). **Figure 1** shows the cascade of involvement of miR-216a in CAD.

Gao et al. have demonstrated high concentrations of lipids, atherosclerotic index, apoptotic index, and KRT1-positive expression while suppression of Notch signaling pathway in the atherosclerotic mice. miR-107 has been shown to bind with KRT1, thus reducing its expression. This miRNA has been down-regulated in animal models of CAD (17). Ren et al. have reported down-regulation of miR-330 in CAD group. Overexpression of miR-330 has been shown to inhibit atherosclerotic plaques creation whereas enhancing proliferation of vascular endothelial cells through modulating MAPK8 via the WNT signaling pathway (18). Lian et al. have shown down-regulation of miR-383-3p and up-regulation of IL1R2 in myocardial tissues of atherosclerotic animals. Forced over-expression of miR-383-3p has reduced expression of IL1R2, caspase-1, IL-1β, IL-6, and IL-18, ameliorated cell apoptosis in the coronary artery endothelial cells, while enhanced IL-10 levels, cell survival, and tube construction (19). Hou et al. have reported down-regulation of miR-939 in the blood of patients with adequate coronary collateral circulation compared with those having insufficient coronary collateral circulation. Up-regulation of miR-939 in HUVECs has remarkably suppressed proliferation, adhesion and tube construction, while increasing migration capacity of these cells. γ-catenin has been identified as a direct target of miR-939 (20). Expressions of both miR-181a-5p and miR-181a-3p have been lower in the aorta plaque and plasma of animal models of CAD. Up-regulation of these miRNAs considerably delays atherosclerotic plaque development in animals. These miRNAs have functional roles in the reduction of expression of pro-inflammatory proteins and diminishing the infiltration of macrophage, leukocyte and T cell into the atherosclerotic plaques through suppression of adhesion molecule expressions in HUVECs (21). miR-376a-3p has also been down-regulated in CAD samples. *In vitro* studies have shown the effects of miR-376a-3p silencing in the suppression of proliferation of HUVECs through modulating NRIP1 expression (22). **Table 1** displays the functional roles of miRNAs in the development of CAD, based on the results of studies which have been conducted in endothelial cells.

Abbreviations: ARMS, Amplification-Refractory Mutation System; ANGII, angiotensinogen; TAB2, binding protein 2, CNVs, Copy Number Variations; CCL2, C-C motif chemokine ligand 2; copy number variations; CAD, Coronary artery disease; EPCs, endothelial progenitor cells; ET-1, endothelin 1;GEO, Gene Expression Omnibus; HF, heart failure; HRM, High resolution Melting; HUVECs, human umbilical vein endothelial cells; ICAM1, intercellular adhesion molecule 1; KRT1, keratin 1; LDL, low-density lipoprotein; LPS, lipopolysaccharide; miRNAs, MicroRNAs; MI, myocardial infarction; MVs, microvesicles; MAPK8, mitogen-activated protein kinase 8; MEF2C, myocyte enhancer factor 2C; MEF2C, myocyte enhancer factor 2C; IκBα, NF-κB inhibitor alpha; NRIP1, nuclear receptor interacting protein 1; eNOS, nitric oxide synthase 3; PBMCs, peripheral blood mononuclear cells; PIK3C2α, phosphatidylinositol-4-phosphate 3-kinase catalytic subunit type 2 alpha; PDCD4, programmed cell death 4; RFLP, Restriction fragment length polymorphism; STEMI, ST-segment elevation myocardial infarction; SNPs, single nucleotide polymorphisms; SMAD3, SMAD family member 3; SPF, specific-pathogen-free; THBS1, thrombospondin 1; MAP3K7, TGF-beta activated kinase 1; TxA2, thromboxane A2 TxA2; TRF2, telomeric repeat binding factor 2; TRAF6, TNF receptor associated factor 6; UA, unstable angina; VEGF, vascular endothelial growth factor; VSMCs, vascular smooth muscle cells; VCAM1, vascular cell adhesion molecule 1; ZDHHC14, zinc finger DHHC-type palmitoyltransferase 14.

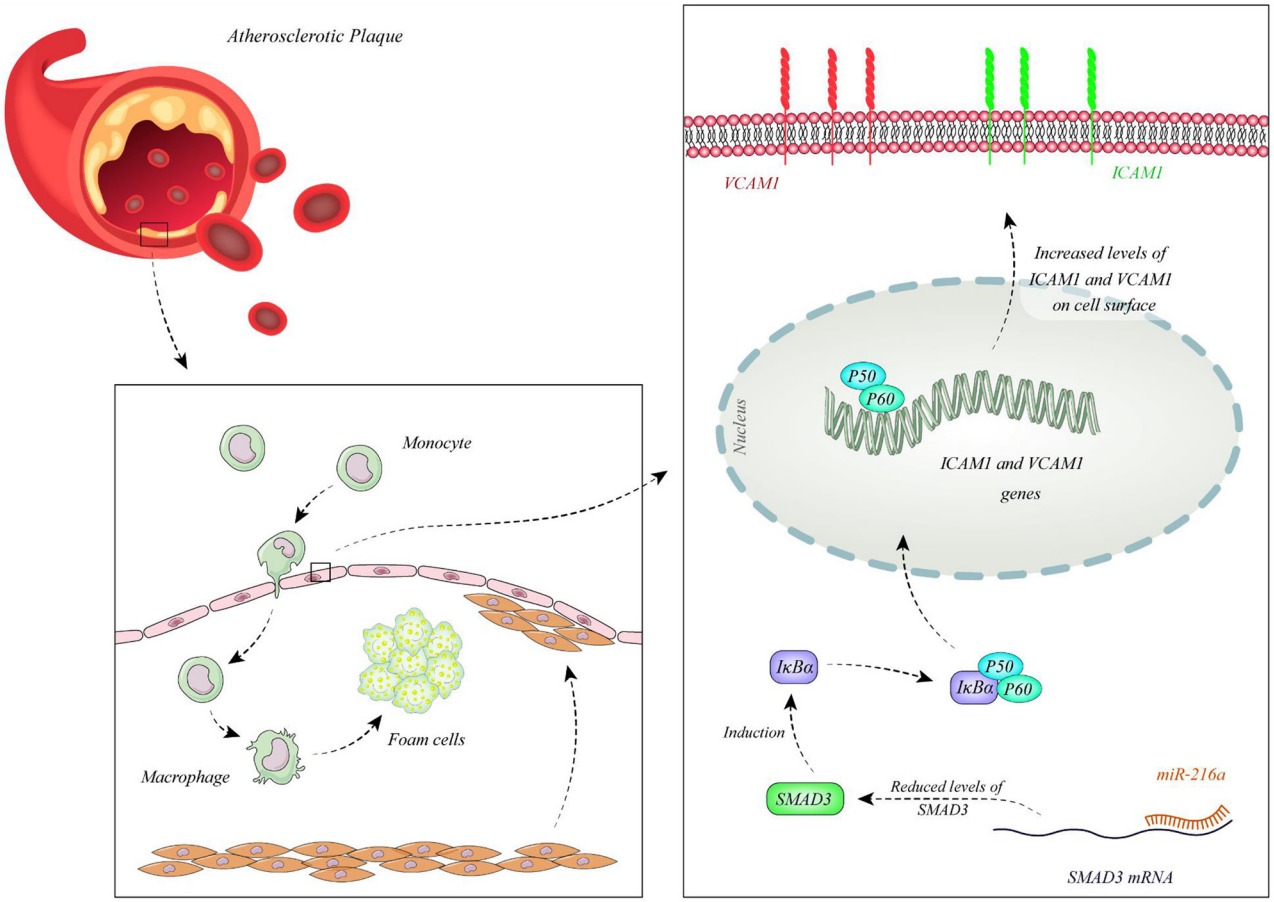

FIGURE 1 | miR-216a is over-expressed in CAD patients. miR-216a attaches to 3' UTR of Smad3 and decreases its levels. Down-regulation of Smad3 leads to reduction of IκBα releasing NF-κB and enhancing its nuclear transport. Subsequent up-regulation of ICAM1 and VCAM1 enhances attachment of monocytes to endothelial cells promoting development of CAD (16).

Lai et al. have reported over-expression of miR-574-5p in the serum samples and vascular smooth muscle cells (VSMCs) of CAD patients. Up-regulation of miR-574-5p has enhanced cell proliferation and suppressed apoptotic processes in VSMCs through targeting ZDHHC14 (27). Down-regulation of miR-146a has been demonstrated to attenuate apoptosis of vascular smooth muscle cells. Autologous injection of endothelial stem cells in a rat model of acute myocardial infarction has led to downregulation of miR-146a levels, reduction of apoptosis in the myocardial cells and decrease in infarct area. Such effects have been accompanied by up-regulation of VEGF (28). Expression of miR-93 has been increased in ventricle tissues and blood samples of mice model of MI. Moreover, miR-93 has been shown to be released from cardiomyocytes cultured in hypoxic conditions. miR-93 suppresses apoptotic processes and guards cardiomyocytes from ischemia/reperfusion damage. miR-93 silencing has deteriorated cardiac remodeling in these animal models. Thus, miR-93 over-expression and release from cardiomyocytes has been regarded as an adaptive mechanism following MI to attenuate cardiac remodeling and heart failure (29). miR-448 has been shown to be over-expressed in vascular smooth muscle cells (VSMCs) obtained from atherosclerotic plaques of coronary artery compared with those obtained from normal arteries. Expression of this miRNA is induced by PDGF-bb, a growth factor that enhances proliferation of VSMCs. MEF2C has been recognized as a direct target of miR-448 in VSMCs, though its down-regulation miR-448 enhances VSMCs migration (30). **Table 2** shows the list of CAD-related miRNAs whose function has been assessed in myocardial cells or vascular smooth muscle cells.

Wang et al. have reported down-regulation of miR-20 in animal models of CAD in association with over-expression of VEGF and PTEN. Levels of miR-20a have been up-regulated following exercise in CAD animals. Up-regulation of miR-20a has reduced levels of ET-1, TxA2, ANGII, PTEN and enhanced levels of eNOS, PGI2, and VEGF. miR-20a exerts its functions through binding with the 3′UTR of PTEN, thus enhancing cell survival and proliferation via induction of the PI3K/Akt signaling (31). Expression of miR-4306 has been decreased in platelets and platelet-originated microparticles of

TABLE 1 | CAD-related miRNAs whose function has been assessed in endothelial cells.

microRNA	Samples	Expression pattern	Assessed cell lines	Gene/protein interactions	Signaling pathway	Function	References
miR-92a-3p	Plasma circulating microvesicles from 41 angiographically excluded CAD patients, 77 patients with stable CAD and 62 patients with acute coronary syndrome	Up-regulated	ECs	THBS1	–	Its knockdown attenuates migration and proliferation of endothelial cells through increasing THBS1 expression	(13)
miR-206	Blood samples from 78 patients with CAD and 65 healthy controls	Up-regulated	EPCs (endothelial progenitor cells)	VEGF	–	Inhibits invasion and cell viability in EPCs can suppress expression of VEGF	(14)
miR-206	Endothelial progenitor cells collected from peripheral blood of 53 CAD patients and 34 healthy controls, Nude mice	Up-regulated	EPCs	PIK3C2α	–	Reduces migration and its knockdown rescued angiogenic and vasculogenic abilities of endothelial progenitor cells	(15)
miR-216a	Blood samples from 176 patients with CAD and 342 age-matched control individuals	Up-regulated	HUVECs	Smad3	–	Promotes monocytes adhesion, endothelial senescence and inflammation through regulating Smad3/IκBα axis	(16)
miR-499	Plasma samples from 216 CAD patients and 90 healthy individuals	Up-regulated	HUVECs	PDCD4	NF-Kβ/TNF-α signaling pathway	Promotes apoptosis rate and decreases survival rate of endothelial cells by reducing expression of PDCD4	(23)
miR-451	Blood samples form 30 patients with coronary heart disease and 30 healthy controls	Up-regulated	HUVECs	VEGFA	PI3K-Akt-mTOR pathway	Suppresses cell proliferation and induces apoptosis in HUVECs by targeting VEGFA	(24)
miR-107	80 specific-pathogen-free (SPF) Kunming mice	Down-regulated	vascular endothelial cells	KRT1	Notch signaling pathway	Its overexpression decreases apoptosis and inflammation so prevents atherosclerosis by targeting KRT1 and activating Notch signaling pathway	(17)
miR-330	Female specific pathogen free (SPF) rats with acute coronary syndrome	Down-regulated	vascular endothelial cells	MAPK8	WNT signaling pathway	Its overexpression inhibits formation of atherosclerotic plaques and promotes proliferation of vascular endothelial cells by targeting MAPK8	(18)
miR-939	Blood samples from 25 CAD patients with poor CCC and 22 CAD patients with sufficient CCC	Down-regulated	HUVECs	γ-catenin	–	Suppresses angiogenesis and abrogates vascular integrity by targeting γ-catenin	(20)
miR-181a-5p *miR-181a-3p*	Plasma samples from 15 CAD patients and 20 healthy controls, $ApoE^{-/-}$ mice	Down-regulated	HUVECs	TAB2, NEMO	NF-κB signaling pathway	miR-181a-5p and miR-181a-3p overexpression prevents endothelium inflammation and atherosclerosis progression by targeting TAB2 and NEMO, respectively. Also they suppresses expression of adhesion molecule	(21)

(Continued)

TABLE 1 | Continued

microRNA	Samples	Expression pattern	Assessed cell lines	Gene/protein interactions	Signaling pathway	Function	References
miR-376a-3p	Analysis of gene and microRNA expression profile datasets	Down-regulated	HUVECs	NRIP1	–	Its overexpression augmented cell proliferation by targeting NRIP1 in NRIP1	(22)
miR-495	Plasma samples form 30 CAD patients and 30 age and sex matched healthy controls	Down-regulated	HUVECs	CCL2	–	Regulated apoptosis and proliferation of HUVECs by targeting CCL2	(25)
miR-383-3p	30 male Sprague-Dawley (SD) rats with coronary artery atherosclerosis	Down-regulated	Coronary artery endothelial cells	IL1R2	–	Its upregulation reduces inflammatory cytokines expression and apoptosis rate in homocysteine-induced coronary artery endothelial cells by interacting with IL1R2	(19)
miR-218	Serum samples from 104 CAD patients and 101 healthy controls	Down-regulated	cardiac microvascular endothelial cells	–	–	Its upregulation promotes angiogenesis, cell proliferation and migration, enhances apoptosis rate and decreases inflammatory injury to CMECs	(26)

TABLE 2 | CAD-related miRNAs whose function has been assessed in myocardial cells or vascular smooth muscle cells.

microRNA	Samples	Expression pattern	Assessed cell lines	Gene/protein interactions	Signaling pathway	Function	References
miR-574-5p	Serum samples from 32 CAD patients and 30 normal individuals	Up-regulated	VSMCs	ZDHHC14	–	Suppresses apoptosis and promotes cell proliferation in VSMCs through targeting ZDHHC14	(27)
miR-146a	20 female Sprague-Dawley rats	Up-regulated	Myocardium	–	–	Injection of endothelial stem cell to rats with acute myocardial infarction caused decreased miR-146a expression and decreased cardiac apoptosis	(28)
miR-93	male C57BL/6 mice established as myocardial infarction (MI) models	Up-regulated	Cardiomyocytes	–	–	Suppresses apoptosis and promotes angiogenesis. Also has antioxidant effects	(29)
miR-448	atherosclerosis plaques and normal coronary artery tissues	Up-regulated	VSMCs	MEF2C	–	Promotes migration and proliferation of VSMCs by targeting MEF2C	(30)

CAD patients. Plasma miRNA-4306 has been mostly fractionated with microparticles rather than Argonaute2 complexes or HDL. These microparticles have the ability to transfer miR-4306 into human monocyte-derived macrophages, thus suppressing their migration and decreasing the quantity of macrophages in cardiac tissue in mouse model of MI. Mechanistically, miR-4306 binds with VEGFA to suppress ERK/NF-κB signaling (32). Expression of miR-23a has been higher in the peripheral blood mononuclear cells (PBMCs) of CAD patients compared with control subjects parallel with down-regulation of TRF2 levels. Aggressive lipid lowering therapy has reduced miR-23a, enhanced TRF2 expression and attenuated telomere erosion through this route (33). Expression of miR-3614 has been decreased by lipopolysaccharide (LPS) in macrophages, while LPS-associated inflammatory damage can be attenuated by up-regulation of miR-3614. This miRNA has been shown to target TRAF6 and suppress phosphorylation of kinases in the MAPK and NF-κB cascades Therefore, miR-3614/TRAF6/MAPK/NF-κB cascade can suppress devastating inflammatory responses (34). Animal studies have shown the role of miR-16 in reduction of development of atherosclerotic plaques and suppression of accretion of inflammatory factors while enhancement of release of anti-inflammatory factors. Mechanistically, miR-16 exerts these effects through downregulation of PDCD4 and activation of p38 and ERK1/2, while inactivation of JNK pathway (35). **Table 3** demonstrates the relevance of miRNAs with the pathogenesis of CAD through summarizing the results of studies which reported function of miRNAs in macrophages/monocytes.

DIAGNOSTIC/PROGNOSTIC SIGNIFICANCE OF miRNAs IN CAD

Altered levels of miRNA in the circulation of CAD patients potentiates their usage as biomarkers in this condition. Zhong et al. have demonstrated differential expressions of tens of miRNAs in patients with UA or ST-segment elevation MI compared with normal controls. Receiver operating characteristics (ROC) curves have revealed miR-142-3p and miR-17-5p as possible markers for diagnosis of these two classes of CAD. Moreover, differential expressed miRNAs have been correlated with the pathological events during the course of CAD (38). Vahed et al. have reported down-regulation of miR-21 in the PBMCs of patients with insignificant coronary artery stenosis compared with CAD patients or healthy subjects. Levels of this miRNA have been negatively correlated with the PTEN. Moreover, they reported a gradual elevation miR-25 expression from healthy subjects to those with insignificant coronary artery stenosis and CAD patients. Expression levels of miR-21 and miR-25 in the PBMCs could differentiate three groups of study participants (39). Yao et al. have demonstrated the capacity of miRNAs in distinguishing CAD patients with heart failure (HF) from those without HF. Among the most significantly dysregulated miRNAs between these two groups of patients have miR-221, miR-19b-5p, and miR-25-5p. Combination of expression levels of these miRNAs in PBMCs and hypertension have been significantly correlated with higher risk of HF risk in CAD patients (40). Another miRNA with promising results in diagnostic approaches is miR-122-5p which could differentiate unstable CAD patients from healthy controls with accuracy of 0.9, yet its accuracy in differentiation of stable patients from controls was not appropriate (41). A brief review of studies which demonstrated this function is presented in **Table 4**.

miRNA POLYMORPHISMS AND COPY NUMBER VARIATIONS IN CAD

Both single nucleotide polymorphisms (SNPs) and copy number variations (CNVs) within miRNA coding genes have been associated with risk of CAD. Sung et al. have examined the relation between miR-146a, miR-149, miR-196a2, and miR-499 SNPs and CAD in a Korean population. They have reported association between the miR-149 rs2292832 and miR-196a2 rs11614913 SNPs and this disorder. Notably, the miR-146a rs2910164 GG genotype has been more prevalent among CAD patients with more than two stents. Moreover, combination of miR-146a G, miR-149 T, miR-196a2 C, and mIR-499 G alleles has been considerably associated with CAD occurrence. Certain SNPs have been reported to increase susceptibility to CAD in different subclasses of study participants such as non-smokers, hypertensive and non-diabetic individuals (61). Sohrabifar et al. have evaluated the presence of CNVs of hsa-miR-93, hsa-miR-122, hsa-miR-192 in CAD patients with or without type 2 diabetes mellitus. They have reported remarkable differences in the distribution of CNVs of hsa-miR-93 between CAD and non-CAD as well as between diabetic CAD and diabetic non-CAD individuals. In addition, hsa-miR-122 CNVs have been differently distributed among three subgroups (62). The rs2292832 miR-149 has been associated with risk of CAD in Iranian population. However, this SNP does not either affect the secondary structure of pre-miR-149 or the stability of the miRNA hairpin structure (63). As this SNP is located outside the sequence of mature miR-149, it has been proposed that it might affect the maturation process and therefore decrease expression of miR-149 (64). T allele of rs2431697 in miR-146a has been associated with higher risk of CAD (65). In addition, the rs2910164 within this miRNA affects risk of CAD (61). This SNP resides in the precursor of miR-146a and results in down-regulation of levels of mature miR-146a (66). **Table 5** reviews the investigations which appraised the role of SNPs/CNVs in conferring risk of CAD.

CONCLUSIONS AND PERSPECTIVES

Aberrant expression of miRNAs in CAD patients has been recognized through high throughput sequencing methods in addition to candidate gene assays. An example of the former type of assays has been conducted through investigation of Gene Expression Omnibus (GEO) database showing frequent differential expression of 150 genes and 5 miRNAs (22). Luciferase reporter assays have shown the functional interactions between a number of miRNAs and mRNAs (24, 72). miRNAs can regulate development of CAD through different mechanisms

TABLE 3 | CAD-related miRNAs whose function has been assessed in macrophages/ monocytes.

microRNA	Samples	Expression pattern	Assessed cell lines	Gene/protein interactions	Signaling pathway	Function	References
miR-23a	Blood samples (PBMCs) from 104 CAD patients and 50 control subjects	Up-regulated	PBMCs	TRF2	–	Contributes to telomere shortening and cellular senescence through targeting TRF2	(33)
miR-4306	Blood samples (platelet-derived microparticles) form CAD patients (24 AMI patients and 16 patients with stable angina pectoris) and 20 controls, C57BL/6 mice	Down-regulated	Primary human monocyte-derived macrophages	–	VEGFA/ERK1/2/NF-κB signaling pathways	Suppresses migration of HMDMs by regulating VEGFA/ERK1/2/NF-κB signaling pathways	(32)
miR-3614	epicardial adipose tissue from 30 CAD patients and 30 controls	Down-regulated	THP-1 (monocyte)	TRAF6	–	Its overexpression regulated inflammatory responses by targeting TRAF6	(34)
miR-124	Plasma samples from 40 patients with CAD and 40 non-CAD individuals, ApoE$^{-/-}$ C57B/L6J mice	Down-regulated	RAW264.7 (mouse macrophage cell line)	p38	MAPK signaling pathway	Its overexpression decreased expression of pro-inflammatory cytokines and enhanced expression of anti-inflammatory cytokines	(36)
miR-16	Blood samples (plasma and PBMCs) from 40 patients with CAD and 40 non-CAD patients, 22 ApoE$^{-/-}$ mice	Down-regulated	Peripheral blood mononuclear cells	PDCD4	–	Its overexpression Suppresses atherosclerotic plaque formation and proinflammatory factors secretion and promotes release of anti-inflammatory factors	(35)
miR-21	Circulating monocytes from CAD patients and non-CAD patients, apoE$^{-/-}$ mice and miR-21$^{-/-}$apoE$^{-/-}$ mice	Up-regulated	Bone-marrow-derived macrophage	Dusp-8	–	Its knockout in mice caused decreased atherosclerotic lesions and smooth muscle cells in aorta also reduced macrophage migration and macrophage-endothelium interaction.	(37)

TABLE 4 | Diagnostic/prognostic significance of miRNAs in CAD (UA, unstable angina; STEMI: ST-segment elevation myocardial infarction).

microRNA	Expression pattern	Samples	Diagnostic/prognostic role	ROC curve analysis			References
				Sensitivity	Specificity	AUC	
miR-142-3p	Upregulated	Blood samples from 52 CAD patients and 26 normal subjects	Distinguishing UA patients from normal subjects	–	–	0.805	(38)
miR-142-3p	Upregulated	Blood samples from 52 CAD patients (including 26 patients with UA and 26 patients with STEMI) and 26 normal subjects	Distinguishing STEMI patients from normal subjects	–	–	0.840	
miR-17-5p	Upregulated	Blood samples from 52 CAD patients (including 26 patients with UA and 26 patients with STEMI) and 26 normal subjects	Distinguishing STEMI patients from normal subjects	–	–	0.845	
miR-223	Upregulated	Plasma samples from 300 patients with coronary heart disease and 100 controls	Diagnostic biomarker	0.86	0.913	0.933	(42)
miR-223-3 p	Upregulated	Serum samples from 314 patients with unstable CAD, 389 patients with stable CAD and 442 controls	Discriminating unstable CAD patients from controls	–	–	0.76	(41)
miR-122-5 p	Upregulated	Serum samples from 314 patients with unstable CAD, 389 patients with stable CAD and 442 controls	Discriminating unstable CAD patients from controls	–	–	0.90	
miR-223-3 p *miR-122-5 p* along with age and gender	Upregulated Upregulated	Serum samples from 314 patients with unstable CAD, 389 patients with stable CAD and 442 controls	discriminating unstable CAD patients from controls	–	–	0.96	
miR-122-5 p	Upregulated	Serum samples from 314 patients with unstable CAD, 389 patients with stable CAD and 442 controls	discriminating stable CAD patients from controls	–	–	0.63	
miR-223-3 p *miR-122-5 p* along with age and gender	Upregulated Upregulated	Serum samples from 314 patients with unstable CAD, 389 patients with stable CAD and 442 controls	Diagnostic biomarker (discriminating stable CAD patients from controls)	–	–	0.80	
miR-495-3p	Upregulated	Blood samples (PBMCs) from 114 patients with stable CAD(including patients with prethrombotic status (PTS) and patients without PTS) and 24 healthy volunteers as controls	Discriminating PTS patients from non-PTS patients	–	–	0.712	(43)
miR-34a-5p	Upregulated	Blood samples (PBMCs) from 114 patients with stable CAD(including patients with prethrombotic status (PTS) and patients without PTS) and 24 healthy volunteers as controls	Discriminating PTS patients from non-PTS patients	–	–	0.780	
miR-34a-5p along with fibrinogen	Upregulated	Blood samples (PBMCs) from 114 patients with stable CAD(including patients with prethrombotic status (PTS) and patients without PTS) and 24 healthy volunteers as controls	Discriminating PTS patients from non-PTS patients	–	–	0.885	

(Continued)

TABLE 4 | Continued

microRNA	Expression pattern	Samples	Diagnostic/prognostic role	ROC curve analysis			References
				Sensitivity	Specificity	AUC	
miR-93-5p along with FHS risk factors	Upregulated	Plasma samples from 50 patients with stable CAD, 50 patients with STEMI and 50 controls	Distinguishing CAD patients from controls	–	–	0.77	(44)
miR-499a-5p along with FHS risk factors	Upregulated	Plasma samples from 50 patients with stable CAD, 50 patients with STEMI, and 50 controls	Distinguishing STEMI patients from controls	–	–	0.93	
miR-146a	Upregulated	Plasma samples from 34 CAD patients with good coronary collateral circulation (CCC) and 44 CAD patients with poor CCC	Discriminating CAD patients with good and poor CCC	–	–	0.939	(45)
miR-208a	Upregulated	Plasma samples from 290 patients with coronary heart disease (CHD) and 110 individuals without CHD	Diagnostic biomarker	0.75	0.93	0.919	(46)
miR-208a	Upregulated	Plasma samples from 95 patients with CAD and 50 individual without CAD	Diagnostic biomarker	–	–	0.819	(45)
miR-370	Upregulated	Plasma samples from 95 patients with CAD and 50 individual without CAD	Diagnostic biomarker	–	–	0.745	
miR-208a *miR-370*	Upregulated Upregulated	Plasma samples from 95 patients with CAD and 50 individual without CAD	Diagnostic biomarker	–	–	0.856	
miR-21	Upregulated	Serum samples from 45 patients with diabetes mellitus (DM) and CAD, 45 patients with DM and heart failure (HF), 45 patients with DM, and 45 matched control subjects	discriminating CAD + DM group from controls	0.800	0.911	0.944	(47)
miR-21	Upregulated	Serum samples from 45 patients with diabetes mellitus (DM) and CAD, 45 patients with DM and heart failure (HF), 45 patients with DM, and 45 matched control subjects	discriminating CAD + DM group from DM group	0.778	0.667	0.755	
miR-21	Upregulated	Serum samples from 45 patients with diabetes mellitus (DM) and CAD, 45 patients with DM and heart failure (HF), 45 patients with DM, and 45 matched control subjects	discriminating CAD + DM form HF + DM group	0.711	0.511	0.640	
miR-21	Upregulated (in ACS patients compared with CAD patients)	50 patients with acute coronary syndrome (ACS) and 50 patients with stable CAD	Distinguishing ACS patients from CAD patients	–	–	0.775	(48)
miR-151-3p	Upregulated (in STEMI group)	Plasma samples from 20 patients with STEMI, 20 patients with stable CAD and 20 individuals without CAD	Distinguishing patients with STEMI form non-CAD individuals	–	–	0.758	(49)
miR-151-3p	Upregulated (in STEMI group)	Plasma samples from 20 patients with STEMI, 20 patients with stable CAD and 20 individuals without CAD	Distinguishing patients with STEMI form patients with stable CAD	–	–	0.754	

(Continued)

TABLE 4 | Continued

microRNA	Expression pattern	Samples	Diagnostic/prognostic role	ROC curve analysis			References
				Sensitivity	Specificity	AUC	
miR-331	Upregulated (in STEMI group)	Plasma samples from 20 patients with STEMI, 20 patients with stable CAD and 20 individuals without CAD	Distinguishing patients with STEMI form non-CAD individuals	–	–	0.790	
miR-331	Upregulated (in STEMI group)	Plasma samples from 20 patients with STEMI, 20 patients with stable CAD and 20 individuals without CAD	Distinguishing patients with STEMI form patients with stable CAD	–	–	0.773	
miR-221 *miR-25-5p* *miR-19b-5p*	Upregulated Upregulated Downregulated	50 CAD patients with heart failure and 48 CAD patients without heart failure	CAD patients with heart failure and CAD patients without heart failure	–	–	0.860	(40)
miR-221 *miR-25-5p* *miR-19b-5p* together with hypertension	Upregulated Upregulated Downregulated	50 CAD patients with heart failure and 48 CAD patients without heart failure	CAD patients with heart failure and CAD patients without heart failure	–	–	0.871	
miR-941	Upregulated	Blood samples from 56 CAD patients [18 patients with STEMI, 18 patients non-ST elevation ACS (NSTE-ACS), and 20 patients with stable angina (SA)] and 16 patients without CAD	Distinguishing STEMI patients form patients without CAD	–	–	0.896	(50)
miR-941	Upregulated	Blood samples from 56 CAD patients (18 patients with STEMI, 18 patients non-ST elevation ACS (NSTE-ACS) and 20 patients with stable angina (SA)) and 16 patients without CAD	distinguishing STEMI patients form patients with SA	–	–	0.808	
miR-941	Upregulated	Blood samples from 56 CAD patients [18 patients with STEMI, 18 patients non-ST elevation ACS (NSTE-ACS), and 20 patients with stable angina (SA)] and 16 patients without CAD	Distinguishing STEMI patients form patients with NSTE-ACS	–	–	0.781	
miR-133a	Upregulated (in patients with PMI)	Serum samples from 80 CAD patients (48 patients with periprocedural myocardial injury (PMI) after percutaneous coronary intervention (PCI) and 32 patients without PMI)	Prognostic biomarker (predicting occurrence of PMI)	0.938	0.719	0.891	(51)
miR-25	Upregulated	Blood samples (PBMCs) from 72 CAD patients, 30 patients with ICAD and 74 controls	Distinguishing CAD patients from controls)	0.85	0.78	0.83	(39)
miR-25	Upregulated		Distinguishing CAD patients from patients with ICAD	0.57	0.76	0.66	
miR-25	Upregulated		Distinguishing ICAD patients from controls	0.62	0.88	0.76	
miR-25	Upregulated		Distinguishing CAD patients from other subjects	0.85	0.67	0.78	
miR-21	Downregulated (in ICAD group)		Distinguishing CAD patients from patients with ICAD	0.58	0.83	0.66	

(Continued)

TABLE 4 | Continued

microRNA	Expression pattern	Samples	Diagnostic/prognostic role	ROC curve analysis			References
				Sensitivity	Specificity	AUC	
miR-21	Downregulated (in ICAD group)		Distinguishing ICAD patients from controls	0.79	0.68	0.76	
miR-218	Downregulated	Serum samples from 104 CAD patients and 101 healthy controls	Diagnostic biomarker	0.86	0.86	0.889	(26)
Let-7f *miR-19a* *miR-126* *miR-210* *miR-296*	Downregulated Downregulated Downregulated Downregulated Downregulated	Plasma samples from 286 patients with CAD (including 113 patients with rapid angiographic stenotic progression (RASP) and 173 patients without RASP)	Distinguishing RASP patients from non-RASP patients	–	–	0.879	(51)
miR-126	–	Plasma samples from 46 patients with diabetes and CAD, 54 patients with diabetes but without CAD and 20 healthy controls	Discriminating diabetic patients with and without CAD	0.91	1	–	(52)
miR-210	–	Plasma samples from 46 patients with diabetes and CAD, 54 patients with diabetes but without CAD and 20 healthy controls	Discriminating diabetic patients with and without CAD	0.93	1	–	
miR-378	Downregulated	Plasma samples from 215 CAD patients and 52 matched healthy subjects	Diagnostic biomarker	–	–	0.789	(53)
let-7c	Downregulated	Plasma samples from 69 CAD patients and 30 control individuals	Diagnostic biomarker	–	–	0.654	(54)
miR-145	Downregulated		Diagnostic biomarker	–	–	0.670	
miR-155	Downregulated		Diagnostic biomarker	–	–	0.620	
let-7c *miR-145* *miR-155*	Downregulated Downregulated Downregulated		Diagnostic biomarker	–	–	0.706	
miR-132	–	Serum samples from 1112 patients with CAD (682 patients with stable angina pectoris and 430 patients with acute coronary syndrome)	Prognostic biomarker (prediction of cardiovascular death)	–	–	0.737	(55)
miR-140-3p	–		Prognostic biomarker (prediction of cardiovascular death)	–	–	0.756	
miR-210	–		Prognostic biomarker (prediction of cardiovascular death)	–	–	0.754	
miR-150	–	Blood samples (PBMCs) from 72 CAD patients with significant stenosis, 30 CAD patients with insignificant stenosis (ICAD) and 74 healthy controls	discriminating CAD patients from healthy controls)	0.90	0.62	0.79	(56)

(Continued)

TABLE 4 | Continued

microRNA	Expression pattern	Samples	Diagnostic/prognostic role	ROC curve analysis			References
				Sensitivity	Specificity	AUC	
miR-223	–		discriminating CAD patients from healthy controls)	0.37	0.91	0.62	
miR-150 *miR-223*	–		Discriminating CAD patients from healthy controls)	0.89	0.65	0.79	
miR-150	-		Discriminating CAD patients form ICAD patients	0.40	0.96	0.70	
miR-223	–		Discriminating CAD patients form ICAD patients	0.55	0.89	0.71	
miR-150 *miR-223*	–		Discriminating CAD patients form ICAD patients	0.74	0.83	0.80	
miR-423-3p	–	Serum samples form 64 CAD patients and 2,748 control individuals	Diagnostic biomarker	–	–	0.8	(57)
miR-26	Downregulated	45 patients with type 2 diabetes, 45 patients with type 2 diabetes and CAD and 45 healthy controls	Discriminating patients with type 2 diabetes and CAD from healthy controls	–	–	0.948	(58)
miR-26	Downregulated	45 patients with type 2 diabetes, 45 patients with type 2 diabetes and CAD and 45 healthy controls	discriminating type 2 diabetes patients with and without CAD	–	–	0.807	
miR-196-5p	Downregulated	60 patients with early-onset CAD and 60 age- and gender-matched normal subjects	Diagnostic biomarker	0.85	0.72	0.824	(59)
miR-3163-3p	Downregulated	60 patients with early-onset CAD and 60 age- and gender-matched normal subjects	Diagnostic biomarker	0.57	0.84	0.758	
miR-145-3p	Downregulated	60 patients with early-onset CAD and 60 age- and gender-matched normal subjects	Diagnostic biomarker	0.67	0.82	0.753	
miR-190a-5p	Downregulated	60 patients with early-onset CAD and 60 age- and gender-matched normal subjects	Diagnostic biomarker	0.70	0.75	0.782	
miR-196a	Downregulated	72 patients with CAD, 30 patients with ICAD and 74 healthy controls	distinguishing ICAD patients from CAD patients	–	–	0.75	(60)

TABLE 5 | miRNA polymorphisms in CAD.

microRNA	Polymorphism	Samples	Population	Assay method	Association	References
miR-196a2	SNP (rs11614913)	Blood samples from 505 CAD patients and 1,109 control subjects	Chinese	SNPscan^{TM} genotyping assay	Was associated with reduced risk of myocardial infarction and also was correlated with reduced risk of CAD in females	(67)
miR-196a2	SNP (rs11614913)	Blood samples form 218 CAD patients and 611 healthy individuals	Mexican	5′ exonuclease TaqMan assays	T allele of this polymorphism was correlated with elevated risk of CAD	(68)
miR-196a2	SNP (rs11614913)		Greek population	PCR-RFLP, High resolution Melting (HRM), and Sanger sequencing	This polymorphism was correlated with elevated risk of CAD	(69)
miR-499	SNP (rs3746444)	Blood samples form 200 CAD patients and 200 healthy individuals as controls	Greek population		This polymorphism was correlated with elevated risk of CAD	
miR-196a2	SNP (rs11614913)	Blood samples from 522 CAD patients and 535 control individuals	South Korean	PCR-RFLP	Is associated with enhanced risk of CAD in females and patients aged >63 years old. Also correlated with prevalence of CAD	(61)
miR-149	SNP (rs2292832)		South Korean	PCR-RFLP	Is associated with enhanced risk of CAD in females and patients aged >63 years old. Also correlated with prevalence of CAD	
miR-146a	SNP (rs2910164)		South Korean	PCR-RFLP	GG genotype of this SNP was correlated with risk of CAD in stent ≥2 group. Also this polymorphism was associated with elevated risk of CAD in non-smoking, hypertensive and non-diabetic subgroups	
miR-146a	SNP (rs2431697, rs2910164)	Blood sample from 353 patients with CAD and 368 control subjects	Chinese	Sequenom MassARRAY system and matrix-assisted laser desorption/ionization time-of-flight mass spectrometry	Carriers of T allele in rs2431697 had enhanced risk of CAD. G allele of rs2910164 was associated with reduced risk of CAD.	(65)
miR-423	SNP (rs6505162)	Blood samples from 100 patients with CAD and 117 gender-matched healthy subjects	Indian	ARMS-PCR	A allele and CA genotype of this SNP was associated with augmented risk of CAD	(70)
miR-224	SNP (rs188519172)	Blood samples from 100 CAD patients and 100 matched healthy subjects	–	ARMS-PCR	GA genotype of this SNP was associated with reduced CAD predisposition	(71)
miR-4513	SNP (rs2168518)	100 CAD patients and 100 healthy controls	Indian	ARMS-PCR	T allele and CT genotype of this SNP was correlated with enhanced predisposition to CAD	(71)
pre-mir-499	SNP (rs3746444)	288 patients with CAD and 150 control subjects	Iranian	PCR-RFLP	Frequency of GG genotype of this SNP was significantly higher in CAD patients than controls	(63)
miR-149	SNP (rs2292832)	272 patients with CAD and 149 control subjects	Iranian	PCR-RFLP	TT genotype of rs2292832 was associated with CAD risk	(63)

(Continued)

TABLE 5 | Continued

microRNA	Polymorphism	Samples	Population	Assay method	Association	References
hsa-miR-93	copy number variation (CNV)	Blood samples from 50 CAD patients (25 diabetic and 25 non-diabetic) and 50 subjects without CAD (25 diabetic and 25 non-diabetic)	Iranian	Real-time PCR	CNVs in hsa-miR-93 were significantly different between CAD patients and non-CAD subjects. CNVs of this miRNA were significantly different between CAD patients CAD patients type 2 diabetes mellitus (T2DM) and non-CAD individuals without T2DM.	(62)
hsa-miR-192	CNV		Iranian	Real-time PCR	CNVs of hsa-miR-192 were significantly different between CAD patients with T2DM and non-CAD individuals without T2DM.	
hsa-miR-122	CNV		Iranian	Real-time PCR	CNVs of hsa-miR-122 were significantly different between: CAD patients and non-CAD subjects CAD patients with T2DM and CAD patients without T2DM CAD patients with T2DM and non-CAD individuals without T2DM	

such as modulation of angiogenesis [miR-92a-3p (13), miR-939 (20), and miR-206 (14)], inflammatory responses [miR-181a-5p, miR-181a-3p (21), miR-216a (16), and miR-383-3p (19)], leukocyte adhesion [miR-21 (37) and miR-25 (39)] and modulation of activity of VSMCs [miR-574-5p (27)]. Notably, a number of miRNAs influence different aspects of this process or different targets in a certain process. For instance, miR-206 regulated expressions of VEGF, PIK3C2α, Akt, and endothelial nitric oxide synthase, all of them being involved in the angiogenic processes. NF-Kβ/TNF-α, PI3K-Akt-mTOR, WNT, and VEGFA/ERK1/2/NF-κB are among signaling pathways which are regulated by miRNAs in the context of CAD.

In addition to dysregulation of expression of miRNAs in endothelial cells and VSMCs, microvesicles originated from these cells have been shown to contain abnormal levels of miRNAs, thus these particles can broaden the extent of miRNAs effects on diverse cells. The presence of miRNAs in the circulation of CAD patients endowed them the ability to predict disease course and distinguish CAD patients from healthy subjects. Both plasma and PBMC levels of miRNAs could be used as diagnostic markers for CAD. Most importantly, miRNAs signature can predict the occurrence of CAD-related complications such as HF. Their ability in distinguishing UA from MI is another promising result of recent investigations, potentiating them as accurate diagnostic marker for stratifying patients who need urgent interventions. However, a major limitation of application of miRNAs as diagnostic or prognostic markers in CAD is the influence of other age-related factors on their expression. Identification of CAD-specific miRNAs whose expressions are not affected by patients' health condition is a major issue in this regard. Longitudinal assessment of miRNA profile in relation with health status of CAD patients and measurement of possible confounding parameters would help in identification of markers for clinical application.

Finally, several SNPs and CNVs within miRNA coding genes have been associated with risk of CAD, providing further evidence for crucial partake of miRNAs in the pathogenesis of CAD. Most notably, some genotypes of these SNPs have been associated with risk of CAD in patients with specific lifestyles or habits (61, 62), demonstrating the possible interaction between these genetic variants and environmental factors. However, the impact of these SNPs on CAD-related biological processes such as cell adhesion, inflammation, proliferation or apoptosis has not been appraised *in vitro*. Conduction of these types of studies would pave the way for design of targeted therapeutic interventions in CAD. Taken together, miRNAs participate in different aspects of CAD pathogenesis and could be used as specific/sensitive markers for this condition. The therapeutic application of miRNAs in CAD should be judged in upcoming studies.

AUTHOR CONTRIBUTIONS

MT and SG-F wrote the draft and revised it. MG designed the tables and collected the data. All authors contributed to the article and approved the submitted version.

REFERENCES

1. Roth GA, Johnson C, Abajobir A, Abd-Allah F, Abera SF, Abyu G, et al. Global, regional, and national burden of cardiovascular diseases for 10 causes, 1990 to 2015. *J Am Coll Cardiol.* (2017) 70:1–25. doi: 10.1016/j.jacc.2017.04.052
2. Mathers CD, Loncar D. Projections of global mortality and burden of disease from 2002 to 2030. *PLoS Med.* (2006) 3:e442. doi: 10.1371/journal.pmed.0030442
3. Spiekerman RE, Brandenburg JT, Achor RW, Edwards JE. The spectrum of coronary heart disease in a community of 30,000: A clinicopathologic study. *Circulation.* (1962) 25:57–65. doi: 10.1161/01.CIR.25.1.57
4. Davies MJ, Thomas AC. Plaque fissuring–the cause of acute myocardial infarction, sudden ischaemic death, and crescendo angina. *Br Heart J.* (1985) 53:363. doi: 10.1136/hrt.53.4.363
5. Ghafouri-Fard S, Gholipour M, Taheri M. The emerging role of long non-coding RNAs and circular RNAs in coronary artery disease. *Front Cardiovas Med.* (2021) 8:42. doi: 10.3389/fcvm.2021.632393
6. Ambrose JA, Singh M. Pathophysiology of coronary artery disease leading to acute coronary syndromes. *F1000Prime Rep.* (2015) 7:08. doi: 10.12703/P7-08
7. Sutton MGSJ, Sharpe N. Left ventricular remodeling after myocardial infarction: pathophysiology and therapy. *Circulation.* (2000) 101:2981–8. doi: 10.1161/01.CIR.101.25.2981
8. Gheorghiade M, Sopko G, De Luca L, Velazquez EJ, Parker JD, Binkley PF, et al. Navigating the crossroads of coronary artery disease and heart failure. *Circulation.* (2006) 114:1202–13. doi: 10.1161/CIRCULATIONAHA.106.623199
9. Melak T, Baynes HW. Circulating microRNAs as possible biomarkers for coronary artery disease: a narrative review. *EJIFCC.* (2019) 30:179–94.
10. Pasquinelli AE. MicroRNAs and their targets: recognition, regulation and an emerging reciprocal relationship. *Nat Rev Genet.* (2012) 13:271–82. doi: 10.1038/nrg3162
11. Bajan S, Hutvagner G. Regulation of miRNA processing and miRNA mediated gene repression in cancer. *Microrna.* (2014) 3:10–7. doi: 10.2174/22115366026661401102340 46
12. Landskroner-Eiger S, Moneke I, Sessa WC. miRNAs as modulators of angiogenesis. *Cold Spring Harbor Perspect Med.* (2013) 3:a006643. doi: 10.1101/cshperspect.a006643
13. Liu Y, Li Q, Hosen MR, Zietzer A, Flender A, Levermann P, et al. Atherosclerotic conditions promote the packaging of functional microRNA-92a-3p into endothelial microvesicles. *Circul Res.* (2019) 124:575–87. doi: 10.1161/CIRCRESAHA.118.314010
14. Wang M, Ji Y, Cai S, Ding W. MiR-206 suppresses the progression of coronary artery disease by modulating vascular endothelial growth factor (VEGF) expression. *Med Sci Monit.* (2016) 22:5011. doi: 10.12659/MSM.898883
15. Tang Y, Zhang Y, Chen Y, Xiang Y, Xie Y. Role of the micro RNA, miR-206, and its target PIK 3C2α in endothelial progenitor cell function–potential link with coronary artery disease. *FEBS J.* (2015) 282:3758–72. doi: 10.1111/febs.13372
16. Yang S, Mi X, Chen Y, Feng C, Hou Z, Hui R, et al. MicroRNA-216a induces endothelial senescence and inflammation via Smad3/IκBα pathway. *J Cell Mol Med.* (2018) 22:2739–49. doi: 10.1111/jcmm.13567
17. Gao ZF, Ji XL, Gu J, Wang XY, Ding L, Zhang H. microRNA-107 protects against inflammation and endoplasmic reticulum stress of vascular endothelial cells via KRT1-dependent Notch signaling pathway in a mouse model of coronary atherosclerosis. *J Cell Physiol.* (2019) 234:12029–41. doi: 10.1002/jcp.27864
18. Ren J, Ma R, Zhang ZB, Li Y, Lei P, Men JL. Effects of microRNA-330 on vulnerable atherosclerotic plaques formation and vascular endothelial cell proliferation through the WNT signaling pathway in acute coronary syndrome. *J Cell Biochem.* (2018) 119:4514–27. doi: 10.1002/jcb.26584
19. Lian Z, Lv FF, Yu J, Wang JW. The anti-inflammatory effect of microRNA-383-3p interacting with IL1R2 against homocysteine-induced endothelial injury in rat coronary arteries. *J Cell Biochem.* (2018) 119:6684–94. doi: 10.1002/jcb.26854
20. Hou S, Fang M, Zhu Q, Liu Y, Liu L, Li X. MicroRNA-939 governs vascular integrity and angiogenesis through targeting γ-catenin in endothelial cells. *Biochem Biophys Res Commun.* (2017) 484:27–33. doi: 10.1016/j.bbrc.2017.01.085
21. Su Y, Yuan J, Zhang F, Lei Q, Zhang T, Li K, et al. MicroRNA-181a-5p and microRNA-181a-3p cooperatively restrict vascular inflammation and atherosclerosis. *Cell Death Dis.* (2019) 10:1–15. doi: 10.1038/s41419-019-1599-9
22. Du L, Xu Z, Wang X, Liu F. Integrated bioinformatics analysis identifies microRNA-376a-3p as a new microRNA biomarker in patient with coronary artery disease. *Am J Transl Res.* (2020) 12:633–48.
23. Liang S, Gong X, Zhang G, Huang G, Lu Y, Li Y. The lncRNA XIST interacts with miR-140/miR-124/iASPP axis to promote pancreatic carcinoma growth. *Oncotarget.* (2017) 8:113701. doi: 10.18632/oncotarget.22555
24. Lin J, Jiang J, Zhou R, Li X, Ye J. MicroRNA-451b participates in coronary heart disease by targeting VEGFA. *Open Med.* (2019) 15:1–7. doi: 10.1515/med-2020-0001
25. Liu D, Zhang X-l, Yan C-h, Li Y, Tian X-x, Zhu N, et al. MicroRNA-495 regulates the proliferation and apoptosis of human umbilical vein endothelial cells by targeting chemokine CCL2. *Thrombosis Res.* (2015) 135:146–54. doi: 10.1016/j.thromres.2014.10.027
26. Gao W, Cui H, Li Q, Zhong H, Yu J, Li P, et al. Upregulation of microRNA-218 reduces cardiac microvascular endothelial cells injury induced by coronary artery disease through the inhibition of HMGB1. *J Cell Physiol.* (2020) 235:3079–95. doi: 10.1002/jcp.29214
27. Lai Z, Lin P, Weng X, Su J, Chen Y, He Y, et al. MicroRNA-574-5p promotes cell growth of vascular smooth muscle cells in the progression of coronary artery disease. *Biomed Pharmacotherap.* (2018) 97:162–7. doi: 10.1016/j.biopha.2017.10.062
28. Fang Y, Chen S, Liu Z, Ai W, He X, Wang L, et al. Endothelial stem cells attenuate cardiac apoptosis via downregulating cardiac microRNA-146a in a rat model of coronary heart disease. *Exp Therap Med.* (2018) 16:4246–52. doi: 10.3892/etm.2018.6702
29. Li K, Lin T, Chen L, Wang N. MicroRNA-93 elevation after myocardial infarction is cardiac protective. *Med Hypotheses.* (2017) 106:23–5. doi: 10.1016/j.mehy.2017.07.003
30. Zhang R, Sui L, Hong X, Yang M, Li W. MiR-448 promotes vascular smooth muscle cell proliferation and migration in through directly targeting MEF2C. *Environ Sci Pollut Res Int.* (2017) 24:22294–300. doi: 10.1007/s11356-017-9771-1
31. Wang D, Wang Y, Ma J, Wang W, Sun B, Zheng T, et al. MicroRNA-20a participates in the aerobic exercise-based prevention of coronary artery disease by targeting PTEN. *Biomed Pharmacotherap.* (2017) 95:756–63. doi: 10.1016/j.biopha.2017.08.086
32. Yang Y, Luo H, Liu S, Zhang R, Zhu X, Liu M, et al. Platelet microparticles-containing miR-4306 inhibits human monocyte-derived macrophages migration through VEGFA/ERK1/2/NF-κB signaling pathways. *Clin Exp Hypertens.* (2019) 41:481–91. doi: 10.1080/10641963.2018.1510941
33. Satoh M, Nasu T, Takahashi Y, Osaki T, Hitomi S, Morino Y, et al. Expression of miR-23a induces telomere shortening and is associated with poor clinical outcomes in patients with coronary artery disease. *Clin Sci.* (2017) 131:2007–17. doi: 10.1042/CS20170242
34. Guo T, Wang J, Cheng G, Huang H. miR-590-5p may regulate colorectal cancer cell viability and migration by targeting PDCD4. *Exp Ther Med.* (2020) 20:55. doi: 10.3892/etm.2020.9183
35. Zhou Y, Cheng X, Wan Y, Chen T, Zhou Q, Wang Z, et al. MicroRNA-421 inhibits apoptosis by downregulating Caspase-3 in human colorectal cancer. *Cancer Manag Res.* (2020) 12:7579–87. doi: 10.2147/CMAR.S255787
36. Liang X, Wang L, Wang M, Liu Z, Liu X, Zhang B, et al. MicroRNA-124 inhibits macrophage cell apoptosis via targeting p38/MAPK signaling pathway in atherosclerosis development. *Aging.* (2020) 12:13005. doi: 10.18632/aging.103387
37. Bai F, Yu Z, Gao X, Gong J, Fan L, Liu F. Simvastatin induces breast cancer cell death through oxidative stress up-regulating miR-140-5p. *Aging.* (2019) 11:3198. doi: 10.18632/aging.101974
38. Zhong Z, Hou J, Zhang Q, Zhong W, Li B, Li C, et al. Circulating microRNA expression profiling and bioinformatics analysis of dysregulated microRNAs of patients with coronary artery disease. *Medicine.* (2018) 97:e11428. doi: 10.1097/MD.0000000000011428
39. Vahed SZ, Aghaee-Bakhtiari SH, Daraei A, Saadatian Z, Kafil HS, Yousefi B, et al. Expression pattern of miR-21, miR-25 and PTEN in peripheral

blood mononuclear cells of patients with significant or insignificant coronary stenosis. *Gene.* (2019) 698:170–8. doi: 10.1016/j.gene.2019.02.074
40. Yao Y, Song T, Xiong G, Wu Z, Li Q, Xia H, et al. Combination of peripheral blood mononuclear cell miR-19b-5p, miR-221, miR-25-5p, and hypertension correlates with an increased heart failure risk in coronary heart disease patients. *Anatolian J Cardiol.* (2018) 20:100. doi: 10.14744/AnatolJCardiol.2018.43255
41. Singh S, de Ronde MW, Kok MG, Beijk MA, De Winter RJ, van der Wal AC, et al. MiR-223-3p and miR-122-5p as circulating biomarkers for plaque instability. *Open Heart.* (2020) 7:e001223. doi: 10.1136/openhrt-2019-001223
42. Guo J-F, Zhang Y, Zheng Q-X, Zhang Y, Zhou H-H, Cui L-M. Association between elevated plasma microRNA-223 content and severity of coronary heart disease. *Scand J Clin Lab Invest.* (2018) 78:373–8. doi: 10.1080/00365513.2018.1480059
43. Gao J, Liu J, Zhang Y, Guan B, Qu H, Chai H, et al. PBMCs-Derived microRNA signature as a prethrombotic status discriminator in stable coronary artery disease. *Thromb Haemostasis.* (2020) 120:121–31. doi: 10.1055/s-0039-1700518
44. John F, Neylon A, McGorrian C, Blake GJ. miRNA-93-5p and other miRNAs as predictors of coronary artery disease and STEMI. *Int J Cardiol.* (2016) 224:310–6. doi: 10.1016/j.ijcard.2016.09.016
45. Wang J, Yan Y, Song D, Liu B. Reduced plasma miR-146a is a predictor of poor coronary collateral circulation in patients with coronary artery disease. *BioMed Res Int.* (2016) 2016:4285942. doi: 10.1155/2016/4285942
46. Zhang Y, Li H-H, Yang R, Yang B-J, Gao Z-Y. Association between circulating microRNA-208a and severity of coronary heart disease. *Scand J Clin Lab Invest.* (2017) 77:379–84. doi: 10.1080/00365513.2017.1328740
47. Al-Hayali MA, Sozer V, Durmus S, Erdenen F, Altunoglu E, Gelisgen R, et al. Clinical value of circulating microribonucleic acids miR-1 and miR-21 in evaluating the diagnosis of acute heart failure in asymptomatic type 2 diabetic patients. *Biomolecules.* (2019) 9:193. doi: 10.3390/biom9050193
48. Darabi F, Aghaei M, Movahedian A, Pourmoghadas A, Sarrafzadegan N. The role of serum levels of microRNA-21 and matrix metalloproteinase-9 in patients with acute coronary syndrome. *Mol Cell Biochem.* (2016) 422:51–60. doi: 10.1007/s11010-016-2805-z
49. Horváth M, Horváthová V, Hájek P, Štěchovský C, Honěk J, Šenolt L, et al. MicroRNA-331 and microRNA-151-3p as biomarkers in patients with ST-segment elevation myocardial infarction. *Sci Rep.* (2020) 10:5845. doi: 10.1038/s41598-020-62835-w
50. Bai R, Yang Q, Xi R, Li L, Shi D, Chen K. miR-941 as a promising biomarker for acute coronary syndrome. *BMC Cardiovasc Disord.* (2017) 17:227. doi: 10.1186/s12872-017-0653-8
51. Dai R, Liu Y, Zhou Y, Xiong X, Zhou W, Li W, et al. Potential of circulating pro-angiogenic microRNA expressions as biomarkers for rapid angiographic stenotic progression and restenosis risks in coronary artery disease patients underwent percutaneous coronary intervention. *J Clin Lab Anal.* (2020) 34:e23013. doi: 10.1002/jcla.23013
52. Amr K, Abdelmawgoud H, Ali Z, Shehata S, Raslan H. Potential value of circulating microRNA-126 and microRNA-210 as biomarkers for type 2 diabetes with coronary artery disease. *Br J Biomed Sci.* (2018) 75:82–7. doi: 10.1080/09674845.2017.1402404
53. Wang Y, Luo X, Liu Y, Han G, Sun D. Long noncoding RNA RMRP promotes proliferation and invasion via targeting miR-1-3p in non–small-cell lung cancer. *J Cell Biochem.* (2019) 120:15170–81. doi: 10.1002/jcb.28779
54. Faccini J, Ruidavets J-B, Cordelier P, Martins F, Maoret J-J, Bongard V, et al. Circulating miR-155, miR-145 and let-7c as diagnostic biomarkers of the coronary artery disease. *Sci Rep.* (2017) 7:42916. doi: 10.1038/srep42916
55. Karakas M, Schulte C, Appelbaum S, Ojeda F, Lackner KJ, Münzel T, et al. Circulating microRNAs strongly predict cardiovascular death in patients with coronary artery disease—results from the large AtheroGene study. *Eur Heart J.* (2017) 38:516–23. doi: 10.1093/eurheartj/ehw250
56. Saadatian Z, Nariman-Saleh-Fam Z, Bastami M, Mansoori Y, Khaheshi I, Parsa SA, et al. Dysregulated expression of STAT1, miR-150, and miR-223 in peripheral blood mononuclear cells of coronary artery disease patients with significant or insignificant stenosis. *J Cell Biochem.* (2019) 120:19810–24. doi: 10.1002/jcb.29286
57. Li P, Cai J-X, Han F, Wang J, Zhou J-J, Shen K-W, et al. Expression and significance of miR-654-5p and miR-376b-3p in patients with colon cancer. *World J Gastrointestinal Oncol.* (2020) 12:492. doi: 10.4251/wjgo.v12.i4.492
58. Al-Kafaji G, Al-Mahroos G, Abdulla Al-Muhtaresh H, Sabry MA, Abdul Razzak R, Salem AH. Circulating endothelium-enriched microRNA-126 as a potential biomarker for coronary artery disease in type 2 diabetes mellitus patients. *Biomarkers.* (2017) 22:268–78. doi: 10.1080/1354750X.2016.1204004
59. Ying D, Yang SH, Sha L, Cui CJ, Zhang Y, Zhu CG, et al. Circulating microRNAs as novel diagnostic biomarkers for very early-onset ($\leq$ 40 years) coronary artery disease. *Biomedical and Environmental Sciences.* (2016) 29:545–54. doi: 10.3967/bes2016.073
60. Saadatian Z, Nariman-Saleh-Fam Z, Khaheshi I, Mansoori Y, Daraei A, Ghaderian SMH, et al. Peripheral blood mononuclear cells expression levels of miR-196a and miR-100 in coronary artery disease patients. *Immunol Invest.* (2020) 1–11. doi: 10.1080/08820139.2020.1791177. [Epub ahead of print].
61. Sung JH, Kim SH, Yang WI, Kim WJ, Moon JY, Kim IJ, et al. miRNA polymorphisms (miR-146a, miR-149, miR-196a2 and miR-499) are associated with the risk of coronary artery disease. *Mol Med Rep.* (2016) 14:2328–42. doi: 10.3892/mmr.2016.5495
62. Sohrabifar N, Ghaderian SMH, Vakili H, Ghaedi H, Rouhani B, Jafari H, et al. MicroRNA-copy number variations in coronary artery disease patients with or without type 2 diabetes mellitus. *Arch Physiol Biochem.* (2019) 1–7. doi: 10.1080/13813455.2019.1651340. [Epub ahead of print].
63. Ghaffarzadeh M, Ghaedi H, Alipoor B, Omrani MD, Kazerouni F, Shanaki M, et al. Association of miR-149 (RS2292832) variant with the risk of coronary artery disease. *J Med Biochem.* (2017) 36:251–8. doi: 10.1515/jomb-2017-0005
64. Wei WJ, Lu ZW, Li DS, Wang Y, Zhu YX, Wang ZY, et al. Association of the miR-149 Rs2292832 polymorphism with papillary thyroid cancer risk and clinicopathologic characteristics in a Chinese population. *Int J Mol Sci.* (2014) 15:20968–81. doi: 10.3390/ijms151120968
65. Wang Y, Wang X, Li Z, Chen L, Zhou L, Li C, et al. Two single nucleotide polymorphisms (rs2431697 and rs2910164) of miR-146a are associated with risk of coronary artery disease. *Int J Environ Res Public Health.* (2017) 14:514. doi: 10.3390/ijerph14050514
66. Ramkaran P, Khan S, Phulukdaree A, Moodley D, Chuturgoon AA. miR-146a polymorphism influences levels of miR-146a, IRAK-1, and TRAF-6 in young patients with coronary artery disease. *Cell Biochem Biophys.* (2014) 68:259–66. doi: 10.1007/s12013-013-9704-7
67. Qiu H, Chen Z, Lv L, Tang W, Hu R. Associations between microRNA polymorphisms and development of coronary artery disease: a case–control study. *DNA Cell Biol.* (2020) 39:25–36. doi: 10.1089/dna.2019.4963
68. Fragoso JM, Ramírez-Bello J, Martínez-Ríos MA, Peña-Duque MA, Posadas-Sánchez R, Delgadillo-Rodríguez H, et al. miR-196a2 (rs11614913) polymorphism is associated with coronary artery disease, but not with in-stent coronary restenosis. *Inflamm Res.* (2019) 68:215–21. doi: 10.1007/s00011-018-1206-z
69. Agiannitopoulos K, Samara P, Papadopoulou M, Efthymiadou A, Papadopoulou E, Tsaousis GN, et al. miRNA polymorphisms and risk of premature coronary artery disease. *Hellenic J Cardiol.* (2020) doi: 10.1016/j.hjc.2020.01.005 (in press).
70. Mir R, Jha CK, Elfaki I, Rehman S, Javid J, Khullar N, et al. MicroRNA-224 (rs188519172 A> G) gene variability is associated with a decreased susceptibility to coronary artery disease: A case-control study. *MicroRNA.* (2019) 8:198–205. doi: 10.2174/2211536608666181211153859
71. Mir R, Elfaki I, Javid J, Rehman S, Khullar N, Banu S, et al. Incidence of MicroR-4513C/T gene variability in coronary artery disease-a case-control study. *Endocr Metab Immune Disord Drug Targets.* (2019) 19:1216–23. doi: 10.2174/1871530319666190417111940
72. Lin Y, Dan H, Lu J. Overexpression of microRNA-136-3p alleviates myocardial injury in coronary artery disease via the Rho A/ROCK signaling pathway. *Kidney Blood Pressure Res.* (2020) 45:477–96. doi: 10.1159/000505849

Conflict of Interest: The authors declare that the research was conducted in the absence of any commercial or financial relationships that could be construed as a potential conflict of interest.

frontiers in Cardiovascular Medicine

ORIGINAL RESEARCH
published: 16 April 2021
doi: 10.3389/fcvm.2021.645541

MicroRNA Profiles in Normotensive and Hypertensive South African Individuals

Don M. Matshazi[1], Cecil J. Weale[1], Rajiv T. Erasmus[2], Andre P. Kengne[3,4], Saarah F. G. Davids[1], Shanel Raghubeer[1], Stanton Hector[1], Glenda M. Davison[1] and Tandi E. Matsha[1]**

[1] South African Medical Research Council/Cape Peninsula University of Technology Cardiometabolic Health Research Unit, Department of Biomedical Sciences, Faculty of Health and Wellness Sciences, Cape Peninsula University of Technology, Cape Town, South Africa, [2] Division of Chemical Pathology, Faculty of Health Sciences, National Health Laboratory Service and Stellenbosch University, Cape Town, South Africa, [3] Non-communicable Diseases Research Unit, South African Medical Research Council, Cape Town, South Africa, [4] Department of Medicine, University of Cape Town, Cape Town, South Africa

OPEN ACCESS

Edited by:
BuChun Zhang, University of Science and Technology of China, China

Reviewed by:
Valdo Jose Dias Da Silva, Universidade Federal do Triângulo Mineiro, Brazil
Elisa Cairrão, Universidade da Beira Interior, Portugal

***Correspondence:**
Don M. Matshazi
matshazid@gmail.com
Tandi E. Matsha
matshat@cput.ac.za;
tandimatsha@gmail.com

Specialty section:
This article was submitted to General Cardiovascular Medicine, a section of the journal Frontiers in Cardiovascular Medicine

Received: *23 December 2020*
Accepted: *23 March 2021*
Published: *16 April 2021*

Citation:
Matshazi DM, Weale CJ, Erasmus RT, Kengne AP, Davids SFG, Raghubeer S, Hector S, Davison GM and Matsha TE (2021) MicroRNA Profiles in Normotensive and Hypertensive South African Individuals. Front. Cardiovasc. Med. 8:645541. doi: 10.3389/fcvm.2021.645541

Hypertension has a complex pathogenesis and symptoms appear in advanced disease. Dysregulation of gene expression regulatory factors like microRNAs has been reported in disease development. Identifying biomarkers which could help understand the pathogenesis and prognosis of hypertension is essential. The study's objective was to investigate microRNA expression profiles according to participant blood pressure status. Next generation sequencing was used to identify microRNAs in the whole blood of 48 body mass index-, smoking- and age-matched normotensive ($n = 12$), screen-detected hypertensive ($n = 16$) and known hypertensive ($n = 20$) female participants. Quantitative reverse transcription polymerase chain reaction was used to validate the next generation sequencing findings in a larger, independent sample of 84 men and 179 women. Using next generation sequencing, 30 dysregulated microRNAs were identified and miR-1299 and miR-30a-5p were the most significantly differentially expressed. Both microRNAs were upregulated in known hypertensives or screen-detected hypertensives compared to the normotensives. Kyoto Encyclopedia of Genes and Genomes pathway enrichment analysis indicated possible involvement of platelet activation, calcium signaling and aldosterone synthesis pathways. Further validation of miR-1299 and miR-30a-5p using quantitative reverse transcription polymerase chain reaction confirmed sequencing results while yielding new findings. These findings demonstrate microRNA dysregulation in hypertension and their expression may be related to genes and biological pathways essential for blood pressure homeostasis.

Keywords: hypertension, microRNA, blood pressure, cardiovascular, non-coding, sub-Saharan Africa

INTRODUCTION

The 8th report released by the Joint National Committee on Prevention, Detection and Evaluation of High Blood Pressure describes hypertension (HPT) as the persistent elevation of blood pressure (BP) above the 140/90 mmHg threshold (1, 2). Despite efforts to understand the pathogenesis of the condition, HPT remains a leading public health concern affecting both developed and developing countries (3, 4). It has been identified as one of the most important modifiable risk factors for

cardiovascular disease, renal disease, and stroke, and accounts for over 10 million deaths throughout the world annually (5–7). In 90–95% of HPT patients, the cause is unknown, and is thus termed primary or essential HPT (8, 9). However, research has demonstrated the involvement of genetic and environmental factors in the development of HPT. The influence of epigenetic factors such as deoxyribonucleic (DNA) methylation and histone modification on the pathogenesis of HPT has been a subject of intense research, with several important conclusions being made along the way (10). However, there is a paucity of research regarding microRNAs (miRNAs) in the context of HPT.

MiRNAs are a group of small, endogenous, non-coding ribonucleic (RNA) sequences that are 17–25 base pairs long (11). These molecules are involved in gene expression regulation at the post-transcriptional level. This is achieved by binding to the 3′untranslated region of complementary messenger RNA (mRNA) molecules and inhibiting translation into protein or inducing mRNA degradation (12). MiRNAs are present in almost every cell and disturbances in their regulation are usually associated with disease processes, including HPT (13, 14). Herein, we investigated the miRNA profiles in South African individuals with normal BP, as well as those presenting with known or screen-detected HPT.

MATERIALS AND METHODS

Ethics Statement

This investigation was based on the Cape Town Vascular and Metabolic Health (VMH) study, which was approved by the Research Ethics Committees of the Cape Peninsula University of Technology (CPUT) and Stellenbosch University (respectively, NHREC: REC−230 40−014 and N14/01/003). Ethical approval was also obtained for this cross-sectional sub-study from the CPUT Health and Wellness Sciences Research Ethics Committee (CPUT/HW-REC 2019/H7). The study was conducted as per the provisions of the Declaration of Helsinki. All procedures were explained to the participants in their language of choice. Once the participants fully understood their participation, they signed informed consent forms to allow the collection of blood and anthropometric data.

Study Design and Procedures

Data collection and procedures have been described previously (15). Briefly, participants underwent anthropometric and BP measurements, as well as oral glucose tolerance tests (OGTT). Anthropometric measurements for each participant were taken three times and the average reported. BP was measured according to the World Health Organization (WHO) guidelines (16), using a semi-automatic digital BP monitor (Omron M6 comfort-preformed cuff BP Monitor, China) on the right arm in a sitting position and at rest for at least 10 min. Three BP readings were taken at 3-min intervals and the lowest systolic BP and corresponding diastolic BP-values were used. Participants were grouped into three categories based on; the use of anti-hypertensive medication as known HPT, BP measurement of 140/90 mm Hg or greater as screen-detected HPT and normal BP measurement (<140/90 mm Hg) as normotensive. Body Mass Index (BMI) was calculated as weight per square meter (kg/m^2), where kg was the participant's weight in kilograms and m^2, the square of their height.

The following biochemical parameters were analyzed at an ISO 15189 accredited Pathology practice (PathCare Reference Laboratory, Cape Town, South Africa): glycated hemoglobin (HbA1c) by High Performance Liquid Chromatography (BioRad Variant Turbo, BioRad, Hercules, CA, USA); serum insulin by a paramagnetic particle chemiluminescence assay (Beckman DXI, Beckman Coulter, South Africa); serum cotinine by Competitive Chemiluminescent (Immulite 2000, Siemens, Munich, Germany); plasma glucose by enzymatic hexokinase method (Beckman AU, Beckman Coulter, Brea, CA, USA); total cholesterol (TC); high density lipoprotein cholesterol (HDL-c) by enzymatic immunoinhibition—end point (Beckman AU, Beckman Coulter, Brea, CA, USA); triglycerides (TG) by glycerol phosphate oxidase-peroxidase, end point (Beckman AU, Beckman Coulter, Brea, CA, USA); low density lipoprotein cholesterol (LDL) by enzymatic selective protection—end point (Beckman AU, Beckman Coulter, Brea, CA, USA); and ultrasensitive C-reactive protein (CRP) by Latex Particle Immunoturbidimetry (Beckman AU, Beckman Coulter, Brea, CA, USA). In addition, blood samples were collected in a Tempus RNA tube (ThermoFisher Scientific, Waltham, MA, USA) and stored at −80°C for total RNA extraction and analysis.

RNA Isolation

Total RNA, including miRNA, was isolated from whole blood using the MagMax for Stabilized Blood RNA isolation kit (ThermoFisher Scientific) according to manufacturer's instructions. The concentration and purity of each RNA extract was determined using a NanoDrop One spectrophotometer. Total RNA extracts with 260/280 values between 1.8 and 2.0, and concentrations >20 ng/μl were used for microRNA sequencing (miRNA-seq) using next generation sequencing (NGS) and quantitative reverse transcription PCR (RT-qPCR).

MicroRNA Sequencing

This was conducted on total RNA samples from 48 female participants representing three different HPT statuses. The inclusion of females only in this part of the study was to avoid introducing potential sources of variation due to gender effect in an already small cohort. Small RNA library construction, deep sequencing, and data processing were performed at Arraystar Inc., Rockville, USA as previously described by Matsha et al. (15). Briefly, the total RNA of each sample was used to prepare the miRNA sequencing library as follows: (1) 3′-adapter ligation with T4 RNA ligase 2 (truncated); (2) 5′-adapter ligation with T4 RNA ligase; (3) complementary DNA (cDNA) synthesis with RT primer; (4) PCR amplification; (5) extraction and purification of ∼130–150 bp PCR amplified fragments (correspond to ∼15–35 nt small RNAs) from the polyacrylamide gel electrophoresis gel. The Agilent 2100 Bioanalyzer was used to quantify completed libraries, thereafter DNA fragments were denatured with 0.1 M sodium hydroxide to generate single-stranded DNA molecules, then captured on Illumina flow cells, amplified *in situ*, and finally sequenced for 51 cycles on the Illumina HiSeq system

according to the manufacturer's instructions. Raw sequences were generated as clean reads from the Illumina HiSeq using real-time base calling and quality filtering. The clean reads that passed the quality filter were processed to remove adaptor sequences as the trimmed reads. The trimmed reads (length $\geq$ 15 nt) were aligned to the human pre-miRNA in miRBase 21, using NovoAlign software. The miRNA expression levels were measured and normalized as transcripts per million of total aligned miRNA reads.

Gene Ontology and Functional Enrichment Analysis

The Gene Ontology (GO) analysis was performed to describe gene and gene product attributes (http://www.geneontology.org). The ontology covers three domains: Biological Process, Cellular Component and Molecular Function. Commonly predicted gene targets were subjected to functional analysis using Kyoto Encyclopedia of Genes and Genomes (KEGG). A conservative Fisher's exact-test and false discovery rate method were used to calculate the targeted pathways.

Validation of NGS miRNA Expression Results

To confirm the expression of miRNAs, the validation of NGS results was performed on total RNA from an independent sample of 263 male and female participants randomly selected from an existing database and 48 females on which NGS had been conducted. MiRNAs were converted to cDNA using the TaqMan MicroRNA Reverse Transcription Kit according to the manufacturer's protocol (Life Technologies, USA). The miRNA expression levels were assessed using TaqMan miRNA Assay primers on the QuantStudio 7 Flex real-time PCR instrument (Life Technologies, USA) analyzer. In order to determine miRNA expression in each sample and between two groups, the $2^{-\Delta Ct}$ and $2^{-\Delta\Delta Ct}$ (17), respectively, were used and normalized using miR-16-5p as the endogenous control. The suitability of miR-16-5p as an endogenous control in RT-qPCR was assessed and confirmed, as there was minimal variation in its expression in normotensive and hypertensive participants.

Statistical Analysis

Data were analyzed using R statistical software version 3.2.2 (The R Foundation for Statistical Computing, Vienna, Austria) and TIBCO Statistica version 13.5.0.17 (TIBCO Software Inc., California, USA). The Shapiro-Wilk W-test was employed to determine whether the data were normally distributed, based on probability thresholds of $p > 0.1$. Continuous variables were summarized as mean and standard deviation (SD) when normally distributed, while median, and 25th and 75th percentiles were used for skewed variables, whilst categorical variables were reported as counts and percentages. When comparing groups, for continuous variables, the analysis of variance (ANOVA) was used for normally distributed data; Kruskal Wallis-H test with Dunn *post-hoc*-test was used for skewed data, whilst the chi-square-test was used for categorical variables. Multivariable regression analysis was conducted to investigate the possible effects of these differences in baseline characteristics on the expression of miRNAs in screen-detected and known HPT. Various models were used, with variations to the crude model being used to analyse the effect or relationship of a baseline characteristic with miRNA expression in HPT. All comparisons were made with the normotensive group as the reference. A p-value < 0.05 was used to characterize statistically significant results. MicroRNAs with fold changes $\geq$1.3, and p-values ≤ 0.1 were selected as the differentially expressed miRNAs. Novel miRNAs were predicted using miRDeep.

RESULTS

General Participant Characteristics

Of the 1988 VMH survey participants, 311 (227, 73.0% female) were selected for inclusion into this sub-study. Of these, 48 (all female) took part in the NGS part of the study while an additional 263 randomly selected male and female participants were included in the RT-qPCR validation study. The distribution of the NGS and RT-qPCR participants by BP status is shown in **Table 1**. The 48 women in the NGS sample included 20 with known HPT, 16 with screen-detected HPT and 12 normotensives, whilst the validation sample included 106 known hypertensives, 52 screen-detected hypertensives and 105 normotensives. The expected differences by status for HPT in the cardiovascular risk profile were apparent across the two sub-samples (**Table 1**).

NGS miRNA Expression Profiling

All 48 samples met the quality control standards. We generated Heat Map and Unsupervised Hierarchical Clustering on all miRNAs that were expressed in at least one sample, to produce miRNA or condition trees that would allow us to pick out groups of similar miRNAs. The result of hierarchical clustering on conditions showed a distinguishable miRNA expression profile amongst the groups (**Figures 1A–C**). For the identification of differentially expressed miRNAs, we computed "fold changes" (i.e., the ratio of the group averages) and p-values between each group. MicroRNAs with fold changes $\geq$ 1.3 and p-values $\leq$ 0.1 were selected as the differentially expressed miRNAs. Based on pre-specified criteria, we then used volcano plots to visualize the significantly differentially expressed pre-miRNAs between the study groups as shown in **Figures 2A–C**. A total of 30 significantly differentially expressed mature miRNAs were identified at varying expression levels and are summarized in **Table 2**. Of the thirty differentially expressed miRNAs, two (6.7%) were novel, and whilst one of these novel miRNAs was upregulated in known HPT vs. normotensive, the other was upregulated in known HPT vs. screen-detected HPT. Whilst miR-1299 exhibited the highest fold change of all significantly upregulated miRNAs as seen in screen-detected HPT vs. normotensive (fold change = 3.38, $p = 0.0812$), miR-30a-5p upregulation was greatest in known HPT vs. normotensive (fold change = 2.44, $p = 0.0631$) and known HPT vs. screen detected HPT (fold change = 2.02, $p = 0.0715$; **Table 2**).

Kyoto Encyclopedia of Genes and Genomes pathway analysis revealed 84 pathways, five of which are essential for platelet activation, calcium signaling, vascular smooth muscle contraction, vasopressin-mediated water reabsorption

TABLE 1 | Characteristics of the participants, based on hypertension status.

	Next generation sequencing sample				Validation sample (RT-qPCR)			
	Normotensive, *n* = 12	**Screen-detected HPT, *n* = 16**	**Known HPT, *n* = 20**	***p*-value**	**Normotensive, *n* = 105**	**Screen-detected HPT, *n* = 52**	**Known HPT, *n* = 106**	***p*-value**
Female, *n* (%)	12 (100%)	16 (100%)	20 (100%)	-	57 (54.29)	36 (69.23)	86 (81.13)	<0.001
Male, *n* (%)	-	-	-	-	48 (45.71)	16 (30.77)	20 (18.87)	
Age (years)	49.6 ± 9.3	52.8 ± 7.1	56.1 ± 7.7	0.086	40 ± 15.32	51.12 ± 13.43	61.1 ± 10.6	<0.001
Body mass index (kg/m^2)	29.1 ± 8.1	30.6 ± 9.0	32.3 ± 6.4	0.509	25.08 ± 6.45	28.71 ± 7.96	30.85 ± 7.06	<0.001
Waist circumference (cm)	87.5 ± 16.2	92.0 ± 22.1	97.9 ± 11.4	0.226	81.99 ± 13.71	91.32 ± 16.71	95.86 ± 14.75	<0.001
Hip circumference (cm)	101.7 ± 17.7	106.1 ± 18.4	108.8 ± 14.2	0.504	97.55 ± 12.69	103.76 ± 15.3	106.05 ± 13.85	<0.001
Waist to hip Ratio	0.86 ± 0.06	0.86 ± 0.09	0.90 ± 0.06	0.139	0.84 ± 0.07	0.88 ± 0.08	0.90 ± 0.08	<0.001
Systolic blood pressure (mmHg)	113.4 ± 14.5	147.7 ± 22.2	144.7 ± 27.7	<0.001	118.77 ± 12.95	149.12 ± 19.96	148.50 ± 23.81	<0.001
Diastolic blood pressure (mmHg)	74.8 ± 11.9	90.6 ± 14.8	89.7 ± 17.7	0.018	74.95 ± 10.47	97.19 ± 12.32	89.11 ± 13.56	<0.001
Fasting blood glucose (mmol/L)	6.18+3.87	7.50+4.58	8.28+4.27	0.413	4.87 ± 1.43	5.55 ± 2.72	6.70 ± 3.49	<0.001
2-h fasting glucose	8.63 ± 4.39	9.84 ± 6.53	12.83 ± 4.54	0.172	5.69 ± 2.8	6.8 ± 4.37	7.74 ± 4.47	0.002
HbA1c (%)	6.28 ± 1.60	7.10 ± 2.82	7.77 ± 2.67	0.276	5.79 ± 1.14	6.19 ± 1.49	6.70 ± 1.74	<0.001
Fasting insulin (mIU/L)	5.88 ± 3.49	7.89 ± 3.89	15.44 ± 8.66	<0.001	6.81 ± 6.65	8.03 ± 6.24	11.14 ± 14.33	0.011
Diabetes mellitus, *n* (%)	5 (41.7)	6 (37.5)	13 (65.0)	0.093	7 (6.7)	7 (13.7)	35 (33.3)	<0.001
Triglycerides-S (mmol/L)*	1.12 (0.86–1.64)	1.26 (1.00–1.50)	1.74 (1.43–3.31)	0.008	1.05 (0.72; 1.42)	1.28 (0.9; 1.67)	1.40 (1.05; 1.83)	<0.001
Total cholesterol (mmol/L)	5.93 ± 1.14	5.66 ± 1.12	5.93 ± 1.23	0.757	4.75 ± 1.18	5.13 ± 0.97	5.42 ± 1.04	<0.001
LDL-cholesterol (mmol/L)	3.76 ± 1.09	3.48 ± 0.97	3.96 ± 1.06	0.402	2.86 ± 1	3.13 ± 0.96	3.37 ± 0.91	0.001
HDL-cholesterol (mmol/L)	1.57 ± 0.50	1.48 ± 0.59	1.17 ± 0.21	0.032	1.36 ± 0.41	1.35 ± 0.38	1.37 ± 0.34	0.984
usCRP (mg/L)	6.32 ± 8.79	9.73 ± 13.20	11.00 ± 6.89	0.44	7.32 ± 13.51	6.24 ± 7.09	7.24 ± 14.03	0.871
Serum cotinine (ng/mL)*	10.0 (10.0–22.5)	209.5 (10.0–261.0)	99.4 (10.0–195.5)	0.146	137 (10; 265.5)	10 (10; 287)	10 (10; 135.75)	0.002
JIS MetS criteria	4 (33.33)	9 (56.25)	18 (90.00)	0.014	22 (21.15)	21 (41.18)	61 (58.65)	<0.001

Values presented as mean ± SD unless marked with an asterisk, in which case the median and (25th-75th percentiles) are reported. The Kruskal-Wallis-test and analysis of variance (ANOVA) were used to compare the median and mean baseline characteristics, respectively, across blood pressure groups. SD, standard deviation; usCRP, ultrasensitive CRP; MetS, Metabolic Syndrome.*

and aldosterone synthesis and secretion. Based on GO analyses, we retrieved the biological processes, cellular components and molecular functions of dysregulated miRNAs. In **Figure 3**, we present the top enrichment scores for biological processes of dysregulated miRNAs in hypertensive vs. normotensive participants.

Next Generation Sequencing Results Validation

The RT-qPCR data were normalized using miR-16-5p and the raw Ct values, showing its suitability as an endogenous control in our cohort, are shown in **Supplementary Figure 1**. The two miRNAs with the highest fold change between study groups using NGS were selected for validation with RT-qPCR, namely miR-30a-5p and miR-1299. The relative expressions ($2^{-\Delta Ct}$) of each target miRNA in the three participant groups are shown in **Figure 4**. Both miR-30a-5p and miR-1299 were upregulated in known HPT compared to normotensive or screen-detected HPT, $p = 0.015$, whilst miR-30a-5p was also significantly upregulated in screen-detected HPT vs. normotensive, $p = 0.023$. Using the $2^{-\Delta\Delta Ct}$ formula to compute fold changes between two groups, miR-30a-5p expression was 2.58-fold higher in known HPT vs. normotensive and 1.69-fold higher vs. screen-detected HPT. In screen-detected HPT, miR-30a-5p expression was 1.52-fold higher when compared to the normotensives. As for miR-1299, there was a 3.93-fold and 2.78-fold higher expression in known

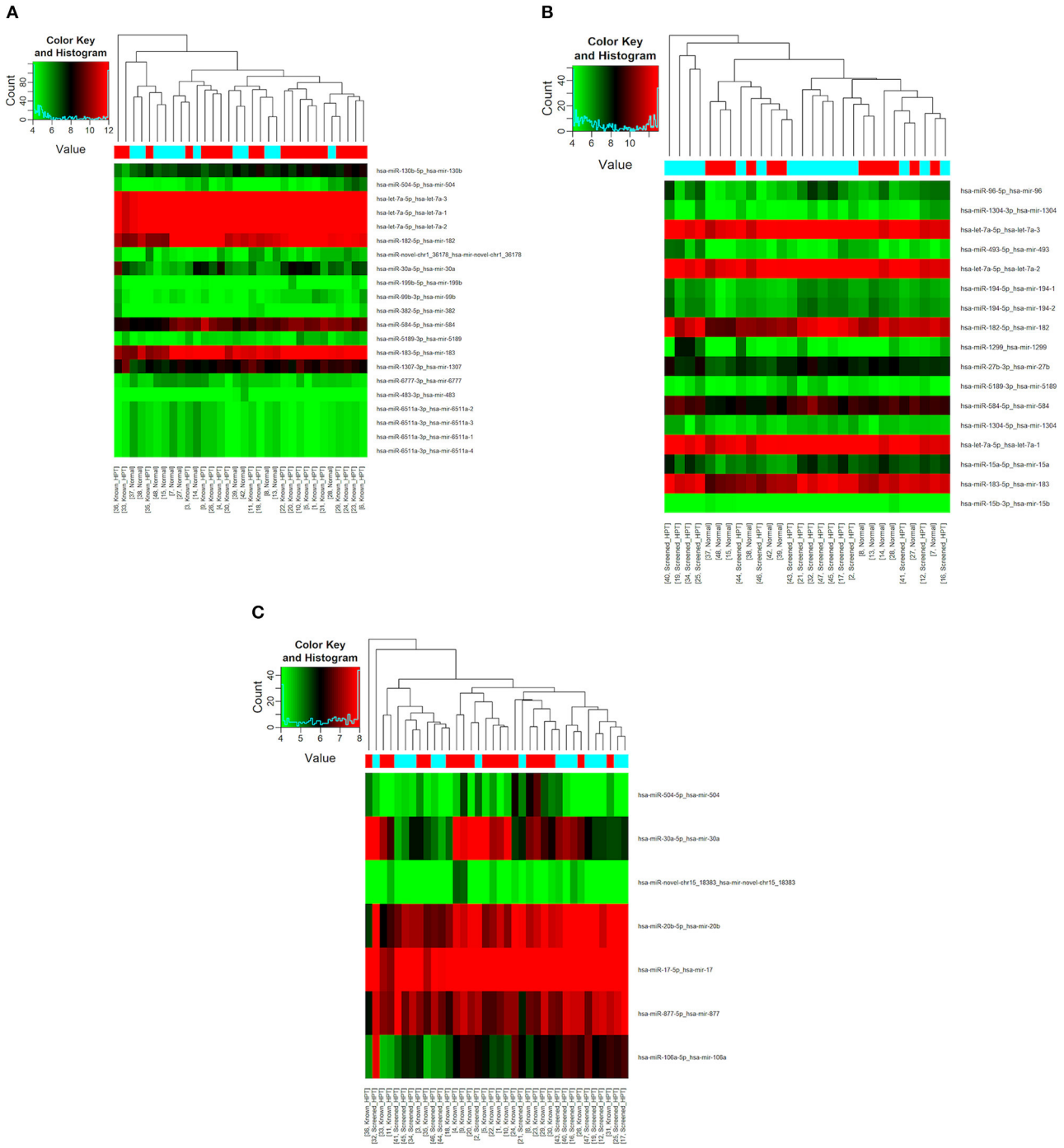

FIGURE 1 | Differential miRNA expression according to HPT status. The heatmap shows all differentially expressed miRNAs at adjusted p-value < 0.05. **(A)** Normotensive vs. known HPT; **(B)** Normotensive vs. screen-detected HPT; **(C)** Known HPT vs. screen-detected HPT.

HPT vs. normotensives and screen-detected HPT, respectively. However, there was not a great difference in the expression of miR-1299 between screen-detected HPT vs. normotensive as shown by the 1.41-fold difference in expression.

Multivariable Regression Analysis

The results of multivariable regression analysis are shown in **Supplementary Table 1**. For miR-30a-5p, the crude odds ratio was 1.31 [95% confidence interval (CI): 1.13–1.51, $p < 0.001$]

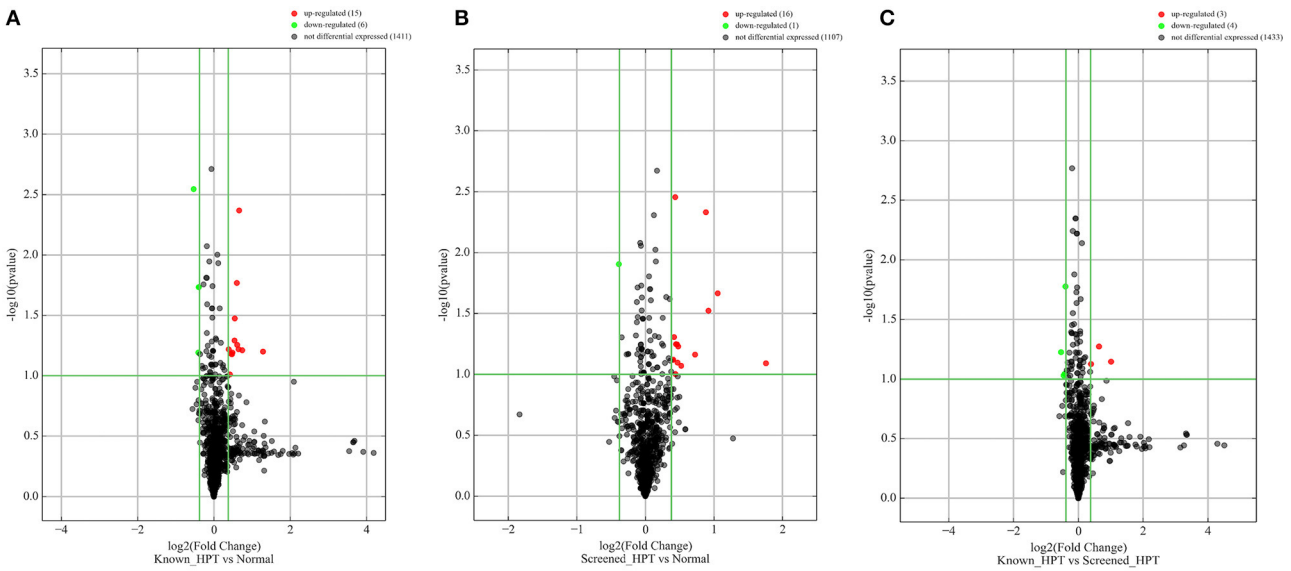

FIGURE 2 | Differentially expressed pre-miRNAs in comparison between blood pressure groups. **(A)** Is a comparison between known hypertensives and normotensives. **(B)** Is a comparison between screen-detected HPT and normotensives. **(C)** Is a comparison between known HPT and screen-detected HPT. Significantly different expression of a pre-miRNA was those in which there was a ≥1.3-fold change difference in expression between comparison groups and $p \leq 0.1$. Red and green dots signify upregulated and downregulated miRNAs, respectively. No differential expression was signified with a black dot.

for screen-detected HPT, whilst for known HPT, the OR was 1.30 (95% CI: 1.13–1.49, $p < 0.001$). When the models were adjusted for different variables, the expression of miR-30a-5p remained significantly associated with both screen-detected and known HPT ($p \leq 0.019$). With regard to miR-1299, the crude odds ratio was 0.80 [95% confidence interval (CI): 0.54–1.20, $p = 0.284$] for screen-detected HPT, whilst for known HPT, the OR was 1.11 (95% CI: 0.96–1.30, $p = 0.164$). There was no significant association between screen-detected and known HPT with miR-1299 expression for all tested models ($p \geq 0.134$). In this cohort of participants, differences in age, sex, diabetes status, BMI, total cholesterol and trigylerides between normotensives and hypertensives (screen-detected and known) did not significantly impact the expression of both miR-30a-5p and miR-1299.

DISCUSSION

To our knowledge, no study has been conducted on miRNA expression in relation to HPT in populations from Africa. Using NGS, we identified 30 (including two novel) mature miRNAs that were differentially expressed in 48 South African women with either screen-detected or treated HPT. These miRNAs were associated with pathways such as platelet activation, calcium signaling and vascular smooth muscle contraction pathways which are particularly important in cardiovascular pathogenesis (18–20). Two miRNAs, namely miR-1299 and miR-30a-5p were the most significantly dysregulated in hypertensive individuals and this was validated using RT-qPCR in 311 study participants, confirming the miRNA sequencing results while yielding new findings. Multivariable regression analysis showed that in our cohort, differences in age, sex, diabetes status, BMI, total cholesterol and trigylerides had no significant effect on the expression of miRNAs. Furthermore, the significant relationship between miR-30a-5p expression and screen-detected and known HPT was demonstrated.

Several studies have reported on a number of dysregulated miRNAs in HPT using different tissues, but results remain inconsistent (21–25). A study similar to ours reported 27 dysregulated miRNAs in a sample of 13 individuals with HPT (21), although the miRNAs were not similar to ours. A recurring theme within these miRNA profiling studies in HPT is the inter-study inconsistency of findings. For example, expression of various miRNAs such as miR-21, miR-145-5p, miR-155-5p, miR-181a (26–34) that had been previously associated with BP and HPT were not found in this study. We suspect this may partially be attributed to the diverse genetic makeup of Africans and in particular, our study participants whose heterogeneous genetic makeup comprises 32–43% Khoisan, 20–36% Bantu-speaking Africans, 21–28% European, and 9–11% Asian ancestry (35). Furthermore, differences in the methods used could account for the discordance in inter-study findings as the tissue specific nature of some miRNAs has been previously described (36). In our study, discordant results with regards to miR-1299 were evident between NGS and RT-qPCR. Other studies have employed the candidate miRNA approach and reported on miRNAs that have not necessarily been identified using microarrays or sequencing, highlighting the need for more studies employing the same methodologies and experimental designs and standardized sample preparation before these miRNAs can be utilized as new biomarkers.

In a previous study, miR-30 was down-regulated in the plasma of patients with essential HPT (37). In contrast, our findings

TABLE 2 | Dysregulated mature miRNAs in screen-detected and known HPT compared to normotensive participants.

Mature miRNA	miRNA accession number	Known HPT vs. normotensive fold change	*p*-value	BH FDR	Mature miRNA	miRNA accession number	Screen-detected HPT vs. normotensive fold change	*p*-value	BH FDR	Mature miRNA	miRNA accession number	Known HPT vs. screen-detected HPT	*p*-value	BH FDR
miR-30a-5p	MIMAT0000087	2.44	0.063	0.7403	miR-1299	MIMAT0005887	3.38	0.081	0.8106	miR-30a-5p	MIMAT0000087	2.02	0.072	0.7031
miR-504-5p	MIMAT0002875	1.67	0.062	0.7403	miR-182-5p	MIMAT0000259	2.08	0.022	0.8106	miR-504-5p	MIMAT0002875	1.56	0.053	0.7031
miR-5189-3p	MIMAT0027088	1.58	0.004	0.7403	miR-96-5p	MIMAT0000095	1.89	0.030	0.8106	miR-novel-chr15_18383	miR-novel-chr15_18383	1.31	0.075	0.7031
miR-182-5p	MIMAT0000259	1.57	0.060	0.7403	miR-183-5p	MIMAT0000261	1.84	0.005	0.8106	miR-877-5p	MIMAT0004949	0.76	0.017	0.7031
miR-183-5p	MIMAT0000261	1.53	0.056	0.7403	miR-493-5p	MIMAT0002813	1.65	0.069	0.8106	miR-106a-5p	MIMAT0000103	0.75	0.091	0.7031
miR-1307-3p	MIMAT0005951	1.52	0.017	0.7403	miR-1304-3p	MIMAT0022720	1.44	0.085	0.8106	miR-17-5p	MIMAT0000070	0.73	0.093	0.7031
miR-novel-chr1_36178	miR-novel-chr1_36178	1.46	0.034	0.7403	miR-5189-3p	MIMAT0027088	1.39	0.059	0.8106	miR-20b-5p	MIMAT0001413	0.69	0.060	0.7031
miR-382-5p	MIMAT0000737	1.45	0.051	0.7403	miR-584-5p	MIMAT0003249	1.38	0.080	0.8106					
miR-584-5p	MIMAT0003249	1.4	0.064	0.7403	miR-27b-3p	MIMAT0000419	1.38	0.057	0.8106					
miR-130b-5p	MIMAT0004680	1.39	0.066	0.7403	miR-194-5p	MIMAT0000460	1.36	0.057	0.8106					
let-7a-5p	MIMAT0000062	1.37	0.066	0.7403	miR-15a-5p	MIMAT0000068	1.36	0.099	0.8106					
miR-199b-5p	MIMAT0000263	1.34	0.098	0.7403	miR-1304-5p	MIMAT0005892	1.35	0.004	0.8106					
miR-99b-3p	MIMAT0004678	1.31	0.060	0.7403	let-7a-5p	MIMAT0000062	1.32	0.076	0.8106					
miR-6511a-3p	MIMAT0025479	0.76	0.019	0.7403	miR-15b-3p	MIMAT0004586	0.76	0.013	0.8106					
miR-483-3p	MIMAT0002173	0.75	0.064	0.7403										
miR-6777-3p	MIMAT0027455	0.69	0.003	0.7403										

A comparison of dysregulated miRNAs between screen-detected HPT and known HPT participants is also shown.
BH FDR, Benjamini-Hochberg False Discovery Rate corrected p-value.

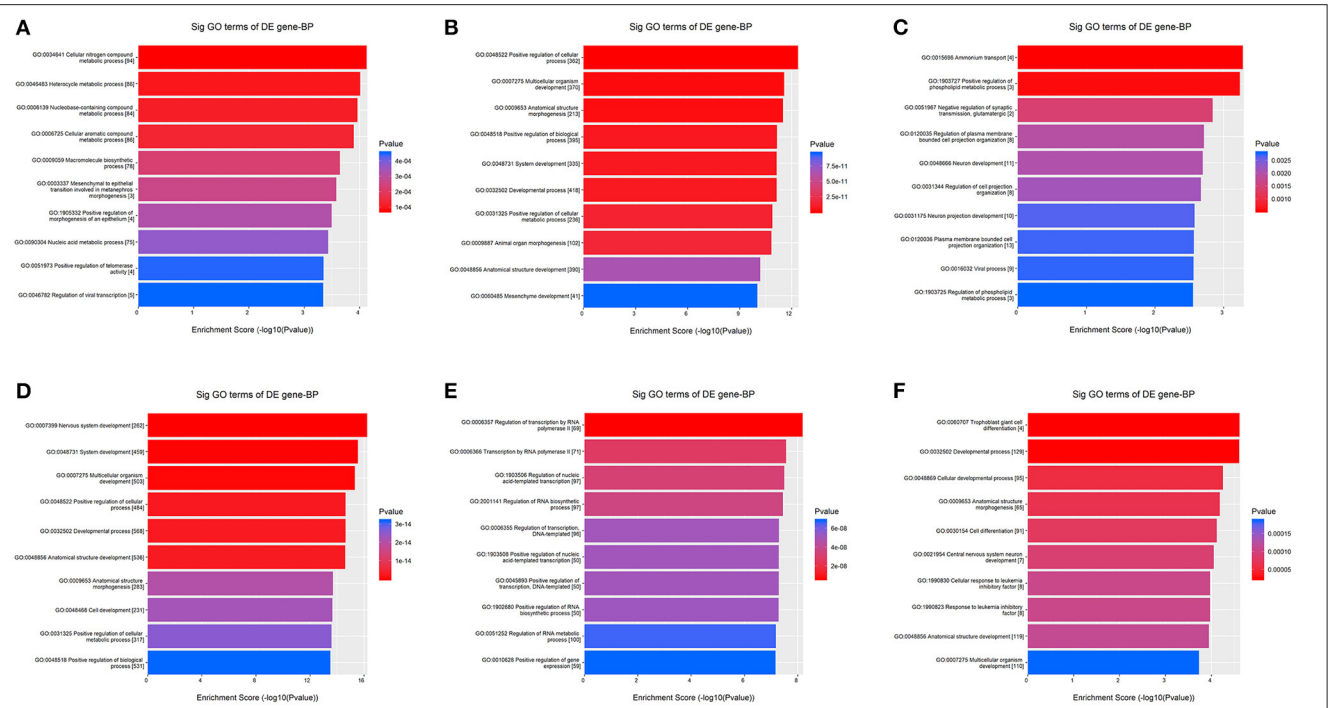

FIGURE 3 | GO analysis—Biological Processes. The bars plots show the top 10 enrichment score values of the significant enrichment terms. X-axis: GOID's enrichment score value; it equals –log10(*p*-value); Y-axis: GO category. **(A)** Upregulated in known HPT vs. normotensive. **(B)** Downregulated in known HPT vs. normotensive. **(C)** Upregulated in screen-detected HPT vs. normotensive. **(D)** Downregulated in screen-detected HPT vs. normotensive. **(E)** Upregulated in known HPT vs. screen-detected HPT. **(F)** Downregulated in known HPT vs. screen-detected HPT.

using both sequencing and RT-qPCR showed an upregulation of miR-30a-5p in both screen-detected or known hypertensive (on antihypertensive treatment) individuals. This difference in expression may be partially explained by the differences in the sample type used for analysis. Whilst our study utilized whole blood (composed of plasma, red blood cells, platelets and white blood cells) for total miRNA expression, the other study made use of plasma (cell-deficient). Pre-analytical sample manipulation using centrifugation, which is required for obtaining plasma from whole blood, affects miRNA expression profiles, as it removes from the plasma, cell-specific miRNAs that would otherwise have been detected in whole blood (38). Findings similar to ours were also reported by Huang et al. who demonstrated increased plasma expression of miR-30a in essential and white coat HPT, relative to normotensive participants (39). Overexpression of miR-30a has been reported to interfere with the removal of damaged or dead endothelial cells, promoting atherosclerosis and predisposing individuals to cardiovascular complications, like heart attacks (40). Similarly, other miRNAs in the miR-30 family have been associated with cardiovascular diseases and suggestions made that they act as predictors for acute myocardial infarction and heart failure (40, 41). For instance, the overexpression of miR-30b-5p was shown to have a downregulatory effect on a muscleblind-like splicing regulator 1 (MBLN1) transcript in atherosclerosis, possibly playing a role in the regulation of vascular smooth muscle cells VSMCs (42). Another miRNA with interesting results was miR-1299, which was significantly upregulated in screen-detected HPT when compared to the normotensive group, fold change = 3.38. This was also confirmed with RT-qPCR, which indicated a 1.41-fold increase in expression of the miRNA in screen-detected HPT compared to the normotensive group. However, multivariable regression analysis did not indicate a relationship between HPT and the expression of miR-1299. Although miR-1299 is yet to be reported in HPT by other groups, the microRNA has been implicated in Rheumatic Heart Disease (RHD), a common complication of which is pulmonary arterial hypertension (PAH) (43). One study identified miR-1299 as an important role player in suppressing the growth of colon cancer cells *via* downregulation of the signal transducers and activators of transcription (STAT3). STAT3 is as an important component in the heart's adaptation to elevated BP (44, 45). It is possible then that elevated expression of miR-1299, as seen in the hypertensive participants, may be a contributing factor in protecting against cardiovascular events associated with elevated BP levels.

As seen in KEGG analysis, the significantly differentially expressed miRNAs had possible involvement in various pathways relevant to HPT, including vascular smooth muscle contraction, vasopressin-mediated water reabsorption, platelet activation, calcium signaling, and aldosterone synthesis and secretion. Alterations to the vascular smooth muscle cells (VSMCs) phenotype has implications in vascular resistance, BP and HPT

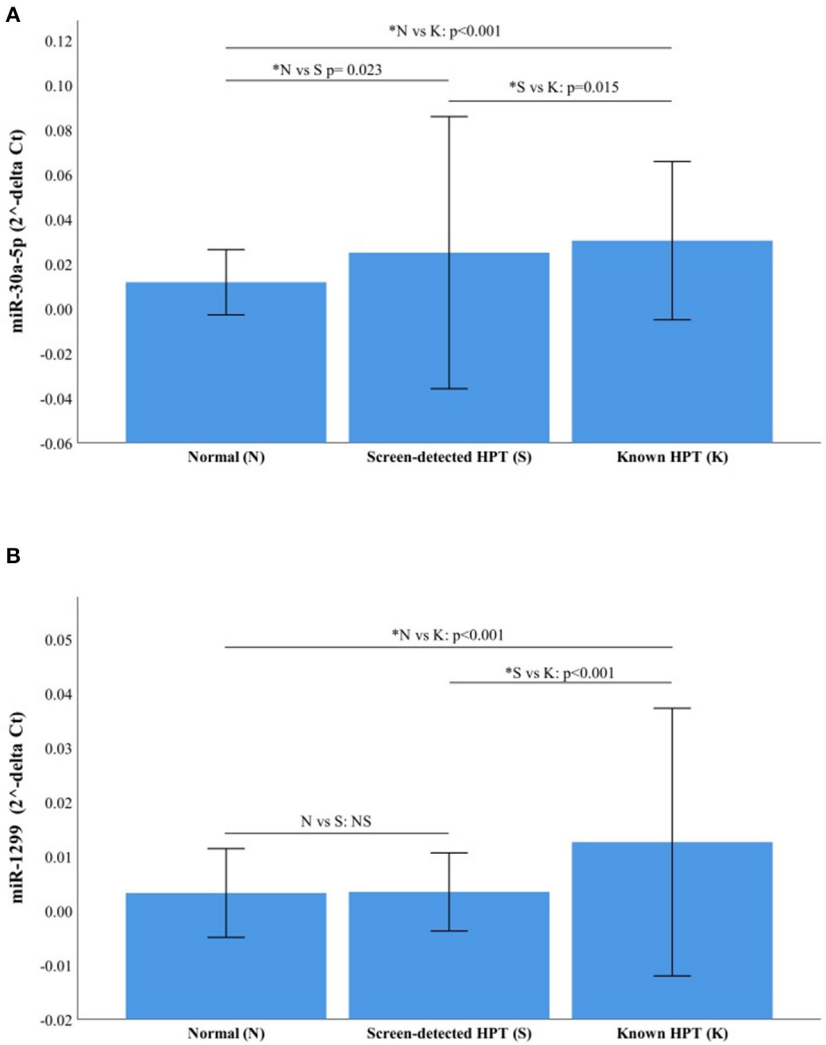

FIGURE 4 | Relative expression of miR-30a-5p and miR-1299. **(A)** miR-30a-5p in normotensive ($n = 116$), screen-detected HPT ($n = 66$) and known HPT ($n = 124$). **(B)** miR-1299p in normotensive, screen-detected HPT and known HPT. Data are represented graphically as the mean ± SD. Not significant (NS) if $p > 0.05$ and significant p-value denoted by an asterisk*.

and Kontaraki et al. demonstrated differential expression of five miRNAs (miR-1, −21, −133, 143, and −145) previously implicated in the alteration of the VSMC phenotype (34). Water retention is also essential in BP regulation and fluid volume maintenance and various miRNAs have been implicated in these processes. Through repression of the methyl CpG binding protein 2 (*Mecp2*) gene and MeCP2 protein, miR-132 regulates vasopressin synthesis and as such, fluid retention (46), whilst miR-32 and −137 regulate water retention by targeting kidney water channels controlled by vasopressin (47, 48). Dysregulations in aldosterone production or secretion pathways may be a risk for the development of HPT and aldosterone production is reduced due to miR-24 targeting of mRNA from the *CYP11B2* gene (49), whilst angiotensin II-mediated overexpression of miR-21 leads to increased aldosterone secretion (50). Dysregulation of calcium signaling leads to altered responses by the vasculature, a common characteristic in HPT (51). In a murine model, Wu et al. demonstrated the regulation of calcium signaling in the kidney by the miR-30 family (52), whilst another study reported miR-214 as a regulator of the calcium pathways through repression of mRNA encoding the sodium-calcium exchanger protein, Ncx1 (53).

Our study had some limitations. Firstly, we did not investigate the effect of antihypertensive drugs, which could have likely influenced the differential expression of miRNAs between treated (known HPT) and untreated (screen-detected HPT) hypertensive individuals. For instance, in a murine model of salt-sensitive HPT, a high salt diet was accompanied by reduced expression of miR-27a, miR-29a, and miR-133a. However, Nebivolol prevented the high salt-mediated lower expression of miR-27a, whilst there was complete and partial reversal of high salt-induced

miR-29a decrease by Nebivolol and Atenolol, respectively. Both medications were able to prevent a decrease in miR-133a expression (54). Second, in our NGS analysis, miRNA expression screening was done in only 48 female participants. However, the RT-qPCR validation was performed in a larger sample that also included male participants. Lastly, only two of the 30 significantly dysregulated miRNAs as shown by NGS were validated by RT-qPCR.

In conclusion, our study demonstrated miRNA dysregulation in hypertensive individuals and to our knowledge, is the first study to do so in a sub-Saharan population. Based on our findings, we have shown a number of miRNAs, particularly, miR-30a-5p and miR-1299 that could be explored further for a potential prognostic role, or as therapeutic targets.

DATA AVAILABILITY STATEMENT

The datasets presented in this study can be found in online repositories. The names of the repository/repositories and accession number(s) can be found below: https://www.ncbi.nlm.nih.gov/, PRJNA680302.

ETHICS STATEMENT

This Investigation was based on the Cape Town Vascular and Metabolic Health (VMH) Study, which was approved by the Research Ethics Committees of the Cape Peninsula University of Technology (CPUT) and Stellenbosch University (respectively, NHREC: REC−230 408−014 and N14/01/003). Ethical approval was also obtained for this cross-sectional sub-study from the CPUT Health and Wellness Sciences Research Ethics Committee (CPUT/HW-REC 2019/H7). The study was conducted as per the provisions of the Declaration of Helsinki. All procedures were explained to the participants in their language of choice. Once the participants fully understood their participation, they signed informed consent forms to allow the collection of blood and anthropometric data. The patients/participants provided their written informed consent to participate in this study.

AUTHOR CONTRIBUTIONS

TM, RE, and AK: conceptualization and funding acquisition. DM, SR, and CW: methodology. DM and SD: formal analysis. DM and CW: investigation. TM: resources. DM, SR, and SD: data curation. DM: writing—original draft preparation. TM, RE, AK, GD, SR, and SH: writing—review and editing. DM, CW, and SR: validation. DM, SD, and TM: visualization. TM, GD, and SH: supervision. TM and SD: project administration. All authors have read and agreed to the published version of the manuscript.

FUNDING

This research was funded by the South African Medical Research Council (SAMRC), with funds from National Treasury under its Economic Competitiveness and Support Package (MRC-RFA-UFSP-01-2013/VMH Study) and South African National Research Foundation (SANRF) (Grant No. 115450).

ACKNOWLEDGMENTS

Our thanks to the Bellville South Ward 009 community for partaking in the study as well as the Bellville South Community Health Forum for supporting the engagement with the Bellville South Community.

SUPPLEMENTARY MATERIAL

The Supplementary Material for this article can be found online at: https://www.frontiersin.org/articles/10.3389/fcvm.2021.645541/full#supplementary-material

Supplementary Figure 1 | A comparison of the raw Ct-values of the RT-qPCR normalizer, miR-16-5p in the three blood pressure groups. No significant difference in expression was observed between groups. Known HPT vs. normotensives, $p = 0.083$; known HPT vs. screen-detected HPT, $p = 0.118$ and normotensive vs. screen-detected HPT, $p = 0.710$.

Supplementary Table 1 | Multivariate regression analysis of miRNAs for the presence of screen-detected and known hypertension.

REFERENCES

1. James PA, Oparil S, Carter BL, Cushman WC, Dennison-Himmelfarb C, Handler J, et al. 2014 Evidence-based guideline for the management of high blood pressure in adults: report from the panel members appointed to the eighth joint national committee (JNC 8). *JAMA*. (2014) 311:507–20. doi: 10.1001/jama.2013.284427
2. Abegaz TM, Abdela OA, Bhagavathula AS, Teni FS. Magnitude and determinants of uncontrolled blood pressure among hypertensive patients in ethiopia: hospital-based observational study. *Pharm Pract (Granada)*. (2018) 16:1173. doi: 10.18549/PharmPract.2018.02.1173
3. Wise IA, Charchar FJ. Epigenetic modifications in essential hypertension. *Int J Mol Sci*. (2016) 17:451. doi: 10.3390/ijms17040451
4. Polsinelli VB, Satchidanand N, Singh R, Holmes D, Izzo JL. Hypertension and aging in Rural Haiti: results from a preliminary survey. *J Hum Hypertens*. (2017) 31:138–44. doi: 10.1038/jhh.2016.52
5. Lim SS, Vos T, Flaxman AD, Danaei G, Shibuya K, Adair-Rohani H, et al. A comparative risk assessment of burden of disease and injury attributable to 67 risk factors and risk factor clusters in 21 regions, 1990-2010: a systematic analysis for the global burden of disease study 2010. *Lancet*. (2012) 380:2224–60. doi: 10.1016/S0140-6736(12)61766-8
6. Babiker FA, Elkhalifa LA, Moukhyer ME. Awareness of hypertension and factors associated with uncontrolled hypertension in sudanese adults. *Cardiovasc J Afr*. (2013) 24:208–12. doi: 10.5830/CVJA-2013-035
7. Peltzer K, Phaswana-Mafuya N. Hypertension and associated factors in older adults in South Africa. *Cardiovasc J Afr*. (2013) 24:66–72. doi: 10.5830/CVJA-2013-002
8. Bátkai S, Thum T. MicroRNAs in hypertension: mechanisms and therapeutic targets. *Curr Hypertens Rep*. (2012) 14:79–87. doi: 10.1007/s11906-011-0235-6
9. Rossier BC, Bochud M, Devuyst O. The hypertension pandemic: an evolutionary perspective. *Physiolgy*. (2017) 32:112–25. doi: 10.1152/physiol.00026.2016
10. Mu S, Shimosawa T, Ogura S, Wang H, Uetake Y, Kawakami-Mori F, et al. Epigenetic modulation of the renal β-adrenergic-WNK4 pathway in salt-sensitive hypertension. *Nat Med*. (2011) 17:573–80. doi: 10.1038/nm.2337
11. Shin VY, Chu K-M. MiRNA as potential biomarkers and therapeutic targets for gastric cancer. *World J Gastroenterol*. (2014) 20:10432–9. doi: 10.3748/wjg.v20.i30.10432

12. Levy E, Spahis S, Bigras J-L, Delvin E, Borys J-M. The epigenetic machinery in vascular dysfunction and hypertension. *Curr Hypertens Rep*. (2017) 19:1–12. doi: 10.1007/s11906-017-0745-y
13. Chen X, Ba Y, Ma L, Cai X, Yin Y, Wang K, et al. Characterization of microRNAs in serum: a novel class of biomarkers for diagnosis of cancer and other diseases. *Cell Res*. (2008) 18:997–1006. doi: 10.1038/cr.2008.282
14. Nemecz M, Alexandru N, Tanko G, Georgescu A. Role of microRNA in endothelial dysfunction and hypertension. *Curr Hypertens Rep*. (2016) 18:87. doi: 10.1007/s11906-016-0696-8
15. Matsha TE, Kengne AP, Hector S, Mbu DL, Yako YY, Erasmus RT. MicroRNA profiling and their pathways in south african individuals with prediabetes and newly diagnosed type 2 diabetes mellitus. *Oncotarget*. (2018) 9:30485–98. doi: 10.18632/oncotarget.25271
16. Chalmers J, MacMahon S, Mancia G, Whitworth J, Beilin L, Hansson L, et al. 1999 World health organization-international society of hypertension guidelines for the management of hypertension. *Clin Exp Hypertens*. (1999) 21:1009–60.
17. Livak KJ, Schmittgen TD. Analysis of relative gene expression data using real-time quantitative PCR and the 2-ΔΔCT method. *Methods*. (2001) 25:402–8. doi: 10.1006/meth.2001.1262
18. Gkaliagkousi E, Passacquale G, Douma S, Zamboulis C, Ferro A. Platelet activation in essential hypertension: implications for antiplatelet treatment. *Am J Hypertens*. (2010) 23:229–36. doi: 10.1038/ajh.2009.247
19. Landstrom AP, Dobrev D, Wehrens XHT. Calcium signaling and cardiac arrhythmias. *Circ Res*. (2017) 120:1969–93. doi: 10.1161/CIRCRESAHA.117.310083
20. Touyz RM, Alves-Lopes R, Rios FJ, Camargo LL, Anagnostopoulou A, Arner A, et al. Vascular smooth muscle contraction in hypertension. *Cardiovasc Res*. (2018) 114:529–39. doi: 10.1093/cvr/cvy023
21. Li S, Zhu J, Zhang W, Chen Y, Zhang K, Popescu LM, et al. Signature microRNA expression profile of essential hypertension and its novel link to human cytomegalovirus infection. *Circulation*. (2011) 124:175–84. doi: 10.1161/CIRCULATIONAHA.110.012237
22. Jairajpuri DS, Malalla ZH, Mahmood N, Almawi WY. Circulating microRNA expression as predictor of preeclampsia and its severity. *Gene*. (2017) 627:543–8. doi: 10.1016/j.gene.2017.07.010
23. Chen S, Chen R, Zhang T, Lin S, Chen Z, Zhao B, et al. Relationship of cardiovascular disease risk factors and noncoding RNAs with hypertension: a case-control study. *BMC Cardiovasc Disord*. (2018) 18:58. doi: 10.1186/s12872-018-0795-3
24. Özkan G, Ulusoy S, Geyik E, Erdem Y. Down-regulation of miRNA 145 and up-regulation of miRNA 4516 may be associated with primary hypertension. *J Clin Hypertens*. (2019) 21:1724–31. doi: 10.1111/jch.13704
25. Yildirim E, Ermis E, Allahverdiyev S, Ucar H, Yavuzer S, Cengiz M. Circulating miR-21 levels in hypertensive patients with asymptomatic organ damage. *Medicine (Baltimore)*. (2019) 98:e17297. doi: 10.1097/MD.0000000000017297
26. Santovito D, Mandolini C, Marcantonio P, De Nardis V, Bucci M, Paganelli C, et al. Overexpression of microRNA-145 in atherosclerotic plaques from hypertensive patients. *Expert Opin Ther Targets*. (2013) 17:217–23. doi: 10.1517/14728222.2013.745512
27. Cengiz M, Yavuzer S, Klçkran Avc B, Yürüyen M, Yavuzer H, Dikici SA, et al. Circulating miR-21 and eNOS in subclinical atherosclerosis in patients with hypertension. *Clin Exp Hypertens*. (2015) 37:643–9. doi: 10.3109/10641963.2015.1036064
28. Sethupathy P, Borel C, Gagnebin M, Grant GR, Deutsch S, Elton TS, et al. Human microRNA-155 on chromosome 21 differentially interacts with its polymorphic target in the AGTR1 3′ untranslated region: a mechanism for functional single-nucleotide polymorphisms related to phenotypes. *Am J Hum Genet*. (2007) 81:405–13. doi: 10.1086/519979
29. Li H, Zhang X, Wang F, Zhou L, Yin Z, Fan J, et al. MicroRNA-21 lowers blood pressure in spontaneous hypertensive rats by upregulating mitochondrial translation. *Circulation*. (2016) 134:734–51. doi: 10.1161/CIRCULATIONAHA.116.023926
30. Ceolotto G, Papparella I, Bortoluzzi A, Strapazzon G, Ragazzo F, Bratti P, et al. Interplay between miR-155, AT1R A1166C polymorphism, and AT1R expression in young untreated hypertensives. *Am J Hypertens*. (2011) 24:241–6. doi: 10.1038/ajh.2010.211
31. Jackson KL, Marques FZ, Watson AMD, Palma-Rigo K, Nguyen-Huu TP, Morris BJ, et al. A novel interaction between sympathetic overactivity and aberrant regulation of renin by miR-181a in BPH/2J genetically hypertensive mice. *Hypertension*. (2013) 62:775–81. doi: 10.1161/HYPERTENSIONAHA.113.01701
32. Marques FZ, Campain AE, Tomaszewski M, Zukowska-Szczechowska E, Yang YHJ, Charchar FJ, et al. Gene expression profiling reveals renin mRNA overexpression in human hypertensive kidneys and a role for microRNAs. *Hypertension*. (2011) 58:1093–8. doi: 10.1161/HYPERTENSIONAHA.111.180729
33. Parmacek MS. MicroRNA-modulated targeting of vascular smooth muscle cells. *J Clin Invest*. (2009) 119:2526–8. doi: 10.1172/JCI40503
34. Kontaraki JE, Marketou ME, Zacharis EA, Parthenakis FI, Vardas PE. Differential expression of vascular smooth muscle-modulating MicroRNAs in human peripheral blood mononuclear cells: novel targets in essential hypertension. *J Hum Hypertens*. (2014) 28:510–6. doi: 10.1038/jhh.2013.117
35. De Wit E, Delport W, Rugamika CE, Meintjes A, Möller M, Van Helden PD, et al. Genome-wide analysis of the structure of the south african coloured population in the Western Cape. *Hum Genet*. (2010) 128:145–53. doi: 10.1007/s00439-010-0836-1
36. Ludwig N, Leidinger P, Becker K, Backes C, Fehlmann T, Pallasch C, et al. Distribution of miRNA expression across human tissues. *Nucleic Acids Res*. (2016) 44:3865–77. doi: 10.1093/nar/gkw116
37. Huang Y, Chen J, Zhou Y, Yu X, Huang C, Li J, et al. Circulating miR-30 is related to carotid artery atherosclerosis. *Clin Exp Hypertens*. (2016) 38:489–94. doi: 10.3109/10641963.2016.1163370
38. Felekkis K, Papaneophytou C. Challenges in using circulating micro-RNAs as biomarkers for cardiovascular diseases. *Int J Mol Sci*. (2020) 21:561. doi: 10.3390/ijms21020561
39. Huang YQ, Huang C, Chen JY, Li J, Feng YQ. The association of circulating miR-30a, miR-29 and miR-133 with white-coat hypertension. *Biomark Med*. (2016) 10:1231–9. doi: 10.2217/bmm-2016-0215
40. Zhang T, Tian F, Wang J, Jing J, Zhou SS, Chen YD. Endothelial cell autophagy in atherosclerosis is regulated by miR-30-mediated translational control of ATG6. *Cell Physiol Biochem*. (2015) 37:1369–78. doi: 10.1159/000430402
41. Maciejak A, Kostarska-Srokosz E, Gierlak W, Dluzniewski M, Kuch M, Marchel M, et al. Circulating miR-30a-5p as a prognostic biomarker of left ventricular dysfunction after acute myocardial infarction. *Sci Rep*. (2018) 8:9883. doi: 10.1038/s41598-018-28118-1
42. Woo CC, Liu W, Lin XY, Dorajoo R, Lee KW, Richards AM, et al. The interaction between 30b-5p miRNA and MBNL1 mRNA is involved in vascular smooth muscle cell differentiation in patients with coronary atherosclerosis. *Int J Mol Sci*. (2020) 21:11. doi: 10.3390/ijms21010011
43. Li N, Lian J, Zhao S, Zheng D, Yang X, Huang X, et al. Detection of differentially expressed microRNAs in rheumatic heart disease: miR-1183 and miR-1299 as potential diagnostic markers. *Biomed Res Int*. (2015) 2015:524519. doi: 10.1155/2015/524519
44. Zouein FA, Zgheib C, Hamza S, Fuseler JW, Hall JE, Soljancic A, et al. Role of STAT3 in angiotensin II-induced hypertension and cardiac remodeling revealed by mice lacking STAT3 serine 727 phosphorylation. *Hypertens Res*. (2013) 36:496–503. doi: 10.1038/hr.2012.223
45. Wang Y, Lu Z, Wang N, Zhang M, Zeng X, Zhao W. MicroRNA-1299 is a negative regulator of STAT3 in colon cancer. *Oncol Rep*. (2017) 37:3227–34. doi: 10.3892/or.2017.5605
46. Bijkerk R, Trimpert C, van Solingen C, de Bruin RG, Florijn BW, Kooijman S, et al. MicroRNA-132 controls water homeostasis through regulating MECP2-mediated vasopressin synthesis. *Am J Physiol Ren Physiol*. (2018) 315:F1129–38. doi: 10.1152/ajprenal.00087.2018
47. Gomes A, da Silva IV, Rodrigues CMP, Castro RE, Soveral G. The emerging role of microRNAs in aquaporin regulation. *Front Chem*. (2018) 6:238. doi: 10.3389/fchem.2018.00238
48. Kim J-E, Jung HJ, Lee Y-J, Kwon T-H. Vasopressin-regulated miRNAs and AQP2-targeting miRNAs in kidney collecting duct cells. *Am J Physiol Ren Physiol*. (2015) 308:F749–64. doi: 10.1152/ajprenal.00334.2014
49. Robertson S, Mackenzie SM, Alvarez-Madrazo S, Diver LA, Lin J, Stewart PM, et al. MicroRNA-24 is a novel regulator of aldosterone and cortisol production in the human adrenal cortex.

Hypertension. (2013) 62:572–8. doi: 10.1161/HYPERTENSIONAHA.113.01102

50. Romero DG, Plonczynski MW, Carvajal CA, Gomez-Sanchez EP, Gomez-Sanchez CE. Microribonucleic acid-21 increases aldosterone secretion and proliferation in H295R human adrenocortical cells. *Endocrinology*. (2008) 149:2477–83. doi: 10.1210/en.2007-1686
51. Wilson C, Zhang X, Buckley C, Heathcote HR, Lee MD, McCarron JG. Increased vascular contractility in hypertension results from impaired endothelial calcium signaling. *Hypertension*. (2019) 74:1200–14. doi: 10.1161/HYPERTENSIONAHA.119.13791
52. Wu J, Zheng C, Wang X, Yun S, Zhao Y, Liu L, et al. MicroRNA-30 family members regulate calcium/calcineurin signaling in podocytes. *J Clin Invest*. (2015) 125:4091–106. doi: 10.1172/JCI81061
53. Aurora AB, Mahmoud AI, Luo X, Johnson BA, Van Rooij E, Matsuzaki S, et al. MicroRNA-214 protects the mouse heart from ischemic injury by controlling Ca2+ overload and cell death. *J Clin Invest*. (2012) 122:1222–32. doi: 10.1172/JCI59327
54. Ye H, Ling S, Castillo AC, Thomas B, Long B, Qian J, et al. Nebivolol induces distinct changes in profibrosis microRNA expression compared with atenolol, in salt-sensitive hypertensive rats. *Hypertension*. (2013) 61:1008–13. doi: 10.1161/HYPERTENSIONAHA.111.00892

Conflict of Interest: The authors declare that the research was conducted in the absence of any commercial or financial relationships that could be construed as a potential conflict of interest.

frontiers in Cardiovascular Medicine

ORIGINAL RESEARCH
published: 13 May 2021
doi: 10.3389/fcvm.2021.631650

Integrated DNA Methylation and Gene Expression Analysis Identified S100A8 and S100A9 in the Pathogenesis of Obesity

Ningyuan Chen[1†], Liu Miao[2†], Wei Lin[3], Donghua Zou[4], Ling Huang[1], Jia Huang[5], Wanxin Shi[5], Lilin Li[5], Yuxing Luo[5], Hao Liang[5], Shangling Pan[1] and Junhua Peng[1*]*

[1] Department of Pathophysiology, School of Preclinical Medicine, Guangxi Medical University, Nanning, China, [2] Department of Cardiology, Liuzhou People's Hospital, Guangxi Medical University, Liuzhou, China, [3] Department of Neurological Rehabilitation, Guangxi Jiangbin Hospital, Nanning, China, [4] Department of Neurology, The Fifth Affiliated Hospital of Guangxi Medical University, Nanning, China, [5] The First Clinical Medical School, Guangxi Medical University, Nanning, China

OPEN ACCESS

Edited by:
Xiangming Ding,
University of Southern California,
United States

Reviewed by:
Xiao Huang,
Second Affiliated Hospital of Nanchang University, China
Xiaoyue Pan,
New York University, United States

***Correspondence:**
Liu Miao
dr.miaoliu@qq.com
Junhua Peng
pengjh@gxmu.edu.cn

[†] These authors have contributed equally to this work

Specialty section:
This article was submitted to General Cardiovascular Medicine, a section of the journal Frontiers in Cardiovascular Medicine

Received: 03 December 2020
Accepted: 30 March 2021
Published: 13 May 2021

Citation:
Chen N, Miao L, Lin W, Zou D, Huang L, Huang J, Shi W, Li L, Luo Y, Liang H, Pan S and Peng J (2021) Integrated DNA Methylation and Gene Expression Analysis Identified S100A8 and S100A9 in the Pathogenesis of Obesity. Front. Cardiovasc. Med. 8:631650. doi: 10.3389/fcvm.2021.631650

Background: To explore the association of DNA methylation and gene expression in the pathology of obesity.

Methods: (1) Genomic DNA methylation and mRNA expression profile of visceral adipose tissue (VAT) were performed in a comprehensive database of gene expression in obese and normal subjects. (2) Functional enrichment analysis and construction of differential methylation gene regulatory networks were performed. (3) Validation of the two different methylation sites and corresponding gene expression was done in a separate microarray dataset. (4) Correlation analysis was performed on DNA methylation and mRNA expression data.

Results: A total of 77 differentially expressed mRNAs matched with differentially methylated genes. Analysis revealed two different methylation sites corresponding to two unique genes—s100a8-cg09174555 and s100a9-cg03165378. Through the verification test of two interesting different expression positions [differentially methylated positions (DMPs)] and their corresponding gene expression, we found that methylation in these genes was negatively correlated to gene expression in the obesity group. Higher S100A8 and S100A9 expressions in obese subjects were validated in a separate microarray dataset.

Conclusion: This study confirmed the relationship between DNA methylation and gene expression and emphasized the important role of S100A8 and S100A9 in the pathogenesis of obesity.

Keywords: obesity, DNA methylation, mRNA expression, function enrichment, correlation analyses

INTRODUCTION

With continuous improvement of living conditions, many countries have to pay more attention to the prevalence of obesity because obesity has reached the proportion of epidemic that is still rising (1). According to the World Health Organization's report in 2015, about one third or more adults are overweight, 43% of whom are male and 45% are female (2). Obesity is implicated in

many diseases, such as metabolic syndrome (MetS), type 2 diabetes mellitus (T2DM), hypertension, arteriosclerosis, cardiovascular disease (CVD), and so on (3), and thus incurs heavy economic burdens on countries around the world (4). Obesity results from interactions between genetic and environmental factors, but for individuals, epigenetic factors can increase susceptibility to obesity (5).

In recent years, with the deepening of research, epigenetics has emerged as a bridge between genes and environmental factors. It can change gene expression and induce long-term changes in phenotype and disease susceptibility (6). Extensive epigenome-wide association studies (EWAS) on DNA methylation conducted in many populations have revealed the relationship between DNA methylation and obesity (7). Changes in gene methylation changes can alter the transcription of genes resulting in abnormal gene expression and eventually obesity (8).

Gene Expression Omnibus (GEO) database hosted the sequencing data of thousands of researchers, and its most important feature was that it provided open access to the data we needed to conduct our research. In the present study, we explored innovative methylation sites of obesity-related DNA by conducting an integration study using two microarray datasets and established the relationship between the expression of obesity-related genes and methylation Differential Expression of Methylated Genes (DEMGs). We then validated the DEMGs in a separate microarray dataset to explore the potential relationship between DNA methylation and mRNA expression on the regulation of obesity.

METHODS

Gene Expression Profile and Probe Labeling

Three microarray datasets (GSE88837, GSE88940, and GSE109597) were downloaded from the gene expression database (https://www.ncbi.nlm.nih.gov/geo/) for analysis. GSE88837 was extracted from the U133 + 2.0 sequence of gpl570 Affymetrix human genome for gene expression. The purpose of this study was to use global gene expression to identify obesity-induced changes in gene expression profiles of lean and obese adolescent females. In our study, subjects with body mass index (BMI) $\geq$30 were defined as obese (1). A total of 30 subjects (including 15 obese and 15 healthy controls) were analyzed. We used the Affy package in R (9) to convert the cel files into an expression value matrix and the Robust Multichip Average (RMA) method to normalize the matrix. The Bioconductor package in R software was used to convert probe data into genes (10). If a gene corresponded to several probes, we chose the average expression value for further analysis. GSE88940 extracted from gpl13534, a human methylation 450 gene chip, was used for DNA methylation analysis, which consisted of 10 objects and 10 lean controls. Genomic DNA was extracted from visceral adipose tissue (VAT) of lean and obese adolescent females. Illumina Infinium Human Methylation 450 k BeadChips were utilized for global methylation profiles in VAT. All data processing was done in GEO2R (https://www.ncbi.nlm.nih.gov/geo/geo2r/). In these two datasets (GSE88837 and GSE88940), there are 20 samples of the same person. We only analyze these 20 samples. GSE109597 was used as the validation dataset and aimed to predict obesity risk with genetic data, specifically, obesity-associated gene expression profiles. Genetic risk score was computed. The genetic risk score was significantly correlated with BMI when an optimization algorithm was used. Linear regression and built support vector machine models predicted obesity risk using gene expression profiles and the genetic risk score with a new mathematical method. The analysis method was the same as used for GSE 88837.

Differential Expression and Analysis of Methylated Genes (DEMGs)

We compared obese with control subjects to explore the differentially expressed genes (DEGs) of the marginal envelope in R (11). The threshold value was set as | log2 fold change |$\geq$ 2, $P < 0.05$. GEO2R was used to determine the methylation sites [differentially methylated positions (DMPs)] by comparing the differences between normal and obese subjects. DMPs located in gene regions were assigned to corresponding genes, which were defined as differentially methylated genes (DMGs). The threshold value was set as $|\log_2$ fold-change$|$ $(\Delta\beta) > 0.05$, $P < 0.05$. Then, we matched the DEGs with DMGs, and only the matched genes (DEMGs) were selected for further analysis.

Functional Enrichment Analysis

All functional enrichment analysis on DEGs was performed on clusterProfiler and Dose package in R (12). The complete functional enrichment analysis includes Gene Ontology (GO), Kyoto Encyclopedia of Genes and Genomes (KEGG) approach, and Disease Ontology (DO). The threshold value of analysis was set as adjust-$P < 0.05$ and error detection rate [false discovery rate (FDR)] <0.05.

Protein–Protein Interaction Network and Module Analysis

We used the string database (version 11.0) (13) to explore protein prediction and experimental interactions. There are many methods of database prediction, including co-expression experiment, text mining, co-occurrence, gene fusion, database, and neighborhood. Also, we used the combination fraction to reveal the protein pair interactions in the database. Then, we localized DEMGs to PPIs to identify the key genes in the network with the cutoff value set to a comprehensive score >0.9 (14). As a valuable method, a degree is used to study the role of protein nodes in the network. Using the molecular complex detection (MCODE) on Cytoscape (version 3.71), the most significant clustering module and the main clustering module were explored (15, 16). For further analysis, we set ease $\leq$0.05 and set $\geq$2 as the cutoff value and MCODE score >8 as the threshold value.

Validation of DEMGs

We used prism 8.0 GraphPad (17) for scatterplots of methylation and gene expression to detect the relationship between methylation and gene expression. Then, we calculated the

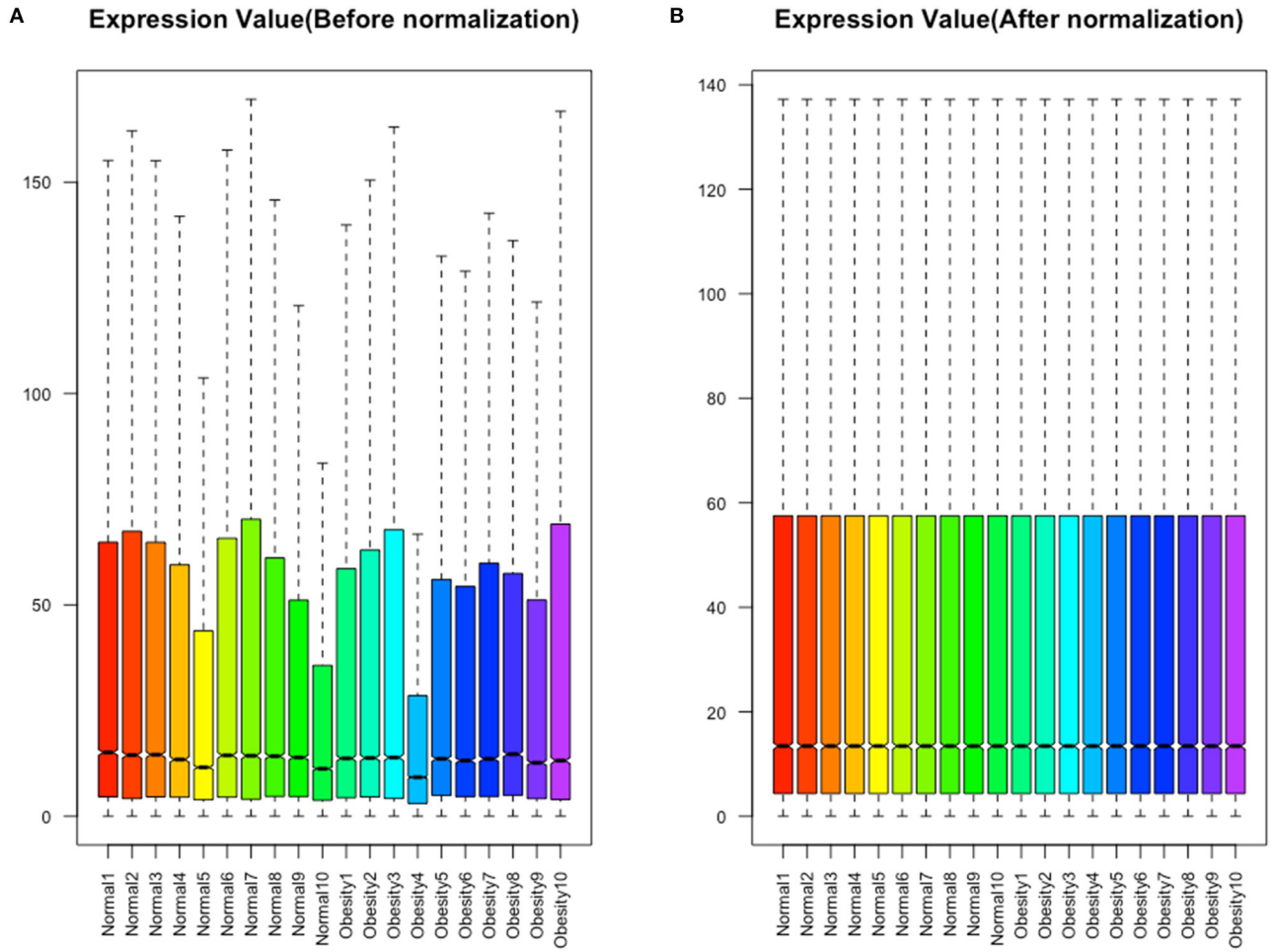

FIGURE 1 | Normalization of all samples. (**A**) Before normalization. (**B**) After normalization.

correlation equation to judge whether the equation has statistical significance. The DEMGs were validated in GSE109597, which contained 84 unrelated samples. After grouping according to BMI (>30 and <30), the expression of DMEGs in the two groups was compared with ggplot2 in R.

RESULTS

Data Preprocessing

A quality control processing of GSE88837 showed that when all the means in the strip chart lie on the same horizontal line, all samples were normalized (**Figure 1**). We obtained 54,560 expression probes from each gene map and expression. Probes with too low or too high probe expression were defined as outliers and eliminated from further analysis. An average expression value was used to screen the DEGs to prevent too many probes corresponding to one gene. The limma software package was used to calculate the DEGs, which yielded 1,814 DEGs with P values <0.05. We use the obese population as a reference, among these, 150 with a log2 (fold change) > 2 were defined as upregulated and 199 with a log2 (fold change) < 2 as downregulated. The heat map and volcano map of DEGs are shown in **Figures 2A,B**.

Out of the 485,579 DNA methylation sites in GSE88940 VAT that were screened for quality control, 454,325 methylation sites were selected for analysis. Here, 10,016 DMPs ($|\Delta\beta| > 0.05$, $P < 0.05$) were identified, of which 666 were hypermethylated and 3,349 were hypomethylated. After annotation, 10,016 DMPs are located in 4,024 unique genes, which were identified as DMGs. The thermal and volcanic maps of the DMGs are shown in **Figures 2C,D**.

Matching DMGs with DEGs yielded 77 genes for the next analysis (**Figure 3**). The details of 77 genes are shown in **Table 1** and **Figure 4**.

Functional Annotation

The cluster profiler package in R for DO function, KEGG pathway enrichment, and GO analysis was used to clarify the role of the DEGs. Here, 104 cell components, seven

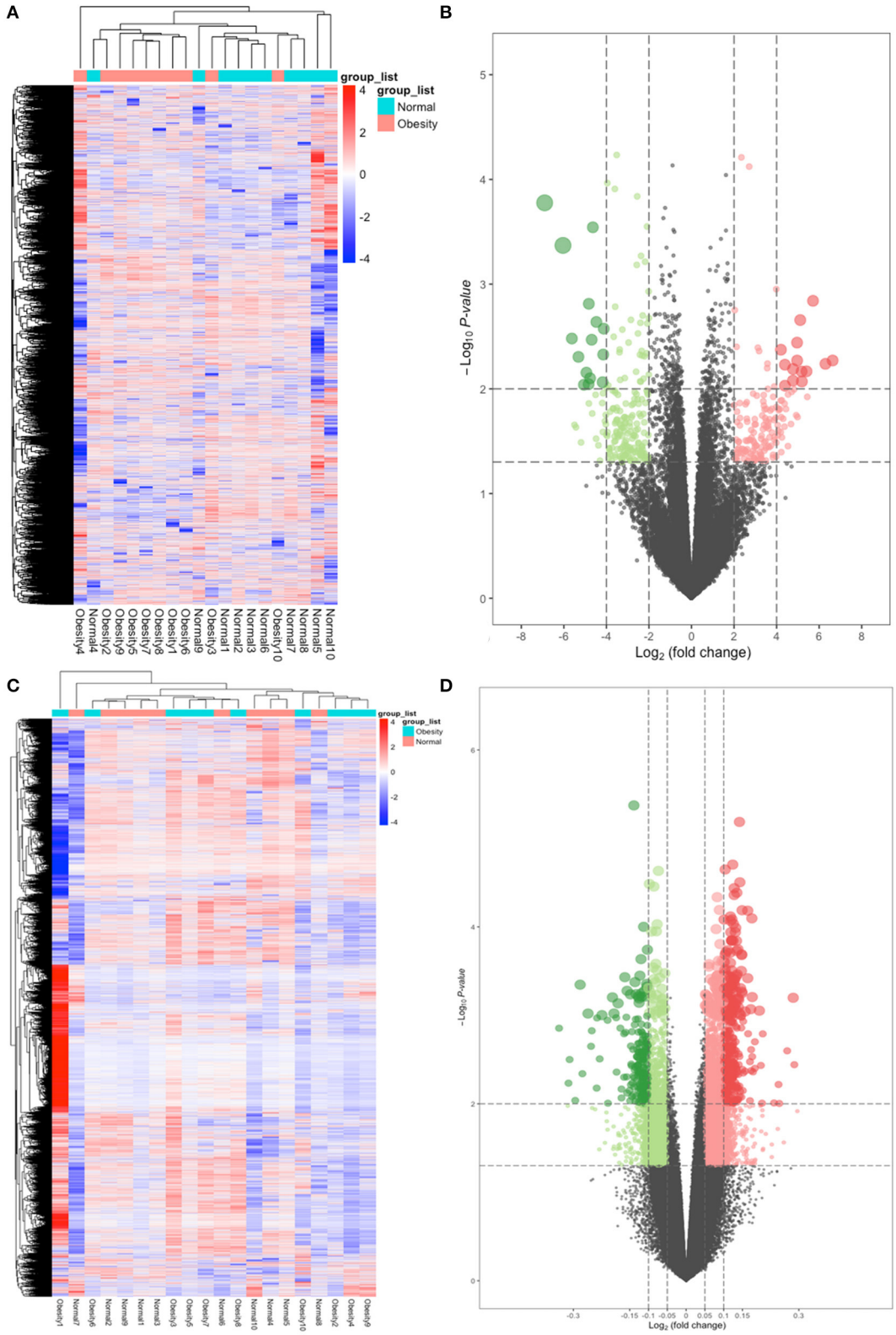

FIGURE 2 | Heatmap and volcano plots of differentially expressed genes (DEGs) and differentially methylated positions (DMPs). **(A)** Heatmap for DEGs. Obesity groups are in the red cluster, and normal samples are in the green cluster. **(B)** Volcano plot for DEGs. The two vertical lines are the 2-fold change boundaries, and the horizontal line is the statistical significance boundary ($P < 0.05$). Red dots show upregulated genes, and green dots are downregulated genes. **(C)** Heatmap for DMPs. Obesity groups are in the green cluster, and normals are in the blue cluster. **(D)** Volcano plot for DMPs. The vertical lines are the 0.05-fold change boundaries, and the horizontal line is the statistical significance boundary ($P < 0.05$). Upregulated DMPs are marked with red dots, and downregulated DMPs are marked with green dots.

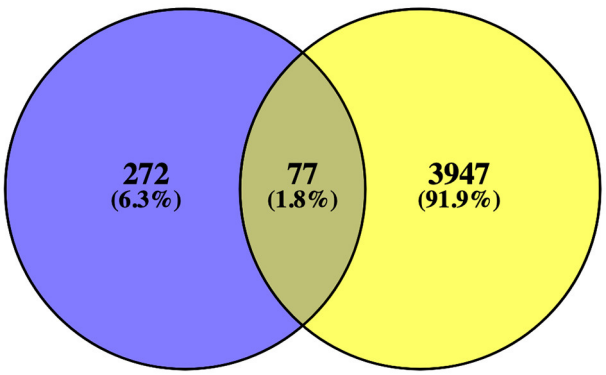

FIGURE 3 | Venn diagram showing the intersection of differentially expressed genes (DEGs) and differentially methylated genes (DMGs).

molecular functions, and 329 biological processes were significantly enriched in GO (corrected $P < 0.05$; **Figure 5A**, **Supplementary Table 1**). Also, 22 pathways were enriched in KEGG, and 77 DO items were identified at $P < 0.05$ after correction (error detection rate, FDR <0.05). The results are shown in **Figures 5B,C** and **Supplementary Tables 2**, **3**.

Enrichments including GO: 0061448 connective tissue development, GO: 0007584 nutritional response, GO: 0022600 digestive system process, GO: 0045444 adipocyte differentiation, hsa04010 MAPK signal pathway, hsa04657 IL-17 signal pathway, hsa0061 fatty acid biosynthesis, hsa04933 age-old signal pathway in diabetic complications, DOID: 9352 Type 2 diabetes mellitus; DOID: 374 nutritional diseases; DOID: 654 over nutrition; DOID: 9970 obesity have been previously reported to be related to obesity, and thus genes in these clusters were selected for further analysis.

Construction of Protein–Protein Interaction Network and Identification of Key Genes

The string database was used to clarify gene interaction networks of the selected genes on Cytoscape, which revealed 5,598 pairs of proteins and 1,003 nodes when the cutoff value was set to a comprehensive score >0.9 (**Figure 6A**). MCODE analysis showed that the scores of the four modules were more than 10 (**Figures 6B–E**). Analysis of 98 genes in these four modules revealed that two of them were highly correlated and carried out submodule analysis to screen out GO, DO, and KEGG data. The two genes were S100 calcium-binding protein A8 (S100A8) and S100 calcium-binding protein A9 (S100A9).

Hub Genes Validation

First, we tested the relationship between S100A8 and S100A9 methylation and gene expression in the same 20 individuals in GSE88837 and GSE88940. We found that there was a negative correlation between methylation level and gene expression. The results also showed that the two correlation equation lines were statistically significant ($P < 0.05$; **Figure 7**). Validation in GSE109597 showed that the expression of S100A8 and S100A9 was significantly higher in obese vs. normal subjects ($P < 0.05$; **Figure 8**).

DISCUSSION

Emerging evidence has shown that obesity is not only a simple nutritional excess but also a metabolic disorder, which is the precursor of many metabolic diseases (18). More and more studies have confirmed that chronic inflammation is the result of the accumulation of fat cells caused by abnormal gene function (19). In the present study, the relationship between gene expression and obesity in 20 obese patients was analyzed using a gene-chip dataset. We found that the high expression of S100A8 and S100A9 was related to obesity. Also, a significant increase in S100A8 and S100A9 expression was observed in the validation microarray dataset of 84 samples. Whole-genome methylation analysis showed hypomethylation of the S100A8 and S100A9 promoters. Changes in methylation often lead to abnormal gene function and diseases and, in this case, may be an important cause of obesity.

Calprotectin is a heterodimer composed of S100A8 (calprotectin a, MRP8) and S100A9 (calprotectin B, MRP14) subunits, which are low-molecular weight members of S100 calprotectin subfamily (20). Previous studies have found that S100A8 and S100A9 are related to obesity, insulin resistance, and atherosclerosis (21). Sekimoto et al. (22) found that serum S100A8/A9 complex level was related to leukocyte count, BMI, subcutaneous fat area, and visceral fat area. At the same time, compared with lean mice, obese mice had higher S100A8 mRNA expression in the mature adipocyte component and obese mice had higher S100A9 expression in the matrix vascular component (22). Lylloff et al. (23) found that Roux-en-Y gastric bypass surgery (RYGB) significantly decreased BMI and circulating mRNA levels of S100A8 and S100A9 in obese patients. These findings are consistent with the present findings.

Epigenetics has become an intense topic of research in recent years. It refers to the regulation of gene expression without changing the basic structure of the gene. At present, epigenetics usually refers to histone modification and methylation of noncoding RNA and DNA (24, 25). Many studies have found that epigenetic mechanisms are associated with obesity. Sonne et al. (26) found changes in the methylation and expression of nine genes in epididymal adipocytes, including ehd2 and kctd15, which are known to be obesity-related genes, and a new candidate gene IRF8, which may be related to the 1/2 balance of immune type. Similarly, Bell (27) and van Dijk et al. (28) also explained the relationship between DNA methylation and obesity. It is worth noting that these two studies are comprehensive in content, more stringent in inclusion criteria, extensive in research content, and very reliable in conclusions (27, 28). Benton et al. (29) demonstrated the relationship between DNA methylation profiles of adipose tissue and weight loss before and after gastric bypass. This study provided a strong basis for future work and additional evidence for the role of DNA methylation

TABLE 1 | The matched pairs of DEG and DMP.

	DMPs							DEGs	
SYMBOL	**CpG site**	**START**	**END**	**CHR**	**Position**	**Δβ**	***P* values**	**FC**	***P* values**
ADH4	cg12011299	100065546	100065669		TSS200	7.95E-02	1.13E-02	−4.15	4.70E-03
ASPHD1	cg05192831	29913007	29913130	16	1stExon	5.42E-02	1.13E-02	−5.50	2.21E-02
ASPHD1	cg02488299	29913223	29913346	16	1stExon	6.23E-02	1.13E-02	−5.50	2.21E-02
BNC1	cg27169020	83954229	83954352	15	TSS1500	7.85E-02	1.13E-02	−2.54	3.92E-02
BNC1	cg23741520	83954231	83954354	15	TSS1500	7.86E-02	1.13E-02	−2.54	3.92E-02
BNC1	cg12250049	83951663	83951786	15	Body	8.56E-02	1.13E-02	−2.54	3.92E-02
BNC1	cg10275315	83954246	83954369	15	TSS1500	9.20E-02	1.13E-02	−2.54	3.92E-02
BNC1	cg00768409	83954392	83954515	15	TSS1500	9.23E-02	1.13E-02	−2.54	3.92E-02
BNC1	cg16049391	83954395	83954518	15	TSS1500	1.06E-01	1.13E-02	−2.54	3.92E-02
C1orf87	cg17238766	60539675	60539798	1	TSS1500	8.87E-02	1.13E-02	3.84	1.19E-02
C1orf87	cg09851465	60539671	60539794	1	TSS1500	1.07E-01	1.13E-02	3.84	1.19E-02
C3orf22	cg07743179	126278943	126279066	3	TSS1500	−5.14E-02	1.13E-02	2.63	4.95E-02
CFB	cg12124018	31916683	31916806	6	Body	−6.73E-02	1.13E-02	−3.60	1.23E-04
CFB	cg21606287	31916705	31916828	6	Body	−6.17E-02	1.13E-02	−3.60	1.23E-04
CGN	cg07596668	151509825	151509948	1	3'UTR	8.20E-02	1.13E-02	−4.83	1.38E-02
CGN	cg25198049	151509723	151509846	1	Body	8.29E-02	1.13E-02	−4.83	1.38E-02
CHI3L1	cg14085262	203155938	203156061	1	TSS200	5.79E-02	1.13E-02	−3.09	1.38E-02
CRB2	cg15922174	126135998	126136121	9	Body	−8.61E-02	1.13E-02	−4.69	3.40E-03
CRB2	cg02625222	126135169	126135292	9	Body	5.30E-02	1.13E-02	−4.69	3.40E-03
CRB2	cg11431402	126135408	126135531	9	Body	5.76E-02	1.13E-02	−4.69	3.40E-03
CRB2	cg13884995	126126377	126126500	9	Body	7.19E-02	1.13E-02	−4.69	3.40E-03
DMRTA1	cg14338345	22447679	22447802	9	1stExon	5.36E-02	1.13E-02	4.92	1.79E-02
DUSP1	cg08452061	172199642	172199765	5	TSS1500	5.88E-02	1.13E-02	5.41	6.80E-03
EPHA1	cg21294616	143093848	143093971	7	Body	−6.88E-02	1.13E-02	3.61	3.53E-02
EPHA1	cg26960083	143106298	143106421	7	TSS1500	6.90E-02	1.13E-02	3.61	3.53E-02
ESPN	cg13284574	6519923	6520046	1	Body	7.33E-02	1.13E-02	4.19	2.59E-02
FAM84A	cg12050497	14773274	14773397	2	5'UTR	9.44E-02	1.13E-02	−4.84	9.04E-03
FGF9	cg03688324	22251017	22251140	13	Body	6.28E-02	1.13E-02	−2.68	1.25E-02
FNDC1	cg06764804	159654028	159654151	6	Body	5.46E-02	1.13E-02	−3.50	1.97E-02
GPR143	cg19318920	9693690	9693813	X	3'UTR	5.73E-02	1.13E-02	−2.33	3.60E-02
GPRIN3	cg02734358	90227074	90227197	4	5'UTR	1.06E-01	1.13E-02	−4.03	2.18E-02
GSC	cg01695643	95237330	95237453	14	TSS1500	8.16E-02	1.13E-02	2.62	3.78E-02
GSC	cg15440688	95237637	95237760	14	TSS1500	9.33E-02	1.13E-02	2.62	3.78E-02
ITGA2B	cg14686645	42452426	42452549	17	Body	6.75E-02	1.13E-02	2.59	1.34E-02
KCNK3	cg19115882	26919145	26919268	2	Body	5.71E-02	2.04E-03	−2.31	4.83E-03
KCNK3	cg19991086	26953767	26953890	2	3'UTR	6.04E-02	2.04E-03	−2.31	4.83E-03
KCNN3	cg16296829	154832535	154832658	2	TSS200	6.21E-02	2.04E-03	−2.31	4.83E-03
KCNN3	cg18315680	154833117	154833240	2	Body	8.39E-02	2.04E-03	−2.31	4.83E-03
KLF2	cg02668248	16437789	16437912	19	Body	−7.35E-02	2.04E-03	3.95	1.90E-02
KLHL34	cg20312916	21676605	21676728	X	TSS200	−6.58E-02	2.04E-03	3.99	1.49E-02
KLHL34	cg01828474	21676593	21676716	X	TSS200	−5.27E-02	2.04E-03	3.99	1.49E-02
KLHL34	cg25075572	21673930	21674053	X	1stExon	−5.05E-02	2.04E-03	3.99	1.49E-02
KRT7	cg25313172	52627272	52627395	12	1stExon	−6.67E-02	2.04E-03	−3.94	2.60E-02
KRT7	cg14537533	52626904	52627027	12	TSS200	−6.14E-02	2.04E-03	−3.94	2.60E-02
KRT7	cg07967679	52626814	52626937	12	TSS200	−5.58E-02	2.04E-03	−3.94	2.60E-02
KRT7	cg07022048	52638592	52638715	12	Body	6.70E-02	2.04E-03	−3.94	2.60E-02
KRT71	cg23767977	52947465	52947588	15	TSS1500	5.19E-02	2.04E-03	3.47	3.17E-02
KRT8	cg24504361	53297987	53298110	12	Body	6.83E-02	2.04E-03	−2.20	4.88E-03
LAD1	cg11418783	201369650	201369773	1	TSS1500	5.47E-02	2.04E-03	2.97	1.95E-02
MARCO	cg07554474	119698443	119698566	2	TSS1500	6.99E-02	2.04E-03	−2.45	1.73E-02

(Continued)

TABLE 1 | Continued

		DMPs						DEGs	
SYMBOL	**CpG site**	**START**	**END**	**CHR**	**Position**	**Δβ**	***P* values**	**FC**	***P* values**
MC2R	cg25924472	13884152	13884275	18	3'UTR	−1.15E-01	2.04E-03	4.96	3.62E-03
MFAP4	cg15119221	19290755	19290878	17	TSS1500	6.26E-02	2.04E-03	2.22	3.19E-02
MYT1L	cg14128411	1926907	1927030	2	Body	−1.08E-01	2.04E-03	−2.32	4.16E-02
MYT1L	cg00067742	1926888	1927011	2	Body	−7.81E-02	2.04E-03	−2.32	4.16E-02
MYT1L	cg09022325	1796228	1796351	2	Body	5.95E-02	2.04E-03	−2.32	4.16E-02
MYT1L	cg22388316	2000192	2000315	2	5'UTR	8.38E-02	2.04E-03	−2.32	4.16E-02
NGFR	cg04466214	47581280	47581403	17	Body	5.49E-02	2.04E-03	−2.34	4.35E-03
NGFR	cg17369032	47590326	47590449	17	Body	7.93E-02	2.04E-03	−2.34	4.35E-03
PCDHB3	cg01925738	140480770	140480893	5	1stExon	−7.09E-02	2.04E-03	3.59	1.00E-02
PKD2L2	cg10535132	137224284	137224407	5	TSS1500	6.68E-02	2.04E-03	−3.16	2.52E-02
ROR2	cg14244439	94561075	94561198	9	Body	5.75E-02	2.04E-03	−2.71	2.79E-02
ROR2	cg02785332	94647670	94647793	9	Body	6.55E-02	2.04E-03	−2.71	2.79E-02
RXFP1	cg03875996	159442782	159442905	4	TSS1500	7.56E-02	2.04E-03	4.77	6.47E-03
S100A8	cg09174555	153364020	153364143	1	TSS1500	7.03E-02	2.04E-03	−2.25	8.00E-03
S100A9	cg03165378	153329882	153330005	1	TSS1500	7.51E-02	2.04E-03	−2.05	1.13E-02
SCTR	cg26009192	120282200	120282323	2	TSS200	−5.88E-02	2.04E-03	2.45	4.12E-02
SGPP2	cg14435109	223288714	223288837	2	TSS1500	5.72E-02	2.04E-03	−3.25	2.72E-03
SGPP2	cg07873848	223288635	223288758	2	TSS1500	6.25E-02	2.04E-03	−3.25	2.72E-03
SGPP2	cg11300809	223288637	223288760	2	TSS1500	7.03E-02	2.04E-03	−3.25	2.72E-03
SGPP2	cg10091265	223288331	223288454	2	TSS1500	7.16E-02	2.04E-03	−3.25	2.72E-03
SGPP2	cg16171484	223290515	223290638	2	Body	7.99E-02	2.04E-03	−3.25	2.72E-03
SMPD3	cg07735969	68418473	68418596	16	5'UTR	6.49E-02	2.04E-03	−3.52	2.63E-02
SRGN	cg18278184	70847430	70847553	10	TSS1500	8.69E-02	2.04E-03	3.49	4.83E-02
TNRC18	cg06947694	5389271	5389394	7	Body	−7.03E-02	2.04E-03	−2.58	1.12E-02
TNRC18	cg19679210	5354874	5354997	7	Body	6.58E-02	2.04E-03	−2.58	1.12E-02
TNXB	cg02657865	32077744	32077867	6	TSS1500	−8.95E-02	2.04E-03	2.82	2.92E-02
TNXB	cg13199127	32049196	32049319	6	Body	−8.53E-02	2.04E-03	2.82	2.92E-02
TNXB	cg25596754	32026610	32026733	6	Body	−7.77E-02	2.04E-03	2.82	2.92E-02
TNXB	cg00661399	32049177	32049300	6	Body	−7.60E-02	2.04E-03	2.82	2.92E-02
TNXB	cg24336152	32070785	32070908	6	5'UTR	−7.03E-02	2.04E-03	2.82	2.92E-02
TNXB	cg14669361	32038747	32038870	6	Body	−6.91E-02	0.00589	2.82	2.92E-02
TNXB	cg20858622	32015651	32015774	6	Body	−6.80E-02	9.84E-03	2.82	2.92E-02
TNXB	cg11493661	32016239	32016362	6	Body	−6.70E-02	5.63E-03	2.82	2.92E-02
TNXB	cg05956076	32074934	32075057	6	5'UTR	−6.55E-02	2.97E-02	2.82	2.92E-02
TNXB	cg16478197	32068181	32068304	6	5'UTR	−6.32E-02	2.04E-03	2.82	2.92E-02
TNXB	cg12493058	32052444	32052567	6	Body	5.59E-02	1.69E-02	2.82	2.92E-02
TNXB	cg20928974	32022642	32022765	6	Body	5.68E-02	1.97E-02	2.82	2.92E-02
TNXB	cg16662408	32053637	32053760	6	Body	5.95E-02	2.36E-02	2.82	2.92E-02
TNXB	cg23636802	32054441	32054564	6	Body	7.13E-02	2.36E-02	2.82	2.92E-02
TNXB	cg13606255	32053100	32053223	6	Body	7.94E-02	2.36E-02	2.82	2.92E-02
TNXB	cg13739666	32013974	32014097	6	TSS200	−7.87E-02	2.36E-02	2.82	2.92E-02
TNXB	cg26537323	32014059	32014182	6	TSS200	−7.60E-02	2.36E-02	2.82	2.92E-02
TNXB	cg18178844	32014100	32014223	6	TSS200	−6.24E-02	2.36E-02	2.82	2.92E-02
TNXB	cg25522795	32014096	32014219	6	TSS200	−5.09E-02	2.36E-02	2.82	2.92E-02
TNXB	cg15376677	32011687	32011810	6	Body	5.40E-02	2.36E-02	2.82	2.92E-02
TNXB	cg18340416	32010178	32010301	6	Body	5.89E-02	2.36E-02	2.82	2.92E-02
TNXB	cg20161227	31980836	31980959	6	5'UTR	−7.46E-02	2.36E-02	2.82	2.92E-02
TRIML1	cg04086012	189060900	189061023	4	1stExon	5.25E-02	2.36E-02	−3.35	2.19E-02
UNC13C	cg06530558	54304778	54304901	15	TSS1500	5.72E-02	2.36E-02	2.07	4.67E-02
VWA5B1	cg05805297	20617329	20617452	1	TSS200	7.04E-02	2.36E-02	4.25	1.29E-02

(Continued)

TABLE 1 | Continued

		DMPs						DEGs	
SYMBOL	**CpG site**	**START**	**END**	**CHR**	**Position**	**Δβ**	***P* values**	**FC**	***P* values**
VWA5B1	cg04637372	20617456	20617579	1	5'UTR	7.54E-02	2.36E-02	4.25	1.29E-02
VWA5B1	cg25745746	20617452	20617575	1	5'UTR	8.04E-02	2.36E-02	4.25	1.29E-02
WNK4	cg06795963	40932359	40932482	17	TSS1500	−7.78E-02	2.36E-02	−3.68	1.54E-02
ZDHHC1	cg06139166	67440283	67440406	16	Body	−1.02E-01	2.36E-02	2.14	1.65E-02
ZDHHC1	cg08968184	67433636	67433759	16	Body	5.10E-02	2.36E-02	2.14	1.65E-02
ZFR2	cg09999510	3812479	3812602	19	Body	5.01E-02	2.36E-02	2.71	3.06E-02

CHR, chromosome; DEG, differentially expressed gene; Δβ, difference of methylation between patients with obesity and healthy controls; DMP, differentially methylated position; START/END, position in Build 37; FC, log fold change.

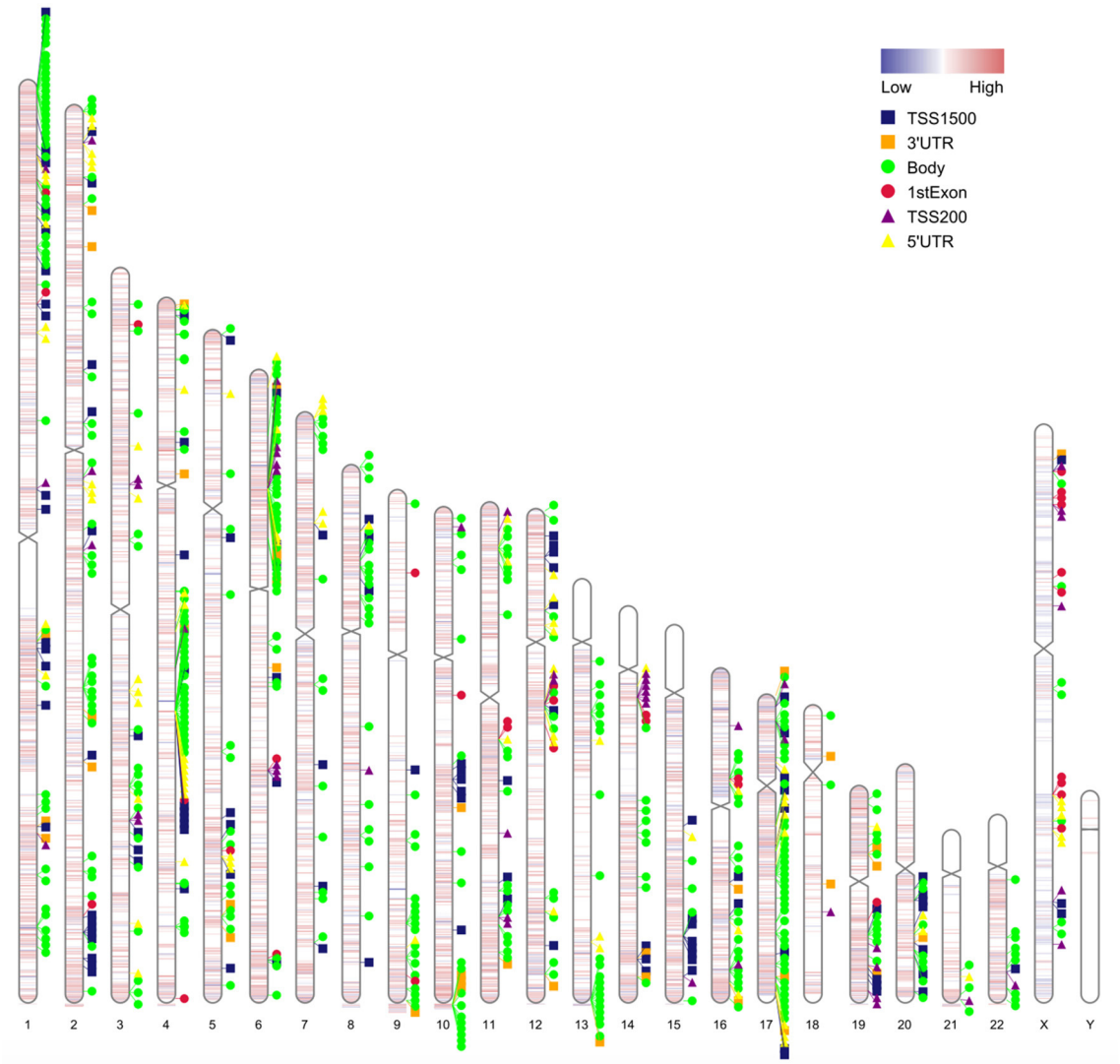

FIGURE 4 | Chromosome distribution of differentially methylated intergenic CpGs. Plot showing the distribution of differential intergenic CpG sites on 22 autosomes and the X and the Y chromosomes. Red is the hypermethylated region and blue is the hypomethylated region with logFC values of the M value between obesity patients and healthy controls.

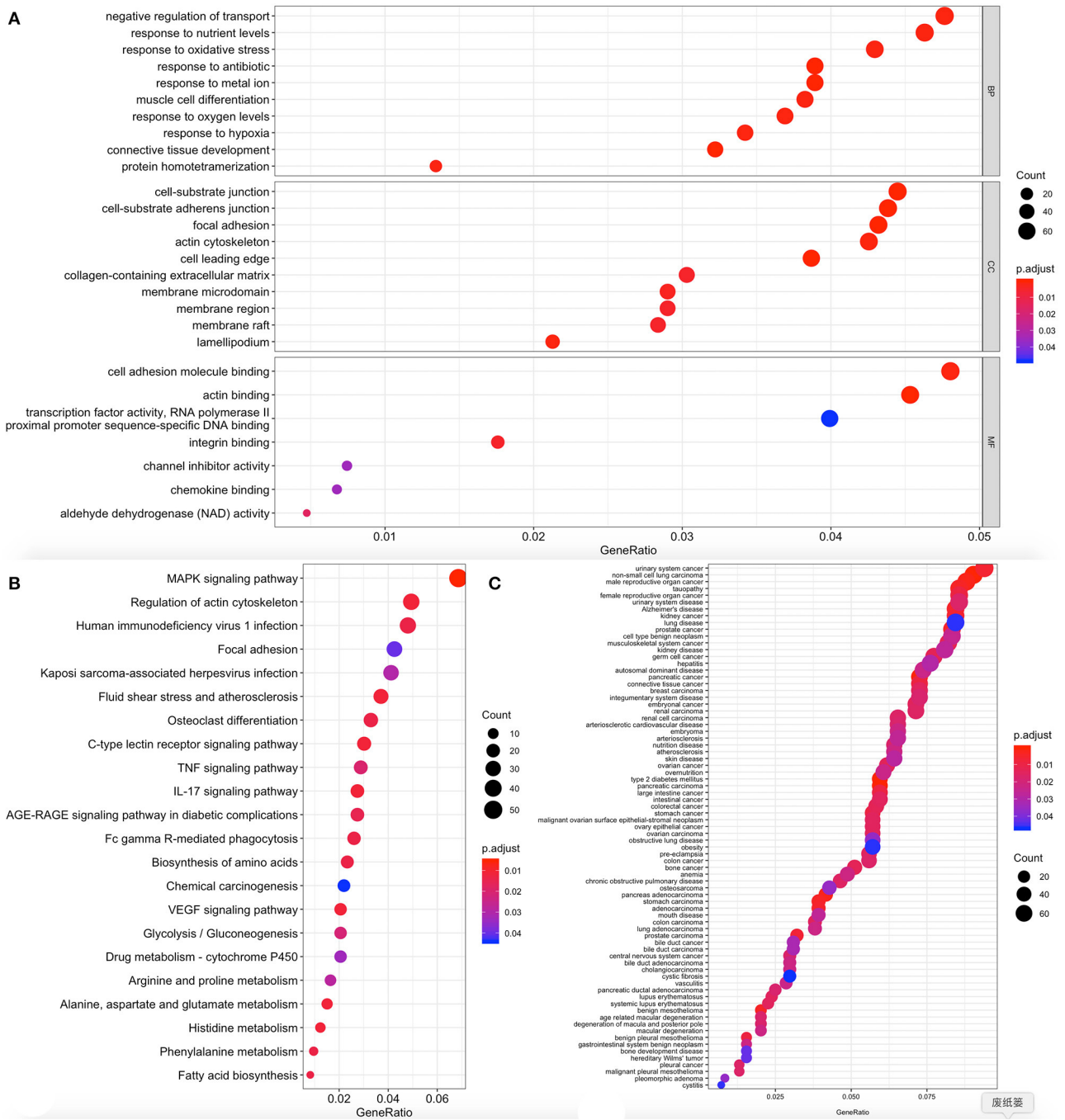

FIGURE 5 | Functional enrichment of differentially expressed genes (DEGs). The x-axis shows the ratio number of genes and the y-axis shows the pathway terms. The -log10 (*P* value) of each term is colored according to the legend. **(A)** Gene Ontology; **(B)** Kyoto Encyclopedia of Genes and Genomes (KEGG) pathway analysis; **(C)** Disease Ontology.

in adipose tissue in obesity. The findings that the promoters of both the S100A8 and S100A9 genes were hypomethylated, in addition to their significantly increased expression in obese people, confirmed the validity of our findings. Other studies showed that methylation is closely associated with changes in adiposity. Brask et al. (26) found that obesity was associated with specific changes in adipocyte DNA methylation and gene expression. In general, obesity was associated with the global DNA hypomethylation significantly and epidermal fat exhibited more obesity-associated Differentially methylated regions (DMRs) than inguinal fat. Among genes that exhibited simultaneous changes in methylation and gene expression,

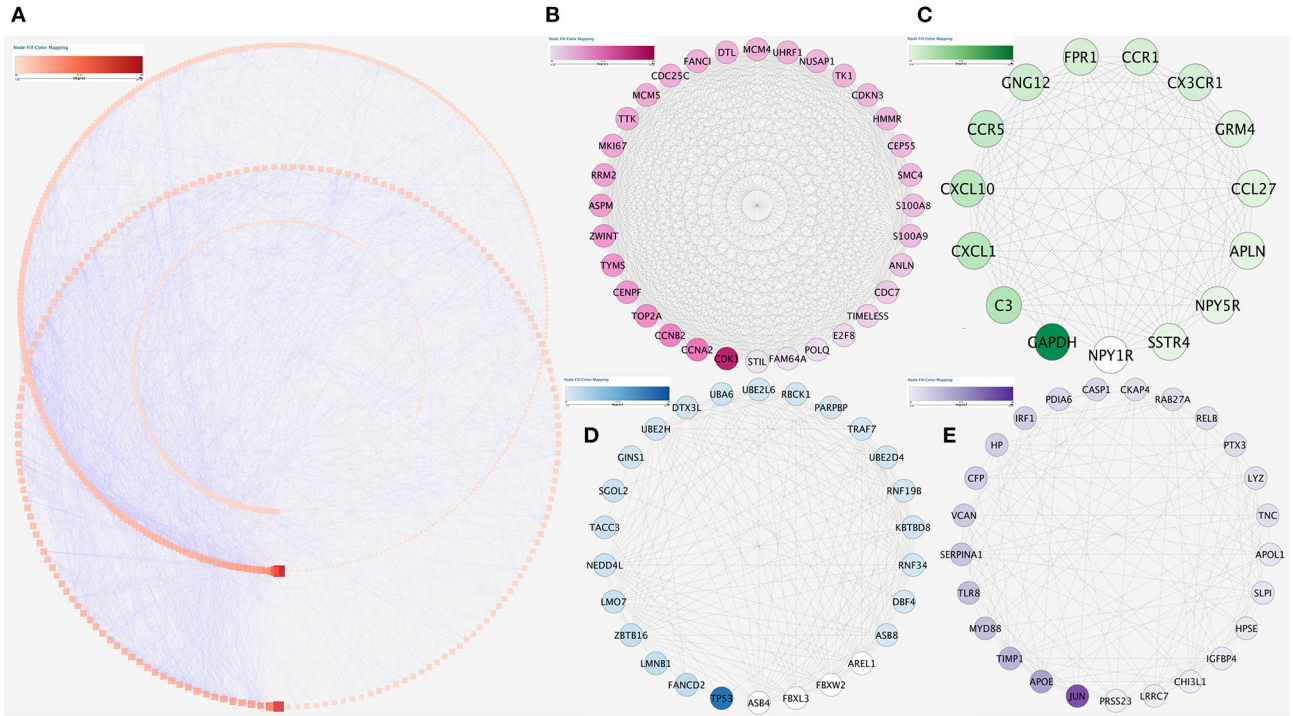

FIGURE 6 | Protein–protein interaction network analysis. **(A)** Protein–protein interaction network of the module genes. Edge stands for the interaction between two genes. A degree was used for describing the importance of protein nodes in the network; darkness red shows a high degree and light presents a low degree. **(B–E)** The significant modules identified from the protein–protein interaction network using the molecular complex detection method with a score of >8.0. $MCODE_B$ score = 22.166, $MCODE_c$ score = 17.442, $MCODE_D$ score = 9.278, and $MCODE_E$ score = 8.963.

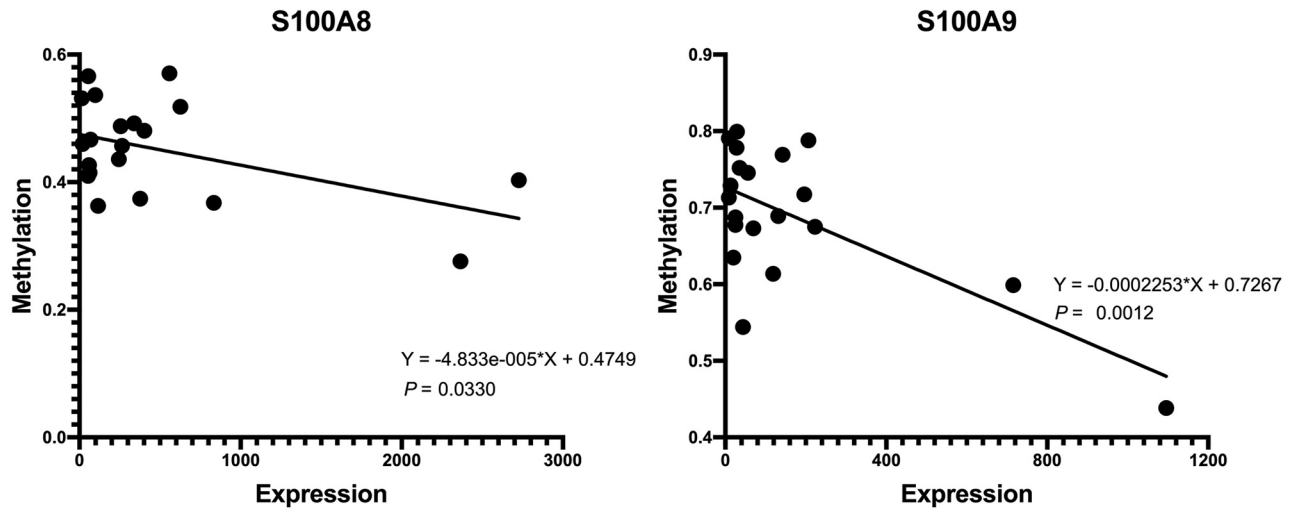

FIGURE 7 | Correlation analysis of DNA methylation and mRNA expression.

some were involved in adipose tissue function in obese mice through hypomethylation-driven changes in expression. On the other hand, Riuzzi et al. (30) found that levels of S100A8/S100A9 were closely correlated with adipocyte size, and the mechanism may be related to the involvement in regulating the cell division cycle. Our study revealed that elevated levels of S100A8/S100A9 were closely associated with the development of obesity, while hypomethylation of the promoter region resulted in upregulation of S100A8/S100A9 expression.

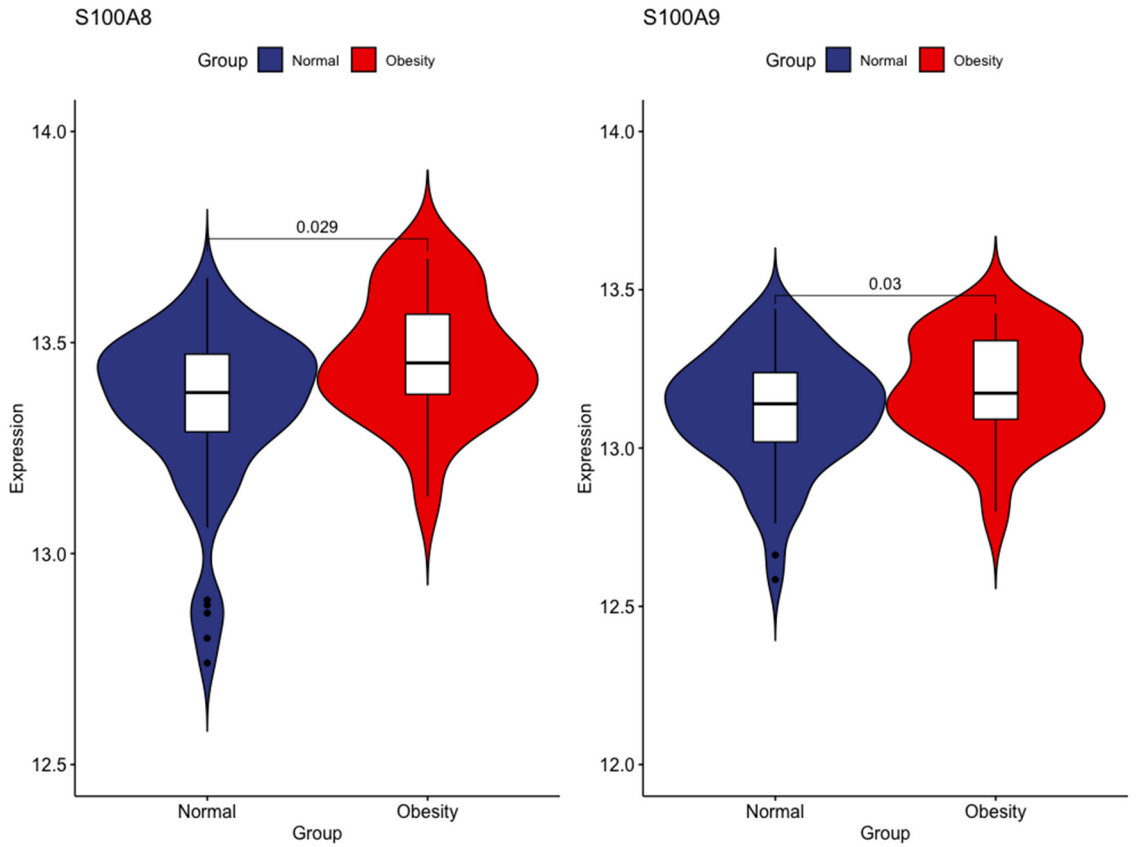

FIGURE 8 | Verification of mRNA expression between obese and healthy samples in GSE109597.

There are a few limitations to this study. First of all, our data results only come from microarrays. Although it is clear that these two hub genes play roles in the pathogenesis of obesity, *in vitro* and *in vivo* studies are required to validate the relationship between these genes and obesity.

CONCLUSION

In summary, two GEO microarrays were explored for differential methylation and gene expression as epigenetic factors of obesity. After the functional analysis, we selected two DEMGs from another microarray dataset (including 84 samples) for verification. Our results showed hypomethylation and upregulation of S100A8 and S100A9 expression in obese patients. Also, correlation analysis showed that DNA methylation can regulate gene expression and lead to obesity.

DATA AVAILABILITY STATEMENT

Publicly available datasets were analyzed in this study. This data can be found here: https://www.ncbi.nlm.nih.gov/geo/; Accession No.'s GSE88837, GSE88940 and GSE109597.

ETHICS STATEMENT

All research protocols on this topic have been approved by the Ethics Committee of Guangxi Medical University (LSGXMU-2019-0028). The patients/participants provided their written informed consent to participate in this study.

AUTHOR CONTRIBUTIONS

NC conceived the study, participated in the design, undertook genotyping, performed the statistical analyses, and drafted the manuscript. LM participated in the design and analyzed the bioinformatics results. WL and DZ conceived the study and helped draft the manuscript. LH, JH, and WS collaborated for the genotyping. LL, YL, and HL carried out the epidemiological survey and collected the samples. SP and JP supervised the whole work. All authors read and approved the final manuscript.

FUNDING

This research was funded by the National Natural Science Foundation of China (No.: 81960266 and 82060072);

Guangxi Province Science Foundation for Youths (2018GXNSFBA281116); National Natural Science Foundation of Guangxi (2020GXNSFAA297003); Open Project of Key Laboratory of Longevity and Aging-related Diseases (Guangxi Medical University), Ministry of Education (KLLAD201902); Guangxi First-class Discipline Project for Basic medicine Sciences (No. GXFCDP-BMS-2018); Guangxi Medical University Science Foundation for Youths (GXMUYSF201823); Project of Liuzhou Science and Technology (2020NBAB0818) and Guangxi Medical and Health Key Discipline Construction Project. Liuzhou People's Hospital High-level Talent Research Fund Project (LRYGCC202107) and Guangxi Medical and Health Key Discipline Construction Project.

ACKNOWLEDGMENTS

The authors would like to acknowledge all the participants of this study.

SUPPLEMENTARY MATERIAL

The Supplementary Material for this article can be found online at: https://www.frontiersin.org/articles/10.3389/fcvm.2021.631650/full#supplementary-material

Supplementary Table 1 | The analysis for Gene Ontology.

Supplementary Table 2 | The analysis for KEGG pathway.

Supplementary Table 3 | The analysis for Disease Ontology.

REFERENCES

1. Jensen MD, Ryan DH, Apovian CM, Ard JD, Comuzzie AG, Donato KA, et al. 2013 AHA/ACC/TOS guideline for the management of overweight and obesity in adults: a report of the American College of Cardiology/American Heart Association Task Force on Practice Guidelines and The Obesity Society. *Circulation.* (2014) 129:S102–38. doi: 10.1161/01.cir.0000437739.71477.ee
2. Collaborators GBDO, Afshin A, Forouzanfar MH, Reitsma MB, Sur P, Estep K, et al. Health effects of overweight and obesity in 195 countries over 25 years. *N Engl J Med.* (2017) 377:13–27. doi: 10.1056/NEJMoa1614362
3. Global Burden of Metabolic Risk Factors for Chronic Diseases C, Lu Y, Hajifathalian K, Ezzati M, Woodward M, Rimm EB, et al. Metabolic mediators of the effects of body-mass index, overweight, and obesity on coronary heart disease and stroke: a pooled analysis of 97 prospective cohorts with 1.8 million participants. *Lancet.* (2014) 383:970–83. doi: 10.1016/S0140-6736(13)61836-X
4. Lozano R, Naghavi M, Foreman K, Lim S, Shibuya K, Aboyans V, et al. Global and regional mortality from 235 causes of death for 20 age groups in 1990 and 2010: a systematic analysis for the Global Burden of Disease Study 2010. *Lancet.* (2012) 380:2095–128. doi: 10.1016/S0140-6736(12)61728-0
5. Sayols-Baixeras S, Subirana I, Fernandez-Sanles A, Senti M, Lluis-Ganella C, Marrugat J, et al. DNA methylation and obesity traits: An epigenome-wide association study. The REGICOR study. *Epigenetics.* (2017) 12:909–16. doi: 10.1080/15592294.2017.1363951
6. Smith ZD, Meissner A. DNA methylation: roles in mammalian development. *Nat Rev Genet.* (2013) 14:204–20. doi: 10.1038/nrg3354
7. Xu X, Su S, Barnes VA, De Miguel C, Pollock J, Ownby D, et al. A genome-wide methylation study on obesity: differential variability and differential methylation. *Epigenetics.* (2013) 8:522–33. doi: 10.4161/epi.24506
8. Rodriguez-Rodero S, Menendez-Torre E, Fernandez-Bayon G, Morales-Sanchez P, Sanz L, Turienzo E, et al. Altered intragenic DNA methylation of HOOK2 gene in adipose tissue from individuals with obesity and type 2 diabetes. *PLoS ONE.* (2017) 12:e0189153. doi: 10.1371/journal.pone.0189153
9. Gautier L, Cope L, Bolstad BM, Irizarry RA. affy–analysis of Affymetrix GeneChip data at the probe level. *Bioinformatics.* (2004) 20:307–15. doi: 10.1093/bioinformatics/btg405
10. Gentleman RC, Carey VJ, Bates DM, Bolstad B, Dettling M, Dudoit S, et al. Bioconductor: open software development for computational biology and bioinformatics. *Genome Biol.* (2004) 5:R80. doi: 10.1186/gb-2004-5-10-r80
11. Miao L, Yin RX, Pan SL, Yang S, Yang DZ, Lin WX. Circulating miR-3659 may be a potential biomarker of dyslipidemia in patients with obesity. *J Transl Med.* (2019) 17:25. doi: 10.1186/s12967-019-1776-8
12. Yu G, Wang LG, Han Y, He QY. clusterProfiler. An R package for comparing biological themes among gene clusters. *OMICS.* (2012) 16:284–7. doi: 10.1089/omi.2011.0118
13. Szklarczyk D, Gable AL, Lyon D, Junge A, Wyder S, Huerta-Cepas J, et al. STRING v11: protein-protein association networks with increased coverage, supporting functional discovery in genome-wide experimental datasets. *Nucleic Acids Res.* (2019) 47:D607–13. doi: 10.1093/nar/gky1131
14. Miao L, Yin RX, Pan SL, Yang S, Yang DZ, Lin WX. Weighted gene co-expression network analysis identifies specific modules and hub genes related to hyperlipidemia. *Cell Physiol Biochem.* (2018) 48:1151–63. doi: 10.1159/000491982
15. Shannon P, Markiel A, Ozier O, Baliga NS, Wang JT, Ramage D, et al. Cytoscape: a software environment for integrated models of biomolecular interaction networks. *Genome Res.* (2003) 13:2498–504. doi: 10.1101/gr.1239303
16. Bader GD, Hogue CW. An automated method for finding molecular complexes in large protein interaction networks. *BMC Bioinformatics.* (2003) 4:2. doi: 10.1186/1471-2105-4-2
17. Miao L, Yin RX, Zhang QH, Hu XJ, Huang F, Chen WX, et al. Integrated DNA methylation and gene expression analysis in the pathogenesis of coronary artery disease. *Aging.* (2019) 11:1486–500. doi: 10.18632/aging.101847
18. Force USPST, Curry SJ, Krist AH, Owens DK, Barry MJ, Caughey AB, et al. Behavioral weight loss interventions to prevent obesity-related morbidity and mortality in adults: US preventive services task force recommendation statement. *JAMA.* (2018) 320:1163–71. doi: 10.1001/jama.2018.13022
19. Yamaoka M, Maeda N, Takayama Y, Sekimoto R, Tsushima Y, Matsuda K, et al. Adipose hypothermia in obesity and its association with period homolog 1, insulin sensitivity, and inflammation in fat. *PLoS ONE.* (2014) 9:e112813. doi: 10.1371/journal.pone.0112813
20. Catalan V, Gomez-Ambrosi J, Rodriguez A, Ramirez B, Rotellar F, Valenti V, et al. Increased levels of calprotectin in obesity are related to macrophage content: impact on inflammation and effect of weight loss. *Mol Med.* (2011) 17:1157–67. doi: 10.2119/molmed.2011.00144
21. Yamaoka M, Maeda N, Nakamura S, Mori T, Inoue K, Matsuda K, et al. Gene expression levels of S100 protein family in blood cells are associated with insulin resistance and inflammation (Peripheral blood S100 mRNAs and metabolic syndrome). *Biochem Biophys Res Commun.* (2013) 433:450–5. doi: 10.1016/j.bbrc.2013.02.096
22. Sekimoto R, Kishida K, Nakatsuji H, Nakagawa T, Funahashi T, Shimomura I. High circulating levels of S100A8/A9 complex (calprotectin) in male Japanese with abdominal adiposity and dysregulated expression of S100A8 and S100A9 in adipose tissues of obese mice. *Biochem Biophys Res Commun.* (2012) 419:782–9. doi: 10.1016/j.bbrc.2012.02.102

23. Lylloff L, Bathum L, Madsbad S, Grundtvig JLG, Nordgaard-Lassen I, Fenger M. S100A8/A9 (Calprotectin), Interleukin-6, and C-Reactive protein in obesity and diabetes before and after Roux-en-Y gastric bypass surgery. *Obes Facts*. (2017) 10:386–95. doi: 10.1159/000478097
24. Wahl S, Drong A, Lehne B, Loh M, Scott WR, Kunze S, et al. Epigenome-wide association study of body mass index, and the adverse outcomes of adiposity. *Nature*. (2017) 541:81–6. doi: 10.1038/nature20784
25. Dick KJ, Nelson CP, Tsaprouni L, Sandling JK, Aissi D, Wahl S, et al. DNA methylation and body-mass index: a genome-wide analysis. *Lancet*. (2014) 383:1990–8. doi: 10.1016/S0140-6736(13)62674-4
26. Sonne SB, Yadav R, Yin G, Dalgaard MD, Myrmel LS, Gupta R, et al. Obesity is associated with depot-specific alterations in adipocyte DNA methylation and gene expression. *Adipocyte*. (2017) 6:124–33. doi: 10.1080/21623945.2017.1320002
27. Bell CG. The epigenomic analysis of human obesity. *Obesity*. (2017) 25:1471–81. doi: 10.1002/oby.21909
28. van Dijk SJ, Molloy PL, Varinli H, Morrison JL, Muhlhausler BS, Members of Epi S. Epigenetics and human obesity. *Int J Obes*. (2015) 39:85–97. doi: 10.1038/ijo.2014.34
29. Benton MC, Johnstone A, Eccles D, Harmon B, Hayes MT, Lea RA, et al. An analysis of DNA methylation in human adipose tissue reveals differential modification of obesity genes before and after gastric bypass and weight loss. *Genome Biol*. (2015) 16:8. doi: 10.1186/s13059-014-0569-x
30. Riuzzi F, Chiappalupi S, Arcuri C, Giambanco I, Sorci G, Donato R. S100 proteins in obesity: liaisons dangereuses. *Cell Mol Life Sci*. (2020) 77:129–47. doi: 10.1007/s00018-019-03257-4

Conflict of Interest: The authors declare that the research was conducted in the absence of any commercial or financial relationships that could be construed as a potential conflict of interest.

frontiers in Cardiovascular Medicine

MINI REVIEW
published: 07 July 2021
doi: 10.3389/fcvm.2021.682357

Circular RNAs as Competing Endogenous RNAs in Cardiovascular and Cerebrovascular Diseases: Molecular Mechanisms and Clinical Implications

Xue Min[1], *Dong-liang Liu*[1] *and Xing-dong Xiong*[1,2]*

[1] *Guangdong Provincial Key Laboratory of Medical Molecular Diagnostics, Institute of Aging Research, Guangdong Medical University, Dongguan, China,* [2] *Institute of Biochemistry and Molecular Biology, Guangdong Medical University, Zhanjiang, China*

Circular RNAs (circRNAs) represent a novel class of widespread and diverse endogenous RNA molecules. This unusual class of RNA species is generated by a back-splicing event of exons or introns, resulting in a covalently closed circRNA molecule. Accumulating evidence indicates that circRNA plays an important role in the biological functions of a network of competing endogenous RNA (ceRNA). CircRNAs can competitively bind to miRNAs and abolish the suppressive effect of miRNAs on target RNAs, thus regulating gene expression at the posttranscriptional level. The role of circRNAs as ceRNAs in the pathogenesis of cardiovascular and cerebrovascular diseases (CVDs) has been recently reported and highlighted. Understanding the underlying molecular mechanism could aid the discovery of therapeutic targets or strategies against CVDs. Here, we review the progress in studying the role of circRNAs as ceRNAs in CVDs, with emphasis on the molecular mechanism, and discuss future directions and possible clinical implications.

Keywords: circRNA, ceRNA, cardiovascular and cerebrovascular diseases, molecular mechanism, clinical implication

OPEN ACCESS

Edited by:
En-Zhi Jia,
Nanjing Medical University, China

Reviewed by:
Annadoray Lavenniah,
National University of Singapore, Singapore
Rushita Bagchi,
University of Colorado Anschutz Medical Campus, United States

***Correspondence:**
Xing-dong Xiong
xiongxingdong@126.com

Specialty section:
This article was submitted to General Cardiovascular Medicine, a section of the journal Frontiers in Cardiovascular Medicine

Received: *18 March 2021*
Accepted: *15 June 2021*
Published: *07 July 2021*

Citation:
Min X, Liu D-l and Xiong X-d (2021) Circular RNAs as Competing Endogenous RNAs in Cardiovascular and Cerebrovascular Diseases: Molecular Mechanisms and Clinical Implications. Front. Cardiovasc. Med. 8:682357. doi: 10.3389/fcvm.2021.682357

INTRODUCTION

Cardiovascular and cerebrovascular diseases (CVDs) are general terms used to refer to all cardiac and cerebral diseases related to vasculopathy. Despite improvements in pharmacotherapy and surgical interventions, as well as lifestyle modifications, morbidity and mortality in patients with CVDs remain high in recent years (1). CVDs are still the leading cause of death worldwide (1). Current treatments primarily alleviate symptoms or slow down disease progression. To develop novel preventive and therapeutic strategies, we should elucidate and understand the underlying molecular mechanisms of these diseases.

Circular RNAs (circRNAs) were first discovered in plant viroids more than 40 years ago (2). A few years later, circRNAs were observed by electron microscopy in the cytoplasmic fractions of eukaryotic cells (3). However, they were mainly considered to be errors of the normal splicing process and did not receive much attention (4). In recent years, advances in the high-throughput sequencing technology and circRNA-specific bioinformatics algorithms have resulted in the discovery and identification of thousands of circRNAs (5–9). Indeed, circRNAs are diverse,

abundant, and expressed in a tissue- and developmental stage-specific manner (5, 8). Although the functions of most circRNAs remain elusive, a select number of circRNAs are known to function as competitive endogenous RNAs (ceRNAs) by decoying miRNAs from other target transcripts, thereby controlling gene expression at the posttranscriptional level (10).

Recent studies have identified circRNAs as ceRNAs in many diseases including CVDs (11–13). Here, we reviewed the role of circRNAs as ceRNAs in atherosclerosis, myocardial infarction, cardiac fibrosis, heart failure, aneurysm, and stroke, with a special focus on the molecular mechanism, which provides a new direction for further research on the pathogenesis and treatment of CVDs.

CircRNA SERVES AS ceRNA

Several years before the discovery of ceRNAs, or natural miRNA sponges, many studies had found that artificial miRNA sponges were able to specifically and effectively inhibit miRNA activity (14–16). These synthetic miRNA sponges are usually expressed from strong promoters, engineered to carry multiple binding sites for a miRNA or miRNA family of interest and have been shown to derepress miRNA targets both *in vitro* and *in vivo* (14). The sponging constructs are not only invaluable tools for miRNA loss-of-function studies *in vitro* and *in vivo*, but also critical for the development of RNA-based therapeutic applications (15, 16).

The theoretical and practical development of the artificial miRNA sponge laid an important foundation for the ceRNA hypothesis. In 2011, Salmena et al. postulated that all endogenous RNA transcripts sharing common miRNA response elements (MREs) can communicate with and regulate each other through competition for a limited pool of miRNAs (17). This hypothesis not only attributes new functions for non-coding RNA transcripts, but also implies coding-independent functions of protein-coding messenger RNAs (17). Given that any transcripts containing MREs can theoretically serve as ceRNAs, they may represent a widespread form of posttranscriptional gene regulation in a variety of physiological and pathophysiological processes.

In 2013, two independent groups firstly discovered that circRNAs can serve as ceRNAs (18, 19). Hansen et al. showed that ciRS-7 (also known as CDR1as) contains 73 conserved binding sites for miR-7 (19). ciRS-7 strongly binds to miR-7 as well as the miRNA effector Argonaute protein 2 (AGO2) and efficiently suppresses miR-7 activity, thereby attenuating the availability of miR-7 to bind to its target mRNAs. *In situ* hybridization showed that miR-7 and ciRS-7 displayed clear co-expression in mouse brain sections and in primary cells isolated from mouse brain, suggesting a high level of endogenous interactivity between them. Another research group demonstrated that ectopic expression of human ciRS-7 in zebrafish impairs midbrain development, consistent with the effect of miR-7 inhibition induced by morpholinos injection (18). The midbrain reduction induced by ciRS-7 expression in zebrafish could be partially rescued by expressing miR-7, indicating the interaction between ciRS-7 and miR-7. These two studies also serve as the first functional analysis of naturally expressed circRNAs. Acting as ceRNAs, circRNAs can bind to miRNAs and inhibit the function of miRNAs, thereby upregulating miRNA target gene expression (**Figure 1**). Because of the lack of free ends, circRNAs are more resistant to exonucleases and more stable than linear RNAs (18, 19). These natures of circRNAs are thought to facilitate their effectiveness as ceRNAs. Indeed, so far many circRNAs have been found to act as ceRNAs both under normal physiological conditions and diseased conditions (20).

CircRNA AS ceRNA IN CVDs

Atherosclerosis

Atherosclerosis (AS) is one group of the most common vasculopathies and a common pathological basis for many cardiovascular diseases, characterized by abnormal lipid metabolism and inflammatory reactions. A number of cells are involved in the pathology and pathophysiology of AS, including vascular endothelial cells (VECs) and vascular smooth muscle cells (VSMCs). Recent studies have found that circRNAs can effectively regulate the proliferation and migration of VECs and VSMCs by acting as ceRNAs, thus modulating the progression of AS (21, 22).

VECs comprise the inner layer of blood vessels and play crucial roles in vascular homeostasis. Endothelial cell injury and dysfunction are critical events that trigger the development of atherosclerotic lesions. Importantly, ox-LDL has been identified to contribute to the progression of AS by inducing VEC injury and apoptosis (23, 24). Zhang et al. found that the circRNA circ_0003204, which is upregulated in ox-LDL-induced human aortic endothelial cells (HAECs), can promote the expression of TGFβR2 and its downstream phospho-SMAD3 by sponging miR-370, leading to inhibition of the proliferation, migration, and capillary-like formation of HAECs exposed to ox-LDL (21). Another study revealed that circ_0124644 exacerbates ox-LDL-induced HUVECs injury through the miR-149-5p/PAPP-A axis (25). In addition, circ-USP36 can bind miR-98-5p, which results in increased levels of VCAM1, thus accelerating ox-LDL-induced apoptosis, inflammatory and viability inhibition of HUVEC cells (26).

VSMCs reside in the tunica media and maintain vascular tension. Abnormal proliferation of VSMCs accelerates the progression of atherosclerosis. A previous study reported that circACTA2 competitively binds miR-548f-5p and upregulates smooth muscle α-actin (α-SMA) expression, thereby facilitating stress fiber formation and cell contraction in human arterial smooth muscle cells (HASMCs) (27). α-SMA participates in the formation of filaments that are major components of the cytoskeleton which is essential for VSMC proliferation and migration (27). Another study reported that circ_Lrp6 competes endogenously by binding to miR-145, thus regulating VSMC migration, proliferation, and differentiation (22). More recently, it has been reported that CircMap3k5 functions as a miRNA sponge to decrease miR-22-3p repression of TET2 (13). As a consequence, CircMap3k5 inhibits the proliferation of smooth muscle cells (SMCs) and attenuates intimal hyperplasia (13). ox-LDL can promote the growth, migration, and differentiation of

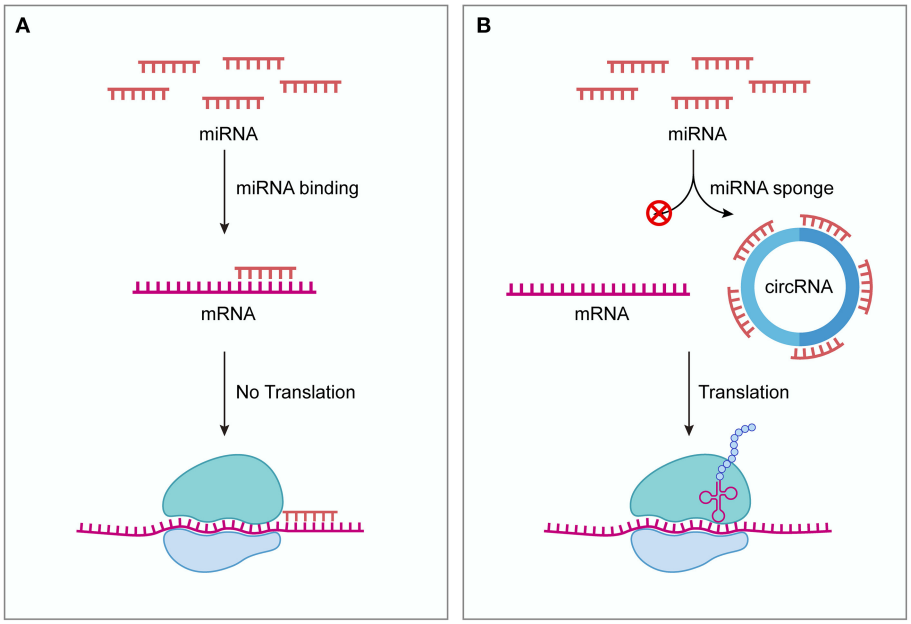

FIGURE 1 | circRNAs function as ceRNAs. **(A)** Without competing transcripts circRNAs, miRNAs bind to target mRNAs through sequence complementarity, blocking the translation of target mRNAs. **(B)** circRNAs can competitively sequestrate miRNAs and derepress their target mRNAs, thus promoting the expression of target genes. ceRNA, competing endogenous RNA; circRNA, circular RNA.

VSMCs, leading to VSMC dysfunction (28). Studies have shown that hsa_circ_0029589 and circ_0010283 are up-regulated in ox-LDL-induced VSMCs (29–32). Knockdown of these circRNAs ameliorates the dysfunction of VSMCs induced by ox-LDL and they exert these biological functions by serving as ceRNAs. VSMCs may preserve phenotype alterations from a highly quiescent and differentiated phenotype (contractile phenotype) to a proliferative and dedifferentiated phenotype (secretory phenotype) (33). The VSMC phenotypic switching is an early event in AS. circ_RUSC2, circ-SATB2, circDHCR24 and circ-Sirt1 have been found to regulate the phenotypic transformation of VSMCs by functioning as ceRNAs (11, 34–36). These circRNAs may be targets for regulating VSMC phenotypic modulation and serve as potential diagnostic biomarkers and therapeutic targets for AS.

Myocardial Infarction

Myocardial infarction (MI), also called acute MI, is characterized by cardiac injury and remodeling caused by a sudden loss of oxygen supply due to acute coronary artery occlusion. Apoptosis has shown great contribution to cardiomyocyte loss during acute MI. Several studies have shown that circRNAs are involved in the regulation of cardiomyocyte apoptosis (37–41). The mitochondrial fission and apoptosis-related circRNA (MFACR) can mediate cardiomyocyte apoptosis and MI by exerting an endogenous competitive effect and regulating the expression of MTP18 (37). circNCX1 is increased in response to ROS and promotes the expression of the pro-apoptosis factor CDIP1 by targeting miR-133a-3p, eventually leading to the death of cardiomyocytes (38). Cdr1as is upregulated in MI mice, and promotes myocardial cell apoptosis and increases cardiac infarct size by targeting the Cdr1as/miR-7a axis (39). Conversely, circMACF1 can attenuate cardiomyocyte apoptosis through the miR-500b-5p-EMP1 axis (40). circ-Ttc3, as a miR-15b-5p sponge, promotes the expression of Arl2 and plays a cardioprotective role in MI (41).

The stimulation of endogenous cardiac regeneration is a promising approach to replace the lost myocardium after MI. Cardiomyocyte proliferation and angiogenesis are essential for structural and functional repair during cardiac regeneration. Gao et al. demonstrated that circFASTKD1 binds directly to miR-106a and relieve its inhibition of LATS1 and LATS2, thereby suppressing the YAP signaling pathway (42). The downregulation of circFASTKD1 ameliorates MI by promoting angiogenesis through the miR-106a-LATS1/2-YAP axis (42). Another study showed that circHipk3 acts as a sponge for miR-133a to promote CTGF expression (43). Upregulation of circHipk3 induces cardiac regeneration and angiogenesis, and decreases the infarct size after MI (43). Huang et al. clarified that circNfix can sponge miR-214 to promote Gsk3β expression and that the knockdown of circNfix promotes cardiomyocyte proliferation and angiogenesis after MI, attenuating cardiac dysfunction and improving prognosis (44).

Cardiac Fibrosis

Cardiac fibrosis is defined as the replacement of normal myocardial tissues with non-beating fibrous tissues caused by the hyperfunction of fibroblasts and differentiation into myofibroblasts. It is a common pathological feature of the most adverse ventricular remodeling, such as MI and diabetic

cardiomyopathy. Some circRNAs have been reported to exert pro-fibrosis effect in cardiac fibroblasts (CFs). circRNA_010567 and circRNA_000203 were upregulated in diabetic mouse myocardium and Ang-II-induced CFs (45, 46). circRNA_010567 can competitively bind to miR-141 and remove the inhibition of TGF-β1 by miR-141, thus increasing TGF-β1 levels (45). circRNA_000203 can competitively bind to anti-fibrotic miR-26b-5p, enhancing the fibrotic phenotype in CFs (46). Similarly, circPAN3 exhibits pro-fibrotic effects via the miR-221/FoxO3/ATG7 axis (47). Another study showed that circHIPK3 is markedly upregulated in CFs and heart tissues treated with Ang-II (48). Knockdown of circHIPK3 prevents Ang-II-induced cardiac fibrosis and improves diastolic function by sponging miR-29b-3p (48). Several circRNAs have been shown to exert anti-fibrotic effect in CFs. circNFIB, which is decreased in post-MI heart samples of mice and TGF-β-treated CFs, can directly sponge miR-433 to inhibit fibroblast proliferation (49). circ_LAS1L can inhibit the activation, proliferation, and migration of CFs by targeting the miR-125b-SFRP5 signaling axis (50). Herein, a better understanding of the molecular mechanisms that regulate cardiac fibrosis could aid the discovery of novel therapeutic approaches for the development of cardiac remodeling.

Heart Failure

Cardiac hypertrophy is characterized by the enlargement of cardiomyocytes and thickening of the ventricular walls. It initially develops as an adaptive response to diverse patho-physiological stimuli; however, chronic sustained cardiac hypertrophy may eventually progress to heart failure (HF). Several reports have revealed that circRNAs function as ceRNAs in the development and progression of HF. Wang et al. found that overexpression of heart-related circRNA (HRCR) increases the expression of ARC by inhibiting miR-223 activity, which attenuates the development of cardiac hypertrophy and HF (51). Lim et al. found that circSlc8a1 inhibition could attenuate cardiac hypertrophy and HF by sponging miR-133a (52). It has been reported that circRNA_000203 exacerbates cardiac hypertrophy by competitively sponging miR-26b-5p and miR-140-3p to derepress Gata4, a pro-hypertrophic transcription factor (53). A recent study showed that circHIPK3 is upregulated in pressure-overload induced cardiomyocytes (54). Knockdown of circHIPK3 plays a protective role against cardiac hypertrophy by sponging miR-185-3p (54). These circRNAs hold promise as prospective therapeutic targets for HF.

Aneurysm

Aneurysm is defined as a pathological condition featured by permanent localized dilation of the vessel wall, involving all layers. Growth impediment and apoptosis of VSMCs can contribute to aneurysm development. Recently, interactions between circRNAs and miRNAs have also been demonstrated in aneurysms. For example, hsa_circRNA_101238 can sequester miR-320a, increasing the expression of MMP9 and leading to thoracic aortic dissection (55). circ_0020397 plays an important role in the phenotypic modulation of intracranial aneurysms by promoting VSMC viability via the miR-502-5p/GREM1 axis (56). Additionally, CDR1as serves as a sponge for miR-7, which increases the expression of CKAP4 to facilitate the proliferation and suppress the apoptosis of VSMCs, leading to VSMC remodeling and progression of abdominal aortic aneurysm (AAA) (57). circCBFB facilitates VSMC proliferation and inhibits VSMC apoptosis via the circCBFB/miR-28-5p/GRIA4/LYPD3 axis (58). circCCDC66 sponges miR-342-3p to upregulate its host gene *CCDC66* in VSMCs and regulates VSMC apoptosis and proliferation (59). These newly identified mechanisms may provide novel options for the treatment of aneurysm.

Stroke

Stroke is a common cardiovascular and cerebrovascular disease and one of the major causes of death and disability worldwide. During the hours after an ischemic stroke, neurons become permanently damaged and undergo cell death. Therefore, novel therapeutic approaches to rescue damaged neurons are urgently needed. The latest study conducted by Dai et al. revealed that knockdown of circHECTD1 attenuates neuronal injury caused by cerebral ischemia via the miR-133b/ TRAF3 axis (60). Chen et al. revealed that circUCK2 functions as a miR-125b-5p sponge to inhibit miR-125b-5p activity, resulting in an increase in GDF11 expression and a subsequent amelioration of neuronal injury (61). Wu et al. demonstrated that circTLK1 acts as an endogenous miR-335-3p sponge to increase the expression of TIPARP, resulting in the exacerbation of neuronal injury (62). It has been shown that circSHOC2 in ischemic-preconditioned astrocyte-derived exosomes attenuates ischemia-induced neuronal apoptosis and ameliorates neuronal damage by acting on the miR-7670-3p/SIRT1 axis (63). The above circRNAs may serve as potential targets for inducing neuroprotection against ischemic stroke.

Astrocytes are the most abundant cells in the brain and play important roles in maintaining normal brain function. Studies have demonstrated that treatments capable of decreasing infarct size are often accompanied by attenuated astrocyte responses (64, 65). Han et al. found that circHECTD1 acts as an endogenous miR-142 sponge to increase the expression of TIPARP, resulting in astrocyte activation, and thus contributes to cerebral infarction (66). Specific blockage of circHECTD1 may be a potential therapeutic target for the inhibition of astrocyte activation in stroke patients.

In addition, Bai et al. firstly reported that endothelial-mesenchymal transition (EndoMT) contributes to blood-brain barrier (BBB) damage during stroke pathogenesis (67). circDLGAP4 competitively binds miR-143 and remove the inhibition of HECTD1 by miR-143, thus increasing HECTD1 levels (67). Overexpression of circDLGAP4 significantly attenuates neuronal deficits, decreases infarct areas, and ameliorates BBB damage through the inhibition of EndoMT (67).

METHODS FOR CHARACTERIZATION OF circRNA-miRNA INTERACTIONS

To investigate the interaction between circRNAs and miRNAs, several bioinformatic tools can be used. For instance, different miRNA-target prediction algorithms, including TargetScan (68), miRanda (69), and PITA (70) have greatly facilitated

TABLE 1 | CircRNAs as ceRNAs in CVDs.

Diseases	circRNAs	miRNAs	mRNAs	Functions	Number of miRNA binding sites	References
Atherosclerosis	circ_0003204	miR-370	TGFβR2	Inhibited proliferation, migration and tube formation of HAECs exposed to ox-LDL	2	(21)
	circ_0124644	miR-149-5p	PAPP-A	Intensified the ox-LDL-induced HUVECs injury	1	(25)
	circUSP36	miR-98-5p	VCAM1	Accelerated ox-LDL-induced apoptosis, inflammatory and viability inhibition of HUVEC cells	1	(26)
	circACTA2	miR-548f-5p	α-SMA	Facilitated stress fiber formation and cell contraction in HASMCs	1	(27)
	circLrp6	miR-145	FASCIN, Yes1, and Lox	Promoted VSMC migration, proliferation, and differentiation	7	(22)
	circMAP3K5	miR-22-3p	TET2	Inhibited SMC proliferation and attenuated intimal hyperplasia	1	(13)
	circ_0029589	miR-214-3p	STIM1	Regulated VSMC proliferation, migration and invasion	1	(29)
	circ_0029589	miR-370	FOXO1	Promoted VSMC the proliferation and migration ability	1	(30)
	circ_0029589	miR-214-3p	Wnt3	Promoted cell growth, migration and inflammation in VSMCs	1	(31)
	circ_0010283	miR-133a-3p	PAPPA	Promoted ox-LDL-induced proliferation, migration and invasion in HVSMCs	1	(32)
	circRUSC2	miR-661	SYK	Promoted VSMC proliferation, enhanced cell migration and inhibited cell apoptosis	–	(34)
	circSATB2	miR-939	STIM1	Promoted proliferation, migration and inhibited apoptosis of VSMC	–	(35)
	circDHCR24	miR-149-5p	MMP9	Promoted HA-VSMC proliferation, migration and phenotypic switching	1	(36)
	circSirt1	miR-132/212	SIRT1	Inhibited inflammatory phenotypic switching of VSMCs	3	(11)
Myocardial infarction	circMFACR	miR-652-3p	MTP18	Regulated mitochondrial dynamics and apoptosis in heart	15	(37)
	circNCX1	miR-133a-3p	CDIP1	Promoted cardiomyocyte apoptosis	8	(38)
	circCdr1as	miR-7a	PARP, SP1	Promoted MCM cell apoptosis	–	(39)
	circMACF1	miR-500b-5p	EMP1	Attenuated cardiomyocyte apoptosis	1	(40)
	circTtc3	miR-15b	Arl2	Protected cardiomyocyte from apoptosis	1	(41)
	circFASTKD1	miR-106a	LATS1, LATS2	Suppressed endothelial cell growth, migration, mobility and angiogenesis.	1	(42)
	circHipk3	miR-133a	CTGF	Promoted coronary vessel endothelial cell proliferation, migration, tube-forming capacity and angiogenesis	2	(43)
	circNfix	miR-214	Gsk3β	Inhibited neonatal cardiomyocyte proliferation and angiogenesis	3	(44)
Cardiac fibrosis	circ_010567	miR-141	TGF-β1	Regulated myocardial fibrosis	1	(45)
	circ_000203	miR-26b-5p	Col1a2, CTGF	Increased cardiac fibrosis	2	(46)
	circPAN3	miR-221	FoxO3	Exerted profibrotic role	1	(47)
	circHIPK3	miR-29b-3p	a-SMA, COL1A1, COL3A1	Promoted cardiac fibroblast proliferation and migration	2	(48)
	circNFIB	miR-433	AZIN1, JNK1	Inhibited cardiac fibroblast activation, proliferation and migration	1	(49)
	circLAS1L	miR-125b	SFRP5	Inhibited cardiac fibroblast activation, proliferation, migration and promoted apoptosis	1	(50)
Heart failure	circHRCR	miR-223	ARC	Attenuated the development of cardiac hypertrophy and heart failure	6	(51)

(Continued)

TABLE 1 | Continued

Diseases	circRNAs	miRNAs	mRNAs	Functions	Number of miRNA binding sites	References
	circSlc8a1	miR-133a	Srf, Ctgf, Adrb1, Adcy6	Induced heart failure	10	(52)
	circ_000203	miR-26b-5p miR-140-3p	Gata4 Gata4	Aggravated cardiac hypertrophy and impaired heart function	1 1	(53)
	circHIPK3	miR-185-3p	CASR	Regulated cardiac hypertrophy	1	(54)
Aneurysm	circ_101238	miR-320a	MMP9	Involved in the pathogenesis of TAD	1	(55)
	circ_0020397	miR-502-5p	GREM1	Promoted VSMC viability	1	(56)
	circCDR1as	miR-7	CKAP4	Facilitated the proliferation and suppressed the apoptosis of VSMCs	1	(57)
	circCBFB	miR-28-5p	LYPD3, GRIA4	Exerted anti-apoptosis effects in VSMCs	1	(58)
	circCCDC66	miR-342-3p	CCDC66	Regulated VSMC apoptosis and proliferation	1	(59)
Stroke	circHECTD1	miR-133b	TRAF3	Attenuated the inhibition of OGD-caused cell apoptosis and NF-κB activation in HT22 cells	1	(60)
	circUCK2	miR-125b-5p	GDF11	Reduced neuronal apoptosis	–	(61)
	circTLK1	miR-335-3p	TIPARP	Aggravated neuronal injury	1	(62)
	circSHOC2	miR-7670-3p	SIRT1	Suppressed neuronal apoptosis and ameliorated neuronal damage	4	(63)
	circHECTD1	miR-142	TIPARP	Promoted astrocyte autophagy	1	(66)
	circDLGAP4	miR-143	HECTD1	Attenuated neuronal deficits, decreased infarct areas, and ameliorated BBB damage	1	(67)

–, Not available.

the discovery of circRNA-miRNA interactions. In addition, some tools incorporate gene expression data including AGO crosslinking-immunprecipitation (CLIP) data, which improve the capability to predict physiologically relevant circRNA-miRNA interactions. starBase 2.0 (http://starbase.sysu.edu.cn/) is the first database containing circRNA-miRNA interactions based on Ago and RNA binding protein (RBP) binding sites (71). It provides comprehensive interaction networks of ncRNAs, mRNA and RBP from 108 CLIP-Seq datasets. CircInteractome (http://circinteractome.nia.nih.gov/) combines many features from other websites, such as circBase, TargetScan, StareBase (72). Similarly, it can be used to explore the interacting miRNAs of circRNAs. Since every database uses distinct rules of targeting and produces different prediction outcomes, a combination of various databases may provide information in a reliable way.

In addition to the above mentioned prediction methods, experimental validation is required to prove that a circRNA has a bona fide miRNA sponging function. First, dual-luciferase reporter assays can be utilized to screen the potential interacting miRNAs. The circRNA sequences containing wild-type (WT) or mutated miRNA binding sites are inserted into luciferase reporter vectors. Transfection of a miRNA mimic can reduce the luciferase activities in the WT group, but not in the mutated group. Second, RNA fluorescence *in situ* hybridization (RNA-FISH) can be used to assess the colocalization of circRNAs with miRNAs in cells and tissues. RNA-FISH probe should target circRNA backspliced junctions in order to avoid recognition of their cognate linear RNAs. It is important to note that RNA-FISH signals for circRNAs and miRNAs appear as distinct puncta in the cell, not as the diffuse signals typically seen when detecting protein. Third, AGO2 RNA immunoprecipitation (RIP) can be employed to confirm a physical interaction between the circRNA, miRNA and AGO2. It is a more direct evidence supporting the miRNA sponging role of a circRNA. Fourth, RNA pull-down assay can be performed using biotinylated probes designed specifically for the circRNA/miRNA of interest. After confirming that the circRNA/miRNA is successfully enriched in the pull-down material, the interacting miRNA/circRNA molecules can be studied by RT-qPCR analysis.

CONCLUSION AND FUTURE PROSPECTS

As discussed in this review, many circRNAs serve as ceRNAs to mediate miRNA functions in CVDs (**Table 1**). These circRNA-miRNA-mRNA competitive endogenous RNA regulatory networks represent a novel section in the pathogenesis and development of CVDs. As lots of circRNAs are deregulated or show a disease-specific profile in CVDs and might play a role in the progression of CVDs, they might serve as promising biomarkers for early diagnosis or therapeutic targets in the future. However, how to effectively regulate circRNA levels in target cells is now still unresolved. Extracellular vesicles are naturally occurring RNA carriers that can induce physiological changes in target cells through the transfer of numerous molecules. These vesicles can be adapted for the delivery of circRNAs or siRNAs targeting the specific backspliced sequence of circRNA. Therefore, exogenous upregulation or downregulation of circRNAs to regulate miRNAs could become

a novel therapy for CVD treatment. In addition, a recent study found that artificial circRNA sponges can competitively inhibit pro-hypertrophic miR-132 and−212, thereby attenuating pressure overload-induced cardiac hypertrophy (73). Thus, introducing synthetic circRNAs sponges into target cells might also serve as new efficient approaches for future CVD therapy. Indeed, the superior ability of circRNA in sponging miRNAs and its unique cellular stability confer them great potential for use as therapeutic drugs. Nevertheless, the real clinical application of circRNAs as molecular drugs or targets is challenging. How to ensure therapeutic efficacy and safety, and avoid off-target adverse effects awaits additional and extensive investigation.

Despite growing evidence for the phenotypic effects of circRNA deregulation in CVDs, the current ceRNA hypothesis is still controversial regarding whether they are really active in the endogenous cellular context. Importantly, optimal ceRNA-mediated regulation is observed when miRNA and ceRNA levels are near equimolarity. The levels of circRNA need to be high enough to relieve the miRNA repression on mRNA. Thus, methods to quantitatively determine absolute expression levels of circRNA and miRNA will allow a more precise determination of ceRNA effectiveness of circRNAs in diverse physiological and pathological conditions. Another important factor is the number of miRNA-binding sites. CircRNAs that harbor multiple binding sites for the same miRNAs may serve as better ceRNA candidates than those with fewer sites. Among the circRNAs we discussed in this review, with the exception of MFACR (37), circSlc8a1 (52), circNCX1 (38), circLrp6 (22), HRCR (51), which contains 15, 10, 8, 7, 6 binding sites for miR-652-3p, miR-133a, miR-133a-3p, miR-145, miR-223, respectively, the majority of circRNAs harbor only a single or very few binding sites for the same miRNAs (**Table 1**). To function as efficient miRNA sponges, the copy numbers of these circRNAs that contain minimal numbers of miRNA-binding sites should attain levels comparable to the miRNAs. However, most of the researches are lack of assessments of absolute levels of circRNAs and miRNAs. Therefore, assessing the stoichiometry of a circRNA with the interacting miRNA is clearly needed in future research. In addition, factors such as miRNA/circRNA binding affinity and RBPs that could occupy MREs can also affect the ceRNA activity of circRNAs. The binding affinity of miRNA and its RNA target, to a great extent, is influenced by matching between MREs and seed sequences. In general, 8-mer seed match has higher affinity than those with 7-mer, and 6-mer has weakest miRNA target-site efficacy (74). As a competitor, circRNA should have a better affinity to miRNA than target mRNAs. RBP can interfere with circRNA-miRNA interactions by directly occupying RNA target sites, or by altering the circRNA secondary structure to influence its affinity for miRNAs. Therefore, technologies such as HITS-CLIP/iCLIP/PAR-CLIP, the mass-spectrometry based quantitative proteomic approaches for capturing RNA-interactome and measuring circRNA-binding protein abundance will help to assess the effect of competitive binding of RBP to MREs.

In summary, circRNAs acting as ceRNAs play important roles in CVDs. Research on the circRNA-mediated ceRNA regulatory network will open up new avenues for basic CVD research, as well as stimulate the development of novel diagnostic and therapeutic strategies for CVDs.

AUTHOR CONTRIBUTIONS

XM and D-lL: wrote the manuscript. X-dX: critically reviewed the manuscript. All authors contributed to the article and approved the submitted version.

FUNDING

The study was supported by grants from the National Natural Science Foundation of China (81871120 and 82071576), the Natural Science Foundation of Guangdong Province (2019A1515010334 and 2019KZDXM059), the discipline construction project of Guangdong Medical University (4SG21008G) and the program for Training High-level Talents of Dongguan (201901019).

REFERENCES

1. Benjamin EJ, Virani SS, Callaway CW, Chamberlain AM, Chang AR, Cheng S, et al. Heart disease and stroke statistics-2018 update: a report from the American heart association. *Circulation.* (2018) 137:e67–492. doi: 10.1161/CIR.0000000000000558
2. Sanger HL, Klotz G, Riesner D, Gross HJ, Kleinschmidt AKJPotNAoS. Viroids are single-stranded covalently closed circular RNA molecules existing as highly base-paired rod-like structures. *Proc Natl Acad Sci USA.* (1976) 73:3852–6. doi: 10.1073/pnas.73.11.3852
3. Hsu MT, Coca-Prados M. Electron microscopic evidence for the circular form of RNA in the cytoplasm of eukaryotic cells. *Nature.* (1979) 280:339–40. doi: 10.1038/280339a0
4. Cocquerelle C, Mascrez B, Hétuin D, Bailleul B. Mis-splicing yields circular RNA molecules. *FASEB J.* (1993) 7:155–60. doi: 10.1096/fasebj.7.1.7678559
5. Jeck WR, Sorrentino JA, Wang K, Slevin MK, Burd CE, Liu J, et al. Circular RNAs are abundant, conserved, and associated with ALU repeats. *RNA.* (2013) 19:141–57. doi: 10.1261/rna.035667.112
6. Wang PL, Bao Y, Yee M-C, Barrett SP, Hogan GJ, Olsen MN, et al. Circular RNA is expressed across the eukaryotic tree of life. *PLoS ONE.* (2014) 9:e90859. doi: 10.1371/journal.pone.0090859
7. Westholm JO, Miura P, Olson S, Shenker S, Joseph B, Sanfilippo P, et al. Genome-wide analysis of drosophila circular RNAs reveals their structural and sequence properties and age-dependent neural accumulation. *Cell Rep.* (2014) 9:1966–80. doi: 10.1016/j.celrep.2014.10.062
8. Salzman J, Chen RE, Olsen MN, Wang PL, Brown PO. Cell-type specific features of circular RNA expression. *PLoS Genet.* (2013) 9:e1003777. doi: 10.1371/journal.pgen.1003777
9. Ivanov A, Memczak S, Wyler E, Torti F, Porath HT, Orejuela MR, et al. Analysis of intron sequences reveals hallmarks of circular RNA biogenesis in animals. *Cell Rep.* (2015) 10:170–7. doi: 10.1016/j.celrep.2014.12.019
10. Rong D, Sun H, Li Z, Liu S, Dong C, Fu K, et al. An emerging function of circRNA-miRNAs-mRNA axis in human diseases. *Oncotarget.* (2017) 8:73271–81. doi: 10.18632/oncotarget.19154
11. Kong P, Yu Y, Wang L, Dou YQ, Zhang XH, Cui Y, et al. circ-Sirt1 controls NF-kappaB activation via sequence-specific interaction and enhancement of

SIRT1 expression by binding to miR-132/212 in vascular smooth muscle cells. *Nucleic Acids Res.* (2019) 47:3580–93. doi: 10.1093/nar/gkz141
12. Liang G, Ling Y, Mehrpour M, Saw PE, Liu Z, Tan W, et al. Autophagy-associated circRNA circCDYL augments autophagy and promotes breast cancer progression. *Mol Cancer.* (2020) 19:65. doi: 10.1186/s12943-020-01152-2
13. Zeng Z, Xia L, Fan S, Zheng J, Qin J, Fan X, et al. Circular RNA CircMAP3K5 acts as a MicroRNA-22-3p sponge to promote resolution of intimal hyperplasia via TET2-mediated smooth muscle cell differentiation. *Circulation.* (2021) 143:354–71. doi: 10.1161/CIRCULATIONAHA.120.049715
14. Ebert MS, Neilson JR, Sharp PA. MicroRNA sponges: competitive inhibitors of small RNAs in mammalian cells. *Nat Methods.* (2007) 4:721–6. doi: 10.1038/nmeth1079
15. Brown BD, Cantore A, Annoni A, Sergi LS, Lombardo A, Della Valle P, et al. A microRNA-regulated lentiviral vector mediates stable correction of hemophilia B mice. *Blood.* (2007) 110:4144–52. doi: 10.1182/blood-2007-03-078493
16. Gentner B, Schira G, Giustacchini A, Amendola M, Brown BD, Ponzoni M, et al. Stable knockdown of microRNA *in vivo* by lentiviral vectors. *Nat Methods.* (2009) 6:63–6. doi: 10.1038/nmeth.1277
17. Salmena L, Poliseno L, Tay Y, Kats L, Pandolfi PP. A ceRNA hypothesis: the rosetta stone of a hidden RNA language? *Cell.* (2011) 146:353–8. doi: 10.1016/j.cell.2011.07.014
18. Memczak S, Jens M, Elefsinioti A, Torti F, Krueger J, Rybak A, et al. Circular RNAs are a large class of animal RNAs with regulatory potency. *Nature.* (2013) 495:333–8. doi: 10.1038/nature11928
19. Hansen TB, Jensen TI, Clausen BH, Bramsen JB, Finsen B, Damgaard CK, et al. Natural RNA circles function as efficient microRNA sponges. *Nature.* (2013) 495:384–8. doi: 10.1038/nature11993
20. Karreth FA, Pandolfi PP. ceRNA cross-talk in cancer: when ce-bling rivalries go awry. *Cancer Discov.* (2013) 3:1113–21. doi: 10.1158/2159-8290.CD-13-0202
21. Zhang S, Song G, Yuan J, Qiao S, Xu S, Si Z, et al. Circular RNA circ_0003204 inhibits proliferation, migration and tube formation of endothelial cell in atherosclerosis via miR-370-3p/TGFbetaR2/phosph-SMAD3 axis. *J Biomed Sci.* (2020) 27:11. doi: 10.1186/s12929-019-0595-9
22. Hall IF, Climent M, Quintavalle M, Farina FM, Schorn T, Zani S, et al. Circ_Lrp6, a circular RNA enriched in vascular smooth muscle cells, acts as a sponge regulating miRNA-145 function. *Circ Res.* (2019) 124:498–510. doi: 10.1161/CIRCRESAHA.118.314240
23. Chen M, Masaki T, Sawamura T. LOX-1, the receptor for oxidized low-density lipoprotein identified from endothelial cells: implications in endothelial dysfunction and atherosclerosis. *Pharmacol Ther.* (2002) 95:89–100. doi: 10.1016/s0163-7258(02)00236-x
24. Rueckschloss U, Galle J, Holtz J, Zerkowski HR, Morawietz H. Induction of NAD(P)H oxidase by oxidized low-density lipoprotein in human endothelial cells: antioxidative potential of hydroxymethylglutaryl coenzyme a reductase inhibitor therapy. *Circulation.* (2001) 104:1767–72. doi: 10.1161/hc4001.097056
25. Wang G, Li Y, Liu Z, Ma X, Li M, Lu Q, et al. Circular RNA circ_0124644 exacerbates the ox-LDL-induced endothelial injury in human vascular endothelial cells through regulating PAPP-A by acting as a sponge of miR-149-5p. *Mol Cell Biochem.* (2020) 471:51–61. doi: 10.1007/s11010-020-03764-0
26. Peng K, Jiang P, Du Y, Zeng D, Zhao J, Li M, et al. Oxidized low-density lipoprotein accelerates the injury of endothelial cells via circ-USP36/miR-98-5p/VCAM1 axis. *IUBMB Life.* (2021) 73:177–87. doi: 10.1002/iub.2419
27. Sun Y, Yang Z, Zheng B, Zhang XH, Zhang ML, Zhao XS, et al. A novel regulatory mechanism of smooth muscle alpha-actin expression by NRG-1/circACTA2/miR-548f-5p axis. *Circ Res.* (2017) 121:628–35. doi: 10.1161/CIRCRESAHA.117.311441
28. Pirillo A, Norata GD, Catapano AL. LOX-1, OxLDL, and atherosclerosis. *Mediators Inflamm.* (2013) 2013:152786. doi: 10.1155/2013/152786
29. Huang Z, Li P, Wu L, Zhang D, Du B, Liang C, et al. Hsa_circ_0029589 knockdown inhibits the proliferation, migration and invasion of vascular smooth muscle cells via regulating miR-214-3p and STIM1. *Life Sci.* (2020) 259:118251. doi: 10.1016/j.lfs.2020.118251
30. Yang L, Yang F, Zhao H, Wang M, Zhang Y. Circular RNA circCHFR facilitates the proliferation and migration of vascular smooth muscle via miR-370/FOXO1/Cyclin D1 pathway. *Mol Ther Nucleic Acids.* (2019) 16:434–41. doi: 10.1016/j.omtn.2019.02.028
31. Zhuang JB, Li T, Hu XM, Ning M, Gao WQ, Lang YH, et al. Circ_CHFR expedites cell growth, migration and inflammation in ox-LDL-treated human vascular smooth muscle cells via the miR-214-3p/Wnt3/beta-catenin pathway. *Eur Rev Med Pharmacol Sci.* (2020) 24:3282–92. doi: 10.26355/eurrev_202003_20696
32. Feng Z, Zhu Y, Zhang J, Yang W, Chen Z, Li B. Hsa-circ_0010283 regulates oxidized low-density lipoprotein-induced proliferation and migration of vascular smooth muscle cells by targeting the miR-133a-3p/pregnancy-associated plasma protein A axis. *Circ J.* (2020) 84:2259–69. doi: 10.1253/circj.CJ-20-0345
33. Owens GK KM, Wamhoff BR. Molecular regulation of vascular smooth muscle cell differentiation in development and disease. *Physiol Rev.* (2004) 84:767–801. doi: 10.1152/physrev.00041.2003
34. Sun J, Zhang Z, Yang S. Circ_RUSC2 upregulates the expression of miR-661 target gene SYK and regulates the function of vascular smooth muscle cells. *Biochem Cell Biol.* (2019) 97:709–14. doi: 10.1139/bcb-2019-0031
35. Mao YY, Wang JQ, Guo XX, Bi Y, Wang CX. Circ-SATB2 upregulates STIM1 expression and regulates vascular smooth muscle cell proliferation and differentiation through miR-939. *Biochem Biophys Res Commun.* (2018) 505:119–25. doi: 10.1016/j.bbrc.2018.09.069
36. Peng W, Li T, Pi S, Huang L, Liu Y. Suppression of circular RNA circDHCR24 alleviates aortic smooth muscle cell proliferation and migration by targeting miR-149-5p/MMP9 axis. *Biochem Biophys Res Commun.* (2020) 529:753–9. doi: 10.1016/j.bbrc.2020.06.067
37. Wang K, Gan TY, Li N, Liu CY, Zhou LY, Gao JN, et al. Circular RNA mediates cardiomyocyte death via miRNA-dependent upregulation of MTP18 expression. *Cell Death Differ.* (2017) 24:1111–20. doi: 10.1038/cdd.2017.61
38. Li M, Ding W, Tariq MA, Chang W, Zhang X, Xu W, et al. A circular transcript of ncx1 gene mediates ischemic myocardial injury by targeting miR-133a-3p. *Theranostics.* (2018) 8:5855–69. doi: 10.7150/thno.27285
39. Geng HH, Li R, Su YM, Xiao J, Pan M, Cai XX, et al. The circular RNA Cdr1as promotes myocardial infarction by mediating the regulation of miR-7a on Its target genes expression. *PLoS ONE.* (2016) 11:e0151753. doi: 10.1371/journal.pone.0151753
40. Zhao B, Li G, Peng J, Ren L, Lei L, Ye H, et al. CircMACF1 attenuates acute myocardial infarction through miR-500b-5p-EMP1 axis. *J Cardiovasc Transl Res.* (2021) 14:161–72. doi: 10.1007/s12265-020-09976-5
41. Cai L, Qi B, Wu X, Peng S, Zhou G, Wei Y, et al. Circular RNA Ttc3 regulates cardiac function after myocardial infarction by sponging miR-15b. *J Mol Cell Cardiol.* (2019) 130:10–22. doi: 10.1016/j.yjmcc.2019.03.007
42. Gao WQ, Hu XM, Zhang Q, Yang L, Lv XZ, Chen S, et al. Downregulation of circFASTKD1 ameliorates myocardial infarction by promoting angiogenesis. *Aging.* (2020) 13:3588–604. doi: 10.18632/aging.202305
43. Si X, Zheng H, Wei G, Li M, Li W, Wang H, et al. circRNA Hipk3 induces cardiac regeneration after myocardial infarction in mice by binding to notch1 and miR-133a. *Mol Ther Nucleic Acids.* (2020) 21:636–55. doi: 10.1016/j.omtn.2020.06.024
44. Huang S, Li X, Zheng H, Si X, Li B, Wei G, et al. Loss of super-enhancer-regulated circRNA Nfix induces cardiac regeneration after myocardial infarction in adult mice. *Circulation.* (2019) 139:2857–76. doi: 10.1161/CIRCULATIONAHA.118.038361
45. Zhou B, Yu JW. A novel identified circular RNA, circRNA_010567, promotes myocardial fibrosis via suppressing miR-141 by targeting TGF-beta1. *Biochem Biophys Res Commun.* (2017) 487:769–75. doi: 10.1016/j.bbrc.2017.04.044
46. Tang CM, Zhang M, Huang L, Hu ZQ, Zhu JN, Xiao Z, et al. CircRNA_000203 enhances the expression of fibrosis-associated genes by derepressing targets of miR-26b-5p, Col1a2 and CTGF, in cardiac fibroblasts. *Sci Rep.* (2017) 7:40342. doi: 10.1038/srep40342
47. Li F, Long TY, Bi SS, Sheikh SA, Zhang CL. circPAN3 exerts a profibrotic role via sponging miR-221 through FoxO3/ATG7-activated autophagy in a rat model of myocardial infarction. *Life Sci.* (2020) 257:118015. doi: 10.1016/j.lfs.2020.118015

48. Ni H, Li W, Zhuge Y, Xu S, Wang Y, Chen Y, et al. Inhibition of circHIPK3 prevents angiotensin II-induced cardiac fibrosis by sponging miR-29b-3p. *Int J Cardiol.* (2019) 292:188–96. doi: 10.1016/j.ijcard.2019.04.006
49. Zhu Y, Pan W, Yang T, Meng X, Jiang Z, Tao L, et al. Upregulation of circular RNA CircNFIB attenuates cardiac fibrosis by sponging miR-433. *Front Genet.* (2019) 10:564. doi: 10.3389/fgene.2019.00564
50. Sun LY, Zhao JC, Ge XM, Zhang H, Wang CM, Bie ZD. Circ_LAS1L regulates cardiac fibroblast activation, growth, and migration through miR-125b/SFRP5 pathway. *Cell Biochem Funct.* (2020) 38:443–50. doi: 10.1002/cbf.3486
51. Wang K, Long B, Liu F, Wang JX, Liu CY, Zhao B, et al. A circular RNA protects the heart from pathological hypertrophy and heart failure by targeting miR-223. *Eur Heart J.* (2016) 37:2602–11. doi: 10.1093/eurheartj/ehv713
52. Lim TB, Aliwarga E, Luu TDA, Li YP, Ng SL, Annadoray L, et al. Targeting the highly abundant circular RNA circSlc8a1 in cardiomyocytes attenuates pressure overload induced hypertrophy. *Cardiovasc Res.* (2019) 115:1998–2007. doi: 10.1093/cvr/cvz130
53. Li H, Xu JD, Fang XH, Zhu JN, Yang J, Pan R, et al. Circular RNA circRNA_000203 aggravates cardiac hypertrophy via suppressing miR-26b-5p and miR-140-3p binding to Gata4. *Cardiovasc Res.* (2020) 116:1323–34. doi: 10.1093/cvr/cvz215
54. Xu X, Wang J, Wang X. Silencing of circHIPK3 inhibits pressure overload-induced cardiac hypertrophy and dysfunction by sponging miR-185-3p. *Drug Des Devel Ther.* (2020) 14:5699–710. doi: 10.2147/DDDT.S245199
55. Zou M, Huang C, Li X, He X, Chen Y, Liao W, et al. Circular RNA expression profile and potential function of hsa_circRNA_101238 in human thoracic aortic dissection. *Oncotarget.* (2017) 8:81825–37. doi: 10.18632/oncotarget.18998
56. Yin K, Liu X. Circ_0020397 regulates the viability of vascular smooth muscle cells by up-regulating GREM1 expression via miR-502-5p in intracranial aneurysm. *Life Sci.* (2021) 265:118800. doi: 10.1016/j.lfs.2020.118800
57. Zhao F, Chen T, Jiang N. CDR1as/miR-7/CKAP4 axis contributes to the pathogenesis of abdominal aortic aneurysm by regulating the proliferation and apoptosis of primary vascular smooth muscle cells. *Exp Ther Med.* (2020) 19:3760–6. doi: 10.3892/etm.2020.8622
58. Yue J, Zhu T, Yang J, Si Y, Xu X, Fang Y, et al. CircCBFB-mediated miR-28-5p facilitates abdominal aortic aneurysm via LYPD3 and GRIA4. *Life Sci.* (2020) 253:117533. doi: 10.1016/j.lfs.2020.117533
59. Yang R, Wang Z, Meng G, Hua L. Circular RNA CCDC66 facilitates abdominal aortic aneurysm through the overexpression of CCDC66. *Cell Biochem Funct.* (2020) 38:830–8. doi: 10.1002/cbf.3494
60. Dai Q, Ma Y, Xu Z, Zhang L, Yang H, Liu Q, et al. Downregulation of circular RNA HECTD1 induces neuroprotection against ischemic stroke through the microRNA-133b/TRAF3 pathway. *Life Sci.* (2021) 264:118626. doi: 10.1016/j.lfs.2020.118626
61. Chen W, Wang H, Feng J, Chen L. Overexpression of circRNA circUCK2 attenuates cell apoptosis in cerebral ischemia-reperfusion injury via miR-125b-5p/GDF11 signaling. *Mol Ther Nucleic Acids.* (2020) 22:673–83. doi: 10.1016/j.omtn.2020.09.032
62. Wu F, Han B, Wu S, Yang L, Leng S, Li M, et al. Circular RNA TLK1 aggravates neuronal injury and neurological deficits after ischemic stroke via miR-335-3p/TIPARP. *J Neurosci.* (2019) 39:7369–93. doi: 10.1523/JNEUROSCI.0299-19.2019
63. Chen W, Wang H, Zhu Z, Feng J, Chen L. Exosome-shuttled circSHOC2 from IPASs regulates neuronal autophagy and ameliorates ischemic brain injury via the miR-7670-3p/SIRT1 axis. *Mol Ther Nucleic Acids.* (2020) 22:657–72. doi: 10.1016/j.omtn.2020.09.027
64. Wang W, Redecker C, Yu ZY, Xie MJ, Tian DS, Zhang L, et al. Rat focal cerebral ischemia induced astrocyte proliferation and delayed neuronal death are attenuated by cyclin-dependent kinase inhibition. *J Clin Neurosci.* (2008) 15:278–85. doi: 10.1016/j.jocn.2007.02.004
65. Fang SH, Wei EQ, Zhou Y, Wang ML, Zhang WP, Yu GL, et al. Increased expression of cysteinyl leukotriene receptor-1 in the brain mediates neuronal damage and astrogliosis after focal cerebral ischemia in rats. *Neuroscience.* (2006) 140:969–79. doi: 10.1016/j.neuroscience.2006.02.051
66. Han B, Zhang Y, Zhang Y, Bai Y, Chen X, Huang R, et al. Novel insight into circular RNA HECTD1 in astrocyte activation via autophagy by targeting MIR142-TIPARP: implications for cerebral ischemic stroke. *Autophagy.* (2018) 14:1164–84. doi: 10.1080/15548627.2018.1458173
67. Bai Y, Zhang Y, Han B, Yang L, Chen X, Huang R, et al. Circular RNA DLGAP4 ameliorates ischemic stroke outcomes by targeting miR-143 to regulate endothelial-mesenchymal transition associated with blood-brain barrier integrity. *J Neurosci.* (2018) 38:32–50. doi: 10.1523/JNEUROSCI.1348-17.2017
68. Friedman RC, Farh KK, Burge CB, Bartel DP. Most mammalian mRNAs are conserved targets of microRNAs. *Genome Res.* (2009) 19:92–105. doi: 10.1101/gr.082701.108
69. John B, Enright AJ, Aravin A, Tuschl T, Sander C, Marks DS. Human MicroRNA targets. *PLoS Biol.* (2004) 2:e363. doi: 10.1371/journal.pbio.0020363
70. Kertesz M, Iovino N, Unnerstall U, Gaul U, Segal E. The role of site accessibility in microRNA target recognition. *Nat Genet.* (2007) 39:1278–84. doi: 10.1038/ng2135
71. Li JH, Liu S, Zhou H, Qu LH, Yang JH. starBase v2.0: decoding miRNA-ceRNA, miRNA-ncRNA and protein-RNA interaction networks from large-scale CLIP-Seq data. *Nucleic Acids Res.* (2014) 42:D92–7. doi: 10.1093/nar/gkt1248
72. Dudekula DB, Panda AC, Grammatikakis I, De S, Abdelmohsen K, Gorospe M. CircInteractome: A web tool for exploring circular RNAs and their interacting proteins and microRNAs. *RNA Biol.* (2016) 13:34–42. doi: 10.1080/15476286.2015.1128065
73. Lavenniah A, Luu TDA, Li YP, Lim TB, Jiang J, Ackers-Johnson M, et al. Engineered circular RNA sponges act as miRNA inhibitors to attenuate pressure overload-induced cardiac hypertrophy. *Mol Ther.* (2020) 28:1506–17. doi: 10.1016/j.ymthe.2020.04.006
74. Bartel DP. MicroRNAs: target recognition and regulatory functions. *Cell.* (2009) 136:215–33. doi: 10.1016/j.cell.2009.01.002

Conflict of Interest: The authors declare that the research was conducted in the absence of any commercial or financial relationships that could be construed as a potential conflict of interest.

frontiers in Cardiovascular Medicine

ORIGINAL RESEARCH
published: 07 July 2021
doi: 10.3389/fcvm.2021.657544

Differentially Expressed Circular Non-coding RNAs in Atherosclerotic Aortic Vessels and Their Potential Functions in Endothelial Injury

Houwei Li[1†], Xue Liu[2†], Na Sun[2†], Tianshuo Wang[2], Jia Zhu[2], Shuang Yang[2], Xia Song[2], Ruishuai Wang[2], Xinhui Wang[2], Yixiu Zhao[2] and Yan Zhang[2*]*

[1] Department of Cardiology at the Second Affiliated Hospital of Harbin Medical University, Harbin, China, [2] Department of Pharmacology (State-Province Key Laboratories of Biomedicine-Pharmaceutics; Key Laboratory of Cardiovascular Medicine Research, Ministry of Education), College of Pharmacy, Harbin Medical University, Harbin, China

OPEN ACCESS

Edited by:
BuChun Zhang,
University of Science and Technology of China, China

Reviewed by:
Aijuan Qu,
Capital Medical University, China
Hui Gong,
Fudan University, China

***Correspondence:**
Yixiu Zhao
zhaoyixiu520@126.com
Yan Zhang
zhangyan@ems.hrbmu.edu.cn

[†]These authors have contributed equally to this work

Specialty section:
This article was submitted to General Cardiovascular Medicine, a section of the journal Frontiers in Cardiovascular Medicine

Received: 23 January 2021
Accepted: 29 March 2021
Published: 07 July 2021

Citation:
Li H, Liu X, Sun N, Wang T, Zhu J, Yang S, Song X, Wang R, Wang X, Zhao Y and Zhang Y (2021) Differentially Expressed Circular Non-coding RNAs in Atherosclerotic Aortic Vessels and Their Potential Functions in Endothelial Injury. Front. Cardiovasc. Med. 8:657544. doi: 10.3389/fcvm.2021.657544

Background: Circular non-coding RNA (circRNA) has a variety of biological functions. However, the expression profile and potential effects of circRNA on atherosclerosis (AS) and vascular endothelial injury have not been fully elucidated. This study aims to identify the differentially expressed circRNAs in atherosclerotic aortic vessels and predict their potential functions in endothelial injury.

Method: ApoE-/- mice were fed with high-fat diet for 12 weeks to induce AS. Atherosclerotic plaques were evaluated by H&E and Masson staining and immunohistochemistry; differentially expressed circRNAs were detected by Arraystar Circular RNA Microarray and verified by RT-PCR; the potential target mircoRNAs of circRNAs were predicted by miRanda, Tarbase, Targetscan and their expression changes were verified by RT-PCR; the potential target genes of mircoRNAs were predicted by Targetscan and verified by Western blot; the signaling pathways that they might annotate or regulate and their potential functions in vascular endothelial injury were predicted by gene enrichment analysis.

Results: Fifty two circRNAs were up-regulated more than twice and 47 circRNAs were down-regulated more than 1.5 times in AS aortic vessels. Mmmu_circRNA_36781 and 37699 were up-regulated both in AS aortic vessels and H_2O_2-treated mouse aortic endothelial cells (MAECs). The expression of miR-30d-3p and miR-140-3p, the target microRNA of circRNA_37699 and circRNA_36781, were downregulated both in AS vessels and H_2O_2-treated MAECs. On the contrary, MKK6 and TP53RK, the potential target gene of miR-140-3p and miR-30d-3p, were upregulated both in AS aortic roots and H_2O_2-treated MAECs. Besides, gene enrichment analysis showed that MAPK and PI3K-AKT signaling pathway were the most potential signaling pathways regulated by the differentially expressed circRNAs in atherosclerosis.

Conclusions: Mmu_circRNA_36781 (circRNA ABCA1) and 37699 (circRNA KHDRBS1) were significantly up-regulated in AS aortic vessels and H_2O_2-treated MAECs. They

have potential regulatory effects on atherosclerosis and vascular endothelial injury by targeting miR-30d-3p-TP53RK and miR-140-3p-MKK6 axis and their downstream signaling pathways.

Keywords: atherosclerosis, circRNA, vascular endothelium, microRNA, ceRNA

INTRODUCTION

Atherosclerosis is a pathological change of blood vessels characterized with narrowed or blocked vascular lumen by cholesterol or fat deposited under vascular endothelium, thereby causing serious cardiovascular events (1). Atherosclerosis is the most dangerous stimulator of cardiovascular and cerebrovascular diseases. There are many contributors to atherosclerosis, such as hyperlipidemia, oxidative stress, hypoxia. These harmful stimuli impair the function of vascular endothelium and destroy the integrity of the vascular endothelium, leading to lipid deposition and plaque formation (2). Lipid metabolism disorder is the most important predisposing cause of atherosclerosis (3). Excessive circulating low density lipoprotein cholesterol (LDL-C) accumulates in vascular endothelial cells and damages the integrity of endothelium (4). Besides, LDL-C can be oxidized to oxidized-LDL (ox-LDL) by excessive oxygen free radicals in endothelial cells. Ox-LDL deposites in endothelial cells and aggravates vascular endothelial injury further (5). The circulating monocytes and lymphocytes then adhere and invade the endothelial cells, transforming into foam cells and lipid streaks. At the same time, vascular smooth muscle cells proliferate and migrate to endothelium, forming fibrous caps and atherosclerotic plaques (6, 7). Therefore, endothelial injury initiates atherosclerosis and plays a vital role in the pathological progression of atherosclerotic cardiovascular diseases (8). Studies have shown that protecting vascular endothelium could effectively delay the development and deterioration of atherosclerosis (9, 10).

Circular non-coding RNAs (circRNAs) are single stranded RNAs with a closed covalent circular structure. Since circRNAs do not have linear 5′ cap and 3′ ploy A terminals, they are stable and insusceptible to RNA exonuclease. Besides, circRNAs are evolutionarily conserved, and the sequences of circRNA from different species are highly consistent. RNA sequencing and bioinformatic studies have proved that endogenous circRNAs are cell, tissue, and disease specific, so they can be potential candidates for biomarkers and therapeutic targets in the diagnosis and treatment of diseases (11, 12). There are many miRNAs binding sites on circRNAs. The main biological function of circRNAs is serving as microRNA sponges. The complementary binding of circRNA and miRNA reduces the ability of miRNA to down-regulate its target mRNAs, leading to up-regulation of target mRNAs, which is called competitive endogenous RNA (ceRNA) (13–15). Studies have confirmed that circRNAs play important roles in atherosclerosis. CircANRIL regulates the maturation of pre-rRNA, inhibits the proliferation of vascular smooth muscle cells, and reduces atherosclerotic lesions (16). Serum circRNA-284 was significantly elevated and its complementary miR-221 was significantly reduced in patients with carotid artery plaque rupture. In addition, the ratio of circRNA-284 to miRNA-221 was significantly increased in the early stage of carotid plaque rupture. Therefore, circRNA-284 may be a potential biomarker of atherosclerotic plaque stability (17). It was also found that circWDR77 inhibited proliferation of vascular smooth muscle cells by targeting the miR-124 /FGF2 axis; has-circ-003575 was involved in the proliferation of vascular endothelial cells and angiogenesis (18, 19). However, the expression of these circRNAs in animal models of atherosclerosis and their regulatory effect on atherosclerosis have been rarely reported. Although the expression profiles of circRNA, miRNA, and mRNA in carotid artery of atherosclerosis rabbits have been detected by RNA-seq analysis, further laboratory verification has not been carried out (20).

In order to elucidate the role of circRNA at the onset and development of vascular endothelial injury and atherosclerosis, we screened and verified the differentially expressed circRNAs in atherosclerotic vessels and oxidative stress induced endothelial cells. Furthermore, the complementary miRNAs of differentially expressed circRNAs and their downstream mRNAs were predicted by bioinformatics techniques. Meanwhile, the expression of miRNAs and their target genes in atherosclerotic vessels and oxidative stress induced endothelial cells were further validated. Besides, the potential regulatory functions of differentially expressed circRNAs were predicted by KEGG gene enrichment analysis. Our work provides new circRNA targets for the intervention of endothelial injury and atherosclerotic associated cardiovascular diseases.

MATERIALS AND METHODS

Establishment of Atherosclerosis Mice Model

ApoE-/- mice (8 weeks old) were purchased from Beijing Vital River Laboratory Animal Technology Co., Ltd. (Beijing, China). The animal experiments were performed in the science and technology park of Harbin Medical University. All animal protocols were approved by the Ethic Committees of Harbin Medical University (IRB of College of Pharmacy, Harbin Medical University, No. IRB3001619) and were in line with the ARRIVE guidelines and recommendations for the care and use of experimental animals. After adaption for a week, ApoE-/- mice were fed with high-fat diet for 12 weeks to induce atherosclerosis (high-fat diet contained 3% cholesterol, 0.5% sodium cholate, 0.2% propyl thiouracil, 0.5% sugar, 10% lard and 81.3% basal feed). ApoE-/- mice fed with ordinary diet for 12 weeks served as control group.

Serum Biochemical Analysis

After 12 weeks of feeding on different diets, all mice were anesthetized with pentobarbital sodium after 12 h fasting. Blood from the inner canthus of eyes was collected and serum was separated. Serum level of total cholesterol, triglyceride, LDL-C and high density lipoprotein cholesterol (HDL-C) lipid were determined by automatic biochemical analyzer (Hitachi, Japan) and corresponding biochemical detection kit (MedicalSystem, Ningbo, China).

Arraystar Circular RNA Microarray

The thoracic aorta was quickly removed from the mouse chest and the aortic root was quickly frozen in the liquid nitrogen. The expression profile of circRNAs in the aortic roots of control and atherosclerosis mice was detected by Arraystar Circular RNA Microarray. These experiments were completed by Kangchen Bio-tech (Shanghai, China).

Hematoxylin-Eosin Staining

The aortic arches were fixed with 4% paraformaldehyde for 48 h, then embedded with paraffin and cut into 6 μm thick tissue sections. The tissue sections were stained with hematoxylin-eosin (H&E) using a H&E staining kit (Beyotime Biotechnology, Shanghai, China). The nucleus were stained blue, and the cytoplasm and connective tissue were stained red. Representative images were taken by Leica microsystems (Solms, Germany).

Masson Staining

The aortic arches were fixed with 4% paraformaldehyde for 48 h, then embedded with paraffin and cut into 6 μm thick tissue sections. The tissue sections were stained with Masson using Masson Staining Kit (Solarbio Life Sciences, Beijing, China). Muscle fibers were stained red, collagen fibers were stained blue or green. Representative images were taken by Leica microsystems (Solms, Germany).

Immunohistochemistry

The aortic arches were fixed with 4% paraformaldehyde for 48 h, then embedded with paraffin and cut into 6 μm thick tissue sections. The tissue sections were fixed on the glass slide pretreated with gelatin and washed in PBS twice with 5 min for each time. Then the tissue sections were treated with 0.1% Triton X-100 penetration solution, washed with PBS for 30 min, and blocked at room temperature for 2 h. Then the sections were incubated with diluted primary antibodies of CD31 (BBI Life Sciences, Shanghai, China) and α-SMA (Boster, Wuhan, China) at 4°C for 24 h and washed in PBS for 6 times with 5 min for each time. Finally, the sections were incubated with diluted secondary antibodies (ZSGB-Bio, Beijing, China) for 2 h, washed with PBS for 6 times with 5 min for each time, and sealed with glycerine sealant. Representative images were taken by Leica microsystems (Solms, Germany).

Cell Culture

MAECs were purchased from Jining Shiye (Shanghai, China). Cells were cultured with complete culture medium containing 89% H-DMEM (Thermo Scientific, Boston, USA), 10% FBS (Thermo Scientific, Boston, USA) and 1% penicillin-streptomycin and cultured in the incubator containing 95% air and 5% CO_2. When the cells fuse to 80–90%, subculture can be carried out by digesting cells into single cell suspension using 0.25% trypsin-0.53mM EDTA (Thermo Scientific, Boston, USA). Then cell suspension was cultured in 12-well plates for further experiments.

RT-PCR

The aortic root tissue or MAECs were treated with 1 mL Trizol (Invitrogen, Boston, USA) and grinded with electric grinder. Then the sample was added with 200 μl chloroform, shocked severely for 20 s, placed on the ice for 10 min, and centrifuged at 4°C and 13,500 r/min for 15 min. Aqueous extract was separated, mixed with equal volume of isopropyl alcohol and blundered slowly, placed on the ice for 10 min, and centrifuged at 4°C and 13,500 r/min for 15 min. Then the supernatant was discarded and the precipitation was washed with 75% ethanol and centrifuged at 4°C, 10,600 r/min for 15 min. The total RNA sample were dissolved with 20 μl DEPC water and transformed into cDNA after reverse transcription using Revert Aid First Strand cDNA Synthesis Kit (Thermo Scientific, Boston, USA). Then cDNA samples were processed into real time PCR using FastStart Universal SYBR Green Master (ROX) (Roche, Basel, Switzerland) to examine the relative level of circRNAs and miRNAs. The primers of circRNAs and miRNAs were listed in **Supplementary Material 5, 6**.

Cell Viability Determination

MAECs were incubated with different concentration of H_2O_2 (Tianli Chemical Reagent Co., Tianjin, China) for 6 h to induce endothelial injury. Then cells were incubated with 5 mg/mL MTT (Solarbio, Beijing, China) for 4 h to determine cell viability (21).

Nitric Oxide Determination

MAECs were incubated with 100, 200 μM H_2O_2 for 6 h to induce endothelial injury. Then nitric oxide (NO) content was determined by DAF-FM DA Fluorescent Probe Kit (Beyotime, Shanghai, China) (22).

ROS Determination

MAECs were incubated with 100, 200 μM H_2O_2 for 6 h to induce endothelial injury. Then the content of reactive oxygen species (ROS) content was determined by ROS Fluorescent Probe Kit (Beyotime, Shanghai, China) (21).

Western Blot Analysis

Western blot analysis was performed according to the previous method (23). Protein extraction should be performed at 4°C. Cells or tissues were lysed with ice-cold protein lysates (RIPA: phosphatase inhibitor: protease: inhibitor = 100:10:1) and the lysed mixture was collected into a tube. The lysed mixture was sonicated and centrifuged at 16,000 g and 4°C for 15 min. The supernatant was collected and the protein concentration was measured. The protein samples were heated in a metal bath at 95°C for 10 min. Then the samples were cooled and subjected

to gel electrophoresis. Protein samples were added to the gel wells for separation. After complete separation, protein was transferred to an NC membrane and blocked with 5% skim milk for 2 h to block non-specific bands. Then the NC membrane was washed with PBST on a shaker for 30 min and incubated with CD31(Abcam, Cambridge, England), MKK6 (Cell signaling technology, Danvers, MA, United States), TP53RK (Sigma-Aldrich, United States), β-actin primary antibody (1:1,000) at 4°C overnight. Then the NC membrane was washed with PBST on a shaker for 30 min and incubated with the anti-HRP antibody (1:10,000) for 50 min in the dark at room temperature. Then the NC membrane was washed with TBST on a shaker in the dark for 30 min. The expression of the target protein was detected by an infrared fluorescence scanning system, and the optical density integral value of the protein bands was analyzed by Odyssey 1.3 software.

Statistical Analysis

Data are presented as means ± SEM and analyzed using *t*-test and one-way ANOVA analysis. *P*-value of <0.05 was regarded as statistically significant.

RESULTS

The Expression Spectrum of circRNAs Altered Significantly in the AS Aortic Roots

ApoE-/- mice were fed with high-fat diet for 12 weeks to induce atherosclerosis (AS). ApoE-/- mice fed with ordinary diet served as control (control). As illustrated in **Figures 1A–D**, serum total cholesterol, triglycerides, and LDL-C level of AS mice were significantly higher than control; while serum HDL-C level of AS mice were significantly lower than control (* $P < 0.05$, *** $P < 0.001$ vs. control, $n = 3$). H&E staining of the AS vessels showed that the arterial intima thickened and lipid deposited under vascular endothelium. Besides, AS vessels showed obvious foam cell aggregation, fat stripe formation, and inflammatory cell aggregation. The intimal surface of AS vessels was covered with atherosclerotic plaques (**Figures 1E,F**). Masson staining of the AS vessels indicated endothelial hyperplasia and collagen deposition (**Figures 1G,H**). CD31 immunohistochemical staining of AS vessels suggested that the intimal integrity of the artery was damaged (**Figure 1J**). α-SMA immunohistochemical staining of AS vessels showed the proliferation and migration of smooth muscle cells to the intima (**Figure 1I**). In all, the above results suggested that the atherosclerosis model was successfully established in this study.

Next, the expression spectrum of circRNAs in Control and AS vessels was detected by Microarray of Arraystar Circular RNA. As illustrated in **Figure 2**, after data standardization, the medians of each group of circRNA chip were at the same level and the probes distributed closely, indicating that the quality of chip data was reliable (**Figure 2A**). Results showed that 52 circRNAs were up-regulated more than twice and 47 circRNAs were down-regulated more than 1.5 times in AS vessels (**Figures 2B–D**). All differentially expressed circRNAs were listed in **Supplementary Materials 1–3**.

Differentially Expressed circRNAs in circRNA Microarray, Aortic Roots of AS Mice and H_2O_2-Treated MAECs

From all differentially expressed circRNAs, 5 up-regulated and 5 down-regulated circRNAs were selected, according to the significance of differences between two groups and their endogenous expression levels, to validate their expression differences in AS and control aortas using RT-PCR. The selected circRNAs were listed in **Table 1**. The whole sequences and primer sequence of selected circRNAs were listed in **Supplementary Materials 4, 5**. Results showed that mmu_circRNA_36781and mmu_circRNA_37699 were significantly up-regulated in AS vessels compared with control. This trend is consistent with the results of chip screening. Besides, mmu_circRNA_42617 and 39714 in AS aortic roots were also significantly altered, but their trends were contrary to the results of microarray screening (**Figure 3**).

Five up-regulated and five down-regulated circRNAs were selected from all differentially expressed circRNAs, according to their expression differences between two groups and their endogenous expression levels, to validate their expression differences further in AS and control vessels using RT-PCR.

In addition, we further verified the expression of mmu_circRNA_36781 and mmu_circRNA_37699 in endothelial injury using oxidative stress injured endothelial cells. MAECs were treated with H_2O_2 for 6 h to induce endothelial injury. As shown in **Figure 4**, H_2O_2 significantly decreased cell viability and NO release, increased reactive oxygen species (ROS) content of MAECs (***$P < 0.001$, **Figures 4A–E**). Then the expression of mmu_circRNA_36781 and mmu_circRNA_37699 were detected in MAECs pretreated with or without H_2O_2. Results showed that both mmu_circRNA_36781 and mmu_circRNA_37699 were significantly up-regulated in H_2O_2-treated MAECs (100 μM, 6 h) (**Figures 4F,G**). The variation trend of mmu_circRNA_36781 and mmu_circRNA_37699 was consistent with the results of microarray and *in vivo* validation.

Expression of Predicted Complementary microRNAs in H_2O_2-Treated MAECs

The target microRNAs of differentially expressed circRNAs and their binding sites were predicted using miRanda and TargetScan database. We analyzed these microRNAs and selected those that have the possibility to regulate atherosclerosis and evolutionarily conserved, including, miR-30d-3p and miR-140-3p, which had conserved binding sites with mmu_circRNA_37699 (circRNA KHDRBS1) and mmu_circRNA_36781 (circRNA ABCA1). 2D structure of binding sites was illustrated in **Figures 5A,B**. Then the expression of predicted complementary microRNAs of above differentially expressed circRNAs were determined in H_2O_2 induced MAECs. The primer sequences of miRNAs were listed in **Supplementary Material 6**. Results showed that miR-30d-3p and miR-140-3p were down-regulated in H_2O_2-treated MAECs (**Figures 5C,D**). In addition, the expression

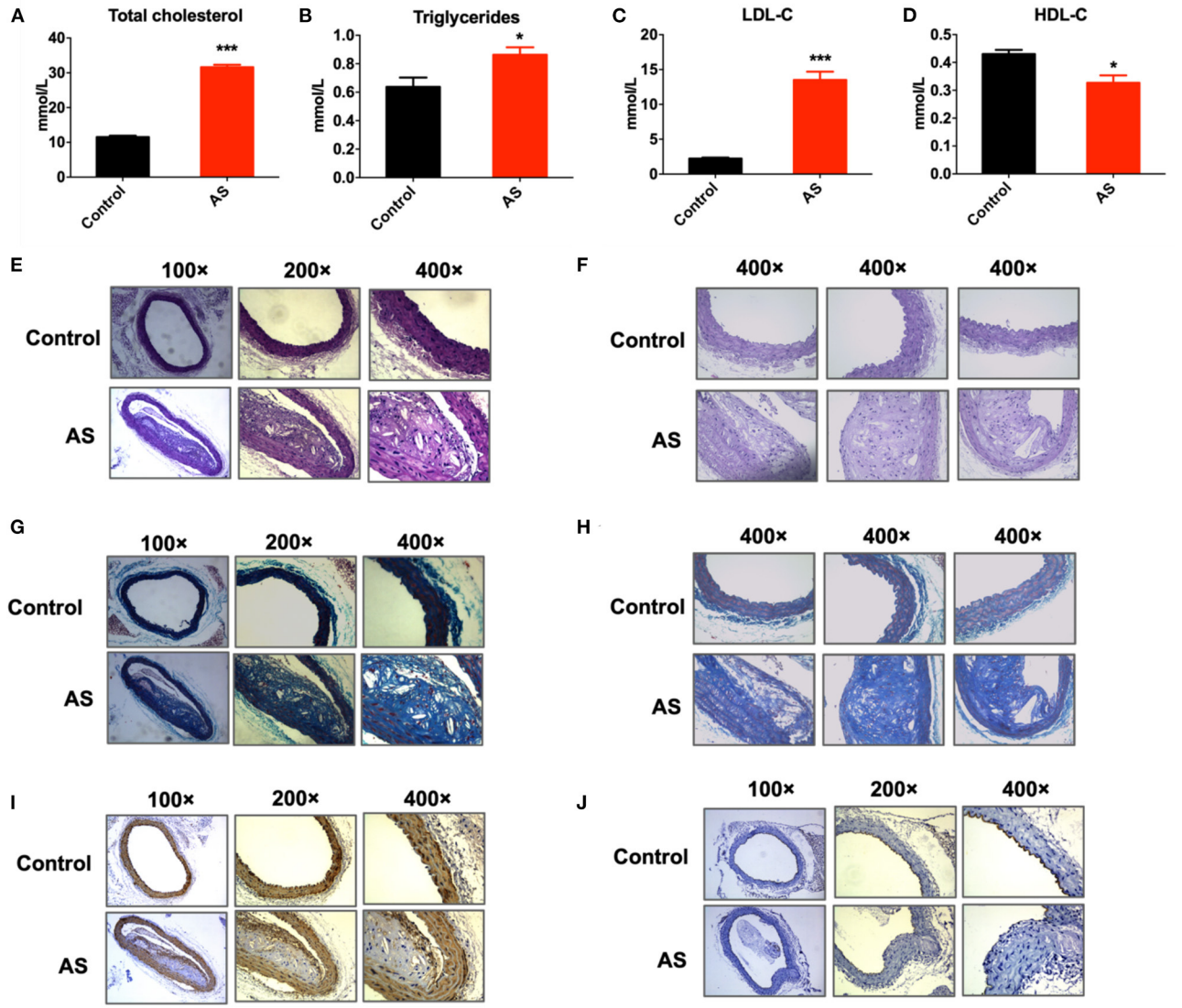

FIGURE 1 | Atherosclerosis mice model was established successfully. **(A–C)** Serum content of total cholesterol, triglycerides, LDL-C of ApoE-/- mice increased significantly after feeding with high fat diet for 12 weeks, $^{*}P < 0.05$, $^{***}P < 0.001$ vs. control, $n = 6$. **(D)** Serum content of HDL-C of ApoE-/- mice decreased significantly after feeding with high fat diet for 12 weeks, $^{*}P < 0.05$ vs. control, $n = 6$. **(E,F)** H & E staining of aortic arches of control and AS mice showed atherosclerotic plaques and foam cell aggregation in AS vessels. **(G,H)** Masson staining of aortic arches of control and AS mice. **(I)** Expression of α-SMA detected by immunohistochemical staining of aortic arches of control and AS mice. **(J)** Expression of CD31 detected by immunohistochemical staining of aortic arches of control and AS mice; $n = 3$.

of these miRNAs was also determined in AS vessels. Results showed that miR-30d-3p and miR-140-3p were all significantly down-regulated in AS vessels. The variation trend of miR-30d-3p and miR-140-3p was consistent with the results of *in vitro* study (**Figures 5E,F**). To further confirm the correlation between miR-30d-3p/miR-140-3p and atherosclerosis, the expressions of miR-30d-3p and miR-140-3p were determined in control aorta (Control), AS aorta near the heart (AS near, susceptible area of atherosclerosis) and AS aorta far away from the heart (AS far, non-susceptible area of atherosclerosis). Results showed that the expressions of miR-30d-3p and miR-140-3p were both significantly downregulated in AS near tissues, while upregulated in control and AS far tissues (**Figures 5G,H**).

Expression of Predicted Complementary mRNAs in AS Vessels and H_2O_2-Treated MAECs

Next, the conserved mRNA sequences and their coding genes with complementary binding sites to miR-30d-3p and

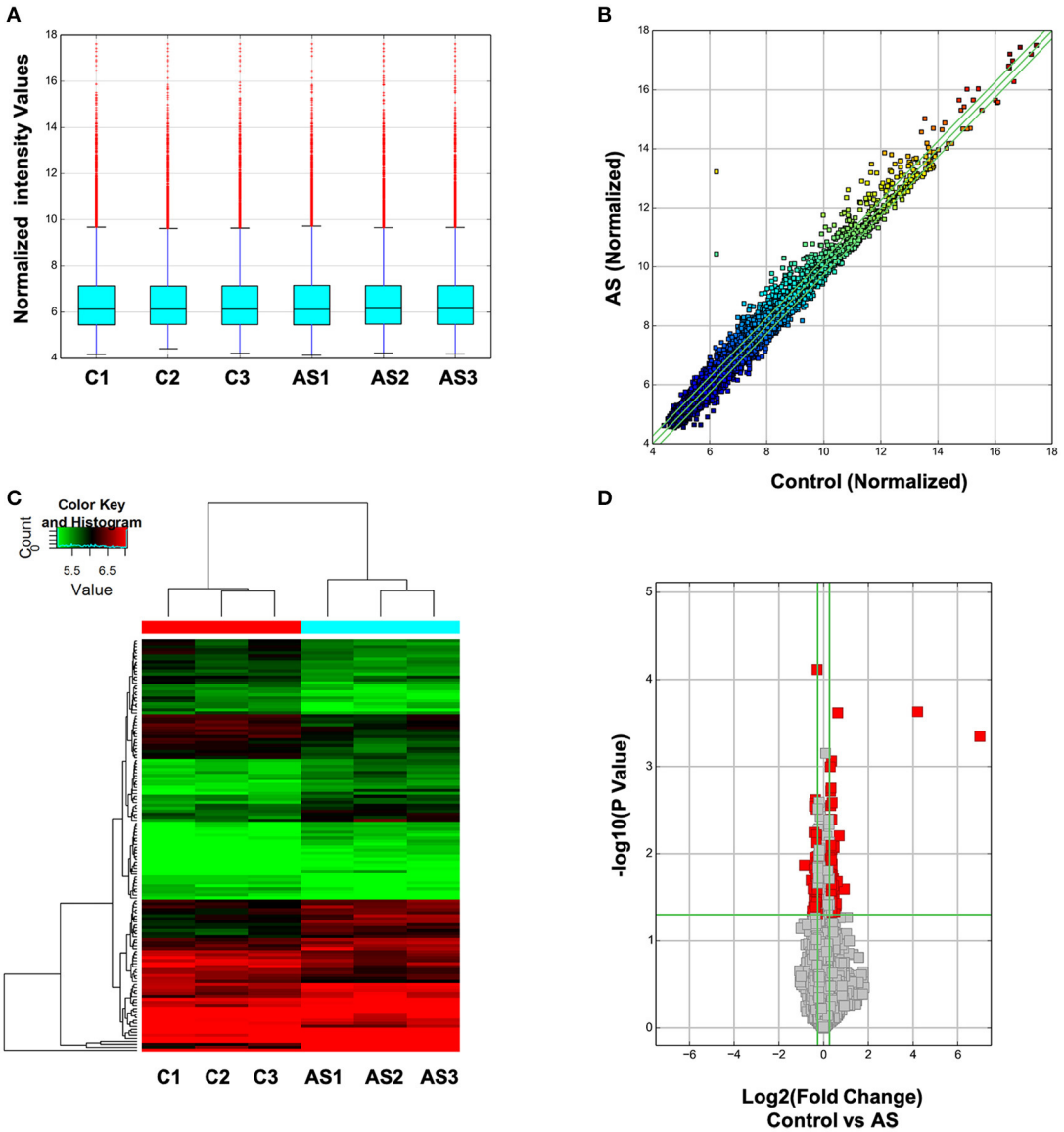

FIGURE 2 | Expression spectrum of circRNAs was screened and analyzed by Arraystar circRNA Microarray Chip. **(A)** Data standardization. **(B)** The overall distribution of chip data. The horizontal and vertical axes represent circRNA expression of different samples respectively. The closer the data get to the center diagonal, the closer the circRNA expressed in two group; while the farther away the data get to the center diagonal, the greater the difference in circRNA expression level between two samples. **(C)** Cluster analysis of differentially expressed circRNA in each sample. Red represents high expressed circRNAs and green represents low expressed circRNAs. **(D)** Differentially expressed circRNA with statistically significant difference between control and AS group.

miR-140-3p were predicted by Target Scan database. The results showed that miR-140-3p and MAP2K6, miR-30d-3p and TP53RK had conservative complementary binding sites (**Figures 6A,B**). Meanwhile, the protein expressions of MKK6 (protein encoded by MAP2K6) and TP53RK in AS aortas and H_2O_2-treated MAECs were detected. Besides, the down-regulation of CD31 expression can be used as a marker of endothelial injury. Results showed that MKK6 and TP53RK were up-regulated in AS aorta near the heart (AS near) and H_2O_2-treated vascular endothelial cells, contrary to the expression of miR-140-3p and miR-30d-3p (**Figures 6C–G**).

Underlying Target Genes of Differentially Expressed miRNAs and Their Potential Roles in Regulating Atherosclerosis and Vascular Endothelial Injury

On the basis of existing studies and bioinformatic database, target genes of differentially expressed microRNAs which have

potential regulatory effects on atherosclerosis and endothelial dysfunction were predicted. Based on the above predicted target genes, the potential functions of circRNAs in atherosclerosis and endothelial injury were predicted by KEGG analysis and summarized in **Table 2**. Results showed that MAPK and PI3K-Akt signaling pathway were top-ranked signaling pathways. Besides, cytokine-cytokine receptor interaction signaling pathway, calcium signaling, TGF-β signaling pathway, Jak-STAT signaling pathway, focal adhesion signaling pathway, HIF-1signaling pathway may also be potential pathways for differentially expressed circRNAs to regulate the pathological process of endothelial injury and atherosclerosis (**Figure 7**).

Term indicates the name of the signaling pathway; gene number indicates the number of differentially expressed genes that are annotated in the pathway; genes indicated the target genes of differentially expressed microRNAs that are annotated in the pathway.

DISCUSSION

Atherosclerosis has continued to be prevalent in developing countries in recent years. The pathogenesis of atherosclerosis is complex. Vascular endothelial injury is the initial stage of atherosclerotic plaques formation, which plays a decisive role in the prognosis of atherosclerosis. CircRNAs are endogenous non-coding RNAs with stable circular structure. Studies have shown that circRNAs have regulative effects on vascular endothelial injury, atherosclerosis and related cardiovascular diseases. This study was the first to analyze the differentially expressed circRNAs in atherosclerotic vessels using microarray. We found that circRNA ABCA1 and circRNA KHDRBS1 were upregulated in atherosclerotic vessels and oxidative-stress damaged endothelial cells, which was consistent with the results of microarray. Besides, miR-30d-3p and miR-140-3p with conserved complementary binding sites for circRNA KHDRBS1 and circRNA ABCA1 were down-regulated in atherosclerotic vessels and oxidative-stress damaged endothelial cells, contrary to the changes of corresponding circRNAs. In addition, MKK6 and TP53RK, the potential targets of miR-30d-3p and miR-140-3p, were up-regulated in atherosclerotic vessels and oxidative-stress damaged endothelial cells, further suggesting that circRNA KHDRBS1 and circRNA ABCA1 may regulate vascular endothelial injury and atherosclerosis through the ceRNA mechanism. Other targets and signaling pathways that may be regulated by miR-30d-3p and miR-140-3p were also predicted and analyzed to provide a basis for further studies on the regulation of circRNA KHDRBS1 and circRNA ABCA1 in vascular endothelial injury and atherosclerosis.

CircRNAs have been reported to be involved in a variety of diseases. Current research suggest that circRNAs perform their

TABLE 1 | Selected significantly differentially expressed circRNAs in AS mice.

circRNA	Up or down	CircRNA type	Gene Symbol	Fold change	*P*-value
mmu_circRNA_42617	Down	exonic	Csmd1	1.8145739	0.013
mmu_circRNA_27503	Down	exonic	Txndc16	1.8483242	0.063
mmu_circRNA_28589	Down	exonic	Csmd3	1.6626629	0.065
mmu_circRNA_014193	Down	Sense overlapping	Rbm39	1.5368923	0.181
mmu_circRNA_24705	Down	exonic	XLOC_004970	2.1051165	0.220
mmu_circRNA_35784	Up	exonic	Il6ra	1.611438	0.006
mmu_circRNA_35619	Up	exonic	Rapgef2	1.888969	0.025
mmu_circRNA_39714	Up	exonic	Wdr95	2.0716431	0.054
mmu_circRNA_36781	Up	exonic	Abca1	1.7430866	0.092
mmu_circRNA_37699	Up	exonic	Khdrbs1	2.1694076	0.139

TABLE 2 | KEGG pathway analysis.

Term	Gene number	Genes
MAPK signaling pathway	16	FGF9, FGF17, MRAS, CACNB2, FAS, RASA1, IL1A, EGFR, TAOK1, FGF21, FGF20, CACNA1S, ATF4, RPS6KA1, RPS6KA2, STMN1
PI3K-Akt signaling pathway	13	FGF9, FGF17, PDPK1, FGFR3, EGFR, FGF21, FGF20, ATF4, CCNB2, ITGA8, VEGFA, JAK2, IL2
Cytokine-cytokine receptor interaction signaling pathway	13	LEPR, IL21R, CXCL9, CCL4, CCL25, IFNAR1, CCR5, FAS, IFNGR2, IL1A, IFNGR1, IL2, ACVR1
Calcium signaling pathway	8	EGFR, TACR2, CACNA1S, VDAC1, ATP2B1, CHRM3, PLN, PLCD1
TGF-beta signaling pathway	7	DCN, CHRD, CUL1, BMP5, PITX2, ACVR1, TFDP1
Jak-STAT signaling pathway	7	LEPR, IL21R, IL20, JAK2, IFNGR2, IFNGR1, IL2
Focal adhesion signaling pathway	7	EGFR, PPP1CC, PDPK1, ITGA6, CCNB2, ITGA8, PPP1R12A
HIF-1 signaling pathway	5	CDC7, MAD2L1, DBF4, CUL1, TFDP1

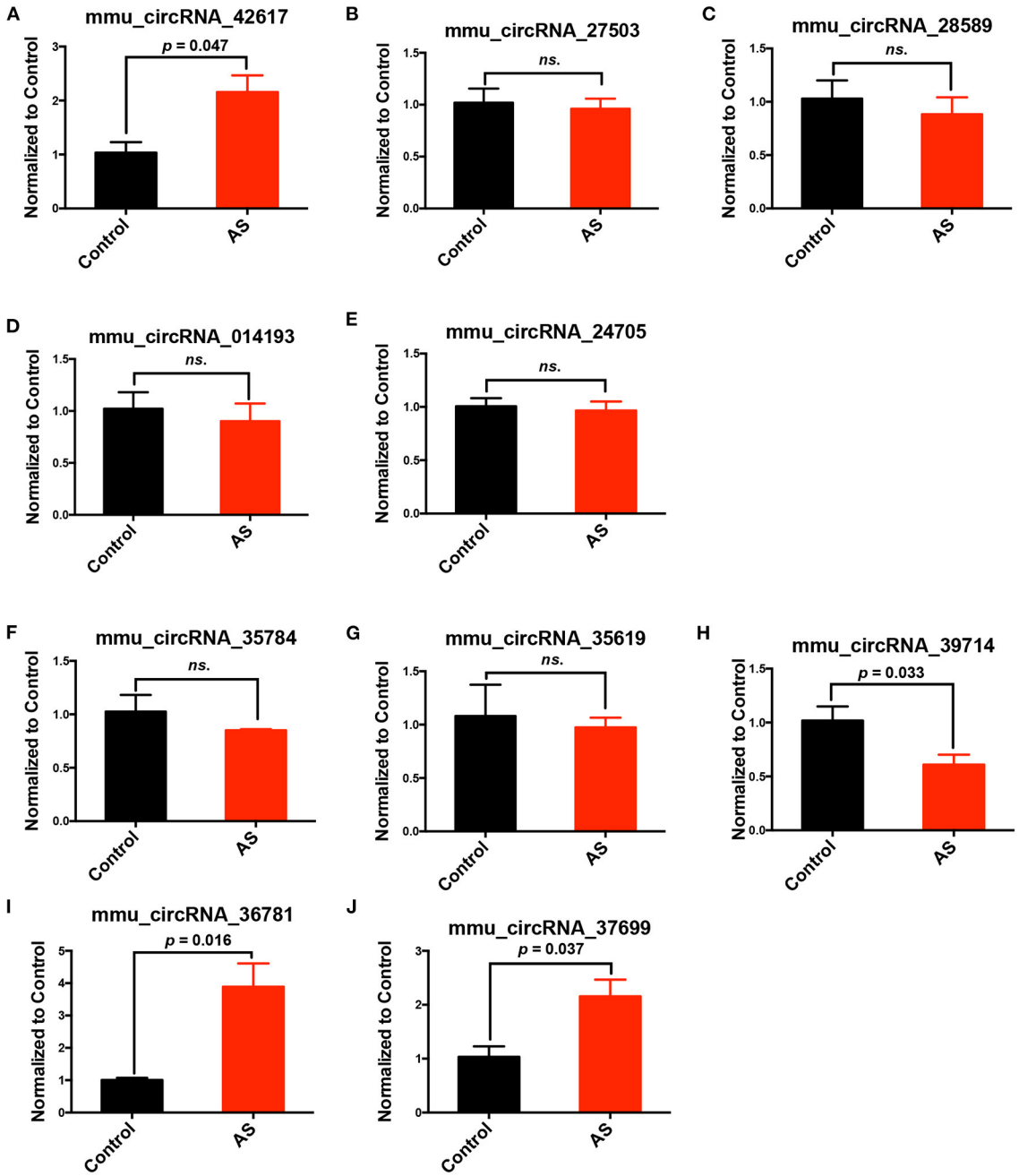

FIGURE 3 | Validation of differentially expressed circRNAs in AS vessels. **(A–E)** Expression of mmu_circRNA_42617, mmu_circRNA_27503, mmu_circRNA_28589, mmu_circRNA_014193, mmu_circRNA_24705 in aortic arches of control and AS mice; **(F–J)** mmu_circRNA_35784, mmu_circRNA_35619, mmu_circRNA_39714, mmu_circRNA_36781,mmu_circRNA_37699 in aortic arches of control and AS mice; $n = 3$. ns, no significant difference.

biological functions through participating in post-transcriptional regulation of genes. Specifically, circRNAs can act as microRNA sponges, competitively inhibiting complementary microRNAs through the ceRNA mechanism and influencing the function of related mRNAs (24). Currently, several studies have reported the potential roles of circRNAs in regulating atherosclerosis, including the regulation of endothelial cell proliferation and angiogenesis by hsa_circRNA_0003575; circANRIL promotes atherosclerosis by modulating ribosomal RNA production and increasing nuclear pressure; reduced circANRIL reduces cell apoptosis, inflammatory factors expression and endothelial damage (16, 19, 25). However, the expression spectrum of

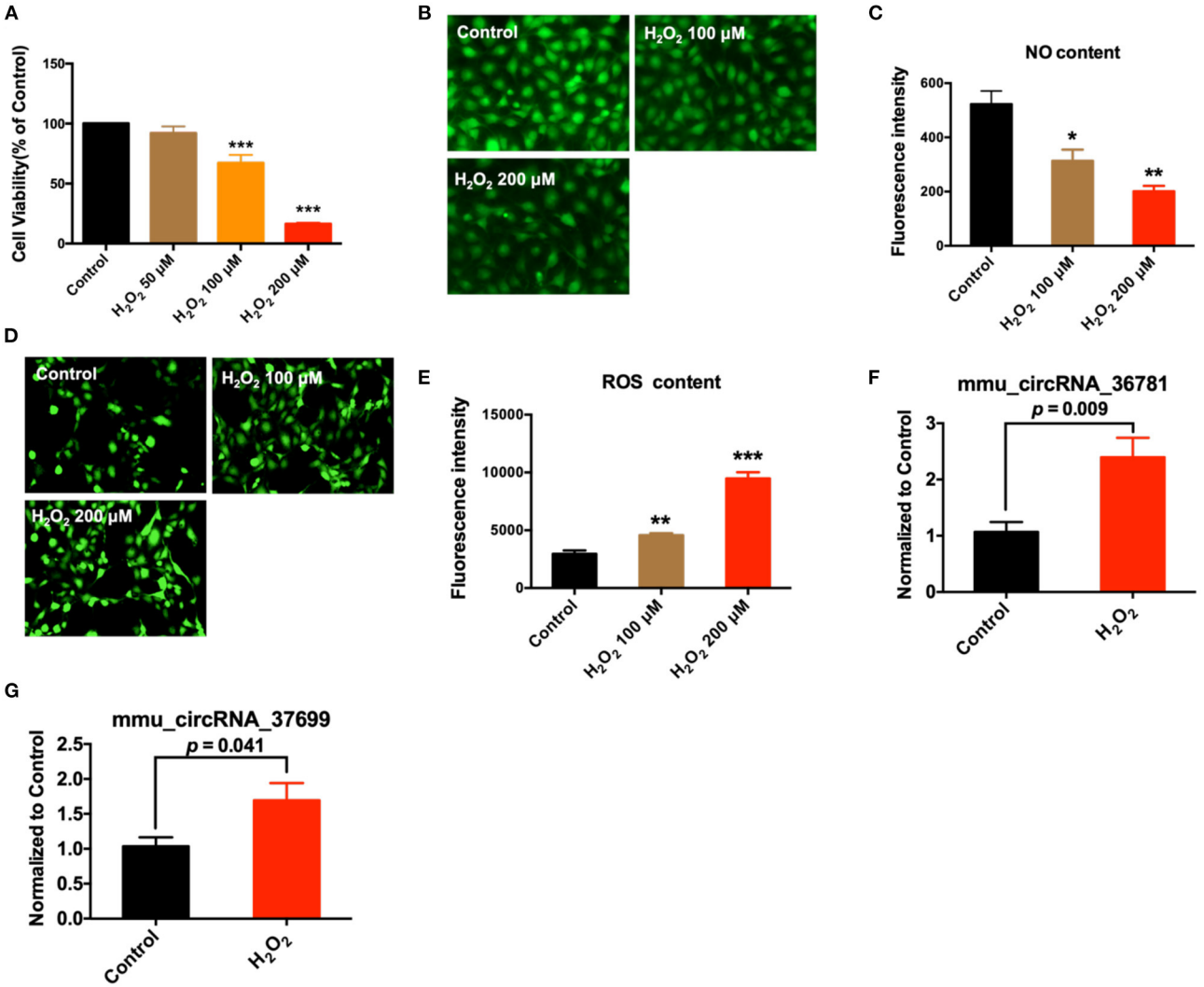

FIGURE 4 | Validation of differentially expressed circRNAs in MAECs induced by H_2O_2. **(A)** Effect of H_2O_2 on cell viability; ***$P < 0.001$ vs. Control, $n = 4$. **(B,C)** Effect of H_2O_2 on NO concentration of MAECs; 400×, $n = 3$. *$P < 0.05$, **$P < 0.01$ vs. Control. **(D,E)** Effect of H_2O_2 on ROS concentration of MAECs; 400×, $n = 3$. **$P < 0.01$, ***$P < 0.001$ vs. Control. **(F,G)** Expression of mmu_circRNA_36781 and mmu_circRNA_37699 in MAECs induced by 100 μM H_2O_2, $n = 5$–6.

circRNAs in atherosclerotic vessels, the relationship between circRNAs and atherosclerosis, and the potential mechanisms of circRNAs regulating atherosclerosis and endothelial injury have not been reported. In this study, we detected and analyzed the differences in circRNA expression profiles between AS and normal vessels. The expression of circRNAs in AS vessels changed significantly compared with normal vessels. Laboratory verification of microarray data showed that mmu_circRNA_36781, mmu_circRNA_37699 in AS vessels were significantly up-regulated and these changes were consistent with the microarray data. Therefore, we screened and verified the differentially expressed circRNAs in atherosclerotic vessels for the first time, providing a basis for further research on the biological functions of circRNAs in regulating atherosclerosis.

Relevant studies have shown that circRNAs regulate downstream target genes by acting as molecular sponges of complementary microRNAs (26). Therefore, we used bioinformatics databases to predict the microRNAs that had specific and conserved binding sites with these differentially expressed circRNAs. Through a comprehensive analysis of interspecies conservatism and binding stability, we selected miR-140-3p and miR-30d-3p as potential microRNA targets. Then, we detected the expression of these microRNAs in AS vessels and H_2O_2-treated MAECs. The results showed that miR-140-3p and miR-30d-3p were significantly down-regulated in H_2O_2-treated MAECs and AS vessels. Therefore, the variation trend of miR-140-3p and miR-30d-3p was consistent in H_2O_2-treated MAECs and AS vessels, contrary

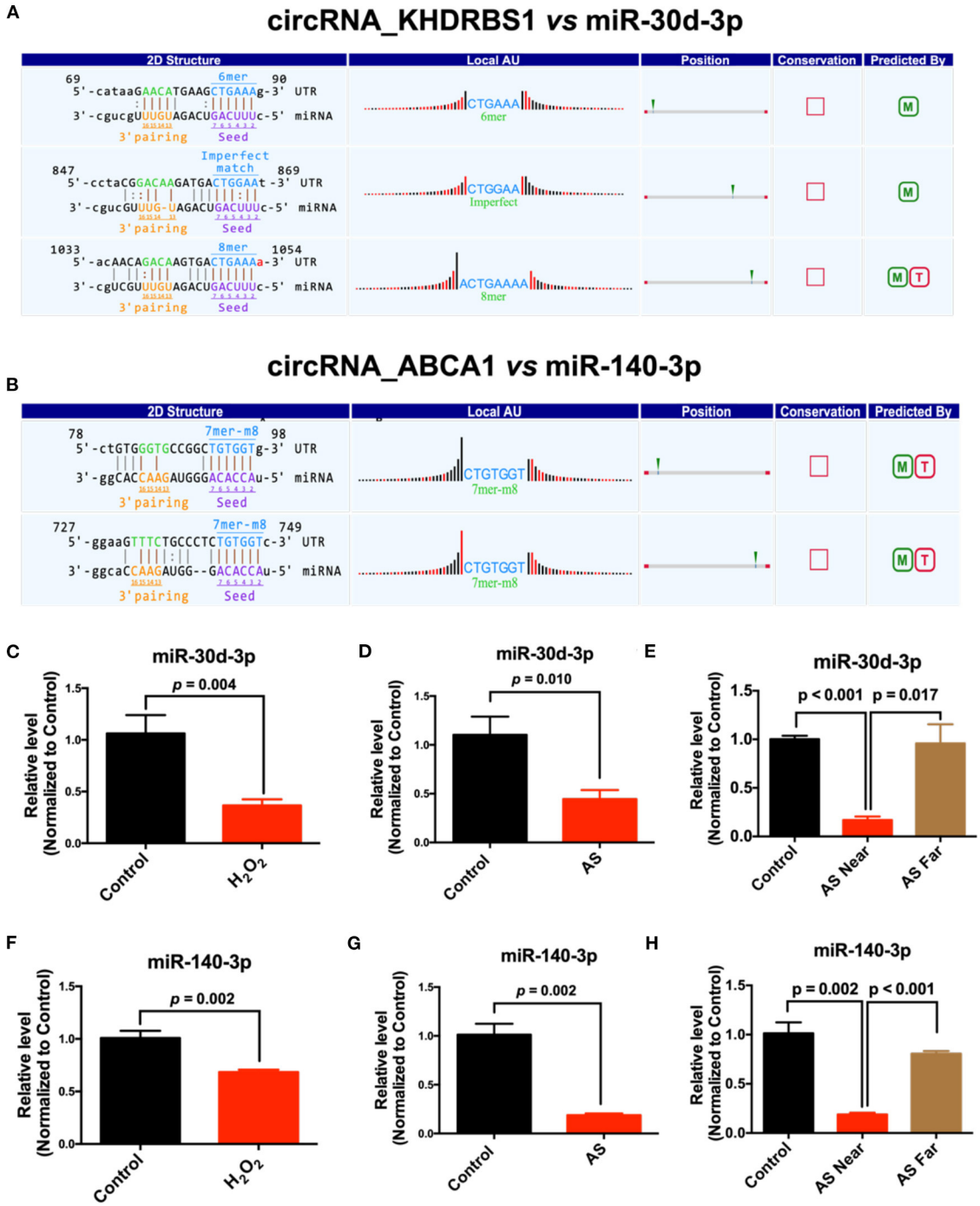

FIGURE 5 | Prediction and validation of complementary microRNAs of differentially expressed circRNAs. **(A)** The binding sites and 2D structure of circRNA KHDRBS1 with miR-30d-3p; **(B)** The binding sites and 2D structure of circRNA ABCA1 with miR-140-3p; **(C–E)** Expression of miR-30d-3p and miR-140-3p in MAECs induced by H_2O_2 and AS aorta, $n = 3–6$; **(F–H)** Expression of miR-140-3p in MAECs induced by H_2O_2 and AS aorta, $n = 3–5$.

to the changes of corresponding circRNAs. Therefore, we speculate that circRNA_ABCA1 and circRNA_KHDRBS1 may regulate vascular endothelial injury by targeting miR-140-3p and miR-30d-3p, respectively.

Current studies on miR-140-3p have shown that miR-140-3p protects against ox-LDL, high glucose and ischemia reperfusion induced endothelial injury, and may have a potential preventive effect on vascular disease (27–29). Recent research

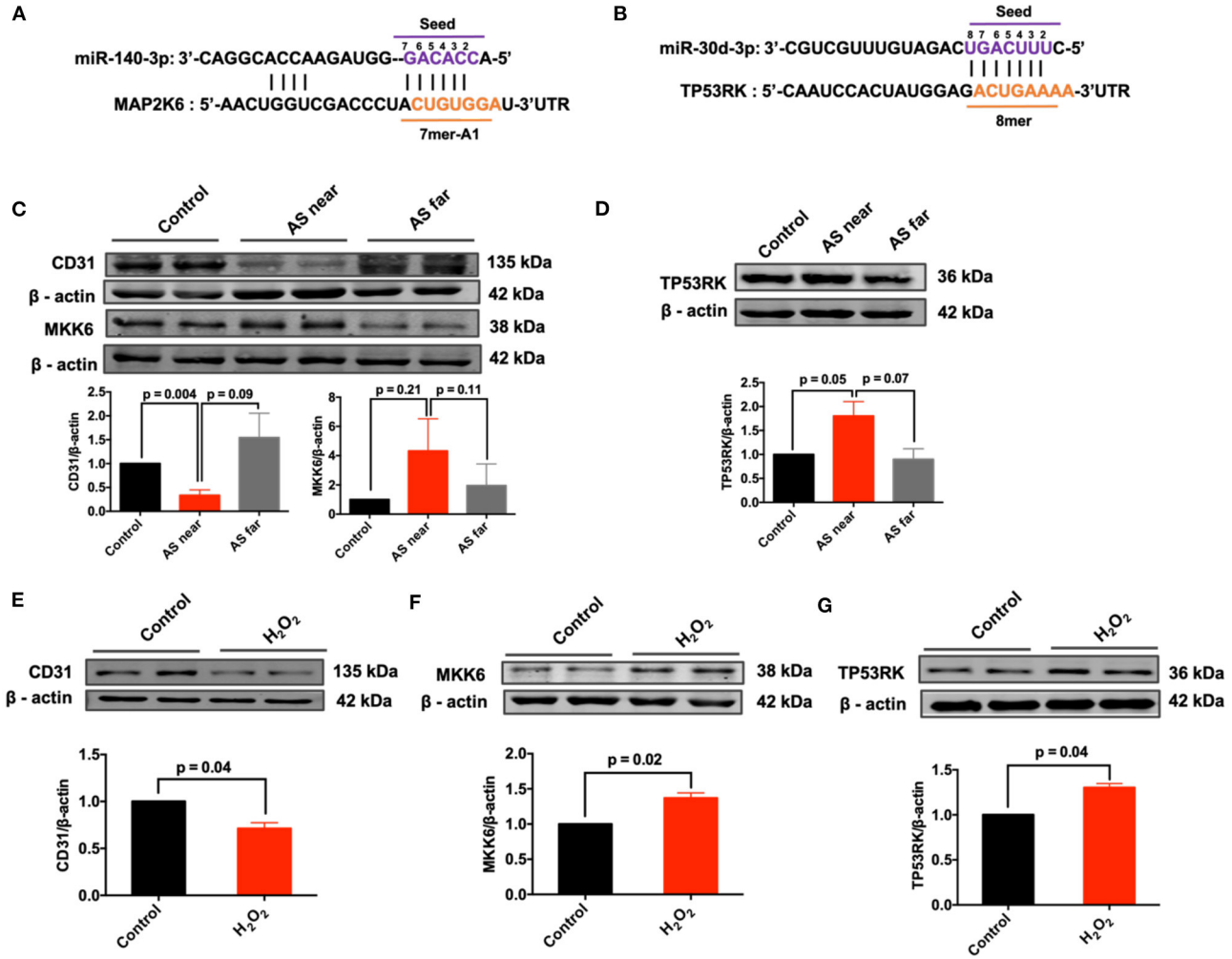

FIGURE 6 | Expression of predicted complementary mRNAs in AS aortas and H_2O_2-treated MAECs. **(A)** The binding sites and 2D structure of miR-140-3p with MAP2K6; **(B)** The binding sites and 2D structure of miR-30d-3p with TP53RK; **(C)** Expression of CD31 and MKK6 in control, AS near and AS far aortas, $n = 3$; **(D)** Expression of TP53RK in control, AS near and AS far aortas, $n = 3$; **(E–G)** Expression of CD31, MKK6 and TP53RK in H_2O_2-treated MAECs, $n = 3$–4.

has reported that miR-30d-3p can reduce cerebral ischemia reperfusion injury (30). Therefore, miR-30d-3p and miR-140-3p may have important biological functions in vascular disease. Based on the protective potential of miR-140-3p and miR-30d-3p on vascular endothelium, their regulative effects on atherosclerosis and whether they can be used as therapeutic targets for atherosclerosis and vascular endothelial injury require further studies. This study found that circRNA_ABCA1 and circRNA_KHDRBS1 had the potential to regulate miR-140-3p and miR-30d-3p and may be key regulators of miRNA abnormalities during disease. Besides, potential target genes of miR-140-3p and miR-30d-3p associated with atherosclerosis or endothelial injury were predicted using bioinformatics databases (TarBase and Targetscan) in this study. In contrast to the expression of microRNA, the protein abundance of MKK6, the potential target of miR-140-3p, and TP53RK, the potential target of miR-30d-3p, were both upregulated in AS vessels and H_2O_2-treated endothelial cells. TP53RK is an upstream kinase of p53. It phosphorylates (serine residue Ser15) and mediates p53 activity (31). MKK6 is a protein kinase that specifically activates p38 (32). p53 and MKK6/p38 stress cascade play crucial roles in endothelial injury associated with hyperglycemia, hyperlipidemia, ischemia, etc. (33–35). In addition, we analyzed the signaling pathways that might be annotated or regulated by these target genes, among which the most significant signal pathways are MAPK and PI3K-AKT signaling pathway. Related studies have confirmed that activation of p38MAPK signaling pathway in endothelial cells is involved in vascular endothelial injury in early atherosclerosis. MAPK signaling pathway in endothelial cells regulates endothelial cell permeability, apoptosis and angiogenesis (36, 37). PI3K-Akt signaling pathway has a broad regulatory effect on cell

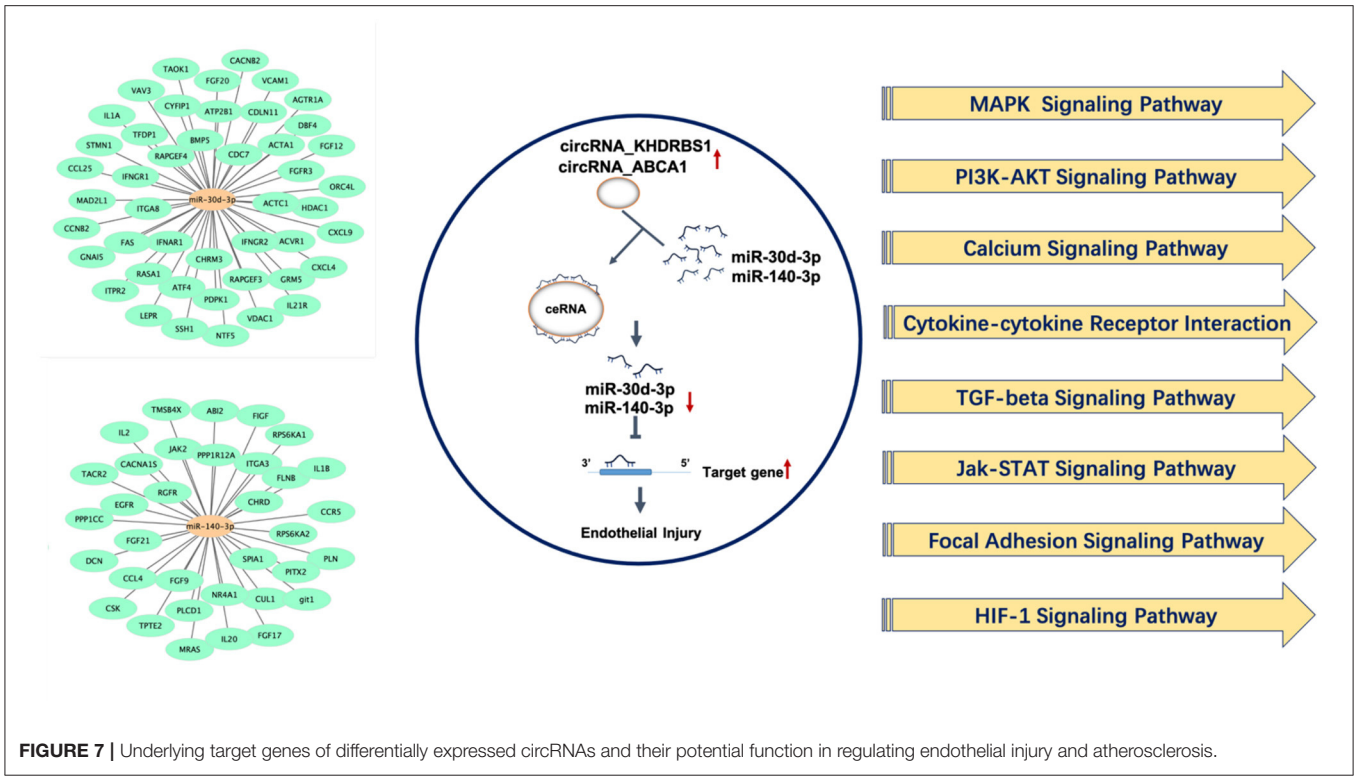

FIGURE 7 | Underlying target genes of differentially expressed circRNAs and their potential function in regulating endothelial injury and atherosclerosis.

function, and is involved in aortic vascular endothelial cell injury and atherosclerotic plaque formation (38, 39). The results of this study preliminarily revealed the correlation between circRNA_ABCA1 and circRNA_KHDRBS1 and MAPK and PI3K signaling pathways, providing reference for clarifying the role of circRNAs in atherosclerosis.

In summary, this study screened and verified the circRNAs differentially expressed in atherosclerosis and oxidative injured endothelial cells. We further verified the potential microRNA and mRNA targets of these differentially expressed circRNAs, and predicted the potential ceRNA mechanism and biological functions of the differentially expressed circRNAs. This study provided new ideas and targets for future studies on the biological functions of circRNA_ABCA1 and circRNA_KHDRBS1 in regulating atherosclerosis and endothelial injury.

DATA AVAILABILITY STATEMENT

The raw data supporting the conclusions of this article will be made available by the authors, without undue reservation.

ETHICS STATEMENT

All animal protocols were approved by the Ethic Committees of Harbin Medical University (IRB of College of Pharmacy, Harbin Medical University, No. IRB3001619) and were in line with the ARRIVE guidelines and recommendations for the care and use of experimental animals.

AUTHOR CONTRIBUTIONS

HL: manuscript preparation and data analysis. XL, NS, TW, JZ, SY, XS, RW, and XW: investigation. YZhao and YZhan: project administration and supervision. YZhao and YZhan: funding acquisition. All authors contributed to the article and approved the submitted version.

FUNDING

This work was supported by National Natural Science Foundation of China [grant number 81903608, 81870259].

ACKNOWLEDGMENTS

We appreciate the Science and Technology Park of Harbin Medical University for providing us with required laboratories and instruments.

SUPPLEMENTARY MATERIAL

The Supplementary Material for this article can be found online at: https://www.frontiersin.org/articles/10.3389/fcvm.2021.657544/full#supplementary-material

REFERENCES

1. Tsivgoulis G, Safouris A, Kim, D, Alexandrov A. Recent advances in primary and secondary prevention of atherosclerotic stroke. *J Stroke.* (2018) 20:145–66. doi: 10.5853/jos.2018.00773
2. Su J. Vascular endothelial dysfunction and pharmacological treatment. *World J Cardiol.* (2015) 7:719–41. doi: 10.4330/wjc.v7.i11.719
3. Auge N, Maupas-Schwalm F, Elbaz M, Thiers JC, Waysbort A, Itohara S, et al. Role for matrix metalloproteinase-2 in oxidized low-density lipoprotein-induced activation of the sphingomyelin/ceramide pathway and smooth muscle cell proliferation. *Circulation.* (2004) 110:571–8. doi: 10.1161/01.CIR.0000136995.83451.1D
4. Chistiakov DA, Orekhov AN, Bobrryshev YV. LOX-1-mediated effects on vascular cells in atherosclerosis. *Cell Physiol Biochem.* (2016) 38:1851–9. doi: 10.1159/000443123
5. Hu YW, Wu SG, Zhao JJ, Ma X, Lu JB, Xiu JC, et al. VNN1 promotes atherosclerosis progression in apoE-/- mice fed a high-fat/high-cholesterol diet. *J Lipid Res.* (2016) 57:1398–411. doi: 10.1194/jlr.M065565
6. Sima AV, Stancu CS, Simionescu M. Vascular endothelium in atherosclerosis. *Cell Tissue Res.* (2009) 335:191–203. doi: 10.1007/s00441-008-0678-5
7. Simionescu M. Impllications of early structural-functional changes in the endothelium for vascular disease. *Arterioscler Thromb Vasc Biol.* (2007) 27:266–74. doi: 10.1161/01.ATV.0000253884.13901.e4
8. Gimbrone MA Jr, Carcia-Cardena G. Endothelial cell dysfunction and the pathobiology of atherosclerosis. *Circ Res.* (2016) 118:620–36. doi: 10.1161/CIRCRESAHA.115.306301
9. Daiber A, Steven S, Weber A, Shuvaev V, Muzykantov V, Laher I, et al. Targeting vascular (endothelial) dysfunction. *Br J Pharmacol.* (2017) 174:1591–619. doi: 10.1111/bph.13517
10. Davignon J, Ganz P. Role of endothelial dysfuntion in atherosclerosis. *Circulation.* (2014) 109:III27–32. doi: 10.1161/01.CIR.0000131515.03336.f8
11. Chen LL., Yang L. Regulation of circRNA biogenesis. *RNA Bio.* (2015) 12:381–8. doi: 10.1080/15476286.2015.1020271
12. Sanger HL, Klotz G, Riesner D, Gross HJ, Kleinschmidt AK. Viroids are single-stranded covalently closed circular RNA molecules existing as highly base-paired rod-like structures. *P Natl Acad Sci USA.* (1976) 73:3852–6. doi: 10.1073/pnas.73.11.3852
13. Memczak S, Jens M, Elefsinioti A, Torti F, Krueger J, Rybak A, et al. Circular RNAs are a large class of animal RNAs with regulatory potency. *Nature.* (2013) 495:333–8. doi: 10.1038/nature11928
14. Zhang Y, Zhang XO, Chen T, Xiang JF, Yin QF, Xing YH, et al. Circular intronic long noncoding RNAs. *Mol Cell.* (2013) 51:792–806. doi: 10.1016/j.molcel.2013.08.017
15. Hansen TB., Jensen T., Clausen BH, Bramsen JB, Finsen B, Damgaard CK, et al. Natural RNA circles function as efficient microRNA sponges. *Nature.* (2013) 495:384–88. doi: 10.1038/nature11993
16. Holdt LM, Stahringer A, Sass K, Pichler G, Kulak NA, Wilfert W, et al. Circular non-coding RNA ANRIL modulates ribosomal RNA maturation and atherosclerosis in humans. *Nat Commun.* (2016) 7:12429. doi: 10.1038/ncomms12429
17. Bazan HA, Hatfield SA, Brug A, Brooks AJ, Lightell DJ Jr, Woods TC. Carotid Plaque Rupture Is Accompanied by an Increase in the Ratio of Serum circR-284 to miR-221 Levels. *Circ Cardiovasc Genet.* (2017) 10:e001720. doi: 10.1161/CIRCGENETICS.117.001720
18. Chen JJ, Cui LQ, Yuan JL, Zhang YQ, Sang HJ. Circular RNA WDR77 target FGF-2 to regulate vascular smooth muscle cells proliferation and migration by sponging miR-124. *Biochem Biophys Res Commun.* (2017) 494:126–32. doi: 10.1016/j.bbrc.2017.10.068
19. Li CY, Ma L, Yu B. Circular RNA hsa_circ_0003575 regulates oxLDL induced vascular endothelial cells proliferation and angiogenesis. *Biomed Pharmacother.* (2017) 95:1514–9. doi: 10.1016/j.biopha.2017.09.064
20. Zhang F, Zhang RY, Zhang XY, Wu YN, Li XY, Zhang S, et al. Comprehensive analysis of circRNA expression pattern and circRNA-miRNA-mRNA network in the pathogenesis of atherosclerosis in rabbits. *Aging.* (2018) 10:2266–83. doi: 10.18632/aging.101541
21. Zhao YX, Zhang X, Luan J, Zhao BC, An N, Sun N, et al. Shenxian-shengmai oral liquid reduces myocardial oxidative stress and protects myocardium from ischemia-reperfusion injury. *Cell Physiol Biochem.* (2018) 48:2503–16. doi: 10.1159/000492688
22. Zhao YX, Zhang X, Li JN, Bian Y, Sheng MM, Liu B, et al. Jujuboside B reduces vascular tension by increasing Ca2+ influx and activating endothelial nitric oxide synthase. *PLoS ONE.* (2016) 11:e0149386. doi: 10.1371/journal.pone.0149386
23. Zhao Y, Wang X, Yang S, Song X, Sun N, Chen C, et al. Kanglexin accelerates diabetic wound healing by promoting angiogenesis via FGFR1/ERK signaling. *Biomed Pharmacother.* (2020) 132:110933. doi: 10.1016/j.biopha.2020.110933
24. Bolha L, Ravnik-Glavac M, Glavac D. Circular RNAs: Biogenesis, function, and a role as possible cancer biomarkers. *Int J Genomics.* (2017) 2017: 6218353. doi: 10.1155/2017/6218353
25. Song CL, Wang JP, Xue X, Liu N, Zhang XH, Zhao Z, et al. (2017). Effect of circular ANRIL on the inflammatory response of vascular endothelial cells in a rat model of coronary atherosclerosis. *Cell Physiol Biochem.* (2017) 42:1202–12. doi: 10.1159/000478918
26. Fang Y. Circular RNAs as novel biomarkers with regulatory potency in human diseases. *Future Sci OA.* (2018) 4:FSO314. doi: 10.4155/fsoa-2018-0036
27. Wang D, Wang H, Liu C, Mu X, Cheng S. Hyperglycemia inhibition of endothelial miR-140-3p mediates angiogenic dysfunction in diabetes mellitus. *J Diabetes Complications.* (2019) 33:374–82. doi: 10.1016/j.jdiacomp.2019.02.001
28. Liang S, Ren K, Li B, Li F, Liang Z, Hu J, et al. LncRNA SNHG1 alleviates hypoxia-reoxygenation-induced vascular endothelial cell injury as a competing endogenous RNA through the HIF-1alpha/VEGF signal pathway. *Mol Cell Biochem.* (2020) 465:1–11. doi: 10.1007/s11010-019-03662-0
29. Qian W, Qian Q, Cai X, Han R, Yang W, Zhang X, et al. Astragaloside IV inhibits oxidized low-density lipoprotein-induced endothelial damage via upregulation of miR-140-3p. *Int J Mol Med.* (2019) 44:847–56. doi: 10.3892/ijmm.2019.4257
30. Hideshima T, Cottini F, Nozawa Y, Seo HS, Ohguchi H, Samur MK, et al. p53-related protein kinase confers poor prognosis and represents a novel therapeutic target in multiple myeloma. Blood. (2017) 129, 1308–19. doi: 10.1182/blood-2016-09-738500
31. Jin DS, Wei W, Song C, Han P, Leng XL. Knockdown EZH2 attenuates cerebral ischemia-reperfusion injury via regulating microRNA-30d-3p methylation and USP22. *Brain Res Bull.* (2021) 169:25–34. doi: 10.1016/j.brainresbull.2020.12.019
32. Anter E, Chen K, Shapira OM, Karas RH, Keaney JF Jr. p38 mitogen-activated protein kinase activates eNOS in endothelial cells by an estrogen receptor alpha-dependent pathway in response to black tea polyphenols. *Circ Res.* (2005) 96:1072–8. doi: 10.1161/01.RES.0000168807.63013.56
33. Grimsey NJ, Aguilar B, Smith TH, Le P, Soohoo AL, Puthenveedu MA, et al. Ubiquitin plays an atypical role in GPCR-induced p38 MAP kinase activation on endosomes. *J Cell Biol.* (2015) 210:1117–31. doi: 10.1083/jcb.201504007
34. Hashimoto S, Gon Y, Matsumoto K, Takeshita I, Horie T. N-acetylcysteine attenuates TNF-alpha-induced p38 MAP kinase activation and p38 MAP kinase-mediated IL-8 production by human pulmonary vascular endothelial cells. *Br J Pharmacol.* (2001) 132:270–6. doi: 10.1038/sj.bjp.0703787
35. Yokoyama M, Shimizu I, Nagasawa A, Yoshida Y, Katsuumi G, Wakasugi T, et al. p53 plays a crucial role in endothelial dysfunction associated with hyperglycemia and ischemia. *J Mol Cell Cardiol.* (2019) 129:105–17. doi: 10.1016/j.yjmcc.2019.02.010
36. Hopkins PN. Molecular biology of atherosclerosis. *Physiol Rev.* (2013) 93:1317–542. doi: 10.1152/physrev.00004.2012
37. Reustle A, Torzewski M. Role of p38 MAPK in atherosclerosis and aortic valve sclerosis. *Int J Mol Sci.* (2018) 19:3761. doi: 10.3390/ijms19123761
38. Durrant TN, Hers I. PI3K inhibitors in thrombosis and cardiovascular disease. *Clin Transl Med.* (2020) 9:8. doi: 10.1186/s40169-020-0261-6
39. Andreas Eisenreich, Ursula Rauch. PI3K inhibitors in cardiovascular disease. *Cardiovasc Ther.* (2011) 29:29–36. doi: 10.1111/j.1755-5922.2010.00206.x

Conflict of Interest: The authors declare that the research was conducted in the absence of any commercial or financial relationships that could be construed as a potential conflict of interest.

frontiers in Cardiovascular Medicine

ORIGINAL RESEARCH
published: 12 July 2021
doi: 10.3389/fcvm.2021.667298

High-Throughput Screening Identifies MicroRNAs Regulating Human PCSK9 and Hepatic Low-Density Lipoprotein Receptor Expression

Coen van Solingen[1], Scott R. Oldebeken[1], Alessandro G. Salerno[1†], Amarylis C. B. A. Wanschel[1†] and Kathryn J. Moore[1,2]*

[1] Leon H. Charney Division of Cardiology, Department of Medicine, New York University Cardiovascular Research Center, New York University School of Medicine, New York, NY, United States, [2] Department of Cell Biology, New York University School of Medicine, New York, NY, United States

OPEN ACCESS

Edited by:
En-zhi Jia,
Nanjing Medical University, China

Reviewed by:
Zhiyong Lei,
University Medical Center Utrecht, Netherlands
Ruijing Zhang,
Second Hospital of Shanxi Medical University, China

***Correspondence:**
Kathryn J. Moore
kathryn.moore@nyulangone.org

†Present address:
Alessandro G. Salerno and Amarylis C. B. A. Wanschel, Interdisciplinary Stem Cell Institute, University of Miami Miller School of Medicine, Miami, FL, United States

Specialty section:
This article was submitted to General Cardiovascular Medicine, a section of the journal Frontiers in Cardiovascular Medicine

Received: *12 February 2021*
Accepted: *11 June 2021*
Published: *12 July 2021*

Citation:
van Solingen C, Oldebeken SR, Salerno AG, Wanschel ACBA and Moore KJ (2021) High-Throughput Screening Identifies MicroRNAs Regulating Human PCSK9 and Hepatic Low-Density Lipoprotein Receptor Expression. Front. Cardiovasc. Med. 8:667298. doi: 10.3389/fcvm.2021.667298

Investigations into the regulatory mechanisms controlling cholesterol homeostasis have proven fruitful in identifying low-density lipoprotein (LDL)-lowering therapies to reduce the risk of atherosclerotic cardiovascular disease. A major advance was the discovery of proprotein convertase subtilisin/kexin type 9 (PCSK9), a secreted protein that binds the LDL receptor (LDLR) on the cell surface and internalizes it for degradation, thereby blunting its ability to take up circulating LDL. The discovery that loss-of-function mutations in *PCSK9* lead to lower plasma levels of LDL cholesterol and protection from cardiovascular disease led to the therapeutic development of PCSK9 inhibitors at an unprecedented pace. However, there remain many gaps in our understanding of PCSK9 regulation and biology, including its posttranscriptional control by microRNAs. Using a high-throughput region(3′-UTR) of human microRNA library screen, we identified microRNAs targeting the 3′ untranslated region of human PCSK9. The top 35 hits were confirmed by large-format PCSK9 3′-UTR luciferase assays, and 10 microRNAs were then selected for further validation in hepatic cells, including effects on PCSK9 secretion and LDLR cell surface expression. These studies identified seven novel microRNAs that reduce PCSK9 expression, including miR-221-5p, miR-342-5p, miR-363-5p, miR-609, miR-765, and miR-3165. Interestingly, several of these microRNAs were also found to target other genes involved in LDLR regulation and potently upregulate LDLR cell surface expression in hepatic cells. Together, these data enhance our understanding of post-transcriptional regulators of PCSK9 and their potential for therapeutic manipulation of hepatic LDLR expression.

Keywords: microRNA, LDL receptor, lipoprotein, proprotein convertase subtilisin kexin type 9, hepatocytes

INTRODUCTION

Cholesterol homeostasis is essential for human health, and its dysregulation results in cardiometabolic diseases, including atherosclerosis. Cells must maintain membrane cholesterol within a narrow concentration to ensure proper membrane function, and this requires an intricate balance of cholesterol synthesis and uptake of cholesterol from plasma lipoproteins (1). Hepatocytes play a major role in the regulation of systemic cholesterol homeostasis through the assembly and secretion of plasma lipoproteins, as well as their eventual clearance through the low-density lipoprotein (LDL) receptor. This highly synchronized process is achieved through a complex network of regulatory and counter-regulatory mechanisms that function at both the transcriptional and post-transcriptional levels. Imbalances in hepatic cholesterol synthesis and uptake can result in elevated levels of LDL cholesterol (LDL-C), a strong, independent risk factor for atherosclerotic cardiovascular disease (ASCVD). Thus, the regulatory networks that maintain cholesterol homeostasis have been the subject of intense research efforts for over 30 years, and discoveries in this area have had major impacts on the management of cardiovascular disease.

Statin drugs have revolutionized the routine management of patients with high LDL-C, significantly lowering the associated cardiovascular morbidity and mortality (2, 3). Statins act to shut off cellular cholesterol biosynthesis by inhibiting 3-HMG-CoA reductase (HMGCR) (4), the rate-limiting enzyme in cholesterol homeostasis. This reduces hepatic cholesterol synthesis, leading to feedback activation of sterol regulatory element (SRE)-binding protein (SREBP), a transcription factor that drives LDL receptor (LDLR) expression (5). The upregulation of hepatic LDLR expression results in increased clearance of circulating LDL, effectively lowering its plasma concentrations and its subsequent negative effects in blood vessels (6). A second major breakthrough came with the identification of proprotein convertase subtilisin/kexin type 9 (PCSK9), a circulating protein that binds to the LDLR and internalizes it for lysosomal degradation (7). The discovery of PCSK9 emerged from seminal studies by Abifadel et al. of a French family with familial hypercholesterolemia, with no known mutations in genes coding for LDLR or its trafficking (8). These patients were found to have gain-of-function mutations in PCSK9, resulting in low levels of hepatic LDLR and LDL clearance. Subsequent studies identified loss-of-function mutations in PCSK9 associated with lifelong low levels of LDL-C and marked reduction in the risk of ASCVD (9–11). This fueled the rapid clinical development of PCSK9 inhibitors, with Food and Drug Administration (FDA) approval of human monoclonal antibodies that bind PCSK9 and reduce LDL-C by 60% (12), occurring in record time less than a decade after the discovery of PCSK9. Despite this success, there is still much to be learned about PCSK9's regulation and function, which may inform not only additional facets of PCSK9 biology but also alternative mechanisms of PCSK9 antagonism.

An area of PCSK9 regulation that remains underexplored is its posttranscriptional inhibition by microRNAs (miRNAs). MiRNAs are short (20–25 base pairs) non-coding RNA sequences that are transcribed from the genome and are capable of binding to complementary sequences in the 3′ untranslated region (3′-UTR) of mRNA transcripts (13). MiRNA targeting of mRNAs results in posttranscriptional inhibition of their translation into protein and/or their degradation (14–16). Previous studies have shown the potential for a handful of miRNAs to directly inhibit the expression and function of PCSK9 in human or murine hepatocytes, including miR-224, miR-191, miR-222, miR-483, and miR-520d (17–20). These studies have uncovered new links for PCSK9 with disease, as well as how miRNAs can integrate the regulation of multiple genes involved in cholesterol metabolism. For example, miR-224 was identified as a potent inhibitor of PCSK9 expression in hepatocytes (18) and subsequently found to regulate PCSK9 in human neuroendocrine tumors (20), where its overexpression restricted tumor cell proliferation and invasion (20). Further studies showed that miR-224 represses not only PCSK9 but also other genes impacting the expression of the LDLR, including HMGCR and a second LDLR chaperone protein called IDOL (19). Notably, hepatic overexpression of miR-224 in mice using nanoparticle mediated delivery of miR-224 mimics decreased plasma LDL-C levels by 15% (19). Similarly, miR-483 was shown to repress expression of PCSK9 in hepatocytes, leading to upregulation of the LDLR and LDL uptake, and adeno-associated virus-mediated delivery of miR-483 in mice overexpressing PCSK9 decreased total plasma cholesterol levels by 20% (17). These studies highlight the feasibility of harnessing miRNA-driven regulation of PCSK9 expression to regulate plasma levels of LDL-C *in vivo*.

To identify novel regulators of PCSK9 expression in humans, we performed a high-throughput screen of human miRNAs targeting the 3′-UTR of *PCSK9* fused to a luciferase gene. Candidate miRNAs that repressed *PCSK9* 3′-UTR luciferase activity were selected using a strictly standardized mean difference (SSMD) analysis of the relative changes in sample luciferase activities and cross-referenced with miRNA target algorithms such as TargetScan and miRanda. The resulting miRNA hits underwent secondary validation in miRNA mimic transfection assays to examine their effect on *PCSK9* mRNA and protein levels in hepatic cell lines, and the top 10 miRNAs were selected for validation assays, including regulation of LDLR protein expression and cell surface localization. Notably, several candidate miRNAs identified to target *PCSK9* were also found to target genes involved in other pathways that regulate LDLR cell surface expression (i.e., *HMGCR* and *IDOL*), suggesting that targeting such miRNAs may have a higher therapeutic impact.

MATERIALS AND METHODS

Cell Culture

HepG2 and HEK-293T cells were obtained from the American Type Culture Collection, authenticated with standard American Type Culture Collection methods (morphology check under microscope and growth curve analysis) and regularly tested for mycoplasma contamination. Cells were maintained in Dulbecco's modified Eagle medium (DMEM; Corning, New York, NY, USA) containing 10% fetal bovine serum (Life Technologies, Carlsbad, CA, USA) and 1% penicillin–streptomycin (Life Technologies). HepG2-LDLR-GFP cells were

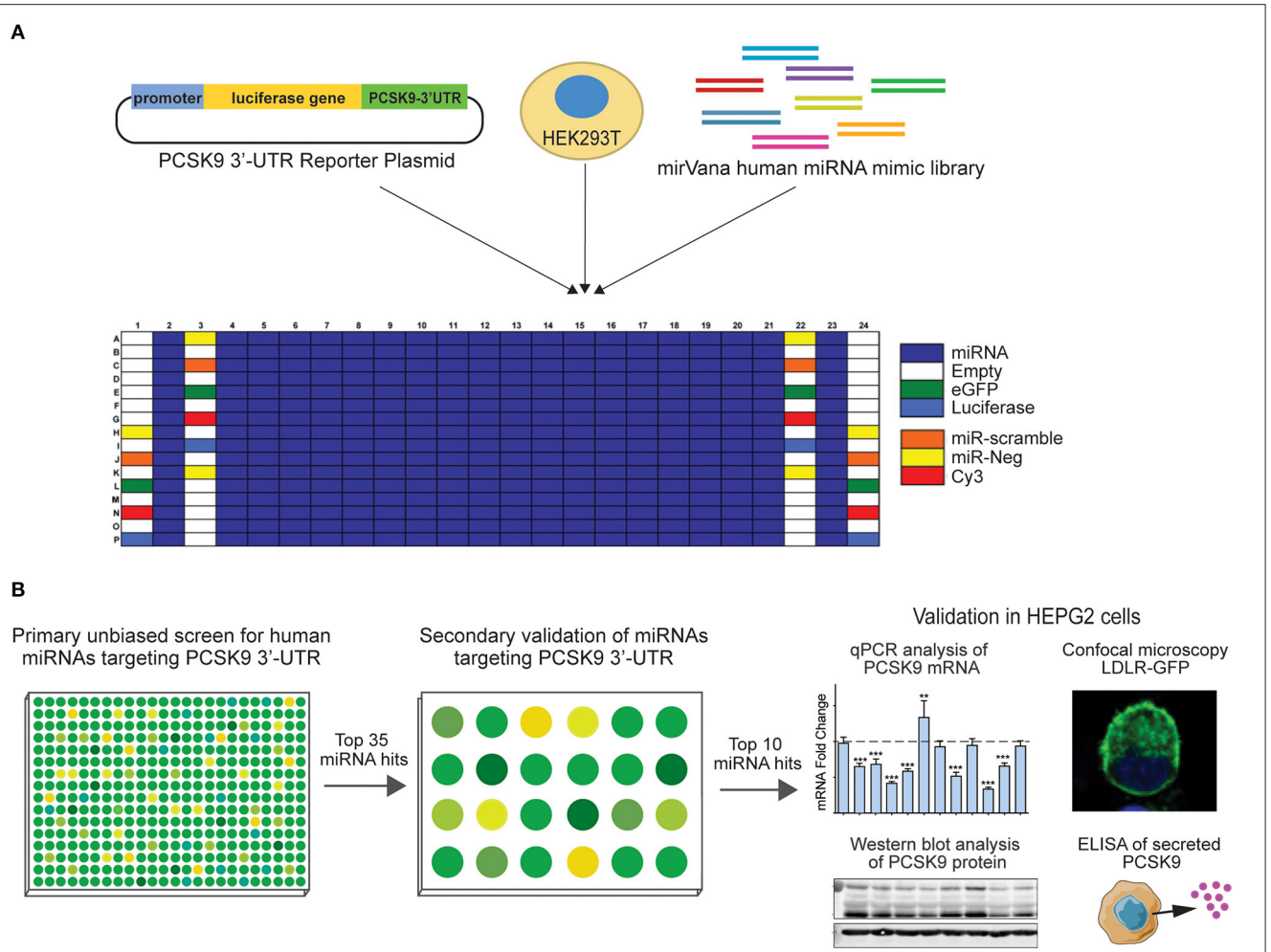

FIGURE 1 | Experimental design for high-throughput human miRNA library screen to identify novel miRNAs targeting *PCSK9*. **(A)** Primary unbiased screen of human miRNAs targeting the 3′-UTR of human *PCSK9*. HEK-293T cells underwent reverse transfection with a luciferase reporter plasmid harboring the 3′-UTR of *PCSK9*, and a human miRvana miRNA mimic library in a 384-well array format. **(B)** Secondary screen of the top 35 miRNA hits using the same *PCSK9* 3′-UTR-luciferase assay in a 24-well format and further validation of the top 10 candidates for effects on PCSK9 mRNA and protein expression, and low-density lipoprotein receptor (LDLR) expression.

grown as previously described (21). All cells were cultured in a humidified incubator at 37°C and 5% CO_2.

High-Throughput Human MicroRNA Library Screens

Primary Screen

A high-throughput human miRNA screen was conducted with the NYU RNAi Core Facility (NYU Grossman School of Medicine). HEK-293T cells were reverse transfected in triplicate with a library of 1,719 miRNA mimics (Life Technologies *mir*Vana Mimic Library, miRbase release 17.0) in Corning 384-well, flat, white-bottom polystyrene TC-treated microplates. Briefly, 5,000 cells/well, 1.5 pmol of miRNA mimic, and 10 ng of total DNA plasmids composed of a 2:1 ratio of *PCSK9* 3′-UTR firefly luciferase reporter plasmid (SwitchGear Genomics, Carlsbad, CA, USA) to renilla luciferase control plasmid using Lipofectamine 2000 (Invitrogen, Carlsbad, CA, USA) were dispensed into the 384-well plates using a WellMate/BioTek Dispenser (Thermo Fisher Scientific, Waltham, MA, USA) outfitted with small-bore tubing. The plates were centrifuged at 1,000 × g for 1 min to settle the contents and then incubated in a humidified incubator at 37°C and 5% CO_2 for 48 h. To measure *PCSK9* 3′-UTR-luciferase activity, media were aspirated, and the wells were washed with 1× phosphate-buffered saline (PBS) using an EL406 Microplate Washer (BioTek). Luciferase activity was measured using the Dual-Glo Luciferase Assay® (Promega, Madison, WI, USA) according to the manufacturer's instructions and read on a spectrophotometer (EnVision; PerkinElmer, Waltham, MA, USA). Positive (miR-224) and negative control miRNAs were included on each screen plate, and the miRNA library was assayed in quadruplicate. *PCSK9* 3′-UTR firefly

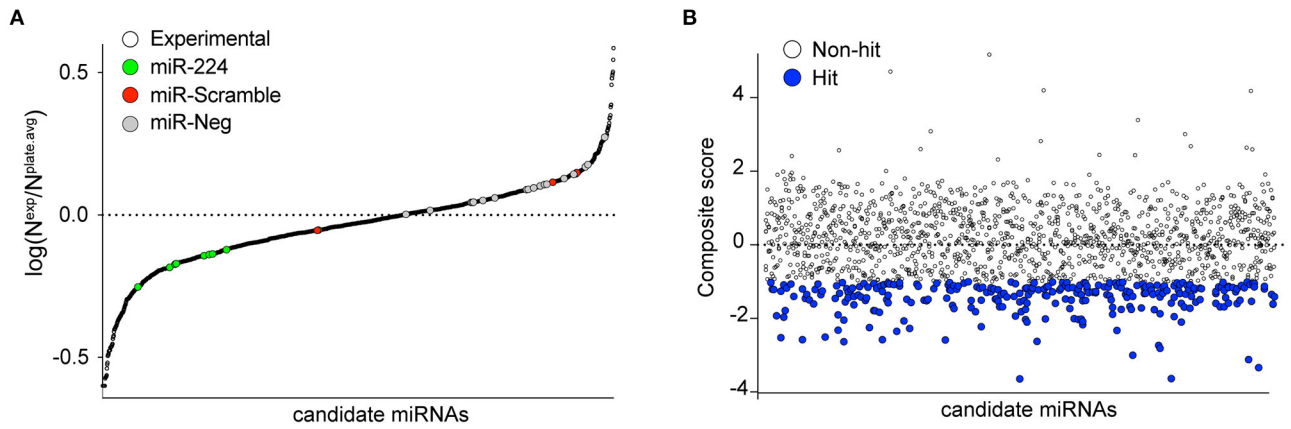

FIGURE 2 | Primary screening of human miRNAs targeting the 3′-UTR of *PCSK9*. **(A)** MiRNAs were tested for their ability to repress a luciferase reporter gene fused to the 3′-UTR of human *PCSK9*. Data represent average log normalized scores [log($N^{exp}/N^{plate.avg}$)] of luciferase activity of three replicates. N^{exp} represents firefly reporter activity normalized to renilla luciferase control per well. $N^{plate.avg}$ represents the average firefly reporter activity normalized to renilla luciferase control for the whole plate. Negative (miR-scramble and miR-negative) and positive (miR-224) controls are indicated by the colored dots. **(B)** Ranking of miRNA hits by composite score of the strictly standardized mean differences (SSMDs) of log($N^{exp}/N^{plate.avg}$), Z-score, and percentage of negative control (POC). MiRNAs with composite SSMD scores of <-1 were identified as positive hits (blue) in the screen.

luciferase values were normalized to those of control renilla luciferase values for each replicate. Normalized firefly luciferase activities were ranked using the SSMDs of log($N^{exp}/N^{plate.avg}$), Z-score (N^{exp}-$N^{plate.avg}$/SD $N^{plate.avg}$), and percent of negative control (POC), relative to plate averages as previously described (22). MiRNA candidates with a composite SSMD score of <-1 were identified as hits.

Secondary Screen

Target prediction algorithms were used to validate putative binding to the human *PCSK9* 3′-UTR, and the top 35 screen hits were selected for a secondary screen, consisting of a similar but larger-format luciferase assay. HEK-293T cells were plated in antibiotic-free media in 24-well plates and co-transfected with 0.2 μg of 3′-UTR luciferase *PCSK9* reporter vector and miRNA mimic or negative control mimic (Dharmacon; Horizon Discovery, Cambridge, UK) utilizing Lipofectamine 2000 (Invitrogen), as previously described. Luciferase activity was measured using the Dual-Glo Luciferase Assay® (Promega). Firefly luciferase activity was normalized to renilla luciferase activity and reported as fold change in activity compared with control mimic. Experiments were performed in triplicate wells of a 24-well plate and repeated three times.

Transfection of Hepatic Cells With MicroRNA Mimics

Human hepatic cells (HepG2) were plated at a density of 10^6 cells per well on 6-well cell culture plates and were transfected with control or miRNA mimics (80 nM, Dharmacon) using Lipofectamine® RNAi MAX (Invitrogen). After 48 h, cells were harvested and lysed with either TRIzol Reagent (Invitrogen) for RNA expression analysis or radioimmunoprecipitation assay (RIPA) buffer (Abcam, Cambridge, UK) for protein expression analysis.

RNA Isolation and Quantitative RT-PCR

Total RNA was isolated with TRIzol Reagent and Direct-zol RNA MiniPrep Columns (Zymo Research, Irvine, CA, USA). RNA was reverse transcribed using iScript™ cDNA Synthesis Kit (Bio-Rad Laboratories, Hercules, CA, USA), according to the manufacturer's protocol. Quantitative RT-PCR analysis was conducted using iQ Sybr Green Supermix (Bio-Rad) in a Mastercycler PCR Machine (Eppendorf, Hamburg, Germany) using the following primers: PCSK9 forward 5′-AGGGGAGGA CATCATTGGTG-3′ and reverse 5′-CAGGTTGGGGGTCAG TACC-3′; HMGCR forward 5′-GTCATTCCAGCCAAGGTT GT-3′ and reverse 5′-GGGACCACTTGCTTCCATTA-3′; IDOL forward 5′-CGAGGACTGCCTCAACCA-3′ and reverse 5′-TGCAGTCCAAAATAGTCAACTTCT-3′; and GAPDH forward 5′GAAGGTGAAGGTCGGAGTC-3′ and reverse 5′-GAAGAT GGTGATGGGATTTC-3′. Fold change in mRNA expression was calculated with the comparative cycle method ($2^{-\Delta\Delta Ct}$) and normalized to the housekeeping gene *GAPDH*.

Western Blotting Analysis and ELISA

PCSK9 (CY-P1037; MBL International Corporation, Woburn, MA, USA) and LDLR (1007665; Cayman Chemical, Ann Arbor, MI, USA), and GAPDH (G9545, Sigma-Aldrich, St. Louis, MO, USA) antibodies were used for immunoblotting of lysates prepared from HepG2 cells transfected with miRNA mimics. Protein bands were visualized using the Odyssey Infrared Imaging System (LI-COR Biosciences, Lincoln, NE, USA). Densitometry analysis of the gels was carried out using ImageJ software from the National Institutes of Health (NIH) (http://rsbweb.nih.gov/ij/). To measure secreted PCSK9 levels,

HepG2 cells were transfected with miRNA mimics and incubated in DMEM containing 5% lipoprotein-deficient serum. After 24 h, the culture medium was collected and centrifuged to remove cellular debris. Cell supernatants were assayed by human PCSK9 Quantikine Enzyme-Linked Immunosorbent Assay (R&D Systems, Minneapolis, MN, USA).

Immunofluorescence Microscopy

HepG2 cells constitutively expressing LDLR-GFP were obtained from Peter Tontonoz (University of California, Los Angeles). Cells were resuspended in 10% lipoprotein-deficient serum (LPDS), plated in chamber slides (LabTekII; Thermo Fisher Scientific) and transfected with miRNA mimics (80 nM, Dharmacon) using Lipofectamine® RNAi MAX (Invitrogen). After 48 h, the cells were washed and fixed with 4% paraformaldehyde and stained with DAPI nuclear stain (D-9542, Sigma-Aldrich) for 10 min. After washing, cells were mounted with coverslips using mounting medium for fluorescence (H-1000; Vector Laboratories Inc., Burlingame, CA, USA). Fluorescent images were collected with an LSM 510 confocal laser-scanning microscope (Carl Zeiss, Oberkochen, Germany) with 63 × /1.4 oil objective. The frame size was 1,024 × 1,024. The manufacturer's software was used for data acquisition and ImageJ for fluorescence profiles. The weighted colocalization coefficients were calculated using AIM (Carl Zeiss). The cells were visualized with an Axiovert 25 (Carl Zeiss) with a 10 × /0.25 or 32 × /0.40 objective.

Statistical Analysis

Screen data were analyzed using SSMDs of percent of control, Z-score, and $\log(N^{well}/N^{plate.avg})$, where N represents firefly luciferase reporter activity divided by renilla luciferase activity in the corresponding well and $N^{plate.avg}$ represents the average firefly reporter activity normalized to renilla luciferase control for the whole plate. The SSMD values were averaged and ranked across the entire screen. Validation data are presented as mean ± standard error of the mean (s.e.m) (n is noted in the figure legends). Statistical significance of differences was evaluated with an unpaired two-sided Student's t-test or one-way ANOVA (as indicated in the figure legends). Significance was accepted at the level of $p < 0.05$. Data analysis was performed using GraphPad Prism Software (GraphPad, La Jolla, CA, USA).

RESULTS

A High-Throughput Screen Identifies MicroRNA Modulators of Human PCSK9

To identify putative miRNA candidates controlling the expression of human *PCSK9*, we conducted an unbiased screen for human miRNAs, which could modulate the activity of a firefly luciferase reporter vector harboring the 3′-UTR of *PCSK9*. The experimental design of the high-throughput 384-well based primary screen is shown in **Figure 1A**. HEK-293T cells were co-transfected with the human *PCSK9* 3′-UTR-luciferase reporter and a renilla luciferase control plasmid, along with a library of human miRNA mimics. Each plate included negative (miR-scramble, miR-Neg, eGFP, Cy3, and miR-21) and positive (miR-224) control wells. Forty-eight hours after transfection, firefly and renilla luciferase activities were measured in each well, and normalized firefly luciferase activities were ranked using SSMDs of percent of control and log values, relative to plate averages (**Figure 2A**). Approximately 100 microRNAs with composite scores of <-1 were identified as positive hits in the assay, indicating strong targeting of the 3′-UTR of *PCSK9* by these miRNAs (blue dots, **Figure 2B**, **Supplementary Table 1**). Corroborating the screen's robustness, we identified previously characterized miRNA modulators of *PCSK9*, including miR-191 and miR-224 (18, 19), as potent inhibitors of *PCSK9* 3′-UTR-luciferase activity (**Figure 3A**).

By integrating the miRNA screen results with target prediction algorithms to confirm *PCSK9* targeting (**Supplementary Figure 1**), we identified 35 miRNAs for secondary screening using larger-format 24-well plate luciferase activity assays. As in the primary assay, HEK-293T cells were co-transfected with the human *PCSK9* 3′-UTR luciferase reporter, control renilla luciferase plasmid, and miRNA mimics or control; and luciferase activity was measured 48 h later. Of the 35 miRNAs identified in the primary screen, all were confirmed to reduce *PCSK9* 3′-UTR luciferase activity by 25% or greater, with 30/35 miRNAs reducing luciferase activity by more than 50% (**Figure 3A**). The top 10 miRNAs, which were found to repress *PCSK9* 3′-UTR luciferase activity by more than 80%, and the positive control miRNA miR-224 (19) were selected for further functional screening in hepatic cells. The full experimental design is summarized in **Figure 1B**.

Endogenous RNA and Protein PCSK9 Are Altered by MicroRNAs Unveiled in Initial Screens

Mapping of the binding sites of top 10 *PCSK9*-targeting miRNAs to its 3′-UTR showed that eight of these had two or more predicted binding sites within the 3′-UTR (miR-221-5p, miR-342-5p, miR-363-5p, miR-491, miR-609, miR-646, miR-650, and miR-3689), as did the positive control miRNA miR-224. This analysis identified hot spots for predicted miRNA binding clustering near both the 5′ and 3′ ends of the UTR (**Figure 3B**). To test the functionality of these binding sites in regulating endogenous PCSK9 expression, we transfected HepG2 cells with miR-mimics for each of the 11 miRNA candidates or a control miRNA, and we measured *PCSK9* mRNA by qRT-PCR and protein levels by Western blotting. Mimics for miR-224, miR-221, miR-342, miR-363, miR-491, miR-609, miR-765, miR-3165, and miR-3689 significantly decreased *PCSK9* mRNA levels, as compared with control mimic (**Figure 3C**). Despite the presence of three putative binding sites for miR-646 and two putative binding sites for miR-650 in the *PCSK9* 3′-UTR, overexpression of these miRNAs did not reduce *PCSK9* mRNA levels in HepG2 cells. Analysis of total cellular PCSK9 protein by Western blotting showed that miR-224, miR-221, miR-342, miR-363, miR-609, miR-646, miR-650, miR-765, and miR-3165 significantly reduced PCSK9 protein levels as compared with control mimic (**Figure 4A**). Interestingly, while mimics for miR-646 and miR-650 showed no effect on the mRNA levels of *PCSK9*,

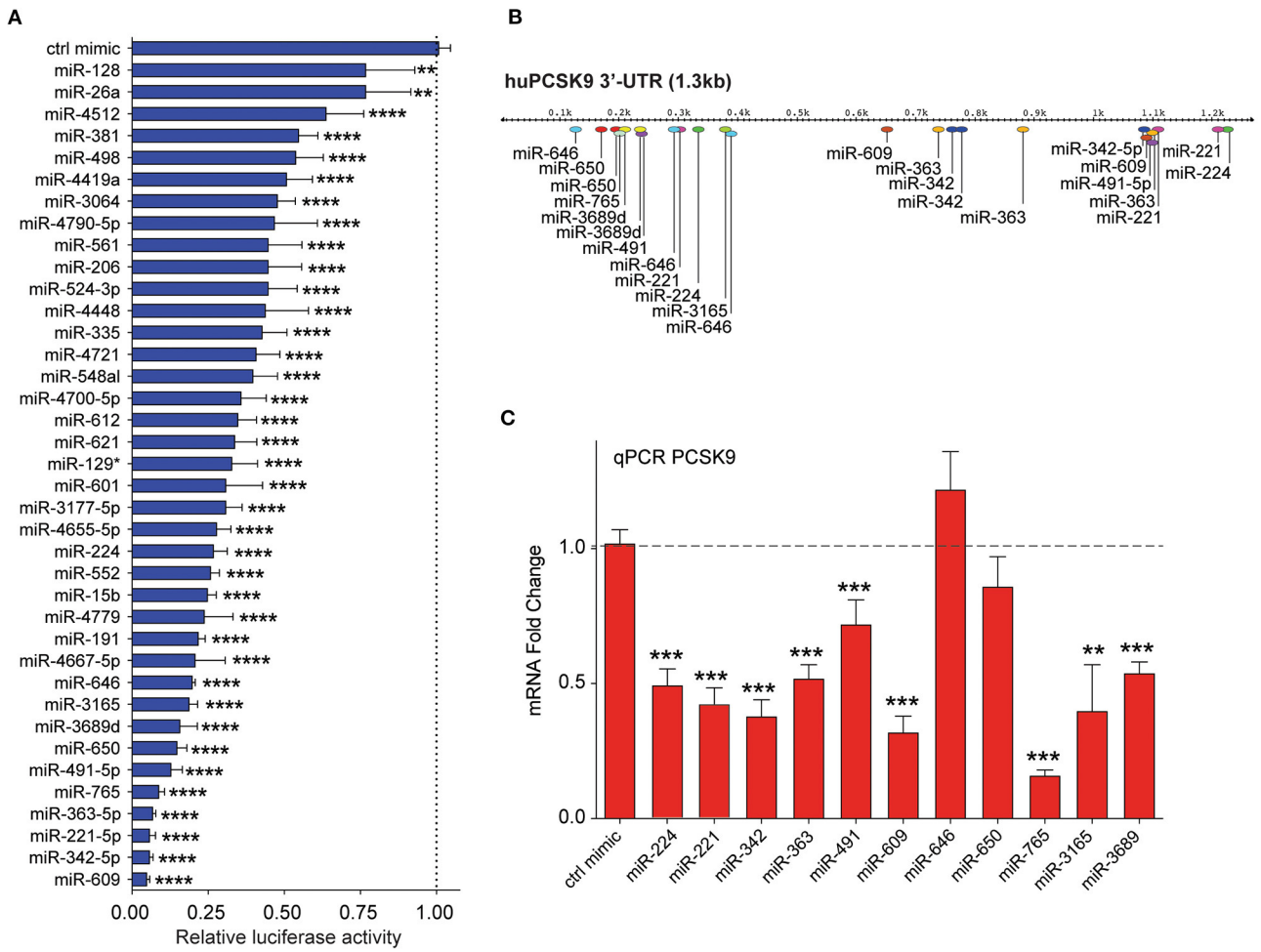

FIGURE 3 | Secondary screening of top miRNA candidates targeting human *PCSK9*. **(A)** Relative luciferase activity of *PCSK9* 3′-UTR luciferase reporter construct in HEK-293T cells transfected with miRNA mimics for the top 35 hits identified from the primary screen. MiR-224 was included as a positive control. Data are presented as percent of control mimic ± standard deviation of three independent experiments. **(B)** Alignment of miRNA binding sites for the top 10 candidate miRNAs on the human *PCSK9* 3′-UTR. **(C)** qRT-PCR analysis of *PCKS9* expression in HepG2 cells transfected with the top 10 candidate miRNAs or control mimic. Data are the mean ± standard deviation from three independent experiments. *p*-Values were calculated by one-way ANOVA and corrected for multiple comparison by Dunnet's *post-hoc* test **(A)** or a two-tailed Student's *t*-test **(C)**. $^{*}p < 0.05$, $^{**}p < 0.01$, $^{***}p < 0.001$, $^{****}p < 0.0001$.

they decreased PCSK9 protein levels by 40 and 25%, respectively (**Figure 4A**), suggesting that binding of miR-646 and miR-650 to the 3′-UTR of *PCSK9* may lead to repression of mRNA translation, but not to degradation of the *PCSK9* transcript.

As PCSK9 is secreted by hepatocytes and modulates cell surface expression of LDLR by binding to the extracellular portion of the receptor, we next measured the effects of the top 10 miRNA candidates on soluble PCSK9 elaborated by HepG2 cells. We treated HepG2 cells with control or miRNA mimics and collected cell culture supernatants 24 h later for analysis by ELISA. Significant reductions in soluble PCSK9 were observed in HepG2 cells expressing miR-224, miR-221, miR-342, miR-363, miR-609, miR-646, and miR-765 compared with control mimics (**Figure 4B**). Consistent with our Western blotting results showing that miR-491 and miR-3689 did not significantly reduce total cellular PCSK9 protein levels in HepG2 (**Figure 4A**), these miRNAs also failed to reduce PCSK9 secretion by HepG2 cells (**Figure 4B**). Collectively, these results identify miR-221, miR-342, miR-363, miR-609, miR-646, miR-765, and miR-3165 as novel regulators of PCSK9.

PCSK9-Targeting MicroRNAs Regulate Low-Density Lipoprotein Receptor Protein Expression and Cellular Distribution

As PCSK9 can bind to the LDLR and promote its degradation, we next tested whether the PCSK9-targeting miRNAs could alter total LDLR expression in HepG2 cells. We transfected HepG2 cells with the top 10 miRNAs identified in our screen or positive (miR-224) and negative (control mimic) control miRNAs, and we measured cellular LDLR protein by Western blotting analysis. Transfection of mimics for miR-224, miR-342, miR-363, miR-491, miR-609, and miR-3165 increased LDLR protein levels

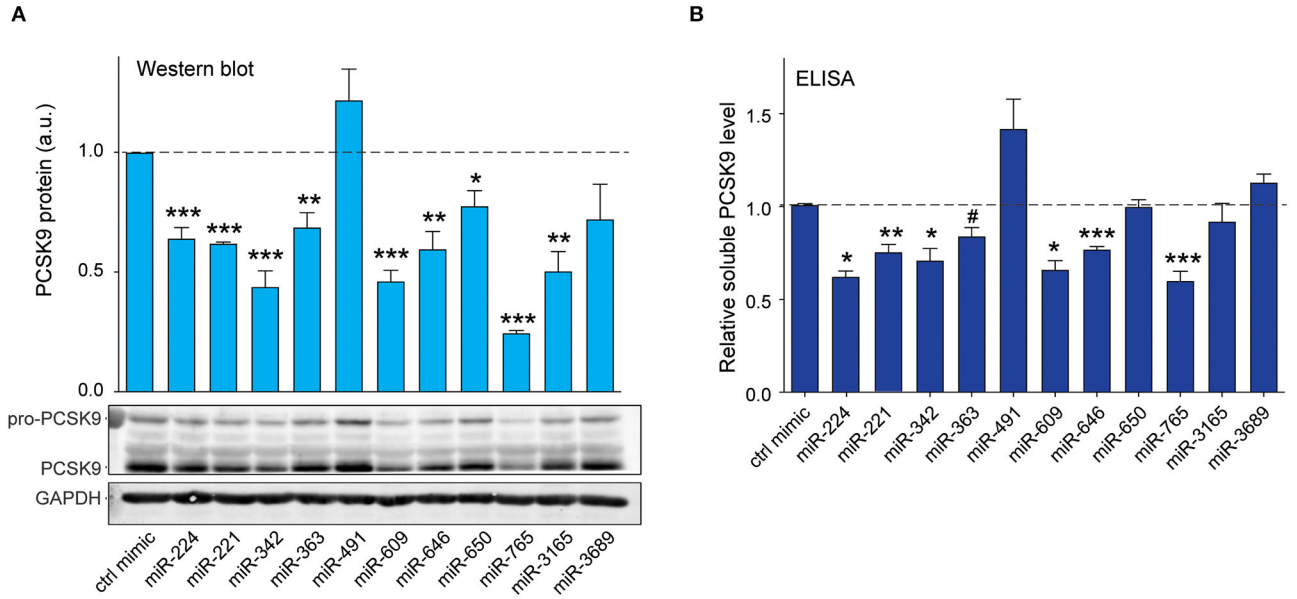

FIGURE 4 | Validation of top 10 candidate miRNAs targeting human PCSK9. **(A)** Western blotting analysis of PCSK9 and GAPDH protein in HepG2 cells transfected with miRNA mimics or a control mimic. Relative quantification of three independent experiments is shown above the blots. **(B)** ELISA quantification of secreted PCSK9 in supernatants derived from HepG2 cells transfected with miRNA mimics or a control mimic. **(A,B)** Data are the mean ± standard error of the mean from three independent experiments. *p*-Values were calculated using two-tailed Student's *t*-test. $^{\#}p < 0.1$, $^{*}p < 0.05$, $^{**}p < 0.01$, $^{***}p < 0.001$.

compared with control mimics (**Figure 5A**). Next, to understand whether these *PCSK9*-targeting miRNAs affect LDLR cell surface expression, we used HepG2 cells stably expressing a GFP-tagged LDLR (HepG2-LDLR-GFP). The LDLR-GFP transgene does not contain the native LDLR 3′-UTR and thus cannot be directly targeted by the miRNA mimics. Transfection of HepG2-LDLR-GFP cells with miR-224, miR-363, miR-491, and miR-3165 increased both whole cell fluorescence and membrane-specific expression of LDLR-GFP when compared with control mimics (**Figures 5B–D**). Similar trends in LDLR-GFP upregulation were observed with miR-221 and miR-609, but the increase did not reach statistical significance (**Figures 5B–D**).

Previous studies from our group showed that in addition to PCSK9, miR-224 targets two additional genes known to modulate LDLR abundance (19): *IDOL*, the chaperone protein that mediates proteasomal degradation of the LDLR (23), and *HMGCR*, the rate-limiting enzyme in cholesterol biosynthesis (4). Interestingly, bioinformatics analysis of the top miRNA hits from our screen showed that 9/35 miRNAs were predicted to target *PCSK9*, *IDOL*, and *HMGCR*, while 6/35 were predicted to target *PCSK9* and *HMGCR* (**Figure 6A**). Included among those miRNAs predicted to repress multiple targets involved in LDLR regulation were four from our top 10 list: miR-221, miR-363, miR-609, and miR-765. To investigate whether our top 10 miRNA candidates also regulate *HMGCR* or *IDOL* expression, we transfected HepG2 cells with miRNA mimics and measured mRNA levels of these genes by qPCR. We observed significant downregulation of *HMGCR* mRNA by miRNA-224, miR-221, miR-342, miR-363, miR-646, miR-765, and miR-3165 when compared with control mimics (**Figure 6B**). By contrast, only two miRNAs, miR-224 and miR-765, reduced *IDOL* mRNA levels in HepG2 cells (**Figure 6C**). Collectively, these data suggest that miR-221, miR-342, miR-363, and miR-3165 may alter hepatic expression of the LDLR by dual targeting of *PCSK9* and *HMGCR* (**Figure 6D**).

DISCUSSION

The discovery that loss-of-function mutations in PCSK9 are associated with lifelong low cholesterol levels and protection from ASCVD sparked intense efforts to develop inhibitors of this circulating protein (7). The first approved PCSK9 inhibitors, human monoclonal antibodies that bind extracellular PCSK9, show remarkable efficacy in reducing LDL-C either as monotherapy (50% reduction) or in combination with a statin (70% reduction) (24). Although highly effective, these monoclonal antibodies require injections every 2–4 weeks, and additional approaches for PCSK9 inhibition are being actively pursued (25). MiRNAs have emerged as exciting new therapeutic targets for manipulation of metabolic pathways, including cholesterol homeostasis (26). In this study, we used a high-throughput screening strategy to identify miRNA regulators of human PCSK9. Using a screening pipeline of 3′-UTR-reporter assays, followed by expression and validation assays, we identify seven novel miRNAs targeting *PCSK9*: hsa-miR-221-5p, hsa-miR-342-5p, hsa-miR-363-5p, hsa-miR-609, hsa-miR-646, hsa-miR-765, and hsa-miR-3165. Furthermore, using measurements of whole cell LDLR protein and a fluorescent LDLR-GFP cell line, we show that miR-221, miR-342, miR-363, and miR-3165 can heighten expression of the LDLR in hepatic cells, validating the effects of these miRNAs in short-circuiting the

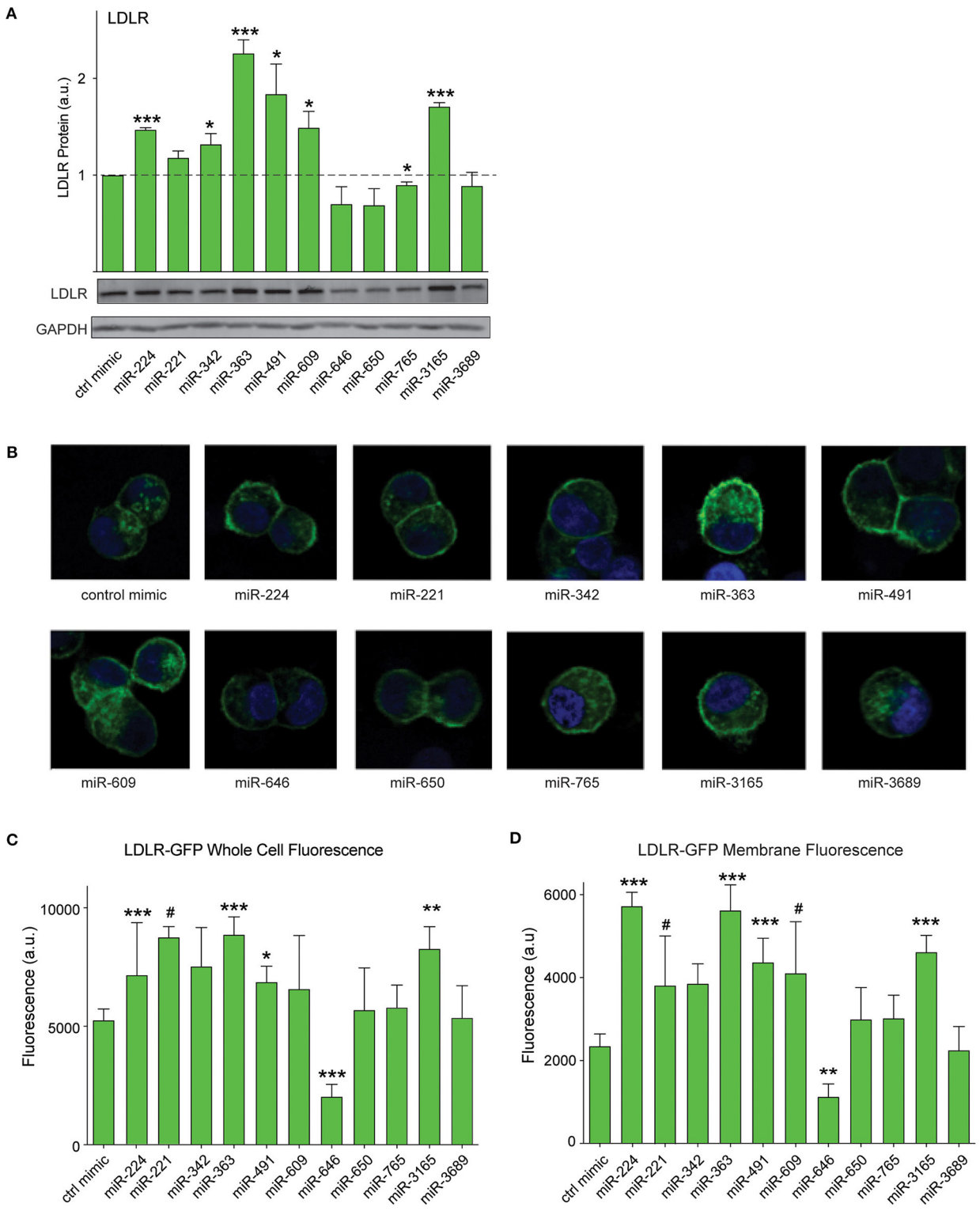

FIGURE 5 | PCSK9-targeting miRNAs regulate hepatic low-density lipoprotein receptor (LDLR) expression. **(A)** Western blotting analysis of LDLR and GAPDH protein in HepG2 cells transfected with miRNA mimics or a control mimic. Relative quantification of three independent experiments (mean ± standard error of the mean) is shown above the blots. **(B)** Representative fluorescent images of HepG2 cells stably expressing LDLR-GFP (green) transfected with miRNAs mimics or a control miR mimic. Counterstaining with DAPI to visualize nucleus (blue). **(C,D)** Quantification of **(C)** whole cell or **(D)** cell surface LDLR-GFP fluorescence intensity in HepG2 cells transfected with miRNA mimics or a control miR mimic. Data are representative of three independent experiments. *p*-Values were calculated using two-tailed Student's *t*-test. $^{\#}p < 0.1$, $^{*}p < 0.05$, $^{**}p < 0.01$, $^{***}p < 0.001$.

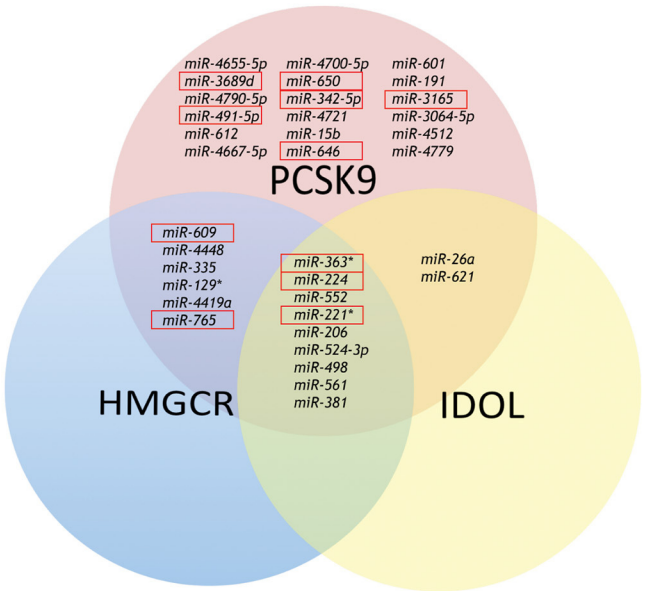

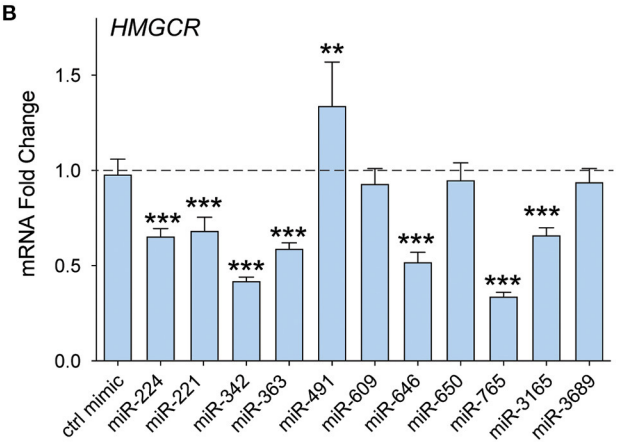

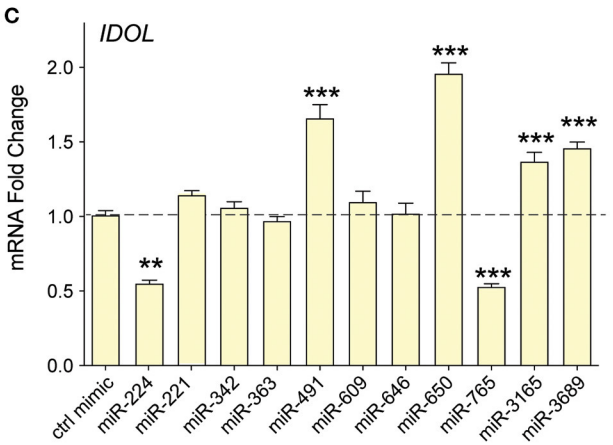

D

up regulation
down regulation

		miR-224	miR-221	miR-342	miR-363	miR-491	miR-609	miR-646	miR-650	miR-765	miR-3165	miR-3689
PCSK9	RNA	●	●	●	●	●	●			●	●	●
	protein	●	●	●	●		●	●	●	●	●	
	secreted protein	●	●	●	●		●	●		●		
LDLR	protein	●		●	●	●	●			●	●	
	cellular expression	●			●	●		●			●	
	membrane expression	●			●	●		●			●	
Other targets	*HMGCR*	●	●	●	●	●		●		●	●	
	IDOL	●				●			●	●	●	●

FIGURE 6 | Common targeting of genes involved in low-density lipoprotein (LDL) receptor regulation by candidate miRNAs. **(A)** Venn diagram of the top 35 miRNAs identified to repress *PCSK9* showing overlapping targeting of *HMGCR* and *IDOL*. The top 10 miRNAs validated for PCSK9 targeting are shown in the red boxes. **(B,C)** qRT-PCR analysis of **(B)** *HMGCR* and **(C)** *IDOL* mRNA in HepG2 cells transfected with the top 10 candidate miRNA mimics or a control miR mimic. Data are the mean ± standard error of the mean from three independent experiments. *p*-Values were calculated using two-tailed Student's *t*-test. $^{**}p < 0.01$, $^{***}p < 0.001$. **(D)** Table summarizing the effects for the top 10 miRNAs targeting PCSK9. Red and blue dots represent significant upregulation or downregulation, respectively.

effect of PCSK9 on endosomal LDLR recycling. Notably, miR-221, miR-342, miR-363, and miR-3165 were also identified to repress *HMGCR*, which would be expected to trigger SREBP-mediated upregulation of LDLR expression, thereby reinforcing the effects of PCSK9 inhibition. Such miRNAs, which simultaneously target multiple genes involved in regulating

LDLR cell surface expression, may offer greater therapeutic potential for regulating LDL-C.

Although the development of PCSK9 inhibitors has moved at an unprecedented pace, there is still much to learn about PCSK9 regulation and biology. At the transcriptional level, PCSK9 has been shown to be regulated by an SRE motif within its promoter (27, 28). Depletion of intracellular cholesterol levels causes translocation of the SREBP transcription factor to the nucleus and transcriptional upregulation of genes involved in cholesterol synthesis and uptake, such as LDLR. Paradoxically, SREBP also upregulates PCSK9, which blunts cholesterol uptake through the LDLR by causing its internalization (29, 30). This is particularly relevant in the setting of statin treatment, where SREBP-mediated upregulation of PCSK9 attenuates LDL-C lowering (29, 30) and why combination therapies of PCSK9 inhibitors with statins are attractive for optimal lipid lowering. In addition to SREBP, the hepatic nuclear factor 1alpha (HNF1α) and peroxisome proliferator-activated receptor gamma (PPARγ) have been shown to contribute to transcriptional regulation of PCSK9 (31, 32). By contrast, relatively little is known about the posttranscriptional mechanisms regulating PCSK9. Previous studies have identified roles for various miRNAs, including miR-224, miR-191, miR-222, miR-483, and miR-520d, in inhibiting the expression and function of PCSK9 in human or murine hepatocytes (17–20), but to our knowledge, this is the first study to perform a systematic screen of miRNAs targeting the human *PCSK9* 3′-UTR. Of the top 35 miRNAs selected for secondary screening, 10 were selected for further validation. Although all 10 miRNAs showed potent repressive effects on the activity of a *PCSK9* 3′-UTR-luciferase reporter (>75%), only seven of these were confirmed to reduce PCSK9 mRNA and/or protein in hepatic HepG2 cells: miR-221, miR-342, miR-363, miR-609, miR-646, miR-765, and miR-3165. Notably, none of these miRNAs have previously been shown to target PCSK9, highlighting the utility of such a screen in identifying novel posttranscriptional regulators of genes of interest.

Therapeutically, the most interesting miRNAs would be ones that not only repress PCSK9 secretion but also show efficacy in upregulating hepatic LDLR surface expression. In that category, miR-221, miR-342, miR-363, and miR-3165 were the most promising candidates. Interestingly, miR-221, miR-342, and miR-363 are each predicted to have three miRNA binding sites within the *PCSK9* 3′-UTR, including sites clustered near the 3′ end of the UTR. To date, no studies have reported links between miR-221 or miR-363 and cholesterol metabolism. However, a recent report showed that miR-342 is upregulated following viral infection and induces a coordinate reduction in the abundance of many genes in the sterol biosynthesis pathway (33), including its master regulator *SREBF2*, as well as *HMGCR* as we showed herein. This type of pathway modulation by miRNAs provides a potent mechanism for synchronized inhibition of gene pathways (34) and also illustrates the complexity of miRNA-mediated posttranscriptional regulatory networks. Although we focused on miRNA repression of human PCSK9 in our study, targeting of PCSK9 by mmu-miR-221-5p, mmu-miR-363-5p, and mmu-miR-342-5p is conserved in mice, which would allow future *in vivo* studies of these miRNAs in mice. Such studies would provide information on whether miR-221, miR-363, and miR-342 targeting of hepatic PCSK9 expression is conserved in mice and whether these miRNAs alter plasma levels of LDL-C.

RNA-based therapeutics against PCSK9 hold promise as alternatives to monoclonal antibody therapy, which requires frequent dosing. Although no miRNA-based therapies are currently in the pipeline, a synthetic siRNA directed against PCSK9, inclisiran, is in advanced stages of development. Inclisiran engages the endogenous RNA interference (RNAi) pathway by binding to the RNA-induced silencing complex (RISC) and enabling cleavage of the *PCSK9* mRNA (35). One potential advantage of this approach, which would also be shared by miRNA-based therapeutics, is that it inhibits the intracellular production of PCSK9 prior to its secretion. Whereas monoclonal antibodies cause significant accumulation of PCSK9-bound antibodies, siRNA- or miRNA-mediated knockdown of *PCSK9* reduces protein production by hepatocytes, similar to what is observed with PCSK9 loss-of-function mutations. Synthetic RNAs can also be conjugated to triantennary *N*-acetylgalactosamine carbohydrates to enhance hepatic uptake via asialoglycoprotein receptors and show an extended duration of action. Indeed, in Phase II clinical trials, two doses of inclisiran resulted in profound suppression of PCSK9 and LDL-C for at least 6 months (24). The success of this siRNA-based therapy reflects the remarkable improvements in the safety and efficacy of RNA-targeted treatment approaches over the last decade and suggests that miRNA-based therapies might not be far behind.

DATA AVAILABILITY STATEMENT

The data that support the findings of this study are available from the corresponding author upon request. The datasets presented in this study can be found in online repositories and are available at the Gene Expression Omnibus (GEO) under accession number GSE166680.

AUTHOR CONTRIBUTIONS

KM, SO, and CvS designed the study, guided the interpretation of the results, and prepared the manuscript, with input from all authors. SO, AS, and AW performed experiments and data analyses. All authors contributed to the article and approved the submitted version.

FUNDING

This work was supported by grants from the National Institutes of Health [R35HL135799 (KM), T32HL098129 (CvS)] and the American Heart Association (19CDA346300066 to CvS).

SUPPLEMENTARY MATERIAL

The Supplementary Material for this article can be found online at: https://www.frontiersin.org/articles/10.3389/fcvm.2021.667298/full#supplementary-material

REFERENCES

1. Goedeke L, Fernandez-Hernando C. Regulation of cholesterol homeostasis. *Cell Mol Life Sci.* (2012) 69:915–30. doi: 10.1007/s00018-011-0857-5
2. Cohen JD. Rationale for aggressive lipid lowering in high-risk patients. *J Am Osteopath Assoc.* (2011) 111:eS7–12.
3. Goldstein JL, Brown MS. A century of cholesterol and coronaries: from plaques to genes to statins. *Cell.* (2015) 161:161–72. doi: 10.1016/j.cell.2015.01.036
4. Endo A, Kuroda M, Tanzawa K. Competitive inhibition of 3-hydroxy-3-methylglutaryl coenzyme A reductase by ML-236A and ML-236B fungal metabolites, having hypocholesterolemic activity. *FEBS Lett.* (1976) 72:323–6. doi: 10.1016/0014-5793(76)80996-9
5. Yokoyama C, Wang X, Briggs MR, Admon A, Wu J, Hua X, et al. SREBP-1, a basic-helix-loop-helix-leucine zipper protein that controls transcription of the low density lipoprotein receptor gene. *Cell.* (1993) 75:187–97. doi: 10.1016/S0092-8674(05)80095-9
6. Goldstein JL, Brown MS. The LDL receptor. *Arterioscler Thromb Vasc Biol.* (2009) 29:431–8. doi: 10.1161/ATVBAHA.108.179564
7. Shapiro MD, Tavori H, Fazio S. PCSK9: from basic science discoveries to clinical trials. *Circ Res.* (2018) 122:1420–38. doi: 10.1161/CIRCRESAHA.118.311227
8. Abifadel M, Varret M, Rabès JP, Allard D, Ouguerram K, Devillers M, et al. Mutations in PCSK9 cause autosomal dominant hypercholesterolemia. *Nat Genet.* (2003) 34:154–6. doi: 10.1038/ng1161
9. Cohen JC, Boerwinkle E, Mosley TH Jr, Hobbs HH. Sequence variations in PCSK9, low LDL, and protection against coronary heart disease. *N Engl J Med.* (2006) 354:1264–72. doi: 10.1056/NEJMoa054013
10. Kathiresan S, Myocardial Infarction Genetics Consortium. A PCSK9 missense variant associated with a reduced risk of early-onset myocardial infarction. *N Engl J Med.* (2008) 358:2299–300. doi: 10.1056/NEJMc0707445
11. Cohen J, Pertsemlidis A, Kotowski IK, Graham R, Garcia CK, Hobbs HH. Low LDL cholesterol in individuals of African descent resulting from frequent nonsense mutations in PCSK9. *Nat Genet.* (2005) 37:161–5. doi: 10.1038/ng1509
12. Crunkhorn S. Trial watch: PCSK9 antibody reduces LDL cholesterol. *Nat Rev Drug Discov.* (2012) 11:11. doi: 10.1038/nrd3633
13. Gebert LFR, MacRae IJ. Regulation of microRNA function in animals. *Nat Rev Mol Cell Biol.* (2019) 20:21–37. doi: 10.1038/s41580-018-0045-7
14. Ambros V. The functions of animal microRNAs. *Nature.* (2004) 431:350–5. doi: 10.1038/nature02871
15. Filipowicz W, Bhattacharyya SN, Sonenberg N. Mechanisms of post-transcriptional regulation by microRNAs: are the answers in sight? Nature reviews. *Genetics.* (2008) 9:102–14. doi: 10.1038/nrg2290
16. Bartel DP. MicroRNAs: target recognition and regulatory functions. *Cell.* (2009) 136:215–33. doi: 10.1016/j.cell.2009.01.002
17. Dong J, He M, Li J, Pessentheiner A, Wang C, Zhang J, et al. microRNA-483 ameliorates hypercholesterolemia by inhibiting PCSK9 production. *JCI Insight.* (2020) 5:e143812. doi: 10.1172/jci.insight.143812
18. Naeli P, Mirzadeh Azad F, Malakootian M, Seidah NG, Mowla SJ. Post-transcriptional regulation of PCSK9 by miR-191, miR-222, and miR-224. *Front Genet.* (2017) 8:189. doi: 10.3389/fgene.2017.00189
19. Salerno AG, Van Solingen C, Scotti E, Wanschel AC, Afonso MS, Oldebeken SR, et al. LDL receptor pathway regulation by miR-224 and miR-520d. *Front Cardiovasc Med.* (2020) 7:81. doi: 10.3389/fcvm.2020.00081
20. Bai JA, Na H, Hua X, Wei Y, Ye T, Zhang Y, et al. A retrospective study of NENs and miR-224 promotes apoptosis of BON-1 cells by targeting PCSK9 inhibition. *Oncotarget.* (2017) 8:6929–39. doi: 10.18632/oncotarget.14322
21. Zelcer N, Hong C, Boyadjian R, Tontonoz P. LXR regulates cholesterol uptake through Idol-dependent ubiquitination of the LDL receptor. *Science.* (2009) 325:100–4. doi: 10.1126/science.1168974
22. Zhang XD. A new method with flexible and balanced control of false negatives and false positives for hit selection in RNA interference high-throughput screening assays. *J Biomol Screen.* (2007) 12:645–55. doi: 10.1177/1087057107300645
23. Hong C, Marshall SM, McDaniel AL, Graham M, Layne JD, Cai L, et al. The LXR-Idol axis differentially regulates plasma LDL levels in primates and mice. *Cell Metab.* (2014) 20:910–8. doi: 10.1016/j.cmet.2014.10.001
24. Katzmann JL, Gouni-Berthold I, Laufs U. PCSK9 inhibition: insights from clinical trials and future prospects. *Front Physiol.* (2020) 11:595819. doi: 10.3389/fphys.2020.595819
25. Warden BA, Fazio S, Shapiro MD. The PCSK9 revolution: current status, controversies, and future directions. *Trends Cardiovasc Med.* (2020) 30:179–185. doi: 10.1016/j.tcm.2019.05.007
26. Feinberg MW, Moore KJ. MicroRNA regulation of atherosclerosis. *Circ Res.* (2016) 118:703–20. doi: 10.1161/CIRCRESAHA.115.306300
27. Costet P, Cariou B, Lambert G, Lalanne F, Lardeux B, Jarnoux AL, et al. Hepatic PCSK9 expression is regulated by nutritional status via insulin and sterol regulatory element-binding protein 1c. *J Biol Chem.* (2006) 281:6211–8. doi: 10.1074/jbc.M508582200
28. Jeong HJ, Lee HS, Kim KS, Kim YK, Yoon D, Park SW. Sterol-dependent regulation of proprotein convertase subtilisin/kexin type 9 expression by sterol-regulatory element binding protein-2. *J Lipid Res.* (2008) 49:399–409. doi: 10.1194/jlr.M700443-JLR200
29. Dubuc G, Chamberland A, Wassef H, Davignon J, Seidah NG, Bernier L, et al. Statins upregulate PCSK9, the gene encoding the proprotein convertase neural apoptosis-regulated convertase-1 implicated in familial hypercholesterolemia. *Arterioscler Thromb Vasc Biol.* (2004) 24:1454–9. doi: 10.1161/01.ATV.0000134621.14315.43
30. Welder G, Zineh I, Pacanowski MA, Troutt JS, Cao G, Konrad RJ. High-dose atorvastatin causes a rapid sustained increase in human serum PCSK9 and disrupts its correlation with LDL cholesterol. *J Lipid Res.* (2010) 51:2714–21. doi: 10.1194/jlr.M008144
31. Dong B, Wu M, Li H, Kraemer FB, Adeli K, Seidah NG, et al. Strong induction of PCSK9 gene expression through HNF1alpha and SREBP2: mechanism for the resistance to LDL-cholesterol lowering effect of statins in dyslipidemic hamsters. *J Lipid Res.* (2010) 51:1486–95. doi: 10.1194/jlr.M003566
32. Li H, Dong B, Park SW, Lee HS, Chen W, Liu J. Hepatocyte nuclear factor 1alpha plays a critical role in PCSK9 gene transcription and regulation by the natural hypocholesterolemic compound berberine. *J Biol Chem.* (2009) 284:28885–95. doi: 10.1074/jbc.M109.052407
33. Robertson KA, Hsieh WY, Forster T, Blanc M, Lu H, Crick PJ, et al. An interferon regulated microRNA provides broad cell-intrinsic antiviral immunity through multihit host-directed targeting of the sterol pathway. *PLoS Biol.* (2016) 14:e1002364. doi: 10.1371/journal.pbio.1002364
34. Selbach M, Schwanhäusser B, Thierfelder N, Fang Z, Khanin R, Rajewsky N. Widespread changes in protein synthesis induced by microRNAs. *Nature.* (2008) 455:58–63. doi: 10.1038/nature07228
35. Sinning D, Landmesser U. Low-density lipoprotein-cholesterol lowering strategies for prevention of atherosclerotic cardiovascular disease: focus on siRNA treatment targeting PCSK9 (Inclisiran). *Curr Cardiol Rep.* (2020) 22:176. doi: 10.1007/s11886-020-01427-6

Conflict of Interest: The authors declare that the research was conducted in the absence of any commercial or financial relationships that could be construed as a potential conflict of interest.

frontiers in Cardiovascular Medicine

ORIGINAL RESEARCH
published: 13 August 2021
doi: 10.3389/fcvm.2021.663832

miR-135b-3p Promotes Cardiomyocyte Ferroptosis by Targeting GPX4 and Aggravates Myocardial Ischemia/Reperfusion Injury

Weixin Sun[1,2,3], *Ruijie Shi*[2,3], *Jun Guo*[2,3], *Haiyan Wang*[2,3], *Le Shen*[2], *Haibo Shi*[2,4], *Peng Yu*[2,3*†] *and Xiaohu Chen*[2,3*†]

[1] Department of Cardiology, Yancheng TCM Hospital Affiliated to Nanjing University of Chinese Medicine, Yancheng, China, [2] Department of Cardiology, Jiangsu Province Hospital of Chinese Medicine, Affiliated Hospital of Nanjing University of Chinese Medicine, Nanjing, China, [3] First Clinical Medical College, Nanjing University of Chinese Medicine, Nanjing, China, [4] Department of Cardiology, Liyang City Hospital of TCM, Changzhou, China

OPEN ACCESS

Edited by:
En-zhi Jia,
Nanjing Medical University, China

Reviewed by:
Owais Bhat,
Virginia Commonwealth University, United States
Julie Pires Da Silva,
University of Colorado Anschutz Medical Campus, United States

***Correspondence:**
Peng Yu
yupengdoctor@126.com
Xiaohu Chen
yfy0007@njucm.edu.cn

†These authors have contributed equally to this work

Specialty section:
This article was submitted to General Cardiovascular Medicine, a section of the journal Frontiers in Cardiovascular Medicine

Received: *03 February 2021*
Accepted: *14 July 2021*
Published: *13 August 2021*

Citation:
Sun W, Shi R, Guo J, Wang H, Shen L, Shi H, Yu P and Chen X (2021) miR-135b-3p Promotes Cardiomyocyte Ferroptosis by Targeting GPX4 and Aggravates Myocardial Ischemia/Reperfusion Injury. Front. Cardiovasc. Med. 8:663832. doi: 10.3389/fcvm.2021.663832

Ferroptosis is a form of cell death induced by excess iron and accumulation of reactive oxygen species in cells. Recently, ferroptosis has been reported to be associated with cancer and ischemia/reperfusion (I/R) injury in multiple organs. However, the regulatory effects and underlying mechanisms of myocardial I/R injury are not well-understood. The role of miR-135b-3p as an oncogene that accelerates tumor development has been confirmed; however, its role in myocardial I/R is not fully understood. In this study, we established an *in vivo* myocardial I/R rat model and an *in vitro* hypoxia/reoxygenation (H/R)-induced H9C2 cardiomyocyte injury model and observed that ferroptosis occurred in tissues and cells during I/R myocardial injury. We used database analysis to find miR-135b-3p and validated its inhibitory effect on the ferroptosis-related gene glutathione peroxidase 4 (*Gpx4*), using a luciferase reporter assay. Furthermore, miR-135b-3p was found to promote the myocardial I/R injury by downregulating GPX4 expression. The results of this study elucidate a novel function of miR-135b-3p in exacerbating cardiomyocyte ferroptosis, providing a new therapeutic target for improving I/R injury.

Keywords: miR-135b-3p, ferroptosis, GPX4, cardiomyocyte ferroptosis, myocardial ischemia/reperfusion injury

INTRODUCTION

Cardiovascular disease is one of the leading causes of death in humans (1). Myocardial ischemia/reperfusion (I/R) may be a therapeutic approach for protecting against acute myocardial ischemic infarction (MI) (2). However, as a result of direct blood flow restoration to ischemic tissue, myocardial I/R also leads to cell death and additional cell dysfunction. For example, the primary pathological manifestation of coronary artery disease is myocardial I/R injury. Myocardial I/R injury does not recover and is involved in inflammation, calcium overload, oxidative stress, cytokine release, and neutrophil infiltration (3). Therefore, elucidation of the molecular mechanisms of myocardial I/R injury has great significance and clinical value and may provide a potential new target for clinical treatment.

The irreversible damage to the heart and brain following I/R has received much attention in recent years. Many scholars have focused their attention on ferroptosis and have confirmed through their studies that ferroptosis plays an important role in I/R injury (4–6). Ferroptosis, first proposed by Dr. Brent R. Stockwell of Columbia University in 2012, is an iron-dependent, novel form of programmed cell death that is distinct from apoptosis, necrosis, and autophagy (7). Ferroptosis occurs primarily due to the failure of the membrane lipid repair enzyme GPX4, resulting in the accumulation of lipid peroxides and reactive oxygen species (ROS) (5). Cancer cells carrying oncogenic Ras appear to be more sensitive to ferritin induction; therefore, this form of cell death has also been explored for cancer therapy (7, 8). Ferroptosis inhibitors are effective in treating other diseases, such as I/R-induced organ damage in experimental models (9, 10). For example, liproxstatin-1 inhibits ferroptosis and promotes cell survival by reducing voltage-dependent anion channel 1 (VDAC1) levels and restoring GPX4 levels to protect the mouse myocardium against I/R injury (11). The mechanistic target of rapamycin (mTOR) has protective effects against excess iron accumulation and ferroptosis in cardiomyocytes (12). Although ferroptosis is strongly implicated in human myocardial I/R injury, the precise molecular mechanisms and biological functions of ferroptosis remain poorly understood. Therefore, in this study, we conducted an in-depth study of the specific mechanisms underlying the occurrence of ferroptosis in I/R.

miRNAs are a class of endogenous non-coding small RNAs that are widely present in the body, with a length of approximately 21–22 nucleotides (13). Studies have shown that miRNAs participate in various life processes, and their abnormal expression is involved in the occurrence and development of multiple diseases, including myocardial I/R injury (14). Previous studies have shown that the presence of miRNAs can regulate cell survival in response to an I/R injury (15). The role of miRNAs in regulating ferroptosis has been reported in several types of cancer (16) but not in myocardial I/R injury. Since GPX4 plays a crucial role in the onset of ferroptosis, we hypothesized that miRNAs are involved in regulating the onset of ferroptosis by targeting GPX4. Through database analysis and experimental validation, we selected miR-135b-3p as a key target of our study and confirmed through *in vitro* and *in vivo* experiments that miR-135b-3p could promote ferroptosis by inhibiting GPX4 expression in myocardial I/R injury.

MATERIALS AND METHODS

Animal Model

Male Sprague–Dawley rats aged 8–10 weeks and weighing 220 g were obtained from the Nanjing Biomedical Research Institute of Nanjing University. All animal experiments complied with the Animal Research: Reporting *in vivo* Experiments (ARRIVE) guidelines (**Supplementary Table 1**. The ARRIVE guidelines 2.0 author checklist). The protocol was approved by the Ethics Committee of the Affiliated Hospital of the Nanjing University of Chinese Medicine. Following acclimatization for 1 week, the rats were divided into five groups of six rats each before the experiment. The establishment of the myocardial I/R model was based on previous studies (14). Sodium pentobarbital (45 mg/kg, i.p.) was used to anesthetize the rats, and the left coronary artery (LCA) was exposed using left thoracotomy at the fifth intercostal space. Following the LCA ligation with 7-0 silk sutures, a smooth catheter was applied to the artery to achieve ischemia for 30 min. The rats were then sacrificed 120 min after reperfusion. Rats in the sham group (without the LCA I/R) underwent surgery and were treated with saline. The miR-135b-3p group rats were injected with miR-135b-3p overexpression virus or knockdown lentivirus (1×10^8 U/ml, 0.2 ml), respectively, for five consecutive days before surgery. The detailed animal grouping information in this study is listed in **Supplementary Figure 1**.

Cell Culture and Establishment of the Hypoxia/Reoxygenation (H/R) Model

The rat myocardial cell line H9C2 was purchased from the Cell Resource Center of the Shanghai Academy of Sciences. H9C2 cells were cultured in DMEM supplemented with 10% fetal bovine serum and 100 units/ml of penicillin-streptomycin (MP Biomedicals). The cells were maintained in a humidified incubator containing 5% CO_2 at 37°C. When the cells reached 80% confluence, the DMEM was replaced with serum-free and sugar-free medium. The cells were then placed in a 37°C hypoxia incubator containing 95% N_2 and 5% CO_2 for 6 h (17, 18). After hypoxia, the medium was replaced with a fresh medium and refilled with air containing 5% CO_2 to establish I/R injury in cells.

Cell Treatment and Cell Transfection

H9C2 cells cultured in 100-mm plastic dishes were allowed to adhere to the plate at 37°C in 5% CO_2 for 6 h. Subsequently, cells were treated with 50 μM ferroptosis activator Erastin (MCE, China) or 1 μM ferroptosis inhibitor ferrostatin-1 (Fer-1, MCE, China) and incubated for 24 h. The cells were seeded in six-well plates at 1.0×10^5/ml. When the confluency of cells reached 60%, transfection was performed. The GPX4 overexpression plasmid, miR-135b-3p mimics, and inhibitor were purchased from Synthgene (Nanjing, China), and the transfection was performed using Lipofectamine 2000 (Thermo-Scientific, USA) according to the manufacturer's instructions.

ELISA

Rat blood was collected after reperfusion. After centrifugation at 3,000 rpm for 10 min at 4°C, 100 μl of serum was obtained. The activities of specific marker enzymes, including creatine phosphokinase (CK), lactic dehydrogenase (LDH), and cardiac troponin T (cTnT), were assessed according to the manufacturer's instructions (R&D Systems).

Iron Assay

Intracellular ferrous iron (Fe^{2+}) levels in rat myocardial tissues or H9C2 cells were measured using an iron assay kit (Abcam, USA) according to the manufacturer's instructions. Briefly, samples were collected and washed in cold PBS and then homogenized in 5X volumes of iron assay buffer on ice. The supernatant was collected, an iron reducer was added to each sample before mixing, and the samples were incubated at 25°C for 30 min.

Thereafter, an iron probe was added to each sample before mixing and incubating at 25°C for 60 min. The output was measured immediately using a colorimetric microplate reader (optical density [OD], 593 nm).

Analysis of Cell Viability

Cells were seeded in 96-well plates at a density of 2×10^3 cells/well (200 μl/well) and cultured for 24 h. Subsequently, 5 mg/ml of the 3-(4,5-dimethyl-2-thiazolyl)-2,5-diphenyl-2H-tetrazolium bromide (MTT) reagent (Sigma, USA) was added (20 μl/well) and incubated at 37°C for another 4 h. Thereafter, the medium was removed and replaced with 150 μl/well DMSO (Sigma, USA), followed by vigorous shaking at room temperature for 10 min to solubilize the dark blue formazan crystals formed. Cell viability was evaluated by measuring the optical absorbance at 490 nm (OD490) using an Elx800 enzyme immunoassay analyzer (Bio-TEK, USA). The cell viability index was calculated as the experimental OD value/control OD value.

RNA Isolation and Reverse Transcription-Quantitative PCR

Total RNA was isolated from the myocardial tissues or cultured cells using TRIzol® reagent (Thermo-Scientific, USA) and RNA was reverse transcribed to cDNA from 1 μg of total RNA using a PrimeScript RT reagent kit with gDNA Eraser (Takara, Japan) according to the manufacturer's protocol. The reaction conditions were as follows: 42°C for 2 min, 37°C for 15 min, and 85°C for 5 s. RT-PCR was performed using the SYBR green PCR kit on an Applied Biosystems 7300 sequence detection system (Applied Biosystems, USA). *U6* levels were used to normalize the relative abundance of miR-135b-3p, and *Gapdh* was used to normalize the expression of *Gpx4*, ferritin heavy chain 1 (*Fth1*), *Ascl4*, nicotinamide adenine dinucleotide phosphate oxidase 1 (*Nox1*), and cyclooxygenase 2 (*Cox2*). RT-qPCR reactions were performed in a 96-well plate at 95°C for 10 min, followed by 40 cycles of 95°C for 15 s, and 60°C for 60 s, according to the manufacturer's specifications. The primers used in this study are listed in **Supplementary Table 2**.

Western Blotting Analysis

Total protein from H9C2 cells or myocardial tissues was extracted using RIPA lysis buffer. Proteins in the samples (20 μg) were separated *via* 10% SDS-PAGE and then transferred to a polyvinylidene difluoride membrane (Millipore, USA). Membranes were then incubated with 5% non-fat milk containing 0.1% PBST for 2 h at room temperature to block nonspecific binding and incubated with primary antibodies against GPX4 (1:1,000, Abcam), FTH1 (1:1,000, Abcam), ACSL4 (1:5,000, Abcam), NOX1 (1:5,000, Abcam), COX1 (1:500, Abcam), and GAPDH (1:1,000, Abcam) at 4°C overnight, followed by incubation with goat anti-rabbit HRP-conjugated secondary antibody (1:5,000, Abcam) at room temperature for 2 h. Protein bands were visualized using an enhanced chemiluminescence kit (Synthgene, China), and GAPDH was used as an internal control for the relative protein expression. Protein bands were quantified using the ImageJ software.

Luciferase Reporter Assay

The entire 3′-UTR of *Gpx4* containing the predicted binding sites for miR-135b-3p was amplified and inserted into a luciferase reporter plasmid (Synthgene, China). To assess the binding specificity, the sequences that interacted with miR-135b-3p were mutated, and the mutant *Gpx4* 3′-UTR was inserted into an equivalent luciferase reporter plasmid. For the luciferase reporter assay, cells were plated in 24-well plates, and each well was transfected with 1 μg of luciferase reporter plasmid, 1 μg of β-galactosidase plasmid (internal control), and 100 pmol of miR-135b-3p mimic or control mimic using Lipofectamine 2000 (Thermo Fisher Scientific, USA). After 48 h, luciferase signals were measured using a luciferase assay kit according to the manufacturer's protocol (Promega Corporation, USA) (19, 20).

Hematoxylin and Eosin Staining

After excising the myocardial tissue from rats, the tissues were fixed with 4% paraformaldehyde for 24 h and paraffin embedded. Sections (4 μm) were cut and stained with HE (21).

The 2,3,5-Triphenyltetrazolium Chloride Staining Assay

At the end of 120 min of reperfusion, the hearts were collected and frozen at −20°C. Frozen hearts were cut into 1-mm sections that were incubated in 1% TTC solution at 37°C for 10 min and then fixed in 4% paraformaldehyde for 24 h. The sections were photographed using a digital camera. The infarcted areas were not stained by TTC (22, 23). The infarcted (unstained) and non-infarcted (stained) areas were measured in each section using ImageJ by a blinded investigator.

Lipid Peroxidation Assay

Cells were treated as indicated, trypsinized, and resuspended in a medium supplemented with 10% FBS. A 10 μM solution of C11-BODIPY (Thermo Fisher, USA) was added, and samples were incubated for 30 min at 37°C with 5% CO_2 and protection from light. The cells were washed twice with PBS to remove excess C11-BODIPY. The fluorescence of C11-BODIPY was measured using a fluorescence microscope (Nikon, Japan) (24).

Echocardiographic Measurements

Cardiac function and structure were assessed using the MyLab^{TM}Eight Platform (Esaote, Italy). Briefly, rats were anesthetized with isoflurane (5%) using ventilation equipment, fur was carefully removed from the left chest, and two-dimensional echocardiographic measurements were obtained. Left ventricular internal diastolic and systolic diameter (LVIDd and LVIDs, respectively) and the left ventricular ejection fraction and fractional shortening (LVEF and LVFS, respectively) were measured using M-mode tracing.

Statistical Analysis

All data are presented as the mean ± standard deviation (SD) of three independent experiments. One-way ANOVA and Duncan's multiple range tests were used to evaluate the mean differences between groups and within groups. Statistical significance was set at $p < 0.05$.

RESULTS

Ferroptosis Involved in the Process of Rat Myocardial I/R

Initially, we established a myocardial I/R injury model in rats and collected myocardial tissue and serum samples. We performed HE staining and ELISA to detect tissue structure and cardiac injury marker expression, respectively. The serum CK, LDH, and cTnT levels were significantly increased in the I/R group compared to those in the sham group (**Figure 1A**). As shown in **Figure 1B**, the myocardial cells were well-ordered with regular structure and myocardial fibers were intact in the sham group, but myocardial cells were disordered and a few myocardial fibers were broken in the I/R group. Results of the analysis of the cardiac injury biomarker expression and HE staining revealed significant damage in the hearts of the rats in the I/R group. To verify the involvement of ferroptosis in the process of cardiac injury, we used the iron assay kit to measure ferrous iron levels in myocardial tissues, and the results showed that in the I/R group, the normalized Fe^{2+} levels were elevated (**Figure 1C**). The ferroptosis-related gene expression results are shown in **Figures 1D–F**. The protein and mRNA expression of GPX4, FTH1, ACSL4, NOX1, and COX2 was detected through Western blotting and RT-qPCR, respectively. ACSL4, NOX1, and COX2 mRNA and protein levels were significantly higher in the I/R group than in the sham group. However, we found that GPX4 and FTH1 were significantly reduced at the protein level in the I/R group but not at the mRNA level, suggesting the presence of factors inhibiting the translation of these two genes.

To visualize the cardiac damage in the I/R group, we performed transthoracic echocardiography and M-mode tracings in rats in the I/R group. The results showed that LVIDs were significantly higher while LVFS and LVEF% were significantly lower in the I/R group than those in the sham group. In addition, the mean LVIDd values were higher in the I/R group than the sham group, and there were no statistically significant differences between the two groups (**Figures 1G–J**). The above results showed that the heart function of rats was disrupted after I/R injury.

miR-135b-3p Targets *Gpx4*, and Its Expression Increases in Myocardial I/R Rats

To explore the miRNA-mediated regulation of *Gpx4* expression, we used TargetScan, miRWalk, and miRada to predict and screen the miRNAs targeting *Gpx4* (**Supplementary Dataset 1**), and the results were presented in the form of a Venn diagram (**Figure 2A**), which was drawn using the tool available from http://bioinformatics.psb.ugent.be/webtools/Venn/. The expression of miRNAs found by database analysis, in the sham and I/R groups, was examined using RT-qPCR. We found that miR-135b-3p expression was significantly increased in myocardial I/R (**Figure 2B**). The prediction results of the TargetScan Release 7.0 database showed that the 3′-UTR of *Gpx4* mRNA possesses putative binding sites for miR-135b-3p (**Figure 2C**). To further confirm the direct binding of miR-135b-3p to the *Gpx4* mRNA 3′UTR, a luciferase activity assay was performed. H9C2 cells were co-transfected with *Gpx4*-3′UTR-WT, *Gpx4*-3′UTR-MUT, miR-135b-3p, or negative control mimics. miR-135b-3p significantly inhibited the luciferase activity of *Gpx4*-3′UTR-WT, whereas that of *Gpx4*-3′UTR-MUT was not decreased (**Figure 2D**), suggesting that miR-135b-3p was able to suppress the translation by binding to the 3′UTR of *Gpx4* mRNA. These results demonstrate that the miR-135b-3p expression increases in myocardial I/R tissue and directly regulates the expression of *Gpx4* in H9C2 cells.

Ferroptosis Occurs in H9C2 Cells After H/R and Is Accompanied by Altered Expression of miR-135b-3p

Erastin is an oncogenic RAS-selective lethal small molecule that triggers a unique iron-dependent form of non-apoptotic cell death in various cell types. Fer-1 inhibits the accumulation of cytoplasmic and lipid ROS induced by erastin (25). To further explore the roles of ferroptosis in myocardial I/R, we cultured rat myocardial H9C2 cells under H/R conditions to induce I/R damage. Cell viability was reduced in the H/R group compared to the control group, and treatment with erastin further reduced cell viability, whereas treatment with Fer-1 restored the viability of H9C2 cells subjected to H/R (**Figure 3A**). These results confirmed that H/R treatment could promote ferroptosis in cells. An iron assay kit was used to measure ferrous iron levels in H9C2 cells. The results showed that the normalized Fe^{2+} level in the H/R group was significantly higher than that in the control group. The normalized Fe^{2+} level in H/R cells was increased after treatment with erastin but decreased after Fer-1 treatment (**Figure 3B**). Subsequently, we examined the expression of ferroptosis-associated proteins by Western blotting. GPX4 and FTH1 expression decreased and ACSL4, NOX1, and COX2 expression increased in H/R cells compared to the control cells. When H/R cells were treated with erastin, GPX4 and FTH1 expression was inhibited, while ACSL4, NOX1, and COX2 expression increased. As shown in **Figures 3C,D**, the ferroptosis-related gene expression in Fer-1-treated cells was completely contrary to that in the erastin-treated cells. Immunofluorescence results showed that ROS levels were upregulated in H/R cells and the erastin-treated H/R cells, whereas Fer-1 treatment downregulated the ROS levels in H/R cells (**Figure 3E**). These results suggest that ferroptosis is involved in myocardial H/R injury. Furthermore, we used RT-qPCR to detect changes in miR-135b-3p expression in different groups and found that miR-135b-3p expression was positively

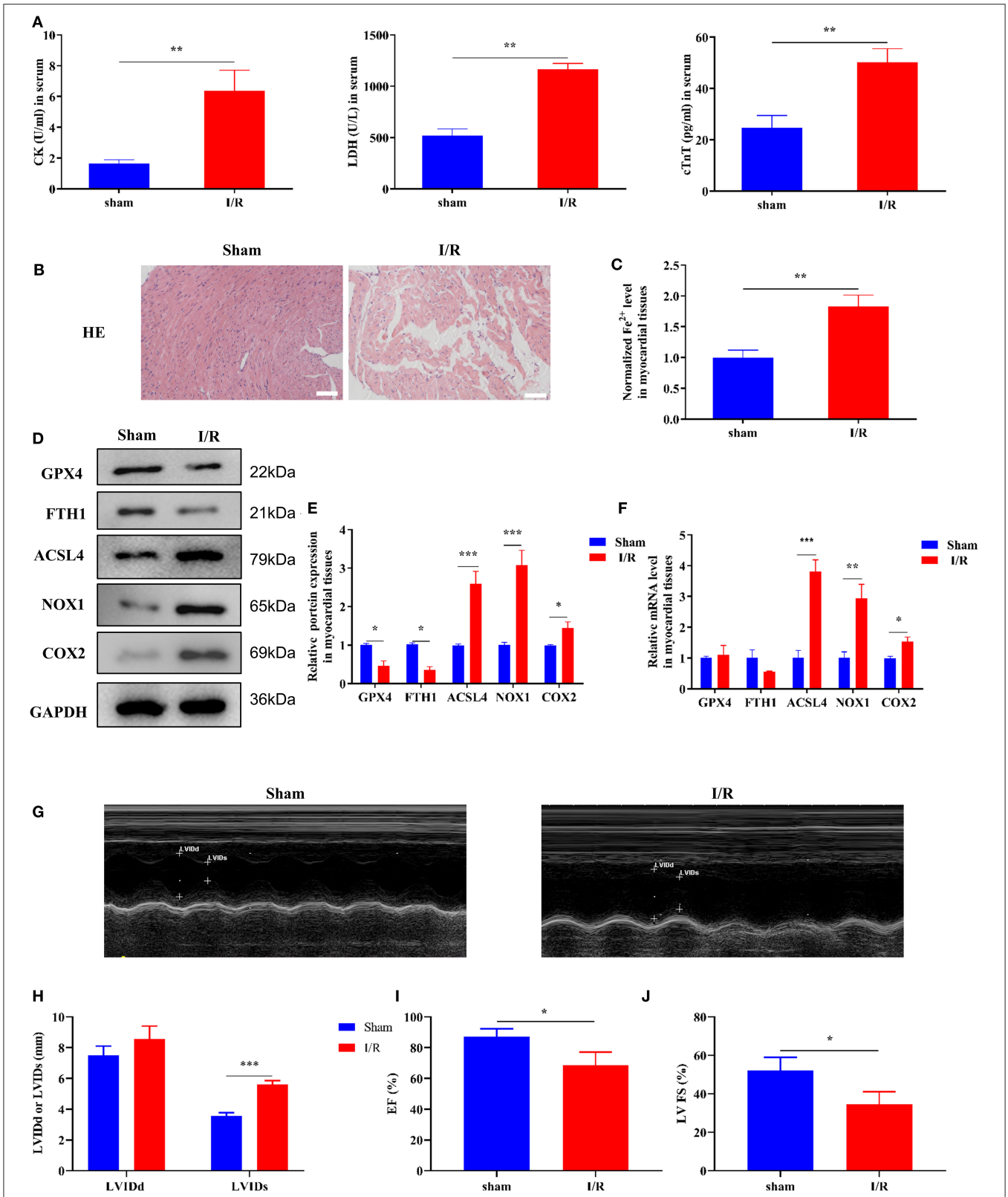

FIGURE 1 | Ferroptosis occurs in myocardial I/R rats. This part of the study was based on sham and I/R rats ($n = 6$). **(A)** The concentration of CK, LDH, and cTnT in serum was determined using ELISA. **(B)** HE staining was performed to detect myocardial tissue injury. Scale bar = 50 μm. **(C)** Iron assay kit was used to measure the

(Continued)

FIGURE 1 | change in ferrous iron levels in the myocardial tissues of sham and I/R rats. Scale bar = 400 μm. **(D,E)** Western blotting was used to detect the levels of GPX4, FTH1, NOX1, ASCL4, and COX2 in sham and I/R rat myocardial tissues; quantitative analysis of the protein levels is shown in E. **(F)** RT-qPCR analysis was used for determining the GPX4, FTH1, NOX1, ASCL4, and COX2 mRNA levels. **(G–J)** LV short-axis view by transesophageal echocardiography in M-mode. ***$p < 0.001$, **$p < 0.01$, *$p < 0.05$. * denotes the difference of the I/R group compared with the sham group. Error bars represent the mean ± SD of the experiments in triplicates.

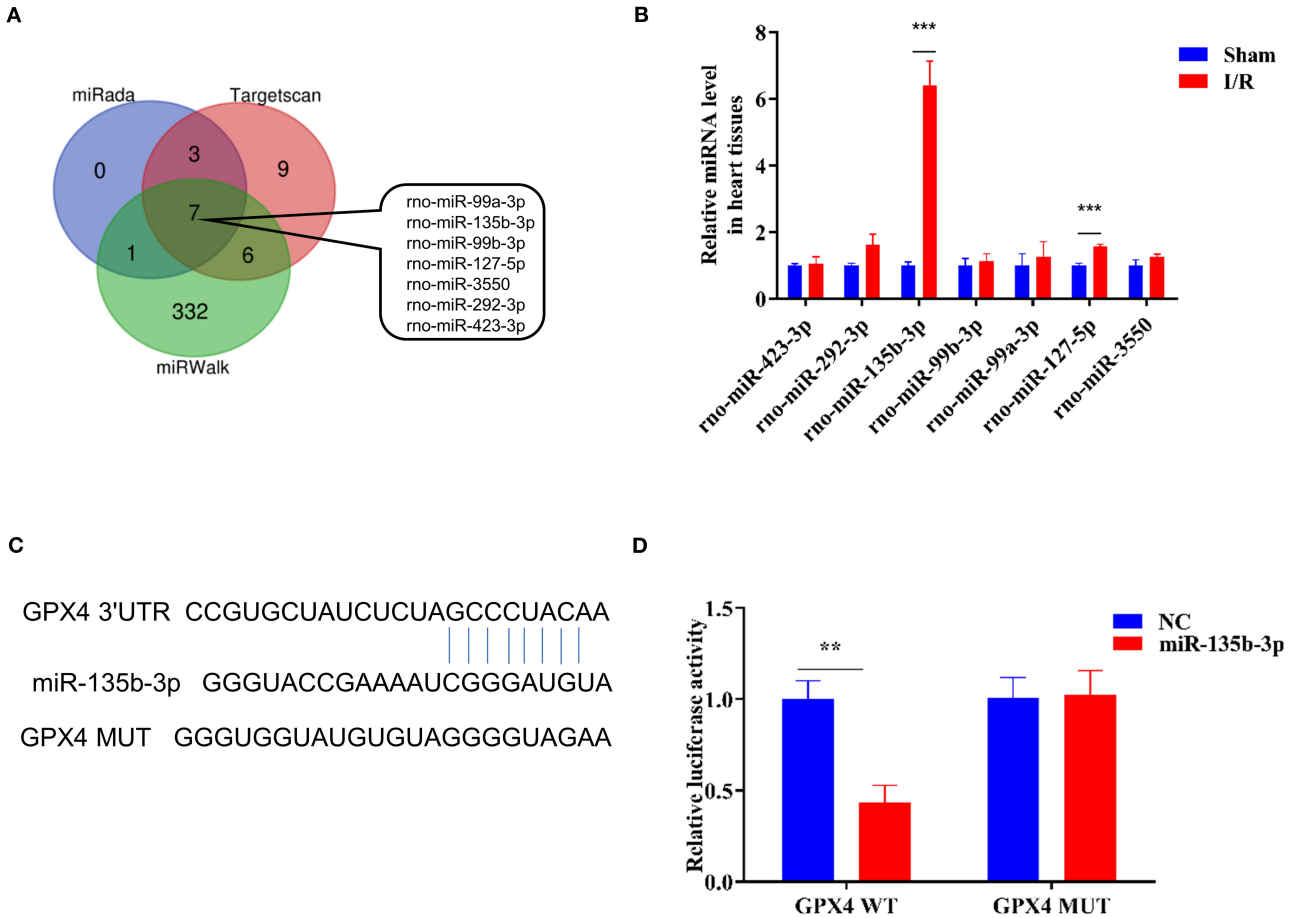

FIGURE 2 | *Gpx4* is a direct target of miR-135b-3p. **(A)** Prediction of miRNAs that target *Gpx4* using TargetScan, miRWalk, and miRada database. **(B)** Detection of miRNA expression in sham and I/R myocardial tissues of rats using RT-qPCR ($n = 3$). **(C)** The putative miR-135b-3p-binding sites in 3'UTR of wild-type and mutant *Gpx4*. **(D)** Relative luciferase activity of the cells co-transfected with constructed luciferase reporters (*Gpx4*-3′UTR-WT and *Gpx4*-3′UTR-MUT), pRL-TK vectors, and miR-135b-3p mimics or negative control ($n = 3$). ***$p < 0.001$, **$p < 0.01$. Error bars represent the mean ± SD of triplicate experiments.

correlated with the severity of ferroptosis (**Figure 3F**). These results suggest that miR-135b-3p may be involved in myocardial cell ferroptosis.

miR-135b-3p Promotes Cell Ferroptosis by Reducing GPX4 Expression in H9C2 Cells After H/R

Previous studies have demonstrated that miR-135b-3p can target GPX4 and is aberrantly expressed in ferroptosis; therefore, we determined whether miR-135b-3p promotes ferroptosis by regulating GPX4 expression. To explore the miR-135b-3p effect in H/R-induced H9C2 cells, we first transfected miR-135b-3p mimics, negative control mimics, miR-135b-3p inhibitor, and negative control inhibitor in H/R-induced H2C9 cells. miR-135b-3p expression detected by RT-qPCR was used to confirm the transfection efficiency (**Figure 4A**). Western blotting results showed a significant negative correlation between miR-135b-3p and GPX4 (**Figures 4B,C**). miR-135b-3p increased the normalized Fe^{2+} levels (**Figure 4D**). The cell viability assay showed that miR-135b-3p mimics significantly decreased the cell viability compared to the negative control mimics group,

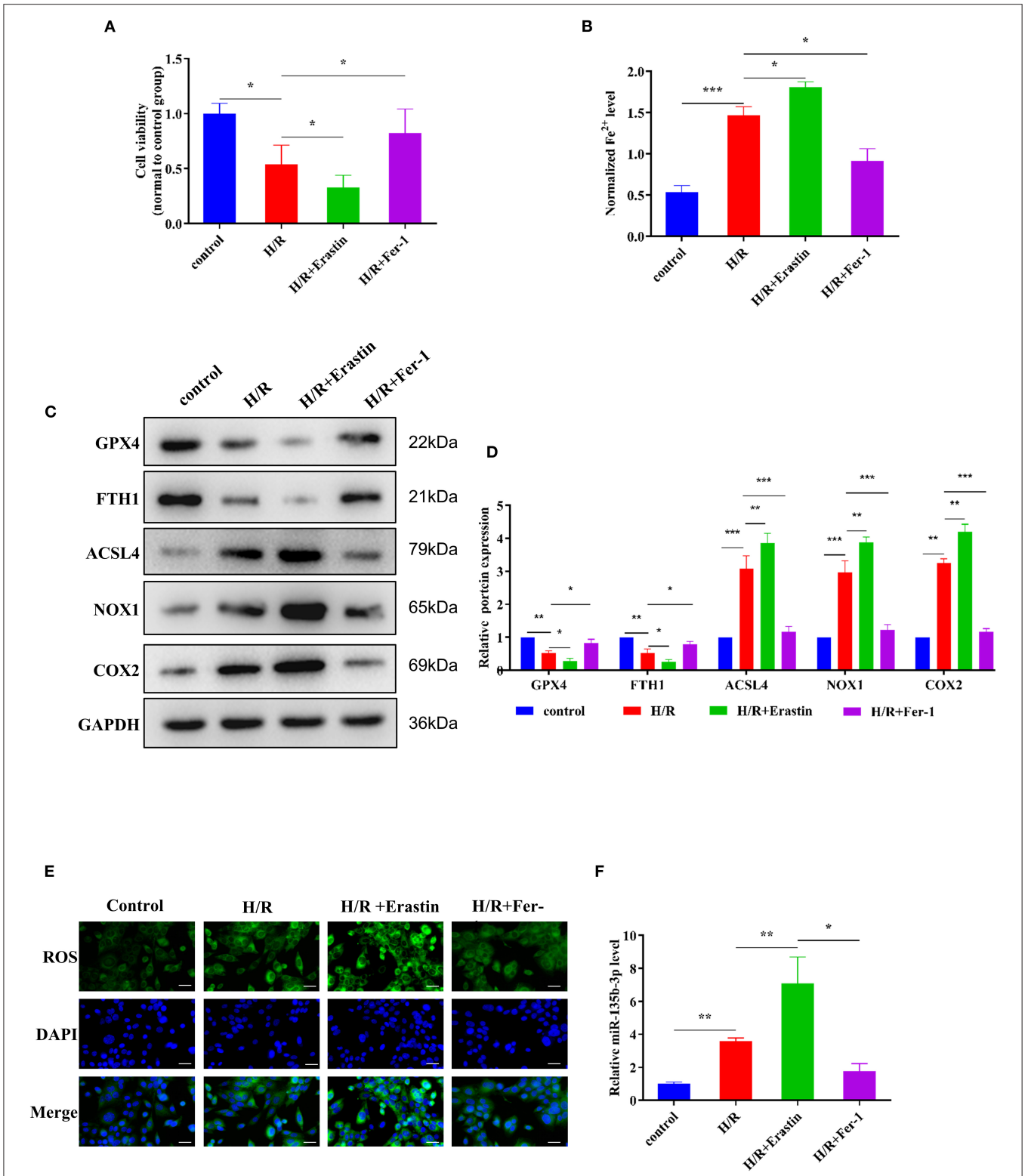

FIGURE 3 | Ferroptosis affects cell survival and miR-135b-3p expression in H9C2 cells after H/R. This part of the study was based on the untreated H9C2 cells and H/R-treated H9C2 cells that were treated with erastin or Fer-1 ($n = 3$). **(A)** MTT assay was conducted to detect the effect of erastin and Fer-1 on the viability of H/R H9C2 cells. **(B)** The ferrous iron level in H9C2 cells with different treatments was measured by using the iron assay kit. **(C)** Western blotting was used for detecting GPX4, FTH1, NOX1, ASCL4, and COX2 expression in different H9C2 cells; quantitative analysis is shown in **(D)**. **(E)** C11-BODIPY was used to detect the ROS level in H9C2 cells subjected to different treatments. DAPI staining was used for nuclear localization. Scale bar = 50 μm. **(F)** RT-qPCR analysis of the expression of miR-135b-3p in H9C2 cells. ***$p < 0.001$, **$p < 0.01$, *$p < 0.05$. Error bars represent the mean ± SD of triplicate experiments.

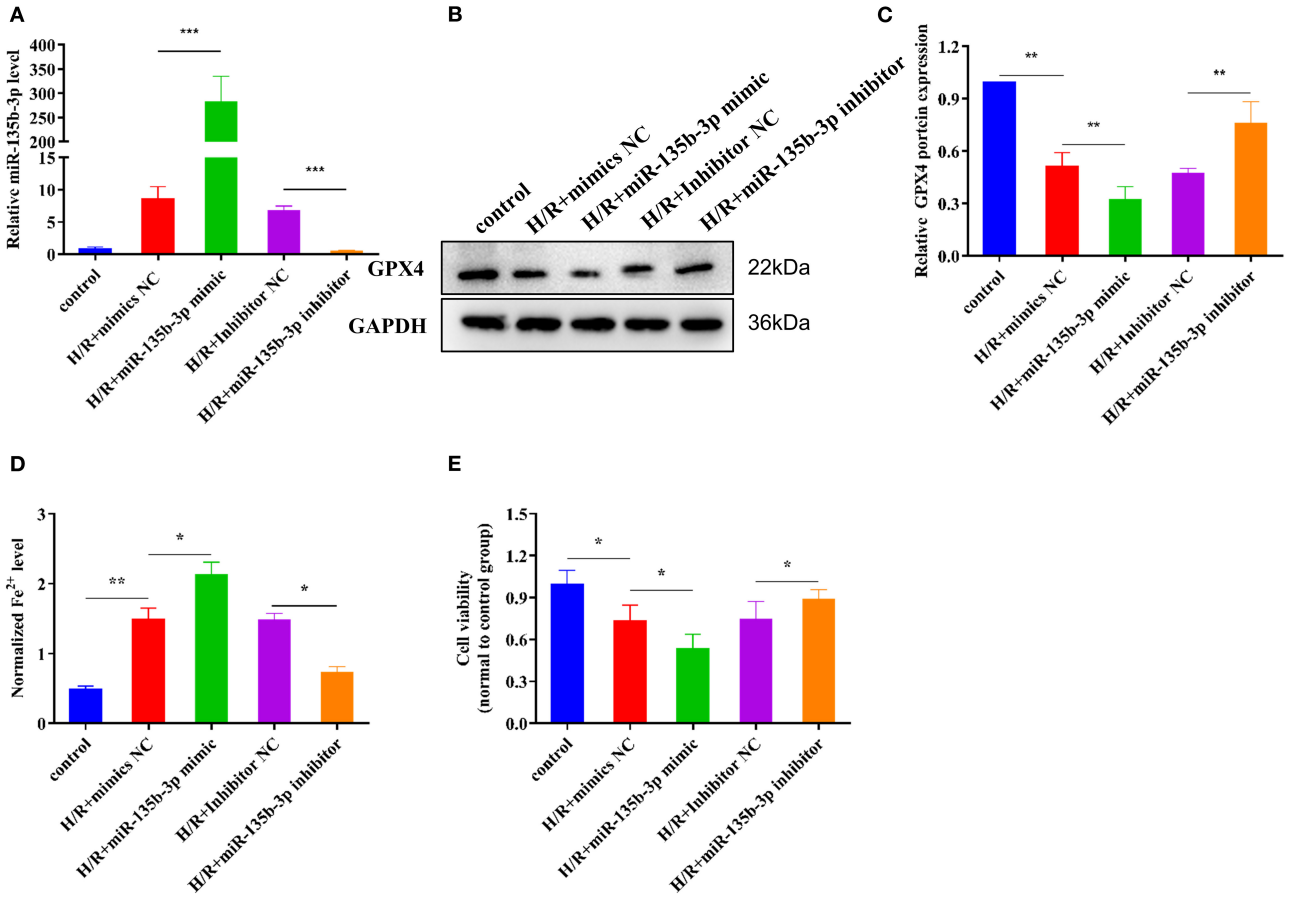

FIGURE 4 | miR-135b-3p promotes ferroptosis in H9C2 cells after H/R. This part of the study was based on untreated H9C2 cells and H/R-treated H9C2 cells, where miR-135b-3p expression was altered by mimics or an inhibitor in H/R H9C2 cells ($n = 3$). **(A)** RT-qPCR-based detection of the expression of miR-135b-3p in control or H/R H9C2 cells after transfection with miR-135b-3p mimics, inhibitor, or corresponding control. **(B)** The expression of GPX4 in miR-135b-3p-overexpressing or miR-135b-3p-knockdown H/R H9C2 cells was detected by Western blotting; quantitative analysis is shown in **(C)**. **(D)** Ferrous iron level was detected in miR-135b-3p-overexpressing or miR-135b-3p-knockdown H/R H9C2 cells by using the iron assay kit. **(E)** MTT assay was used to analyze cell viability after altering the expression of miR-135b-3p. $^{***}p < 0.001$, $^{**}p < 0.01$, $^{*}p < 0.05$. Results represent the average of three independent experiments. Error bars represent the mean ± SD.

whereas the viability of cells transfected with miR-135b-3p inhibitor was increased compared to the negative control group (**Figure 4E**). Based on these results, we concluded that miR-135b-3p regulated the expression of GPX4 and ferroptosis in H/R-induced H9C2 cells.

To further explore the influence of miR-135b-3p on ferroptosis through GPX4, we used the GPX4 plasmid to increase the expression of GPX4, which was confirmed by Western blotting. The Western blot results also showed that the increased expression of GPX4 and miR-135b-3p leads to increased expression of FTH1 and decreased expression of ACSL4, NOX1, and COX2 in H/R myocardial cells, compared to the cells transfected only with miR-135b-3p mimics (**Figures 5A,B**). Results from the assays for normalized Fe^{2+} levels, cell viability, and ROS levels confirmed that restoration of GPX4 expression could reduce cell ferroptosis and increase cell viability (**Figures 5C–E**). These data suggest that miR-135b-3p promotes cell ferroptosis by inhibiting GPX4 expression in H/R myocardial cells.

miR-135b-3p/GPX4 Promotes Cell Ferroptosis and Aggravates Myocardial I/R Injury *In vivo*

To confirm that miR-135b-3p promotes cell ferroptosis by suppressing GPX4 expression *in vivo*, we constructed an I/R rat model by injecting the control virus, miR-135b-3p overexpression virus, or knockdown virus into the tail vein. After reperfusion, the myocardial tissue and serum were collected. ELISA results showed a positive correlation between miR-135b-3p and CK, LDH, and cTnT levels, indicating that miR-135b-3p could aggravate myocardial I/R injury (**Figure 6A**). HE staining

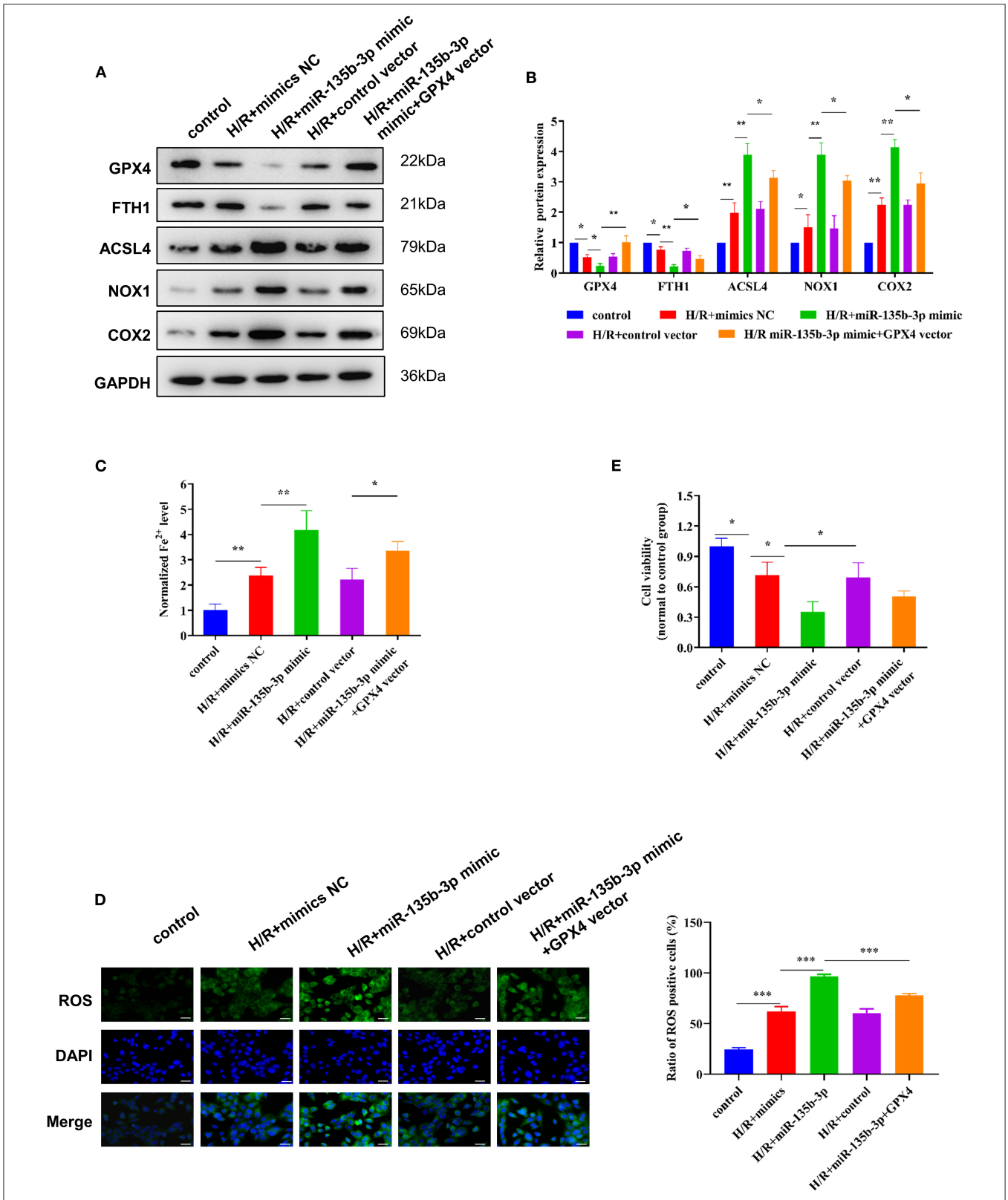

FIGURE 5 | miR-135b-3p promotes ferroptosis through inhibition of GPX4 expression in H9C2 cells after H/R. This part of the study was based on untreated H9C2 cells and H/R-treated H9C2 cells, where miR-135b-3p and GPX4 expression was altered in H/R H9C2 cells ($n = 3$). **(A)** Western blots indicating the levels of GPX4

(Continued)

FIGURE 5 | and other ferroptosis-related proteins in H/R H9C2 cells overexpressing miR-135b-3p or H/R H9C2 cells overexpressing miR-135b-3p and GPX4. The quantitative analysis is shown in **(B)**. **(C)** The ferrous iron concentration was measured in H/R H9C2 cells overexpressing miR-135b-3p or H/R H9C2 cells overexpressing miR-135b-3p and GPX4 by using the iron assay kit. **(D)** C11-BODIPY was used to detect the ROS levels in cells. DAPI staining was used for nuclear localization. Scale bar = 50 μm. The quantitative analysis is shown on the right. **(E)** MTT assay was used to evaluate the viability of H/R H9C2 cells overexpressing miR-135b-3p or H/R H9C2 cells overexpressing miR-135b-3p and GPX4. ***$p < 0.001$, **$p < 0.01$, *$p < 0.05$. Results represent the average of three independent experiments; error bars represent the mean ± SD.

showed that overexpression of miR-135b-3p could lead to myocardial cell disorder and a rise in cell death, and knockdown of miR-135b-3p could restore these effects (**Figure 6B**). Western blot results showed that GPX4 expression was reduced in the I/R group, but inhibiting miR-135b-3p expression restored the GPX4 expression (**Figures 6C,D**).

To visually assess the infarct volume, we performed TTC staining, which showed that the hearts of rats in the I/R group showed distinct areas of infarction compared to the sham group and that the infarction became more severe after miR-135b-3p overexpression (**Figures 6E,F**). In addition, we performed transthoracic echocardiography and M-mode tracing in rats from five groups. The results showed that LVIDd and LVIDs values were significantly higher, whereas LVFS% and LVEF% were significantly lower, in the I/R group than in the sham group, as demonstrated in **Figure 1**. In addition, we found that miR-135b-3p expression had a significant effect on these four indicators: miR-135b-3p overexpression led to an increase in LVIDd and LVIDs and a decrease in LVFS% and LVEF% in rats (**Figures 6G–J**).

Taken together, the *in vivo* experiments confirmed that miR-135b-3p promotes cellular ferroptosis by downregulating GPX4 expression, thereby exacerbating myocardial I/R injury.

DISCUSSION

Myocardial I/R can lead to a large amount of Fe^{2+} influx and ROS production, which is the main mechanism of pathogenesis of cell damage (26). Myocardial I/R is related to the occurrence and development of various clinical diseases, such as myocardial infarction and atherosclerosis, and affects patient recovery (16–18, 27). Therefore, exploring the mechanisms of myocardial I/R injury and its alleviation are of great significance for treating these diseases. In our study, we constructed a myocardial I/R rat model and detected the CK, LDH, and cTnT expression levels in the serum. An increase in the CK, LDH, and cTnT levels is indicative of myocardial I/R injury during myocardial perfusion (19, 20). Our results showed that CK, LDH, and cTnT expression was upregulated in the I/R model group, indicating a successful myocardial I/R model. Induction of ferroptosis has been reported in the myocardial tissue during I/R injury (21, 28). In the present study, we found that the level of Fe^{2+} increased during I/R injury, and the expression of ferroptosis-related genes changed significantly. Moreover, we found that the expression of GPX4 and FTH1 was downregulated at the protein level but there were no significant differences in their mRNA levels, suggesting that the reduced expression of transcription factors or epigenetic modifications may be involved in the inhibition of GPX4 and FTH1 translation. Classical ferroptosis is regulated by GPX4 signaling (5, 6); therefore, we hypothesized that miRNAs involved in regulating GPX4 translation might affect ferroptosis.

Many studies have reported that miRNAs regulate ferroptosis in cancers and other diseases (13, 22, 29). In gastric cancer cells, CAFs secrete exosome miR-522 to inhibit ferroptosis by targeting ALOX15 and blocking lipid-ROS accumulation (23). In upper gastrointestinal cancer, inhibition of AURKA or reconstitution of miR-4715-3p was shown to inhibit GPX4 expression and induce cell ferroptosis; this phenomenon represents a novel epigenetic mechanism mediating miR-4715-3p silencing and AURKA induction (24). However, in myocardial I/R injury, the effects of miRNAs on ferroptosis have not been reported. Nonetheless, miR-21 overexpression in the heart has been reported to reduce cardiomyocyte apoptosis and myocardial infarct size (30). Therefore, we speculated that miRNAs are also involved in myocardial I/R injury. As mentioned earlier, GPX4 plays a crucial role in the occurrence of ferroptosis, which is a key cause of myocardial injury caused by I/R. To investigate *GPX4* expression during myocardial I/R and the functional roles miRNAs may play in the process, we focused on the *GPX4*-targeting miRNAs and found that miR-135b-3p directly targets *GPX4* in I/R tissues. We transfected miR-135b-3p mimics or inhibitors into cultured cardiomyocytes to explore the roles of miR-135b-3p in the H/R model. We determined ferrous iron levels, cell viability, and *Gpx4* expression in the cells and found that transfection of miR-135b-3p mimics increased the ferrous iron levels and decreased *Gpx4 e*xpression and cell viability in cardiomyocytes after H/R. In contrast, transfection with miR-135b-3p inhibitor reduced the ferrous iron levels and increased *Gpx4* expression and cell viability in cardiomyocytes after H/R. These results suggest that miR-135b-3p promotes cell death in an iron-dependent manner *in vitro*. We further found that upregulation of *Gpx4* expression restored cell viability, ferrous iron levels, and lipid ROS levels compared with transfection of miR-135b-3p separately. These results confirm that miR-135b-3p affects ferroptosis in cardiomyocytes after H/R by regulating GPX4 expression. We then confirmed the effect of miR-135b-3p on ferroptosis by injecting a virus to upregulate or downregulate the expression of miR-135b-3p in rats. In addition to miR-135b-3p, we believe that other miRNAs might be involved in the regulation of I/R-related ferroptosis. Further exploration and studies are required to provide adequate experimental evidence for alleviating or avoiding I/R damage in clinical settings by targeting miRNAs.

In summary, we demonstrated the upregulation of miR-135b-3p in myocardial I/R rat cardiac muscle tissues and H/R myocardial cells. Moreover, increased

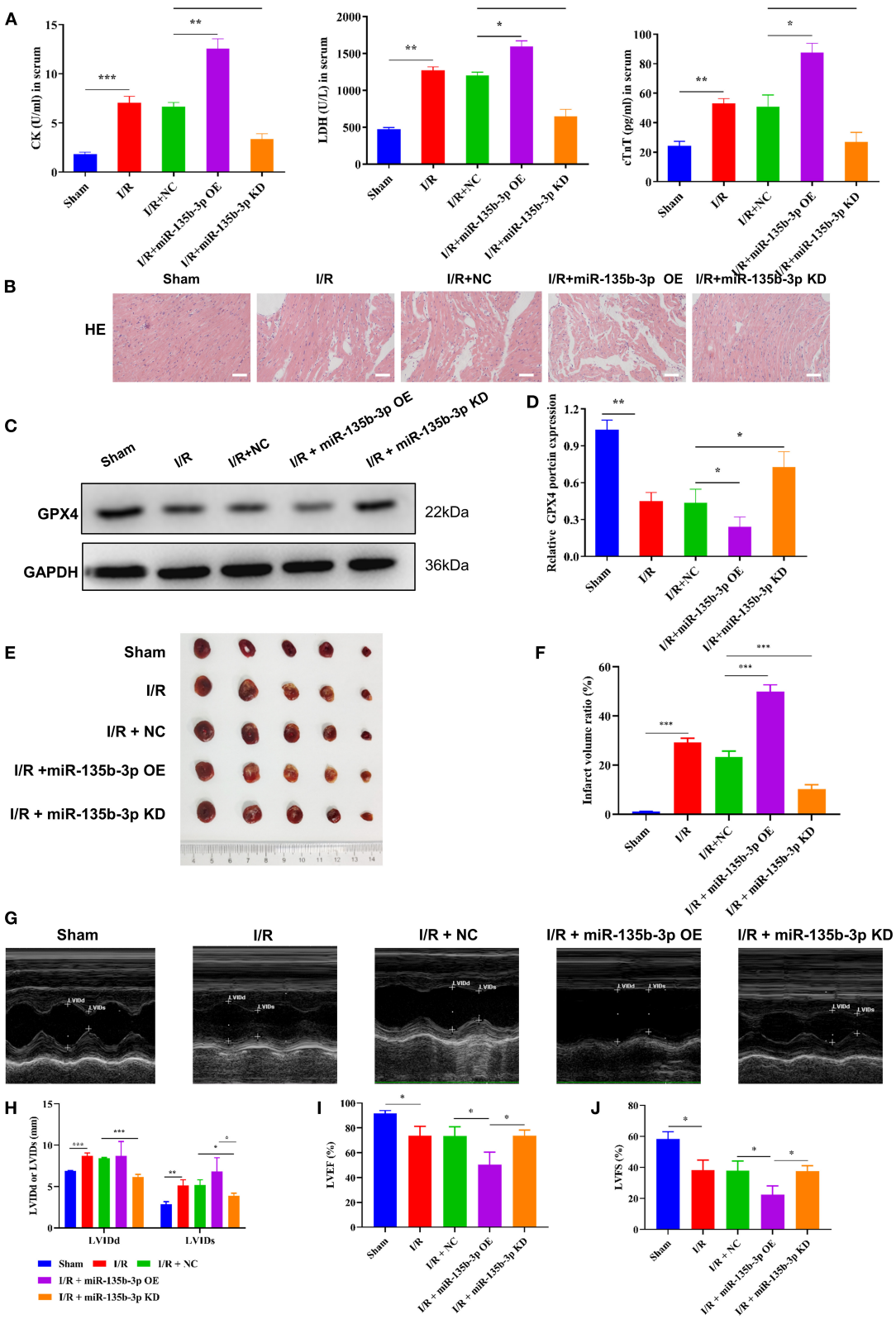

FIGURE 6 | miR-135b-3p enhances ferroptosis by reducing GPX4 expression *in vivo*, ultimately exacerbating myocardial I/R injury. This part of the study was based on sham and I/R rats, where miR expression in I/R rats was regulated by lentivirus injection ($n = 6$). **(A)** The expression of CK, LDH, and cTnT in serum was detected

(Continued)

FIGURE 6 | using ELISA. **(B)** Histopathology was analyzed using HE staining. Scale bar = 400 μm. **(C,D)** Western blotting was used to detect the levels of GPX4 in myocardial tissues of rats, and the quantitative analysis is shown in **(D)**. **(E,F)** Infarct volumes were evaluated by TTC staining of hearts; quantitative analysis is shown in **(F)**. **(G–J)** LV short-axis view by transesophageal echocardiography in M-mode. ***$p < 0.001$, **$p < 0.01$, *$p < 0.05$. Results represent the average of three independent experiments; error bars represent the mean ± SD.

expression of miR-135b-3p worsened the cell injury by promoting ferroptosis through inhibition of GPX4 expression. Therefore, targeting miR-135b-3p may be a potential therapeutic approach for myocardial I/R injury.

DATA AVAILABILITY STATEMENT

The original contributions presented in the study are included in the article/**Supplementary Material**, further inquiries can be directed to the corresponding author/s.

ETHICS STATEMENT

The animal study was reviewed and approved by Ethics Committee of Affiliated Hospital of Nanjing University of Chinese Medicine.

AUTHOR CONTRIBUTIONS

XC: conceptualization and supervision. WS and PY: data curation and project administration. HS, PY, and XC: funding acquisition. RS, JG, and HW: investigation and resources. LS and PY: methodology. WS: software, visualization, and writing—original draft. HS: validation. WS, PY, and XC: writing—review and editing. All authors contributed to the article and approved the submitted version.

FUNDING

This work was supported by the Natural Science Foundation of Jiangsu, China (BK20201500), the Jiangsu Province Traditional Chinese Medicine Leading Talent Project (SLJ0204), the Priority Academic Program Development of Jiangsu Higher Education Institutions (Integration of Chinese and Western Medicine), and 333 High-level Talent Training Project of Jiangsu Province (BRA2020386).

ACKNOWLEDGMENTS

The authors thank the Experimental Center of the First Clinical Medical College at Nanjing University of Chinese Medicine for providing support to our study.

SUPPLEMENTARY MATERIAL

The Supplementary Material for this article can be found online at: https://www.frontiersin.org/articles/10.3389/fcvm.2021.663832/full#supplementary-material

Supplementary Table 1 | The ARRIVE guidelines 2.0 author checklist.

Supplementary Table 2 | The primer sequences of genes in RT-qPCR assay.

Supplementary Dataset 1 | The result of TargetScan, miRWalk, and miRada to predict and screen the miRNAs targeting *Gpx4*.

Supplementary Figure 1 | The detailed animal groupings information.

Supplementary Figure 2 | The Full Scan WB images in the study.

REFERENCES

1. Fares MA. Introduction: challenges and advances in cardiovascular disease. *Cleve Clin J Med.* (2017) 84:11. doi: 10.3949/ccjm.84.s3.01
2. Xie B, Liu X, Yang J, Cheng J, Gu J, Xue S. PIAS1 protects against myocardial ischemia-reperfusion injury by stimulating PPARgamma SUMOylation. *BMC Cell Biol.* (2018) 19:24. doi: 10.1186/s12860-018-0176-x
3. Kalogeris T, Baines CP, Krenz M, Korthuis RJ. Ischemia/reperfusion. *Compr Physiol.* (2016) 7:113–70. doi: 10.1002/cphy.c160006
4. Lei P, Bai T, Sun Y. Mechanisms of ferroptosis and relations with regulated cell death: a review. *Front Physiol.* (2019) 10:139. doi: 10.3389/fphys.2019.00139
5. Cao JY, Dixon SJ. Mechanisms of ferroptosis. *Cell Mol Life Sci.* (2016) 73:2195–209. doi: 10.1007/s00018-016-2194-1
6. Seibt TM, Proneth B, Conrad M. Role of GPX4 in ferroptosis and its pharmacological implication. *Free Radic Biol Med.* (2019) 133:144–52. doi: 10.1016/j.freeradbiomed.2018.09.014
7. Torii S, Shintoku R, Kubota C, Yaegashi M, Torii R, Sasaki M, et al. An essential role for functional lysosomes in ferroptosis of cancer cells. *Biochem J.* (2016) 473:769–77. doi: 10.1042/BJ20150658
8. Liu Q, Wang K. The induction of ferroptosis by impairing STAT3/Nrf2/GPx4 signaling enhances the sensitivity of osteosarcoma cells to cisplatin. *Cell Biol Int.* (2019) 43:1245–56. doi: 10.1002/cbin.11121
9. Friedmann Angeli JP, Schneider M, Proneth B, Tyurina YY, Tyurin VA, Hammond VJ, et al. Inactivation of the ferroptosis regulator Gpx4 triggers acute renal failure in mice. *Nat Cell Biol.* (2014) 16:1180–91. doi: 10.1038/ncb3064
10. Linkermann A, Skouta R, Himmerkus N, Mulay SR, Dewitz C, De Zen F, et al. Synchronized renal tubular cell death involves ferroptosis. *Proc Natl Acad Sci U S A.* (2014) 111:16836–41. doi: 10.1073/pnas.1415518111
11. Vishnoi A, Rani S. MiRNA biogenesis and regulation of diseases: an overview. *Methods Mol Biol.* (2017) 1509:1–10. doi: 10.1007/978-1-4939-6524-3_1
12. Baba Y, Higa JK, Shimada BK, Horiuchi KM, Suhara T, Kobayashi M, et al. Protective effects of the mechanistic target of rapamycin against excess iron and ferroptosis in cardiomyocytes. *Am J Physiol Heart Circ Physiol.* (2018) 314:H659-H668. doi: 10.1152/ajpheart.00452.2017
13. Manz DH, Blanchette NL, Paul BT, Torti FM, Torti SV. Iron and cancer: recent insights. *Ann N Y Acad Sci.* (2016) 1368:149–61. doi: 10.1111/nyas.13008
14. Hampton CR, Shimamoto A, Rothnie CL, Griscavage-Ennis J, Chong A, Dix DJ, et al. HSP70.1 and−70.3 are required for late-phase protection induced by ischemic preconditioning of mouse hearts. *Am J Physiol Heart Circ Physiol.* (2003) 285:H866–74. doi: 10.1152/ajpheart.00596.2002
15. Xiao X, Lu Z, Lin V, May A, Shaw DH, Wang Z, et al. MicroRNA miR-24-3p reduces apoptosis and regulates Keap1-Nrf2 pathway in mouse cardiomyocytes responding to ischemia/reperfusion injury. *Oxid Med Cell Longev.* (2018) 2018:7042105. doi: 10.1155/2018/7042105
16. Valko M, Jomova K, Rhodes CJ, Kuca K, Musilek K. Redox- and non-redox-metal-induced formation of free radicals and their role in human disease. *Arch Toxicol.* (2016) 90:1–37. doi: 10.1007/s00204-015-1579-5

17. Huang C, Li R, Zeng Q, Ding Y, Zou Y, Mao X, et al. Effect of minocycline postconditioning and ischemic postconditioning on myocardial ischemia-reperfusion injury in atherosclerosis rabbits. *J Huazhong Univ Sci Technolog Med Sci.* (2012) 32:524–9. doi: 10.1007/s11596-012-0090-y
18. Chi HJ, Chen ML, Yang XC, Lin XM, Sun H, Zhao WS, et al. Progress in therapies for myocardial ischemia reperfusion injury. *Curr Drug Targets.* (2017) 18:1712–21. doi: 10.2174/1389450117666160401120308
19. Dai Y, Wang Z, Quan M, Lv Y, Li Y, Xin HB, et al. Asiatic acid protests against myocardial ischemia/reperfusion injury via modulation of glycometabolism in rat cardiomyocyte. *Drug Des Devel Ther.* (2018) 12:3573–82. doi: 10.2147/DDDT.S175116
20. Ren GD, Y YC, Li WL, Li FF, Han XY. Research on cardioprotective effect of irbesartan in rats with myocardial ischemia-reperfusion injury through MAPK-ERK signaling pathway. *Eur Rev Med Pharmacol Sci.* (2019) 23:5487–94. doi: 10.26355/eurrev_201906_18218
21. Kobayashi M, Suhara T, Baba Y, Kawasaki NK, Higa JK, Matsui T. Pathological roles of iron in cardiovascular disease. *Curr Drug Targets.* (2018) 19:1068–76. doi: 10.2174/1389450119666180605112235
22. Xiao FJ, Zhang D, Wu Y, Jia QH, Zhang L, Li YX, et al. miRNA-17-92 protects endothelial cells from erastin-induced ferroptosis through targeting the A20-ACSL4 axis. *Biochem Biophys Res Commun.* (2019) 515:448–54. doi: 10.1016/j.bbrc.2019.05.147
23. Zhang H, Deng T, Liu R, Ning T, Yang H, Liu D, et al. CAF secreted miR-522 suppresses ferroptosis and promotes acquired chemo-resistance in gastric cancer. *Mol Cancer.* (2020) 19:43. doi: 10.1186/s12943-020-01168-8
24. Gomaa A, Peng D, Chen Z, Soutto M, Abouelezz K, Corvalan A, et al. Epigenetic regulation of AURKA by miR-4715-3p in upper gastrointestinal cancers. *Sci Rep*. (2019) 9:16970. doi: 10.1038/s41598-019-53174-6
25. Bruni A, Pepper AR, Pawlick RL, Gala-Lopez B, Gamble AF, Kin T, et al. Ferroptosis-inducing agents compromise *in vitro* human islet viability and function. *Cell Death Dis.* (2018) 9:595. doi: 10.1038/s41419-018-0506-0
26. Perera RJ, Ray A. MicroRNAs in the search for understanding human diseases. *BioDrugs.* (2007) 21:97–104. doi: 10.2165/00063030-200721020-00004
27. Neri M, Riezzo I, Pascale N, Pomara C, Turillazzi E. Ischemia/reperfusion injury following acute myocardial infarction: a critical issue for clinicians and forensic pathologists. *Mediators Inflamm.* (2017) 2017:7018393. doi: 10.1155/2017/7018393
28. Feng Y, Madungwe NB, Imam Aliagan AD, Tombo N, Bopassa JC. Liproxstatin-1 protects the mouse myocardium against ischemia/reperfusion injury by decreasing VDAC1 levels and restoring GPX4 levels. *Biochem Biophys Res Commun.* (2019) 520:606–11. doi: 10.1016/j.bbrc.2019.10.006
29. Mokhtari-Zaer A, Marefati N, Atkin SL, Butler AE, Sahebkar A. The protective role of curcumin in myocardial ischemia-reperfusion injury. *J Cell Physiol.* (2018) 234:214–22. doi: 10.1002/jcp.26848
30. Dong S, Cheng Y, Yang J, Li J, Liu X, Wang X, et al. MicroRNA expression signature and the role of microRNA-21 in the early phase of acute myocardial infarction. *J Biol Chem.* (2009) 284:29514–25. doi: 10.1074/jbc.M109.027896

Conflict of Interest: The authors declare that the research was conducted in the absence of any commercial or financial relationships that could be construed as a potential conflict of interest.

Publisher's Note: All claims expressed in this article are solely those of the authors and do not necessarily represent those of their affiliated organizations, or those of the publisher, the editors and the reviewers. Any product that may be evaluated in this article, or claim that may be made by its manufacturer, is not guaranteed or endorsed by the publisher.

frontiers in Cardiovascular Medicine

ORIGINAL RESEARCH
published: 22 September 2021
doi: 10.3389/fcvm.2021.647953

The Integrative Analysis of Competitive Endogenous RNA Regulatory Networks in Coronary Artery Disease

Yuyao Ji[1†], Tao Yan[2†], Shijie Zhu[2†], Runda Wu[1], Miao Zhu[2], Yangyang Zhang[3], Changfa Guo[2*] and Kang Yao[1*]*

[1] Department of Cardiology, Zhongshan Hospital, Shanghai Institute of Cardiovascular Diseases, Fudan University, Shanghai, China, [2] Department of Cardiovascular Surgery, Zhongshan Hospital, Fudan University, Shanghai, China, [3] Department of Cardiovascular Surgery, Shanghai East Hospital, Tongji University School of Medicine, Shanghai, China

Background: Coronary artery disease (CAD) is the leading cause of cardiovascular death. The competitive endogenous RNAs (ceRNAs) hypothesis is a new theory that explains the relationship between lncRNAs and miRNAs. The mechanism of ceRNAs in the pathological process of CAD has not been fully elucidated. The objective of this study was to explore the ceRNA mechanism in CAD using the integrative bioinformatics analysis and provide new research ideas for the occurrence and development of CAD.

Methods: The GSE113079 dataset was downloaded, and differentially expressed lncRNAs (DElncRNAs) and genes (DEGs) were identified using the limma package in the R language. Weighted gene correlation network analysis (WGCNA) was performed on DElncRNAs and DEGs to explore lncRNAs and genes associated with CAD. Functional enrichment analysis was performed on hub genes in the significant module identified *via* WGCNA. Four online databases, including TargetScan, miRDB, miRTarBase, and Starbase, combined with an online tool, miRWalk, were used to construct ceRNA regulatory networks.

Results: DEGs were clustered into ten co-expression modules with different colors using WGCNA. The brown module was identified as the key module with the highest correlation coefficient. 188 hub genes were identified in the brown module for functional enrichment analysis. DElncRNAs were clustered into sixteen modules, including seven modules related to CAD with the correlation coefficient more than 0.5. Three ceRNA networks were identified, including OIP5-AS1-miR-204-5p/miR-211-5p-SMOC1, OIP5-AS1-miR-92b-3p-DKK3, and OIP5-AS1-miR-25-3p-TMEM184B.

Conclusion: Three ceRNA regulatory networks identified in this study may play crucial roles in the occurrence and development of CAD, which provide novel insights into the ceRNA mechanism in CAD.

Keywords: coronary artery disease, non-coding RNA, ceRNA, bioinformatics, WGCNA

OPEN ACCESS

Edited by:
En-Zhi Jia,
Nanjing Medical University, China

Reviewed by:
Xiao Huang,
Second Affiliated Hospital of Nanchang University, China
Jie Yuan,
Fudan University, China
Cláudio Lera Orsatti,
University of Western São Paulo, Brazil

***Correspondence:**
Yangyang Zhang
zhangyangyang_wy@vip.sina.com
Changfa Guo
guo.changfa@zs-hospital.sh.cn
Kang Yao
yao.kang@zs-hospital.sh.cn

[†]These authors have contributed equally to this work

Specialty section:
This article was submitted to General Cardiovascular Medicine, a section of the journal Frontiers in Cardiovascular Medicine

Received: *30 December 2020*
Accepted: *25 August 2021*
Published: *22 September 2021*

Citation:
Ji Y, Yan T, Zhu S, Wu R, Zhu M, Zhang Y, Guo C and Yao K (2021) The Integrative Analysis of Competitive Endogenous RNA Regulatory Networks in Coronary Artery Disease. Front. Cardiovasc. Med. 8:647953. doi: 10.3389/fcvm.2021.647953

INTRODUCTION

Cardiovascular disease (CVD) is one of the leading causes of death in the world. Coronary artery disease (CAD) is the main cause of cardiovascular death (1), which increases the morbidity, mortality, and economic burden on societies worldwide (2). The occurrence of CAD is associated with the interplay of genetic and environmental factors (3). Diabetes, hypertension, obesity, and smoking are significant risk factors for CAD (4, 5). Vascular stenosis caused by CAD is the main cause of coronary atherosclerosis and ischemia. The sclerotic plaques are at risk of rupture, leading to myocardial infarction and eventually death (4, 5). Although considerable efforts have been made, it remains a daunting task to prevent and cure CAD. Therefore, further research is urgently needed to understand its pathophysiological process.

Non-coding RNA (ncRNA), including lncRNA, circRNA, and miRNA, is a kind of RNA that does not encode proteins, which plays an essential role in the occurrence and development of CAD. LncRNAs are transcripts with a length of >200 nucleotides participating in a variety of critical biological processes (6). It was reported that lncRNAs play a significant role in the core stages of CAD, including lipid metabolism, inflammation, vascular cell proliferation, apoptosis, adhesion and migration, and angiogenesis (7). The competitive endogenous RNAs (ceRNAs) hypothesis is a theory that explains the relationship between lncRNAs and miRNAs. In this hypothesis, lncRNAs rich in miRNA binding sites can bind miRNAs and act as a miRNA sponge, leading to changes in expression levels of miRNA-target genes (8, 9). Although a growing body of evidence demonstrated that ncRNAs were associated with the development of CAD, research on the role of ceRNAs in the pathological process of CAD is still insufficient. Therefore, further efforts are warranted to elucidate the ceRNA mechanism in CAD.

In this study, we aimed to explore the complex interaction between lncRNAs, miRNAs, and mRNAs to investigate the potential mechanism of ceRNAs in CAD. We performed weighted gene correlation network analysis (WGCNA) on the GSE113079 to screen out lncRNAs and mRNAs associated with CAD. Then several online databases and tools were used to construct the ceRNA regulatory networks. We hope this study can provide potential targets and new research ideas for understanding the ceRNA mechanism in CAD.

METHODS AND MATERIALS

Data Processing

The GSE113079 dataset was downloaded from the Gene Expression Omnibus (GEO) database. The dataset was based on the GPL20115 platform (Agilent-067406 Human CBC lncRNA + mRNA microarray V4.0), containing 141 samples of peripheral blood mononuclear cells (PBMCs) in 93 patients with CAD and 48 healthy controls. The R language was applied to process the dataset. The Linear Models for Microarray data (limma), a package in the R language, was used to identify differentially expressed genes (DEGs) and differentially expressed lncRNAs (DElncRNAs) with the cut-off point of adj. $p < 0.05$.

WGCNA

DEGs identified by the limma package were imported for WGCNA to construct the gene co-expression network. First, the correlation network was constructed with an appropriate soft-thresholding power β realizing the scale-free topology criterion of $R^2 > 0.85$. Second, the average linkage hierarchical clustering method was applied to cluster DEGs into different modules with different colors. The threshold for module merging was set as 0.25, and the minimum number of genes in each module was thirty. Hub genes correlation threshold was 0.9. Third, the correlation between each module and CAD was calculated using Pearson's correlation method. The module with a $p < 0.05$ and the highest correlation coefficient was screened out for further analysis. Similarly, DElncRNAs were also imported for WGCNA using the same parameters and procedures.

Functional Enrichment

The Database for Annotation, Visualization and Integrated Discovery (DAVID, v6.8) was used to perform the Gene Ontology (GO) enrichment analysis, which revealed the biological processes (BPs), cellular components (CCs), and molecular functions (MFs) related to hub genes in the module identified above. GO terms with a $p < 0.05$ were considered significant enrichment. Metascape, a powerful online tool for gene function annotation, was also applied for functional enrichment.

Construction of the ceRNA Network

The online tool miRWalk applies a machine-learning algorithm to predict miRNA-target interactions, including those that have been validated experimentally. Three online databases, including TargetScan, miRDB, and miRTarBase, combined with miRWalk, were used for the prediction of target miRNAs to ensure the robustness of the interactions between miRNAs and hub genes identified above. The Starbase is a public database that can search for potential miRNA-lncRNA interactions through high-throughput data. It was used to predict the relationships between target miRNAs and DElncRNAs to identify potential interactions. LncRNA-miRNA-mRNA regulatory network was visualized utilizing the Cytoscape software (v3.8.1).

Quantitative Real-Time PCR (qRT-PCR)

Ten patients with CAD and ten without CAD confirmed by coronary angiography were included in this study. This study was in full compliance with the Declaration of Helsinki and approved by the Medical Ethics Committee of Shanghai Tenth People's Hospital, Tongji University. Written informed consent was obtained from all subjects participating in this study. Blood samples were collected and total RNA was extracted following the manufacturer's instruction (QIAGEN, Frankfurt, Germany). Briefly, mix one volume of whole blood with five volumes of buffer in an eppendorf tube. After incubating for 15 min on ice, centrifuge at 3,000 rpm for 10 min at 4°C and discard supernatant. Transfer lysate to spin column to centrifuge at 14,000 rpm and pipet 50 μl of RNase-free water. The Complementary DNA (cDNA) was synthesized by reverse transcription at 42°C for 60 min and then at 95°C for 5 min with the PrimeScript^{TM} RT reagent Kit (Takara, Otsu, Japan).

TABLE 1 | RNA primer sequences for quantitative real-time PCR.

RNA	Sequences
OIP5-AS1	Forward: CCACCACGCTCAGCCTGATTTC
	Reverse: TTTCCACGATGACCCAACCACAAG
DKK3	Forward: ACGAGTGCATCATCGACGAG
	Reverse: GCAGTCCCTCTGGTTGTCAC
SMOC1	Forward: TCAGGTTCAGTCACCGACAAG
	Reverse: TCCTGGTCACACGAATAGACTT
TMEM184B	Forward: ACTACGTGTACTTCGGCACC
	Reverse: CTGGACTCAATGGGTTTTCCTC
GAPDH	Forward: GGAGCGAGATCCCTCCAAAAT
	Reverse: GGCTGTTGTCATACTTCTCATGG
miR-204-5p	Forward: CGCGTTCCCTTTGTCATCCT
	Reverse: AGTGCAGGGTCCGAGGTATT
	RT: GTCGTATCCAGTGCAGGGTCCGAGGTATTCGC
	ACTGGATACGACAGGCAT
miR-211-5p	Forward: CGCGTTCCCTTTGTCATCCT
	Reverse: AGTGCAGGGTCCGAGGTATT
	RT: GTCGTATCCAGTGCAGGGTCCGAGGTATTCGC
	ACTGGATACGACAGGCGA
miR-92b-3p	Forward: GCGTATTGCACTCGTCCCG
	Reverse: AGTGCAGGGTCCGAGGTATT
	RT: GTCGTATCCAGTGCAGGGTCCGAGGTATTCGCAC
	TGGATACGACGGAGGC
miR-25-3p	Forward: GCGCATTGCACTTGTCTCG
	Reverse: AGTGCAGGGTCCGAGGTATT
	RT: GTCGTATCCAGTGCAGGGTCCGAGGTATTCGCACTGGA
	TACGACTCAGAC
U6	Forward: AGAGAAGATTAGCATGGCCCCTG
	Reverse: ATCCAGTGCAGGGTCCGAGG
	RT: GTCGTATCCAGTGCAGGGTCCGAGGTATTCGCA
	CTGGATACGACAAAATA

TB Green® Premix Ex Taq™ II (Takara, Otsu, Japan) was applied to perform qRT-PCR at the temperature of 95°C for 30 s, followed by 40 cycles with the temperature of 95°C for 5 s and 60°C for 34 s on QuantStudio™ 5 System (Thermo Fisher Scientific, Waltham, MA, USA). The expression of RNA levels was normalized by GAPDH and U6, and the $2^{-\Delta\Delta CT}$ method was applied to calculate the relative expression levels. All sequences for RNA primers (Sangon Biotech, Shanghai, China) are shown in **Table 1**.

RESULTS

Identification of DEGs and DElncRNAs

A total of 20,128 DElncRNAs, including 6,103 upregulated and 14,025 downregulated, which were differentially expressed between CAD samples and healthy controls, were identified in the GSE113079 dataset with the limma package. And 11,487 DEGs were identified, including 5,993 upregulated and 5,494 downregulated.

WGCNA

DEGs with |logFC| > 0.5 were selected for WGCNA, and a scale-free co-expression network was established. The soft-thresholding power β was nine with scale-free $R^2 > 0.85$ (**Supplementary Figure 1**). Then DEGs were clustered into ten co-expression modules through the average linkage hierarchical clustering method to ensure that the number of genes in each module is more than thirty. Different modules were represented by different colors, including black, blue, brown, greenyellow, pink, purple, red, tan, yellow, and gray (**Figure 1**). Genes in the gray module were uncorrelated and excluded from the subsequent analysis. We then calculated the correlation between module memberships and the gene significance for CAD (**Supplementary Figure 2**). Modules that meet the following two conditions were selected: (1) the correlation coefficient between the module and CAD was >0.5; (2) the correlation coefficient between module memberships and the gene significance for CAD was more than 0.7. According to the above criteria, 193 hub genes in the brown and pink modules were identified for further analysis. These genes were listed in **Supplementary Table 1**.

DElncRNAs identified by limma package with a $p < 0.001$ were selected for WGCNA. The soft-thresholding power β was ten to ensure scale-free $R^2 > 0.85$ (**Supplementary Figure 3**). The DElncRNAs were clustered into sixteen modules with different colors, including black, darkgray, darkmagenta, darkorange, darkred, darkturquoise, lightgreen, lightyellow, midnightblue, orange, paleturquoise, red, royalblue, salmon, sienna3, and steelblue, excluding the gray module (**Figure 2**). The correlation between module memberships and the gene significance for CAD was also calculated (**Supplementary Figure 4**). Same as the module selection criteria above, the salmon and lightgreen modules were selected to construct the ceRNA networks.

Functional Enrichment

193 hub genes in the brown and pink module were subjected to perform functional enrichment analysis utilizing the DAVID and Metascape online tool to investigate the biological effects. The significant enriched GOBPs included regulation of ion transmembrane transport, O-glycan processing, telencephalon cell migration, positive regulation of glucose import, and renal water homeostasis. In addition, golgi lumen, plasma membrane, and extracellular region were significantly enriched in GOCCs. For MF, the most significant entries were G-protein coupled receptor binding, channel activity, and passive transmembrane transporter activity (**Figure 3**). The results of Metascape demonstrated that hub genes were mainly enriched in the matrisome-associated pathway, cell-cell recognition, regulation of cellular component size, regulation of transmembrane transport, and cell-cell adhesion *via* plasma-membrane adhesion molecules (**Figure 4**).

The ceRNA Regulatory Network

The intersection of the online tool miRWalk and three databases, TargetScan, miRDB, and miRTarBase was established to predict

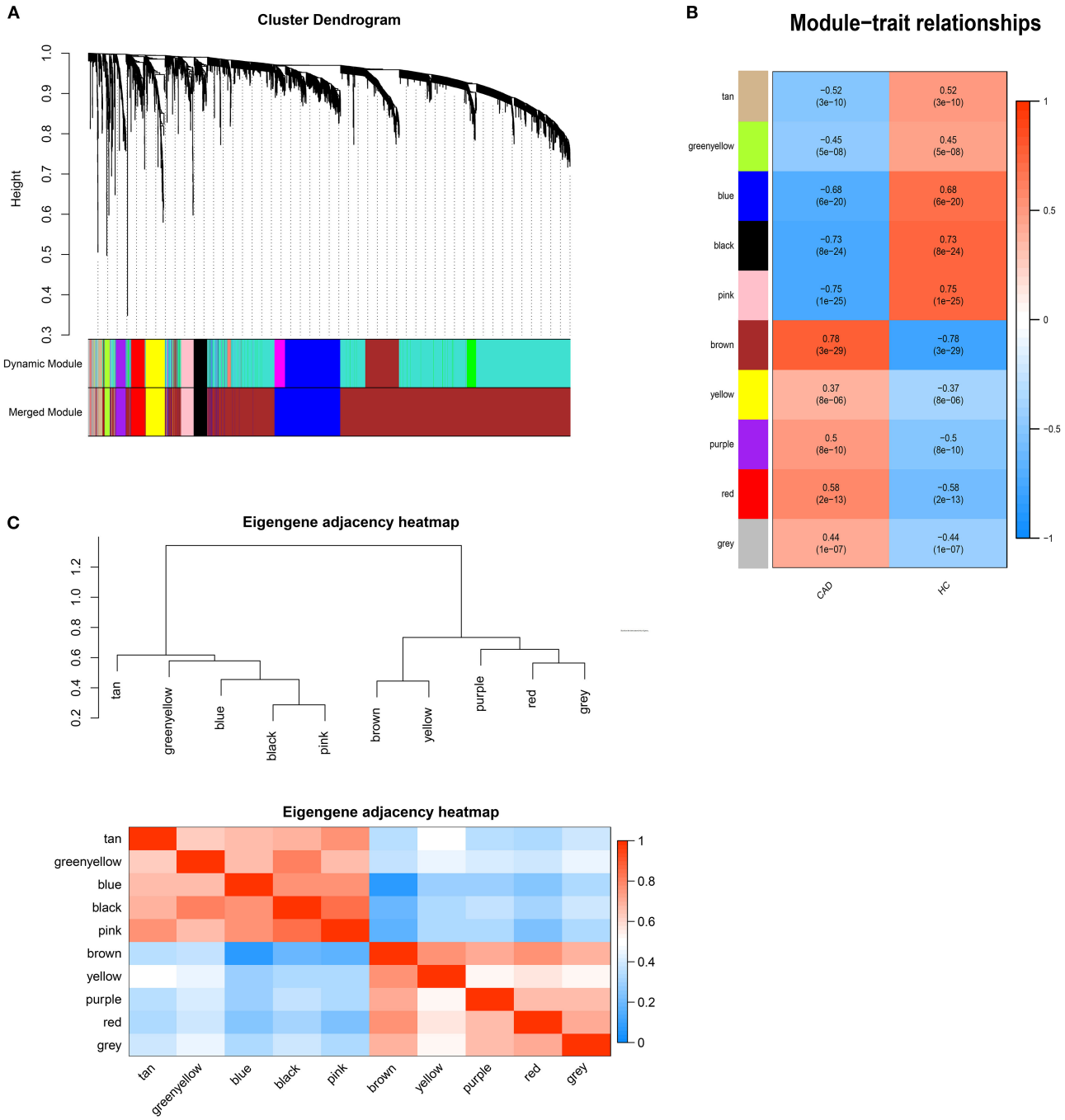

FIGURE 1 | Weighted genes correlation network analysis. **(A)** The dendrogram of differentially expressed genes. **(B)** The heatmap of module-trait correlations. Blue represents negative correlation, and red represents positive correlation. **(C)** The clustering heatmap between modules. Red means closer similarity, and blue means farther similarity.

the target miRNAs of hub genes in the brown module. A total of seven miRNAs were screened out, including hsa-miR-195-3p, hsa-miR-188-5p, hsa-miR-204-5p, hsa-miR-211-5p, hsa-miR-526b-3p, hsa-miR-92b-3p, and hsa-miR-25-3p. Among them, hsa-miR-195-3p and hsa-miR-188-5p regulate UBE2I; hsa-miR-204-5p, hsa-miR-211-5p, and hsa-miR-526b-3p regulate SMOC1; hsa-miR-92b-3p regulates DKK3 and has-miR-25-3p regulates TMEM184B; has-miR-15b-5p and has-miR-503-5p regulate C1orf21. The starbase database was used to predict interaction relationships between miRNAs and lncRNAs, and the intersection of the predicted lncRNAs and DElncRNAs in modules identified above was established to

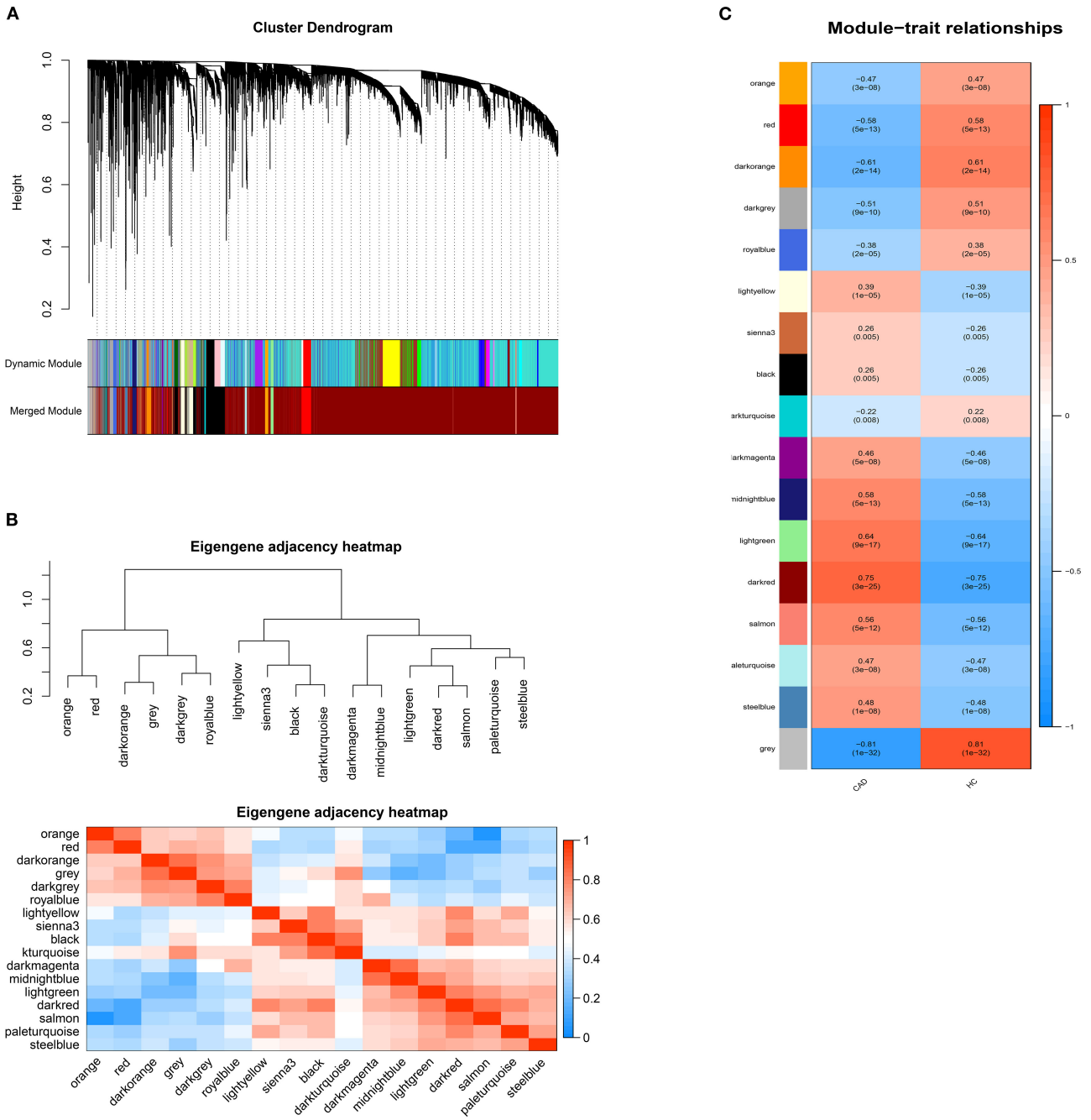

FIGURE 2 | Weighted genes correlation network analysis. **(A)** The dendrogram of differentially expressed lncRNAs. **(B)** The heatmap of module-trait correlations. Blue represents negative correlation, and red represents positive correlation. **(C)** The clustering heatmap between modules. Red means closer similarity, and blue means farther similarity.

search for lncRNAs which may play a potential role in the pathophysiological process of CAD. The lncRNA OIP5-AS1 was identified to regulate hsa-miR-204-5p, hsa-miR-211-5p, hsa-miR-92b-3p, and hsa-miR-25-3p. The ceRNA regulatory network was then visualized using the Cytoscape software (v3.8.1) (**Table 2**; **Figure 5**).

Validation Using qRT-PCR

The lncRNAs, miRNAs, and mRNAs identified above were verified utilizing qRT-PCR. The results demonstrated that the expression levels of OIP5-AS1, DKK3, SMOC1, and TMEM184B were significantly higher in patients with CAD, while miR-204-5p, miR-211-5p, miR-92b-3p, and miR-25-3p levels were

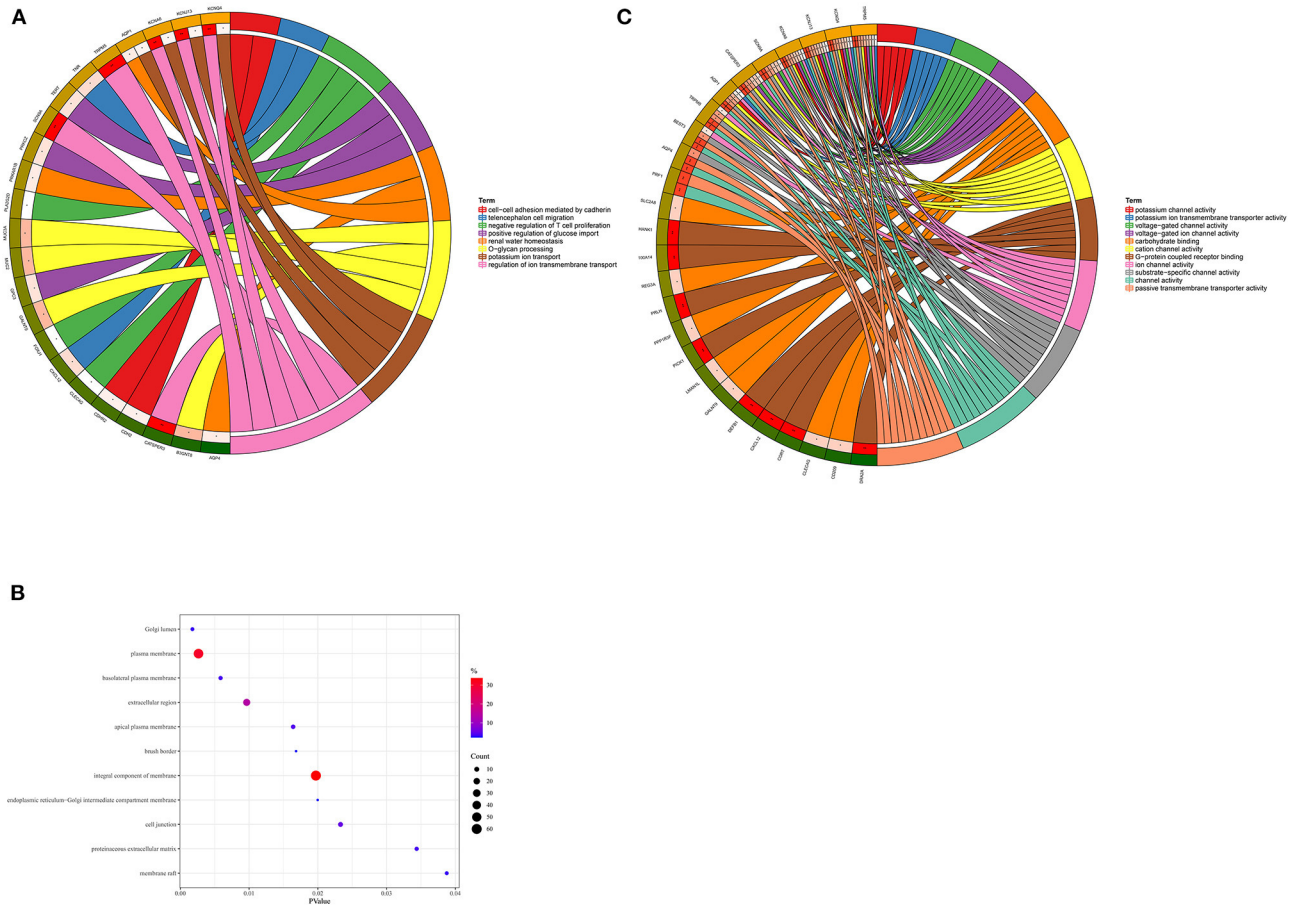

FIGURE 3 | Gene Ontology enrichment analysis. **(A)** Biological process. **(B)** Cellular component. **(C)** Molecular function.

significantly lower, which were consistent with our bioinformatic analysis (**Figure 6**).

DISCUSSION

In this study, we downloaded the GSE113079 dataset from the GEO database for bioinformatics analysis. The limma package in the R language was applied to identify the DEGs and DELncRNAs between patients with CAD and healthy controls. Then WGCNA was performed to cluster DEGs and DELncRNAs into different modules and calculate the relationships between modules and CAD. The brown module of DEGs was identified as the key module with the highest correlation coefficient. 188 hub genes in the brown module were selected for functional enrichment analysis. The significant enriched GOBPs included regulation of ion transmembrane transport, O-glycan processing, telencephalon cell migration, positive regulation of glucose import, and renal water homeostasis. The results of Metascape showed that these hub genes were mainly enriched in the matrisome-associated pathway, regulation of cellular component size, and cell-cell recognition. Then three online databases, including TargetScan, miRDB, and miRTarBase, and the online tool miRWalk were used to predict the potential target miRNAs. Nine miRNAs which may regulate hub genes were identified, including hsa-miR-195-3p, hsa-miR-188-5p, hsa-miR-204-5p, hsa-miR-211-5p, hsa-miR-526b-3p, hsa-miR-92b-3p, hsa-miR-25-3p, has-miR-15b-5p and has-miR-503-5p. The Starbase database was used to predict the relationships between seven miRNAs and DElncRNAs in modules selected above to identify potential interactions. The lncRNA OIP5-AS1 was screened out to regulate hsa-miR-204-5p, hsa-miR-211-5p, hsa-miR-92b-3p, and hsa-miR-25-3p. In all, we identified three novel ceRNA networks, including OIP5-AS1 - miR-204-5p/miR-211-5p - SMOC1, OIP5-AS1 - miR-92b-3p – DKK3, and OIP5-AS1 - miR-25-3p - TMEM184B, which have not been studied in CAD before. In the previous study conducted by He et al. (10), they also utilized the GSE113079 dataset to identify the DEGs and DElncRNAs in CAD. However, we applied WGCNA, which can explore the relationships between gene modules and the clinical phenotypes and make results more reliable, to further analyze DEGs and DElncRNAs in the present study and identified the different regulatory nodes. Moreover, He et al. only verified five miRNAs in ceRNA networks, whereas we verified all lncRNAs, miRNAs, and mRNAs in the ceRNA networks using our clinical

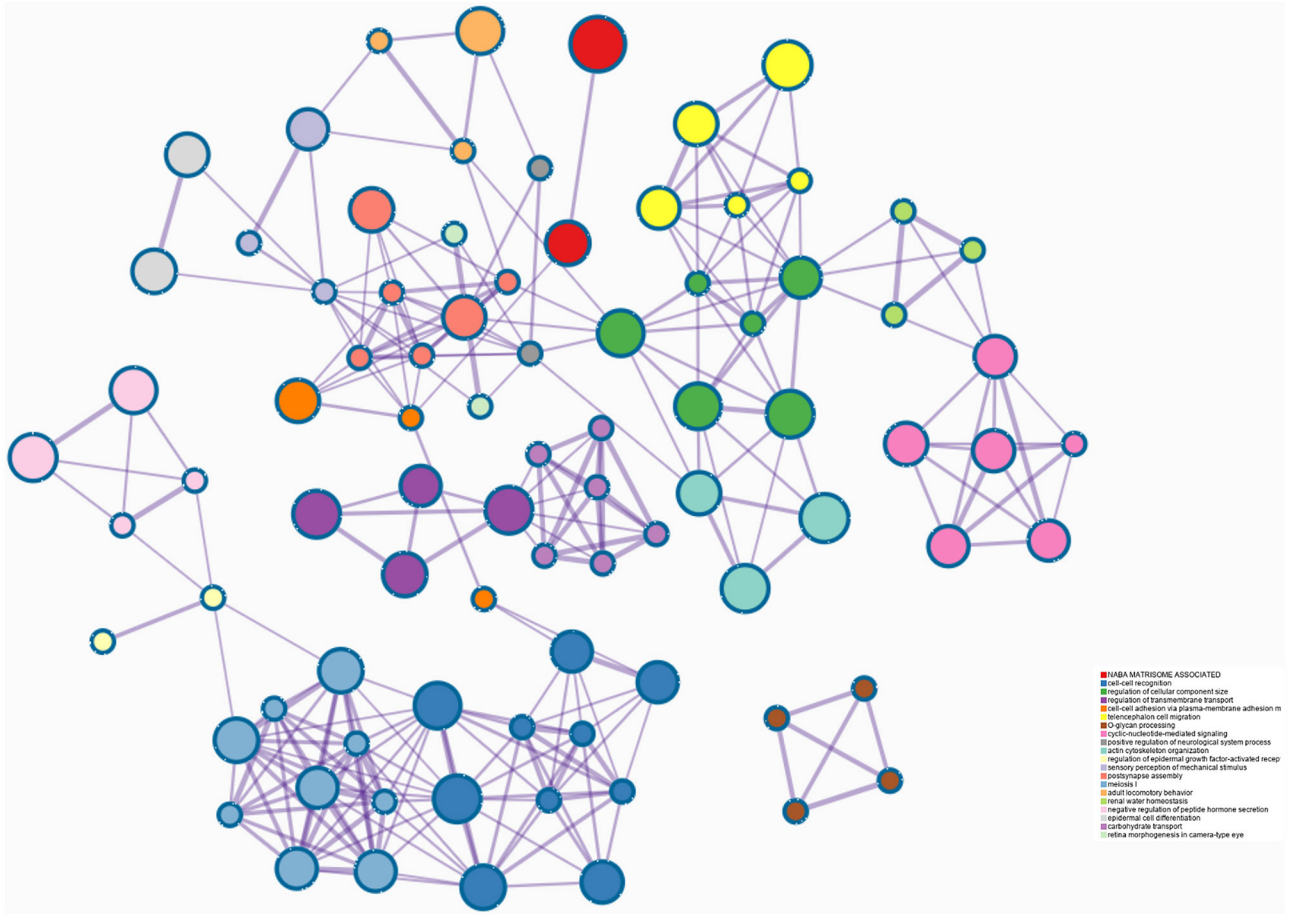

FIGURE 4 | Enrichment analysis using the Meatscape.

TABLE 2 | The regulatory networks between lncRNAs, miRNAs, and mRNAs.

lncRNA	miRNA	mRNA
OIP5-AS1	miR-204-5p	SMOC1
OIP5-AS1	miR-211-5p	SMOC1
OIP5-AS1	miR-92b-3p	DKK3
OIP5-AS1	miR-25-3p	TMEM184B

samples to make our results more credible and worthy of further study in clinical application.

OIP5-AS1 is a long non-coding RNA located on human chromosome 15q15.1, which is involved in regulating cell proliferation (11). Some studies have shown that OIP5-AS1 is related to the pathophysiological process of atherosclerosis. A previous study demonstrated that OIP5-AS1 contributed to the progression of atherosclerosis by targeting miR-26a-5p, and OIP5-AS1 knockdown could promote cell proliferation and reduce apoptosis and inflammatory response (12). A recent integrated analysis identified six key lncRNAs, including OIP5-AS1, whose expression pattern was highly correlated with the disease stage of atherogenesis (13). Another study showed that OIP5-AS1 promoted oxidative low-density lipoprotein induced endothelial cell injury, which may be involved in the pathological process of atherogenesis (14). Moreover, OIP5-AS1 could activate the SIRT1/AMPK/PGC1α pathway by sponging miR-29a to attenuate myocardial ischemia/reperfusion injury (15). OIP5-AS1 is also considered as a carcinoma-related lncRNA in many types of cancer. It was proved to be overexpressed in lung cancer (16, 17), breast cancer (18), osteosarcoma (19, 20), and hepatoblastoma (21), which were related to later cancer stages and metastasis. However, in multiple myeloma and radioresistant colorectal cancer, OIP5-AS1 was downregulated and played an important role in anti-tumor effects (22). In addition, current evidence suggested that OIP5-AS1 was related to osteoarthritis (23), rheumatoid arthritis (24), primary open angle glaucoma (25), and diabetes (26, 27).

The microRNA miR-204-5p and miR-211-5p were predicted to regulate SMOC1. Down-regulation of miR-204-5p was proved to attenuate endothelial cell dysfunction, which was associated with atherogenesis (28, 29). Another study demonstrated that the expression level of miR-204-5p was significantly lower in atherosclerotic plaque tissues and blood samples than

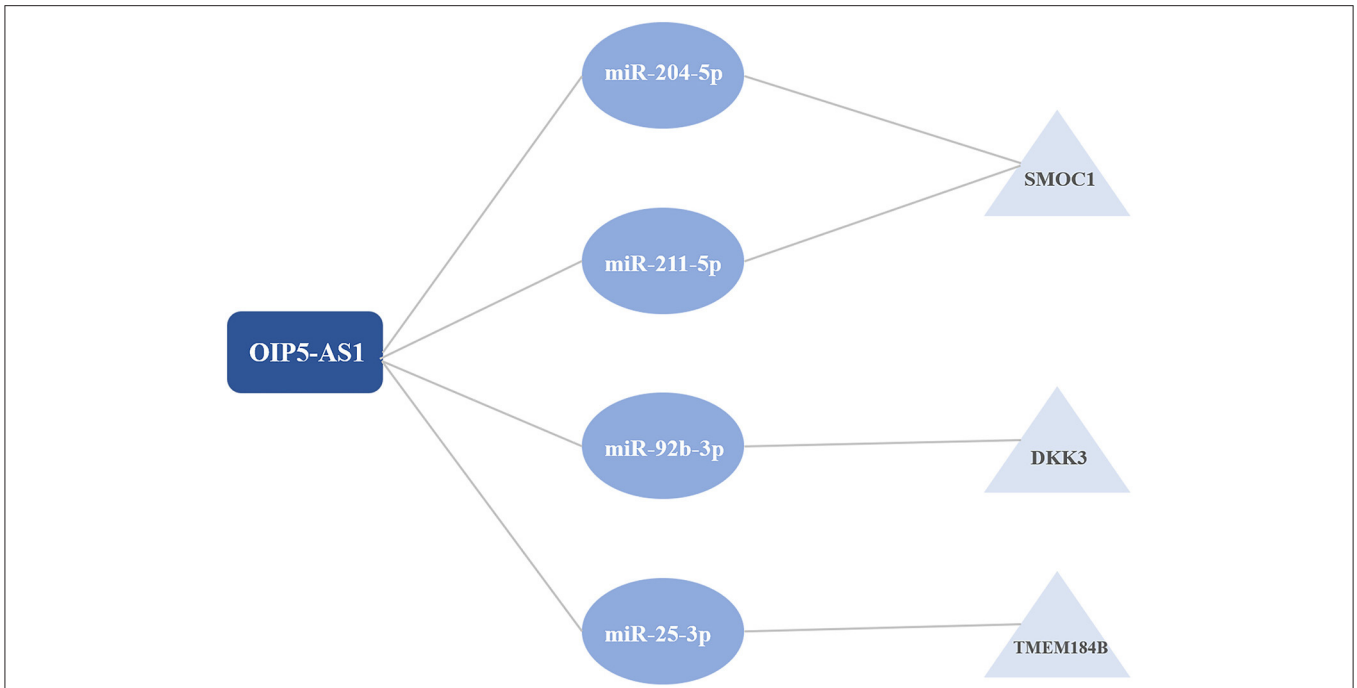

FIGURE 5 | The competitive endogenous RNA (ceRNA) regulatory networks.

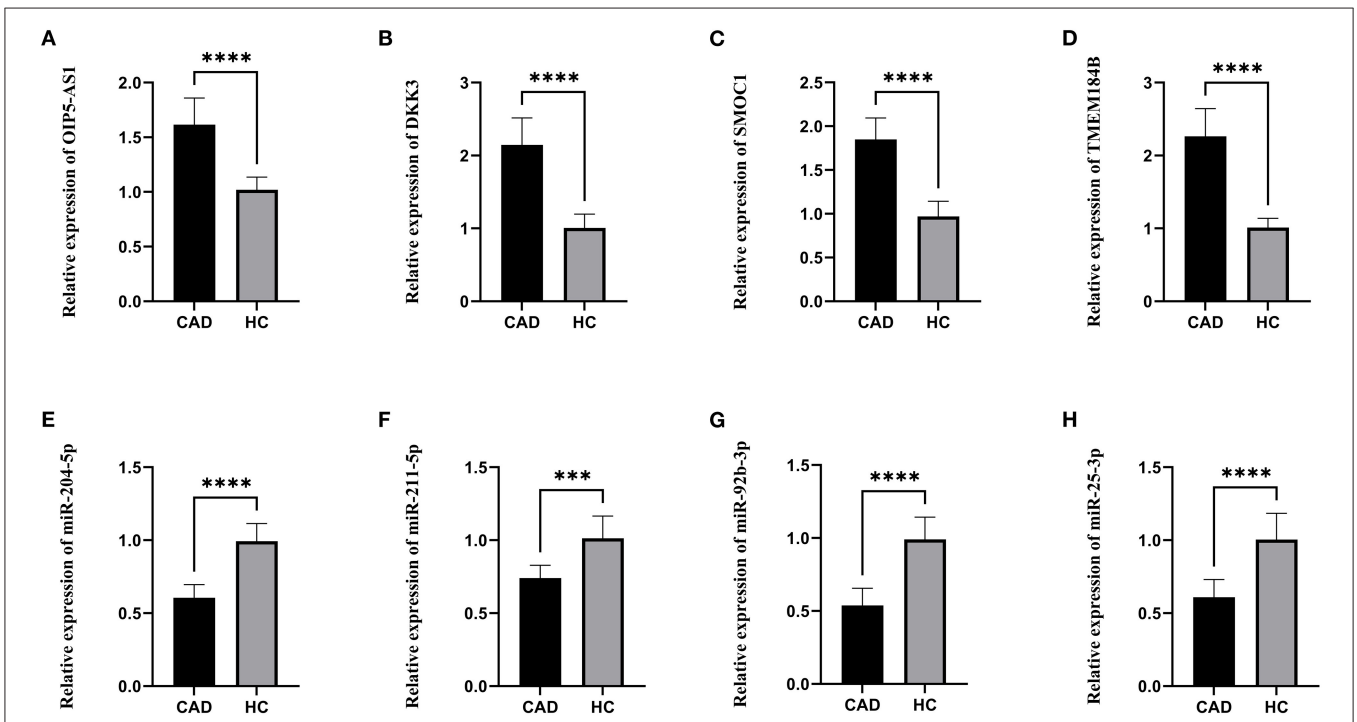

FIGURE 6 | The relative expression levels. **(A)** The relative expression level of OIP5-AS1. **(B)** The relative expression level of DKK3. **(C)** The relative expression level of SMOC1. **(D)** The relative expression level of TMEM184B. **(E)** The relative expression level of miR-204-5p. **(F)** The relative expression level of miR-211-5p. **(G)** The relative expression level of miR-92b-3p. **(H)** The relative expression level of miR-25-3p. CAD, Coronary artery disease; HC, Healthy control. ***$p < 0.001$, ****$p < 0.0001$.

in healthy controls. Further studies indicated that miR-204-5p played a crucial role in the growth and migration of human vascular smooth muscle cells by targeting MMP-9 (30). Moreover, mir-204-5p was also involved in the pathophysiological process of aortic valve calcification, which shared many common characteristics of atherogenesis (31, 32). The microRNA miR-211-5p could inhibit cortical neuron differentiation and survival and strengthen oxidative stress in Alzheimer's disease (33, 34). In osteoarthritis, miR-211-5p contributed to chondrocyte differentiation by suppressing Fibulin-4 expression (35, 36). Several previous studies showed that mir-211-5p was also associated with many types of cancer, including renal cancer, hepatocellular carcinoma, breast cancer, and malignant melanoma (37–43). SMOC1 is a protein-coding gene that may play an important role in ocular development (44–47). Recent studies demonstrated that SMOC1 was also associated with Alzheimer's disease (48–50). However, the role of miR-211-5p and SMOC1 in cardiovascular diseases has rarely been studied.

MiR-92b-3p-DKK3 and miR-25-3p-TMEM184B were also identified in our study. Compared with the peripheral venous circulation, the level of expression was lower for miR-92b-3p in the coronary sinus of patients with heart failure (51). The expression level of miR-92b-3p was lower under the hypoxic condition, and it can inhibit proliferation and cell cycle progression in pulmonary arterial hypertension (52). Previous research indicated that miR-92b-3p played a crucial role in vascular smooth muscle cell proliferation by hypoxia (53). Another study showed that it could inhibit cardiomyocyte hypertrophy by targeting HAND2 (54). DKK3 is a member of the Dickkopf family, which is decreased in a variety of cancers serving as a tumor suppressor gene (55). In ApoE-deficient mice, the expression of DKK3 was involved in the pathogenesis of atherosclerosis *via* the Wnt/β-catenin pathway (56). In a prospective population-based study, the expression of plasma DKK3 was inversely related to the 5-year progression of carotid atherosclerosis (57). Serum DKK3 level was also inversely associated with coronary stenosis in a Chinese cohort (58). Another study demonstrated that DKK3 might have a therapeutic effect in reducing intraplaque hemorrhage related to atherosclerotic plaque phenotype (59). These pieces of evidence indicated that DKK3 might play an important role in CAD. The miR-25-3p inhibited coronary vascular endothelial cell inflammation through the NF-kappaB pathway in $ApoE^{-/-}$ mice (60). It was reported that miR-25-3p could promote endothelial cell angiogenesis in aging mice (61). TMEM184B is a protein-coding gene that may activate the MAPK signaling pathway. The role of TMEM184B in cardiovascular diseases has never been reported, which is worth of further research.

Previous WGCNA studies in CAD all focused on the expression of mRNA. To the best of our knowledge, it is the first time that WGCNA was used to analyze the expression of lncRNA and mRNA between patients with CAD and healthy controls and to construct the ceRNA regulatory networks. Nevertheless, there are some limitations to our study. First, the data we acquired was from the public database, lacking clinical trait data. Second, although we identified three novel ceRNA networks in this study, further mechanistic studies should be conducted for a better understanding of the pathological process in CAD.

CONCLUSION

In this study, we identified three novel ceRNA regulatory networks, including OIP5-AS1-miR-204-5p/miR-211-5p-SMOC1, OIP5-AS1-miR-92b-3p-DKK3, and OIP5-AS1-miR-25-3p-TMEM184B, using integrated bioinformatics analysis, which were worthy of further study. Our research might provide a novel insight into ceRNA mechanisms in CAD progression.

DATA AVAILABILITY STATEMENT

The dataset presented in this study can be found at https://www.ncbi.nlm.nih.gov/geo/query/acc.cgi?acc=GSE113079.

ETHICS STATEMENT

The studies involving human participants were reviewed and approved by Medical Ethics Committee of Shanghai Tenth People's Hospital, Tongji University. The patients/participants provided their written informed consent to participate in this study.

AUTHOR CONTRIBUTIONS

All authors listed have made a substantial, direct and intellectual contribution to the work, reviewed the final manuscript, and approved it for publication.

FUNDING

This study was supported by the General Program of the National Natural Science Foundation of China (No. 81770408).

ACKNOWLEDGMENTS

We thanked Professor Ban Liu, Dr. Qi Wu, and Dr. Zhengyang Hu for their valuable advice.

SUPPLEMENTARY MATERIAL

The Supplementary Material for this article can be found online at: https://www.frontiersin.org/articles/10.3389/fcvm.2021.647953/full#supplementary-material

REFERENCES

1. Roth GA, Johnson C, Abajobir A, Abd-Allah F, Abera SF, Abyu G, et al. Global, regional, and national burden of cardiovascular diseases for 10 causes, 1990 to 2015. *J Am Coll Cardiol.* (2017) 70:1–25. doi: 10.1016/j.jacc.2017.04.052
2. Ohira T, Iso H. Cardiovascular disease epidemiology in Asia: an overview. *Circ J.* (2013) 77:1646–52. doi: 10.1253/circj.cj-13-0702
3. Musunuru K, Kathiresan S. Genetics of common, complex coronary artery disease. *Cell.* (2019) 177:132–45. doi: 10.1016/j.cell.2019.02.015
4. Mahmood SS, Levy D, Vasan RS, Wang TJ. The Framingham Heart Study and the epidemiology of cardiovascular disease: a historical perspective. *Lancet.* (2014) 383:999–1008. doi: 10.1016/S0140-6736(13)61752-3
5. McCullough PA. Coronary artery disease. *Clin J Am Soc Nephrol.* (2007) 2:611–6. doi: 10.2215/CJN.03871106
6. Zhong W, Deng Q, Deng X, Zhong Z, Hou J. Long non-coding RNA expression profiles in peripheral blood mononuclear cells of patients with coronary artery disease. *J Thorac Dis.* (2020) 12:6813–25. doi: 10.21037/jtd-20-3105
7. Meng Q, Pu L, Luo X, Wang B, Li F, Liu B. Regulatory roles of related long non-coding RNAs in the process of atherosclerosis. *Front Physiol.* (2020) 11:564604. doi: 10.3389/fphys.2020.564604
8. Salmena L, Poliseno L, Tay Y, Kats L, Pandolfi PP, A. ceRNA hypothesis: the Rosetta Stone of a hidden RNA language? *Cell.* (2011) 146:353–8. doi: 10.1016/j.cell.2011.07.014
9. Qi X, Zhang DH, Wu N, Xiao JH, Wang X, Ma W. ceRNA in cancer: possible functions and clinical implications. *J Med Genet.* (2015) 52:710–8. doi: 10.1136/jmedgenet-2015-103334
10. He J, Li X, Zhang Y, Zhang Q, Li L. Comprehensive analysis of ceRNA regulation network involved in the development of coronary artery disease. *Biomed Res Int.* (2021) 2021:6658115. doi: 10.1155/2021/6658115
11. Naemura M, Kuroki M, Tsunoda T, Arikawa N, Sawata Y, Shirasawa S, et al. The Long noncoding RNA OIP5-AS1 is involved in the regulation of cell proliferation. *Anticancer Res.* (2018) 38:77–81. doi: 10.21873/anticanres.12194
12. Ren M, Wang T, Han Z, Fu P, Liu Z, Ouyang C. Long noncoding RNA OIP5-AS1 contributes to the progression of atherosclerosis by targeting miR-26a-5p through the AKT/NF-kappaB pathway. *J Cardiovasc Pharmacol.* (2020) 76:635–44. doi: 10.1097/FJC.0000000000000889
13. Qian C, Xia M, Yang X, Chen P, Ye Q. Long noncoding RNAs in the progression of atherosclerosis: an integrated analysis based on competing endogenous RNA theory. *DNA Cell Biol.* (2020) 40:283–92. doi: 10.1089/dna.2020.6106
14. Zheng Z, Zhang G, Liang X, Li T. LncRNA OIP5-AS1 facilitates ox-LDL-induced endothelial cell injury through the miR-98-5p/HMGB1 axis. *Mol Cell Biochem.* (2020) 476:443–55. doi: 10.1007/s11010-020-03921-5
15. Niu X, Pu S, Ling C, Xu J, Wang J, Sun S, et al. lncRNA Oip5-as1 attenuates myocardial ischaemia/reperfusion injury by sponging miR-29a to activate the SIRT1/AMPK/PGC1alpha pathway. *Cell Prolif.* (2020) 53:e12818. doi: 10.1111/cpr.12818
16. Wang M, Sun X, Yang Y, Jiao W. Long non-coding RNA OIP5-AS1 promotes proliferation of lung cancer cells and leads to poor prognosis by targeting miR-378a-3p. *Thorac Cancer.* (2018) 9:939–49. doi: 10.1111/1759-7714.12767
17. Deng J, Deng H, Liu C, Liang Y, Wang S. Long non-coding RNA OIP5-AS1 functions as an oncogene in lung adenocarcinoma through targeting miR-448/Bcl-2. *Biomed Pharmacother.* (2018) 98:102–10. doi: 10.1016/j.biopha.2017.12.031
18. Zeng H, Wang J, Chen T, Zhang K, Chen J, Wang L, et al. Downregulation of long non-coding RNA Opa interacting protein 5-antisense RNA 1 inhibits breast cancer progression by targeting sex-determining region Y-box 2 by microRNA-129-5p upregulation. *Cancer Sci.* (2019) 110:289–302. doi: 10.1111/cas.13879
19. Kun-Peng Z, Chun-Lin Z, Xiao-Long M, Lei Z. Fibronectin-1 modulated by the long noncoding RNA OIP5-AS1/miR-200b-3p axis contributes to doxorubicin resistance of osteosarcoma cells. *J Cell Physiol.* (2019) 234:6927–39. doi: 10.1002/jcp.27435
20. Song L, Zhou Z, Gan Y, Li P, Xu Y, Zhang Z, et al. Long noncoding RNA OIP5-AS1 causes cisplatin resistance in osteosarcoma through inducing the LPAATbeta/PI3K/AKT/mTOR signaling pathway by sponging the miR-340-5p. *J Cell Biochem.* (2019) 120:9656–66. doi: 10.1002/jcb.28244
21. Zhang Z, Liu F, Yang F, Liu Y. Kockdown of OIP5-AS1 expression inhibits proliferation, metastasis and EMT progress in hepatoblastoma cells through up-regulating miR-186a-5p and down-regulating ZEB1. *Biomed Pharmacother.* (2018) 101:14–23. doi: 10.1016/j.biopha.2018.02.026
22. Li Y, Han X, Feng H, Han J. Long noncoding RNA OIP5-AS1 in cancer. *Clin Chim Acta.* (2019) 499:75–80. doi: 10.1016/j.cca.2019.08.031
23. Zhi L, Zhao J, Zhao H, Qing Z, Liu H, Ma J. Downregulation of LncRNA OIP5-AS1 induced by IL-1beta aggravates osteoarthritis via regulating miR-29b-3p/PGRN. *Cartilage.* (2020):940077951. doi: 10.1177/1947603519900801
24. Qing P, Liu Y. Inhibitory role of long non-coding RNA OIP5-AS1 in rheumatoid arthritis progression through the microRNA-448-paraoxonase 1-toll-like receptor 3-nuclear factor kappaB axis. *Exp Physiol.* (2020) 105:1708–19. doi: 10.1113/EP088608
25. Zhou M, Lu B, Tan W, Fu M. Identification of lncRNA-miRNA-mRNA regulatory network associated with primary open angle glaucoma. *BMC Ophthalmol.* (2020) 20:104. doi: 10.1186/s12886-020-01365-5
26. Fu JX, Sun GQ, Wang HL, Jiang HX. LncRNA OIP5-AS1 induces epithelial-to-mesenchymal transition and renal fibrosis in diabetic nephropathy via binding to miR-30c-5p. *J Biol Regul Homeost Agents.* (2020) 34:961–8. doi: 10.23812/20-199-A-68
27. Xie W, Wu D, Ren Y, Jiang Y, Zhang H, Yang S, et al. OIP5-AS1 attenuates microangiopathy in diabetic mouse by regulating miR-200b/ACE2. *World Neurosurg.* (2020) 139:e52–60. doi: 10.1016/j.wneu.2020.03.063
28. Wang Z, Zhang M, Wang Z, Guo Z, Wang Z, Chen Q. Cyanidin-3-O-glucoside attenuates endothelial cell dysfunction by modulating miR-204-5p/SIRT1-mediated inflammation and apoptosis. *Biofactors.* (2020) 46:803–12. doi: 10.1002/biof.1660
29. Lu G, Tian P, Zhu Y, Zuo X, Li X. LncRNA XIST knockdown ameliorates oxidative low-density lipoprotein-induced endothelial cells injury by targeting miR-204-5p/TLR4. *J Biosci.* (2020) 45:52. doi: 10.1007/s12038-020-0022-0
30. Wang N, Yuan Y, Sun S, Liu G. microRNA-204-5p participates in atherosclerosis via targeting MMP-9. *Open Med (Wars).* (2020) 15:231–9. doi: 10.1515/med-2020-0034
31. Wang Y, Han D, Zhou T, Zhang J, Liu C, Cao F, et al. Melatonin ameliorates aortic valve calcification via the regulation of circular RNA CircRIC3/miR-204-5p/DPP4 signaling in valvular interstitial cells. *J Pineal Res.* (2020) 69:e12666. doi: 10.1111/jpi.12666
32. Yu C, Li L, Xie F, Guo S, Liu F, Dong N, et al. LncRNA TUG1 sponges miR-204-5p to promote osteoblast differentiation through upregulating Runx2 in aortic valve calcification. *Cardiovasc Res.* (2018) 114:168–79. doi: 10.1093/cvr/cvx180
33. Zhu R, Qi X, Liu C, Wang D, Li L, Liu X, et al. The silent information regulator 1 pathway attenuates ROS-induced oxidative stress in Alzheimer's disease. *J Integr Neurosci.* (2020) 19:321–32. doi: 10.31083/j.jin.2020.02.1151
34. Fan C, Wu Q, Ye X, Luo H, Yan D, Xiong Y, et al. Role of miR-211 in neuronal differentiation and viability: implications to pathogenesis of Alzheimer's disease. *Front Aging Neurosci.* (2016) 8:166. doi: 10.3389/fnagi.2016.00166
35. Prasadam I, Batra J, Perry S, Gu W, Crawford R, Xiao Y. Systematic identification, characterization and target gene analysis of microRNAs involved in osteoarthritis subchondral bone pathogenesis. *Calcif Tissue Int.* (2016) 99:43–55. doi: 10.1007/s00223-016-0125-7
36. Liu H, Luo J. miR-211-5p contributes to chondrocyte differentiation by suppressing Fibulin-4 expression to play a role in osteoarthritis. *J Biochem.* (2019) 166:495–502. doi: 10.1093/jb/mvz065
37. Wang K, Jin W, Jin P, Fei X, Wang X, Chen X. miR-211-5p suppresses metastatic behavior by targeting SNAI1 in renal cancer. *Mol Cancer Res.* (2017) 15:448–56. doi: 10.1158/1541-7786.MCR-16-0288
38. Jiang G, Wen L, Deng W, Jian Z, Zheng H. Regulatory role of miR-211-5p in hepatocellular carcinoma metastasis by targeting ZEB2. *Biomed Pharmacother.* (2017) 90:806–12. doi: 10.1016/j.biopha.2017.03.081
39. Chen LL, Zhang ZJ, Yi ZB, Li JJ. MicroRNA-211-5p suppresses tumour cell proliferation, invasion, migration and metastasis in triple-negative breast cancer by directly targeting SETBP1. *Br J Cancer.* (2017) 117:78–88. doi: 10.1038/bjc.2017.150

40. Lunavat TR, Cheng L, Einarsdottir BO, Olofsson BR, Veppil MS, Sharples RA, et al. BRAF(V600) inhibition alters the microRNA cargo in the vesicular secretome of malignant melanoma cells. *Proc Natl Acad Sci U S A.* (2017) 114:E5930–9. doi: 10.1073/pnas.1705206114
41. Diaz-Martinez M, Benito-Jardon L, Alonso L, Koetz-Ploch L, Hernando E, Teixido J. miR-204-5p and miR-211-5p contribute to BRAF inhibitor resistance in melanoma. *Cancer Res.* (2018) 78:1017–30. doi: 10.1158/0008-5472.CAN-17-1318
42. Qin X, Zhang J, Lin Y, Sun XM, Zhang JN, Cheng ZQ. Identification of MiR-211-5p as a tumor suppressor by targeting ACSL4 in hepatocellular carcinoma. *J Transl Med.* (2020) 18:326. doi: 10.1186/s12967-020-02494-7
43. De Martino E, Brunetti D, Canzonieri V, Conforti C, Eisendle K, Mazzoleni G, et al. The Association of residential altitude on the molecular profile and survival of melanoma: results of an interreg study. *Cancers (Basel).* (2020) 12:2796. doi: 10.3390/cancers12102796
44. Okada I, Hamanoue H, Terada K, Tohma T, Megarbane A, Chouery E, et al. SMOC1 is essential for ocular and limb development in humans and mice. *Am J Hum Genet.* (2011) 88:30–41. doi: 10.1016/j.ajhg.2010.11.012
45. Abouzeid H, Boisset G, Favez T, Youssef M, Marzouk I, Shakankiry N, et al. Mutations in the SPARC-related modular calcium-binding protein 1 gene, SMOC1, cause waardenburg anophthalmia syndrome. *Am J Hum Genet.* (2011) 88:92–8. doi: 10.1016/j.ajhg.2010.12.002
46. Slavotinek AM. Eye development genes and known syndromes. *Mol Genet Metab.* (2011) 104:448–56. doi: 10.1016/j.ymgme.2011.09.029
47. Slavotinek A. Genetics of anophthalmia and microphthalmia. Part 2: Syndromes associated with anophthalmia-microphthalmia. *Hum Genet.* (2019) 138:831–46. doi: 10.1007/s00439-018-1949-1
48. Wang H, Dey KK, Chen PC Li Y, Niu M, Cho JH, et al. Integrated analysis of ultra-deep proteomes in cortex, cerebrospinal fluid and serum reveals a mitochondrial signature in Alzheimer's disease. *Mol Neurodegener.* (2020) 15:43. doi: 10.1186/s13024-020-00384-6
49. Sathe G, Albert M, Darrow J, Saito A, Troncoso J, Pandey A, et al. Quantitative proteomic analysis of the frontal cortex in Alzheimer's disease. *J Neurochem.* (2020) 156:988–1002. doi: 10.1111/jnc.15116
50. Bai B, Wang X, Li Y, Chen PC Yu K, Dey KK, et al. Deep Multilayer Brain Proteomics Identifies Molecular Networks in Alzheimer's Disease Progression. *Neuron.* (2020) 105:975–91. doi: 10.1016/j.neuron.2019.12.015
51. Ben-Zvi I, Volinsky N, Grosman-Rimon L, Haviv I, Rozen G, Andria N, et al. Cardiac-peripheral transvenous gradients of microRNA expression in systolic heart failure patients. *ESC Heart Fail.* (2020) 7:835–43. doi: 10.1002/ehf2.12597
52. Hao X, Ma C, Chen S, Dang J, Cheng X, Zhu D. Reverse the down regulation of miR-92b-3p by hypoxia can suppress the proliferation of pulmonary artery smooth muscle cells by targeting USP28. *Biochem Biophys Res Commun.* (2018) 503:3064–77. doi: 10.1016/j.bbrc.2018.08.095
53. Lee J, Heo J, Kang H. miR-92b-3p-TSC1 axis is critical for mTOR signaling-mediated vascular smooth muscle cell proliferation induced by hypoxia. *Cell Death Differ.* (2019) 26:1782–95. doi: 10.1038/s41418-018-0243-z
54. Yu XJ, Huang YQ, Shan ZX, Zhu JN, Hu ZQ, Huang L, et al. MicroRNA-92b-3p suppresses angiotensin II-induced cardiomyocyte hypertrophy via targeting HAND2. *Life Sci.* (2019) 232:116635. doi: 10.1016/j.lfs.2019.116635
55. Lee EJ, Nguyen Q, Lee M. Dickkopf-3 in human malignant tumours: a clinical viewpoint. *Anticancer Res.* (2020) 40:5969–79. doi: 10.21873/anticanres.14617
56. Cheng WL, Yang Y, Zhang XJ, Guo J, Gong J, Gong FH, et al. Dickkopf-3 ablation attenuates the development of atherosclerosis in ApoE-deficient mice. *J Am Heart Assoc.* (2017) 6:e004690. doi: 10.1161/JAHA.116.004690
57. Yu B, Kiechl S, Qi D, Wang X, Song Y, Weger S, et al. A cytokine-like protein dickkopf-related protein 3 is atheroprotective. *Circulation.* (2017) 136:1022–36. doi: 10.1161/CIRCULATIONAHA.117.027690
58. Wang L, Liu S, Niu J, Zhao Z, Xu M, Lu J, et al. Serum dickkopf-3 level is inversely associated with significant coronary stenosis in an asymptomatic Chinese cohort. *Int Heart J.* (2020) 61:1107–13. doi: 10.1536/ihj.20-094
59. Karamariti E, Zhai C, Yu B, Qiao L, Wang Z, Potter C, et al. DKK3 (Dickkopf 3) alters atherosclerotic plaque phenotype involving vascular progenitor and fibroblast differentiation into smooth muscle cells. *Arterioscler Thromb Vasc Biol.* (2018) 38:425–37. doi: 10.1161/ATVBAHA.117.310079
60. Yao Y, Sun W, Sun Q, Jing B, Liu S, Liu X, et al. Platelet-derived exosomal MicroRNA-25-3p inhibits coronary vascular endothelial cell inflammation through Adam10 via the NF-kappaB signaling pathway in ApoE(-/-) mice. *Front Immunol.* (2019) 10:2205. doi: 10.3389/fimmu.2019.02205
61. Lian C, Zhao L, Qiu J, Wang Y, Chen R, Liu Z, et al. miR-25-3p promotes endothelial cell angiogenesis in aging mice via TULA-2/SYK/VEGFR-2 downregulation. *Aging (Albany NY).* (2020) 12:22599–613. doi: 10.18632/aging.103834

Conflict of Interest: The authors declare that the research was conducted in the absence of any commercial or financial relationships that could be construed as a potential conflict of interest.

The reviewer JY declared a shared affiliation, with no collaboration, with the authors to the handling editor at the time of review.

Publisher's Note: All claims expressed in this article are solely those of the authors and do not necessarily represent those of their affiliated organizations, or those of the publisher, the editors and the reviewers. Any product that may be evaluated in this article, or claim that may be made by its manufacturer, is not guaranteed or endorsed by the publisher.

frontiers in Cardiovascular Medicine

ORIGINAL RESEARCH
published: 06 October 2021
doi: 10.3389/fcvm.2021.747449

Novel lncRNA-miRNA-mRNA Competing Endogenous RNA Triple Networks Associated Programmed Cell Death in Heart Failure

Yu Zheng[1†], *Yingjie Zhang*[1†], *Xiu Zhang*[1†], *Yini Dang*[2†], *Yihui Cheng*[1], *Wenjie Hua*[1], *Meiling Teng*[1], *Shenrui Wang*[1] *and Xiao Lu*[1*]

[1] *Department of Rehabilitation Medicine, The First Affiliated Hospital of Nanjing Medical University, Nanjing, China,*
[2] *Department of Gastroenterology, The First Affiliated Hospital of Nanjing Medical University, Nanjing, China*

Objective: Increasing evidence has uncovered the roles of lncRNA-miRNA-mRNA regulatory networks in cardiovascular diseases. However, the crosstalk between ceRNA networks and development of heart failure (HF) remains unclear. This study was to investigate the role of lncRNA-mediated ceRNA networks in the pathophysiological process of HF and its potential regulatory functions on programmed cell death.

Methods: We firstly screened the GSE77399, GSE52601 and GSE57338 datasets in the NCBI GEO database for screening differentially expressed lncRNAs, miRNAs and mRNAs. lncRNA-miRNA-mRNA regulatory networks based on the ceRNA theory were subsequently constructed. GO and KEGG enrichment analysis was conducted to predict potential biological functions of mRNAs in ceRNA networks. Differentially expressed mRNAs were then interacted with programmed cell death related genes. lncRNA-mediated ceRNA regulatory pathways on programmed cell death were validated with qRT-PCR testing.

Results: Based on our bioinformatic analysis, two lncRNAs, eight miRNAs and 65 mRNAs were extracted to construct two lncRNAs-mediated ceRNA networks in HF. Biological processes and pathways were enriched in extracellular matrix. Seven lncRNA-mediated ceRNA regulatory pathways on programmed cell death, GAS5/miR-345-5p/ADAMTS4, GAS5/miR-18b-5p/AQP3, GAS5/miR-18b-5p/SHISA3, GAS5/miR-18b-5p/C1orf105, GAS5/miR-18b-5p/PLIN2, GAS5/miR-185-5p/LPCAT3, and GAS5/miR-29b-3p/STAT3, were finally validated.

Conclusions: Two novel ceRNA regulatory networks in HF were discovered based on our bioinformatic analysis. Based on the interaction and validation analysis, seven lncRNA GAS5-mediated ceRNA regulatory pathways were hypothesized to impact programmed cell death including seven for apoptosis, three for ferroptosis, and one for pyroptosis. Upon which, we provided novel insights and potential research plots for bridging ceRNA regulatory networks and programmed cell death in HF.

Keywords: heart failure, competitive endogenous RNA, long non-coding RNA, programmed cell death, apoptosis, ferroptosis

OPEN ACCESS

Edited by:
Xiangming Ding,
University of Southern California, United States

Reviewed by:
Andre Rodrigues Duraes,
Federal University of Bahia, Brazil
Simin Li,
Southern Medical University, China

***Correspondence:**
Xiao Lu
luxiao1972@163.com

[†] These authors have contributed equally to this work and share first authorship

Specialty section:
This article was submitted to General Cardiovascular Medicine, a section of the journal Frontiers in Cardiovascular Medicine

Received: *26 July 2021*
Accepted: *09 September 2021*
Published: *06 October 2021*

Citation:
Zheng Y, Zhang Y, Zhang X, Dang Y, Cheng Y, Hua W, Teng M, Wang S and Lu X (2021) Novel lncRNA-miRNA-mRNA Competing Endogenous RNA Triple Networks Associated Programmed Cell Death in Heart Failure. Front. Cardiovasc. Med. 8:747449. doi: 10.3389/fcvm.2021.747449

INTRODUCTION

Heart Failure (HF) is the terminal stage of various cardiovascular diseases. Advanced interventions, such as pharmacological treatment, cardiac resynchronous treatment, cardiac transplantation, mainly focus on HF related symptom control (1). With these interventions, the mortality of HF has been decreased to some extent (2). Nonetheless, novel therapeutic strategies underlying cellular and molecular pathways are warranted to further decrease the mortality and improve the quality of life in patients with HF. Accordingly, there is an imperative need for further research and deeper insight into the biological mechanisms underlying HF.

Non-coding RNAs (ncRNAs), such as microRNAs (miRNAs), long non-coding RNAs (lncRNAs) and circular RNAs (circRNAs), are a group of RNAs that play critical roles in cellular and molecular physiology and pathology including epigenetic, transcriptional regulation, and post-transcriptional regulation (3). Among these ncRNAs, increasing evidence indicates that lncRNA was widely involved in the pathological process of cardiac development, atherosclerosis, myocardial infarction, hypertension and aneurysm (4–6). Dysfunction of lncRNAs was also reported in a number of studies of HF (7, 8). Specifically, lncRNA MHRT and non-coding NFAT inhibitory factor NRON was found to significantly increase in the plasma of patients with HF (9). LncRNA LIPCA, functioning in the process of cardiac remodeling, was proved to be able to predict the long-term mortality in patients with chronic HF (10). However, evidence also suggests that lncRNAs may not perform modulatory functions independently while create dynamic regulatory crosstalk networks by interacting with other ncRNAs through competitively binding to certain ncRNAs, which was previously termed as the competitive endogenous RNA (ceRNA) network theory (11).

ceRNA network had been reported as a crucial mechanism to explain the regulation of post-transcriptional gene translation (12). It has been found that lncRNA APF targets the regulation of miR-188-3p, thereby affecting the expression of ATG7 in autophagy, which can effectively reduce the area of myocardial infarction, prevent HF, and prolong survival time (13). LncRNA kcnq1ot1 was demonstrated to increase HDAC3 expression by competitively binding to miR-452-3p, followed by the inhibition of ABCA1 and cholesterol efflflux, promoted macrophage lipid accumulation and accelerated the development of atherosclerosis (14). The above findings highlighted the importance of ceRNA network, a global view of lncRNA-mediated ceRNA network may help researchers comprehensively understand the pathophysiological process of cardiovascular diseases. Nonetheless, limited evidence was found in the research field of HF and more regulatory pathways still need further verification. Considering the essential role of programmed cell death in HF, it promoted us to think about the question that "whether there are interactions between lncRNA-mediated ceRNA network and programmed cell death?" Apart from one recent study of circRNA-miRNA-mRNA regulatory network on iron homeostasis (15), there were limited evidence to reveal the interactions between these two elements. The answers to this question may renew our knowledge in the regulation of pathophysiological process after HF.

Upon the above statement, this study was aimed to construct a global lncRNA-mediated triple network (lncRNA-miRNA-mRNA) based on the NCBI GEO dataset including lncRNA, miRNA and mRNA expression profiles. Differential gene expression profiles between HF subjects and healthy controls were analyzed with "Limma" package in R software, and lncRNA-miRNA-mRNA triple regulatory networks were constructed. Gene Ontology (GO) and Kyoto Encyclopedia of Genes and Genomes (KEGG) functional enrichment analyses for the differentially expressed mRNAs in the ceRNA network was analyzed. Afterwards, we interacted the differentially expressed mRNAs in the ceRNA network with genes related to programmed cell death in open source datasets. Finally, programmed cell death-related regulatory pathways in the lncRNA-mediated ceRNA network were further verified through quantitative real-time reverse transcription-polymerase chain reaction (qRT-PCR). This study may add insights into novel molecular mechanisms underlying HF pathogenesis, specifically interactions between lncRNA-mediated ceRNA regulatory networks and programmed cell death in the pathological process of HF, and finally provide novel treatment targets for patients with HF.

MATERIALS AND METHODS

The construction of a global lncRNA-mediated triple ceRNA network (lncRNA-miRNA-mRNA) was conducted following the logic shown in **Figure 1**.

Online Data Collection

The gene expression profiles (GSE77399 for lncRNA, GSE52601 for miRNA and GSE57338 for mRNA) related to HF were downloaded from NCBI GEO (https://www.ncbi.nlm.nih.gov/geo/). The lncRNA data was collected with GPL21384 Platforms (Human Disease-related LncRNA Profiler, Molecular Cardiology, Milan, Italy), and included data from 13 patients with HF and 12 healthy controls. The miRNA array data were measured using GPL10558 Platforms (Illumina HumanHT-12 V4.0 expression beadchip, Laboratory of RNA Molecular Biology, Thomas Tuschl, New York, USA), in 16 patients with HF and eight healthy controls. The mRNA array data in GSE57338 was collected from 177 patients with HF and 136 healthy controls based on GPL11532 {Affymetrix Human Gene 1.1 ST Array [transcript (gene) version], Perelman School of Medicine at the University of Pennsylvania, Philadelphia, USA}.

Screening Strategies for Differentially Expressed lncRNAs, miRNAs and mRNAs

Differential expression analysis of lncRNAs, miRNAs, and mRNAs between patients with HF and healthy controls was conducted with "Limma" package in the R software. The screening threshold for significant difference in gene expression was adjusted with $P < 0.05$ and $|\log2FC \text{ (fold change)}| > 0.5$. For visualization, heat maps and volcano maps were generated

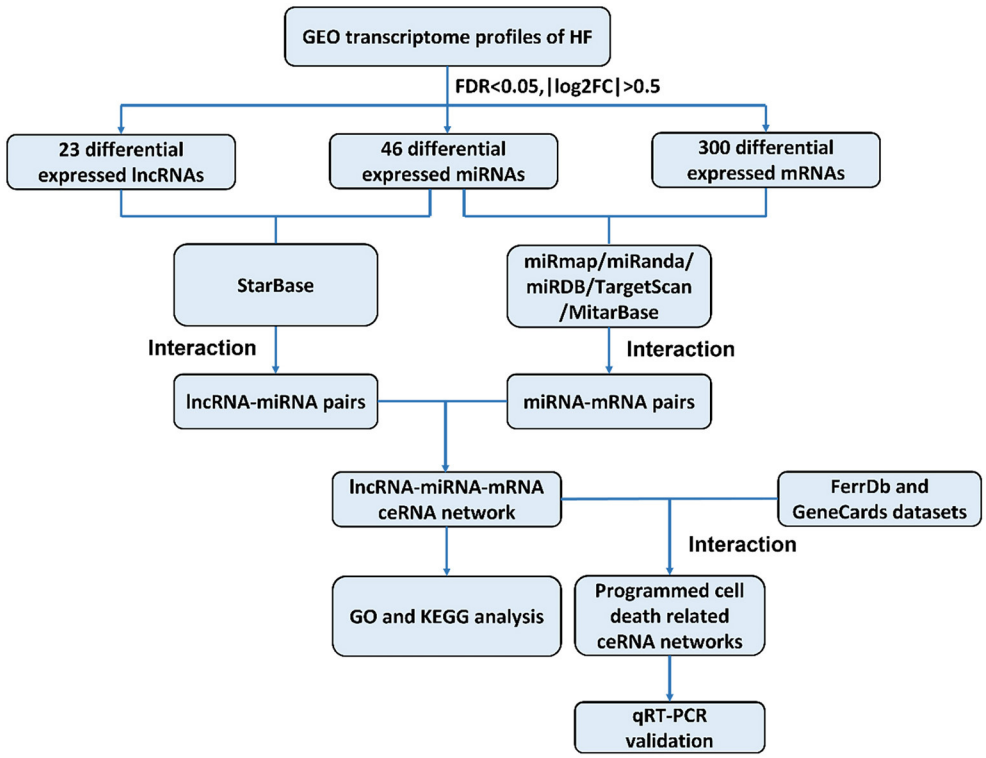

FIGURE 1 | Flowchart of construction and analysis of ceRNA networks. GEO, gene expression omnibus; HF, heart failure; FDR, false discovery rate; FC, fold change; GO, Gene Ontology; KEGG, Kyoto Encyclopedia of Genes and Genomes; qRT-PCR, quantitative real-time reverse transcription-polymerase chain reaction.

by employing the "ggplot2" and "pheatmap" packages in the R software (16).

Construction of the lncRNA-miRNA-mRNA Network

The lncRNA-miRNA-mRNA network was constructed based on ceRNA hypothesis as follows: (1) Interaction information of miRNA-mRNAs in the miRmap, miRanda, miRDB, TargetScan and MitarBase, and miRNA-lncRNAs in the StarBase were extracted (17–22); (2) if both the lncRNA and mRNA were targeted and were co-expressed negatively with one common miRNA, this lncRNA-miRNA-mRNA group was identified as co-expression competing triplet and the corresponding ceRNA regulatory networks were constructed. The ceRNA regulatory networks were visualized with Cytoscape 3.7.1 (23).

GO and KEGG Functional Enrichment Analysis

Enriched GO terms (e.g., biological process, BP; cellular component, CC and molecular function, MF) and KEGG pathways were analyzed to predict potential biological functions of mRNAs underlying our ceRNA network with the "clusterprofiler" package in the R software (24). $P < 0.05$ was considered as statistically significant and results were visualized with bubble chart.

Screening Strategy for Programmed Cell Death Related Genes in the ceRNA Network

We firstly interacted the differentially expressed mRNAs in our ceRNA network with genes related to programmed cell death in FerrDb (http://www.zhounan.org/ferrdb/) and GeneCards (https://www.genecards.org/). Afterwards, we interacted our differentially expressed mRNAs with genes related to apoptosis, pyroptosis and ferroptosis, respectively. Results were visualized by Venn diagram generated with the online tool Venny 2.1.0 [http://bioinfogp.cnb.csic.es/tools/venny/index.html (55)].

Validation of Programmed Cell Death Related Genes in ceRNA Network in HF Animal Model

All the animal experimental protocols were in accordance with all institutional and national guideline for the care and use of laboratory animals and were reviewed and approved by the Ethics Committees of the Nanjing Medical University, Jiangsu Province, China. Healthy male Wistar rats were randomized either into the sham operation (SO) or the HF group. Under anesthesia, a thoracotomy was performed through the fourth intercostal space, the heart was exposed. A suture was placed 1-1.5 mm from the left anterior descending branch (LAD), and the ends were tied loosely in the SO group and firmly in the HF group (25). After 4 weeks, HF followed by myocardial infarction

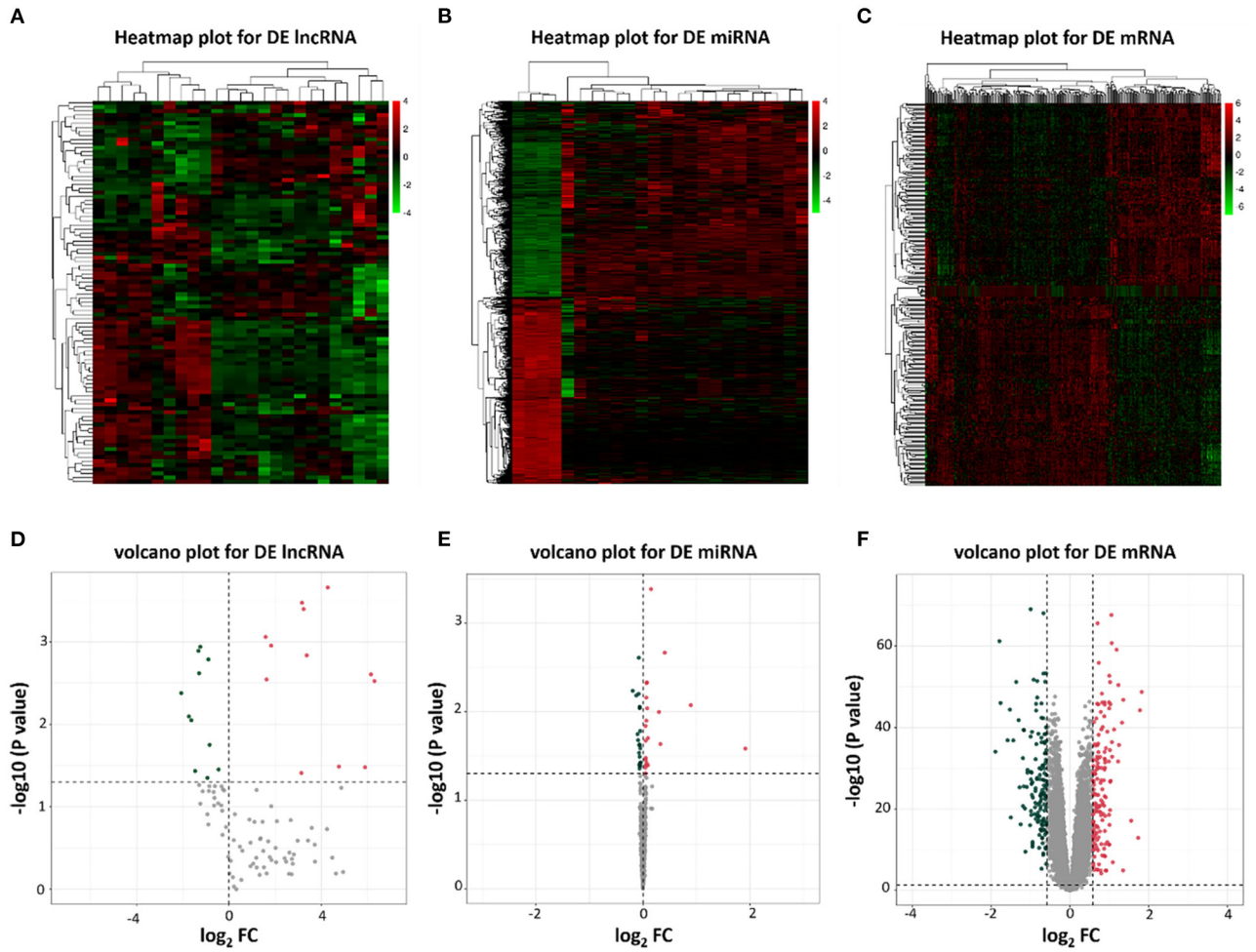

FIGURE 2 | Heatmap plots and volcano plots of differentially expressed lncRNAs, miRNAs, and mRNAs. **(A)** Heatmap of differentially expressed lncRNAs; **(B)** Heatmap of differentially expressed miRNAs; **(C)** Heatmap of differentially expressed mRNAs; **(D)** Volcano plot of 23 differentially expressed lncRNAs; **(E)** Volcano plot of 46 differentially expressed miRNAs; **(F)** Volcano plot of 300 differentially expressed mRNAs. Red represents upregulated genes and green indicates downregulated genes. DE, differentially expressed; FC, fold change.

was confirmed by multiple morphological and hemodynamic parameters (mainly due to LVEF lower than 50%) and myocardial tissues were collected from the infarcted edge area of all eligible rats (26, 27).

For qRT-PCR testing of programmed cell death related ceRNA network, a template equivalent to 400 ng of total RNA extracted from myocardial tissues were subjected to 40 cycles of quantitative PCR using the Takara SYBR Premix Ex TaqTM on StepOnePlus^{TM} Real-Time PCR System (Applied Biosystems, Foster City, California, USA). GAPDH and U6 were used as internal references and the relative expression level was calculated using the $2^{-\Delta\Delta Ct}$ method. Primer sequences used for two lncRNAs, seven miRNAs and 23 mRNAs were listed in **Supplementary Table 1**.

Statistical Analysis

Data are expressed as the mean ± SD. Differentially expressed lncRNAs from the GSE77399 were compared with Student *t*-test. Differentially expressed miRNAs and mRNAs from the GSE52601 and the GSE57338, respectively, were compared with "Limma" package in R software. "Clusterprofiler" package in R software was used to perform GO and KEGG functional enrichment analysis for differentially expressed mRNAs in our ceRNA network. The results of qRT-PCT for validation were analyzed with Student *t*-test. $P < 0.05$ were considered significantly different. All analyses were performed using SPSS 25.0 (IBM, Chicago, Illinois, USA) and GraphPad Prism 8 (GraphPad Software, San Diego, California, USA).

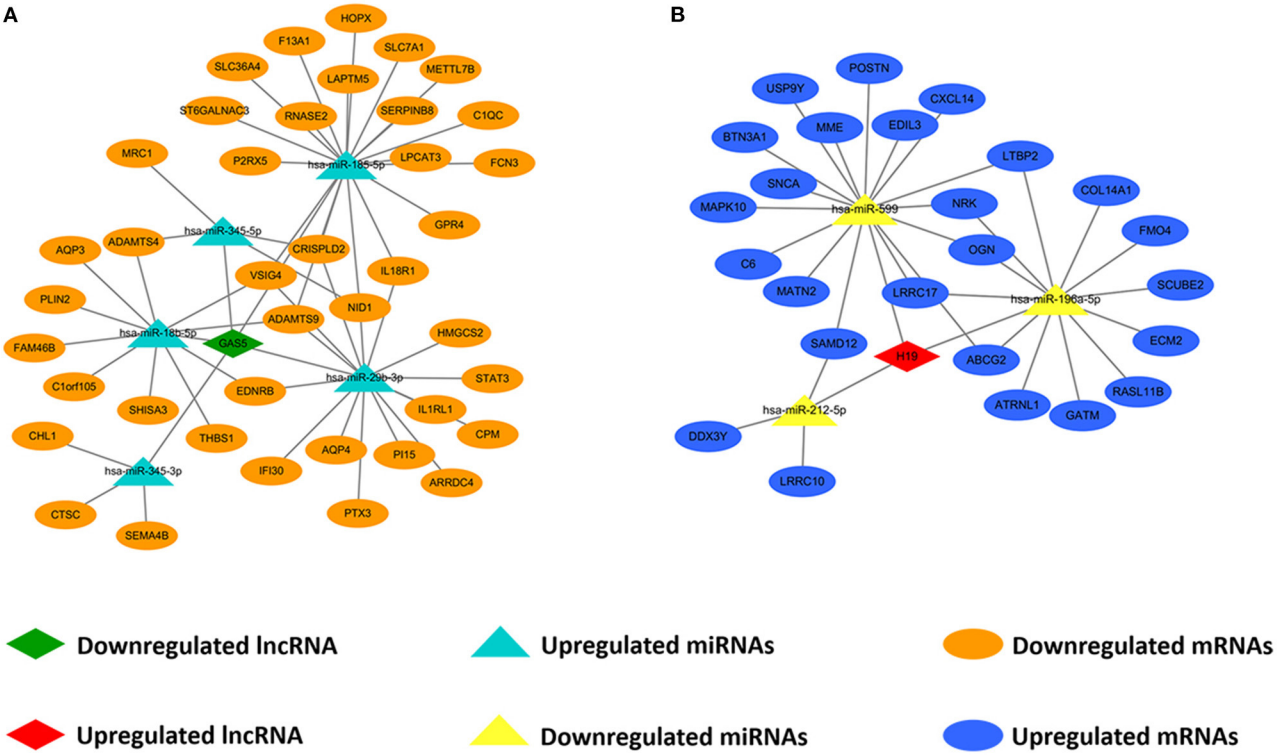

FIGURE 3 | Construction of lncRNA-mediated ceRNA regulatory network. **(A)** The lncRNA-mediated downregulated ceRNA network; **(B)** The lncRNA-mediated upregulated ceRNA network. Green means downregulated LncRNA, red means upregulated LncRNA, blue indicates upregulated miRNAs and mRNAs, yellow represents downregulated miRNAs, orange represents downregulated mRNAs.

RESULTS

Identification of Differentially Expressed lncRNAs, miRNAs and mRNAs

To identify potential differential lncRNAs, miRNAs and mRNAs in HF, a comparative analysis for expression profiles of lncRNAs, miRNAs and mRNAs between patients with HF and healthy controls using GEO dataset was performed with $P < 0.05$ and |log fold change [FC]|>0.5 as threshold. A total of 23 lncRNAs (12 upregulated and 11 downregulated), 46 miRNAs (22 upregulated and 24 downregulated) and 300 mRNAs (157 upregulated and 143 downregulated) were identified as differentially expressed genes between patients with HF and healthy controls (**Supplementary Tables 2–4**). The heatmap plots and volcano plots for differentially expressed lncRNAs, miRNAs and mRNAs were demonstrated in **Figure 2**.

Construction of lncRNA–miRNA–mRNA ceRNA Network

We predicted lncRNA-miRNA and miRNA-mRNA pairs according to both base sequence and expression level. Based on the interaction elements, five miRNA-lncRNA pairs and 51 miRNA-mRNA pairs were identified in the upregulated miRNA ceRNA network, and 3 miRNA-lncRNA pairs and 31 miRNA-mRNA pairs in the downregulated miRNA ceRNA network. Afterwards, the ceRNA regulatory networks were reconstructed, including one lncRNA node, five miRNA nodes and 40 mRNA nodes in the lncRNA mediated downregulated ceRNA network, and one lncRNA node, three miRNA nodes and 25 mRNA nodes in the lncRNA mediated upregulated ceRNA network (**Figure 3**).

Functional Enrichment Analysis of Differentially Expressed mRNAs in ceRNA Networks

To further explore the potential functions associated with our ceRNA network, functional enrichment analysis (including GO and KEGG) was utilized by "Clusterprofiler" package in R software. The results showed that the differentially expressed mRNAs participating in our ceRNA network were particularly enriched in the "extracellular matrix organization" (biological process), "collagen–containing extracellular matrix" (cellular component), "Interleukin−1 receptor activity" (molecular function), "regulation of systemic arterial blood pressure" (biological process), "mitochondrial intermembrane space" (cellular component), "RNA binding" (molecular function) interacted with upregulated or downregulated mRNA (**Figures 4A,B**). Additional KEGG pathway analysis indicated that differentially expressed mRNAs were relevant to "protein digestion and absorption," "complement and coagulation

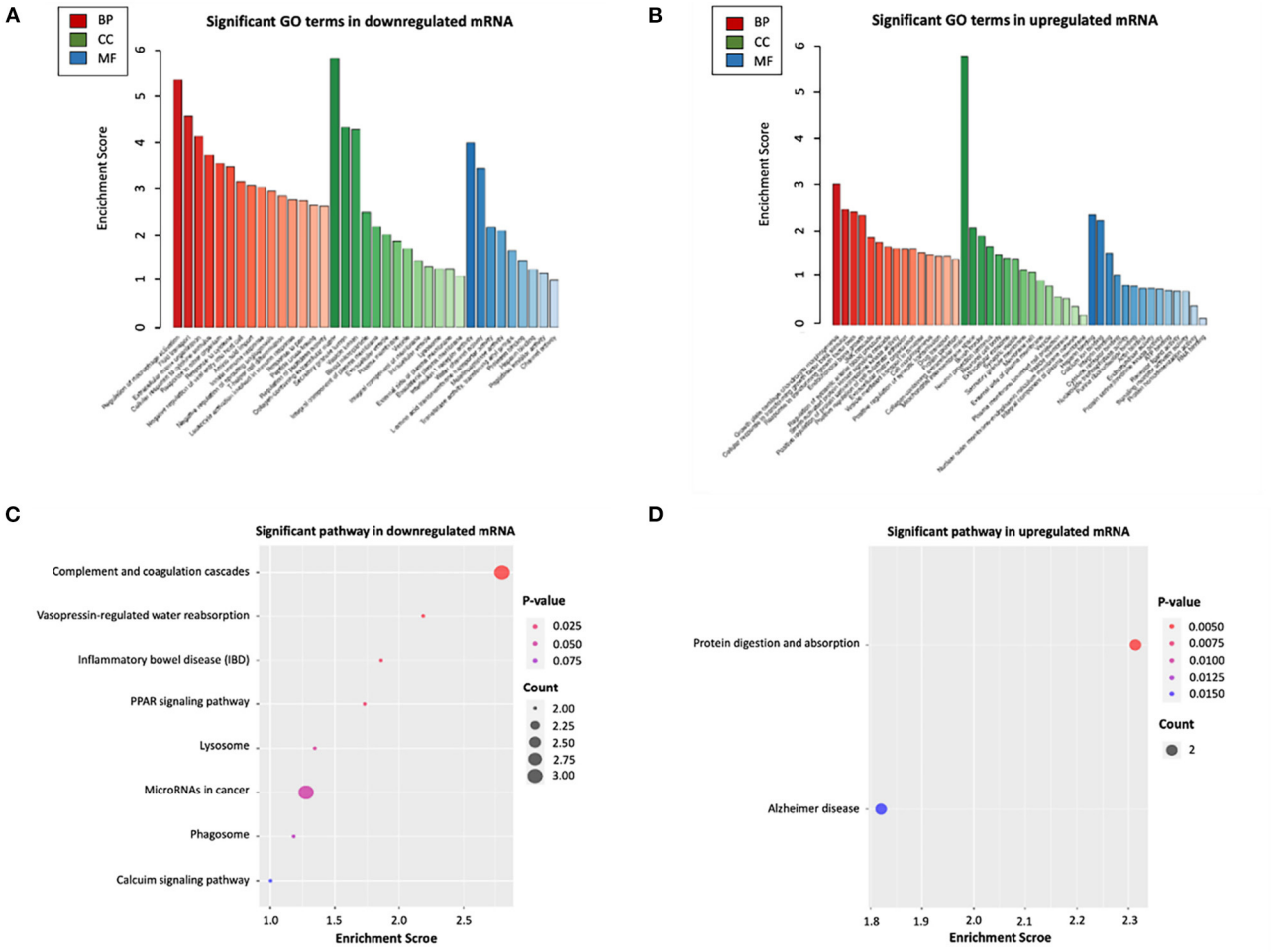

FIGURE 4 | Functional enrichment analysis of differentially expressed mRNAs in ceRNA networks. **(A)** GO biological functional analyses of downregulated mRNA; **(B)** GO biological function analyses of upregulated mRNA; **(C)** KEGG pathway analyses of downregulated mRNA; **(D)** KEGG pathway analyses of upregulated mRNA. BP, biological process; CC, cellular component; MF, molecular function; GO, Gene Ontology.

cascades" and "vasopressin-regulated water reabsorption" in our ceRNA networks (**Figures 4C,D**).

Identification of the Candidate Programmed Cell Death Related Genes in the ceRNA Networks

We interacted 65 differentially expressed mRNAs in our ceRNA networks with 14,031 programmed cell death related genes in FerrDb and GeneCards, 57 common genes were consequently obtained (**Figure 5A**; **Supplementary Table 5**). Afterwards, 65 differentially expressed mRNAs in our ceRNA networks were interacted with 14,004 apoptosis related genes in GeneCards, 57 common genes were obtained (**Figure 5B**; **Supplementary Table 5**). With regard to ferroptosis, three common genes in our ceRNA networks were identified (**Figure 5C**; **Supplementary Table 5**) and one pyroptosis related common gene was identified (**Figure 5D**; **Supplementary Table 5**).

Validation of Genes in the Programmed Cell Death Regulatory Pathways

To validate the expression of programmed cell death related genes, a number of lncRNAs, miRNAs, and mRNAs were selected for qRT-PCR testing. Specifically, two lncRNAs in the ceRNA networks were selected. Twenty apoptosis related genes including top 10 upregulated and downregulated mRNAs in our ceRNA networks (**Figure 6C**) and three common apoptosis related genes (caspase-3, caspase-8 and caspase-12, **Figure 6C**), three ferroptosis related mRNAs (LPCAT3, STAT3 and PLIN2, **Figure 6C**), and one pyroptosis related gene (STAT3, **Figure 6C**) were included. Finally, the above mRNAs targeted miRNAs were also selected for qRT-PCR validation.

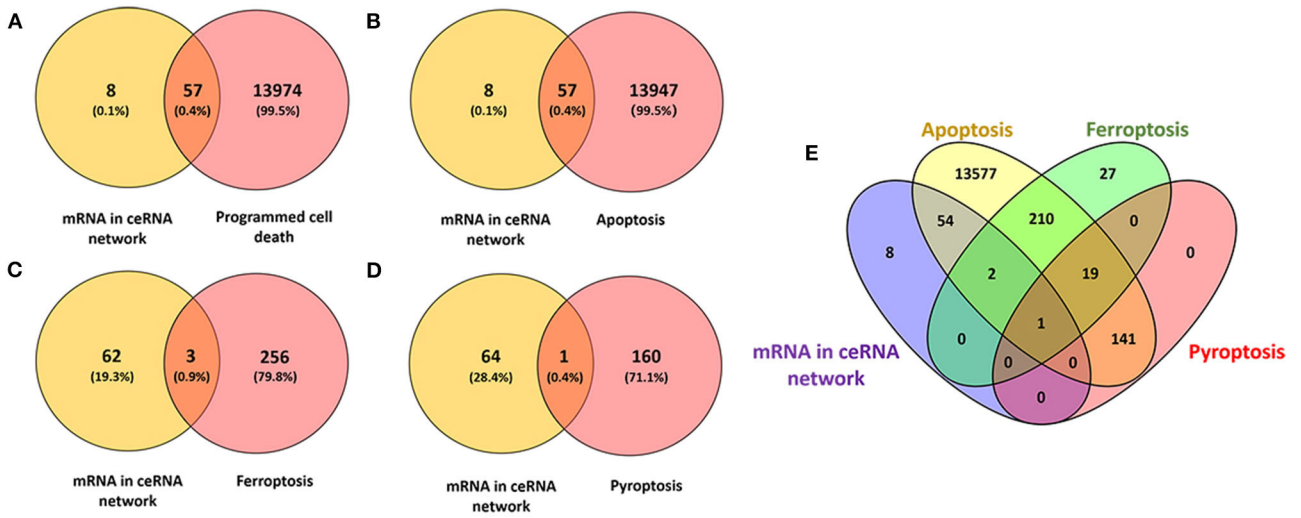

FIGURE 5 | Identification of the candidate programmed cell death related genes in the ceRNA networks. **(A)** Venn diagram to identify common mRNAs between differentially expressed mRNAs in our ceRNA networks and programmed cell death related mRNAs; **(B)** Venn diagram to identify common mRNAs between differentially expressed mRNAs in our ceRNA networks and apoptosis related mRNAs; **(C)** Venn diagram to identify common mRNAs between differentially expressed mRNAs in our ceRNA networks and ferroptosis related mRNAs; **(D)** Venn diagram to identify common mRNAs between differentially expressed mRNAs in our ceRNA networks and pyroptosis related mRNAs; **(E)** Interactions between differentially expressed mRNAs in our ceRNA networks and apoptosis, ferroptosis, pyroptosis related mRNAs.

Comparing SO with HF, qRT-PCR results showed that lncRNA GAS5 was significantly upregulated while lncRNA H19 was significantly downregulated (**Figure 6A**). miR-345-5p, miR-185-5p, miR-18b-5p, miR-29b-3p were significantly upregulated in HF (**Figure 6B**). In addition, ferroptosis related genes, LPCAT3, STAT3, and PLIN2, were confirmed to be differentially downregulated in HF by qRT-PCR analyses (**Figure 6C**). For apoptosis related genes, COL14A1, USP9Y, C6, DDX3Y and MATN2 were significantly upregulated (**Figure 6C**) while ADAMTS4, AQP3, SHISA3, and C1orf105 were significantly downregulated in HF (**Figure 6C**). Finally, we proposed seven lncRNA GAS5-mediated ceRNA regulatory pathways on programmed cell death, and the results are presented in **Figure 7**; **Supplementary Table 6**.

DISCUSSION

In the present study, we demonstrated the lncRNA-mediated ceRNA regulatory networks in HF. We screened the NCBI GEO database and constructed two lncRNA-miRNA-mRNA ceRNA regulatory networks based on the ceRNA theory, including two lncRNAs, eight miRNAs and 65 mRNAs. GO and KEGG enrichment analysis demonstrated that differentially expressed mRNAs participating in our ceRNA network were particularly enriched in the "extracellular matrix organization" and "collagen–containing extracellular matrix." 57 lncRNA-mediated ceRNA regulatory pathways were detected after the interaction between our ceRNA networks with programmed cell death related genes. Finally, qRT-PCR testing demonstrated seven ceRNA regulatory pathways to be significantly associated with programmed cell death in the pathophysiological process of HF, including lncRNA GAS5/miR-345-5p/ADAMTS4, lncRNA GAS5/miR-18b-5p/AQP3, lncRNA GAS5/miR-18b-5p/SHISA3, lncRNA GAS5/miR-18b-5p/C1orf105, lncRNA GAS5/miR-18b-5p/PLIN2, lncRNA GAS5/miR-185-5p/LPCAT3, and lncRNA GAS5/miR-29b-3p/STAT3.

Two ceRNA networks nested with two hub nodes (lncRNAs), including downregulated lncRNA GAS5 and upregulated lncRNA H19, were detected in our comprehensive bioinformatic analysis. lncRNA GAS5, as a growth arrest specific transcription factor, is capable to regulate cell growth, survival and proliferation (28). Recent evidence suggested that the expression of lncRNA GAS5 in chronic HF was downregulated, while the expression of miR-223-3p was upregulated. lncRNA GAS5 and miR-223-3p was demonstrated to predict the occurrence and recurrence of CHF based on the ROC curve analysis (29). In addition, the expression of lncRNA H19 and its encoded miR-675 were verified to be up-regulated in pathological cardiac hypertrophy and HF (30). lncRNA H19 was reported to be upregulated in decompensated right ventricular, further silencing H19 limited pathological right ventricular hypertrophy, fibrosis and capillary rarefaction. However, the dynamic regulatory crosstalk between these lncRNAs with other transcripts is unknown. Consequently, our newly discovered lncRNA-mediated ceRNA regulatory networks may provide novel insights in understanding the mechanisms underlying the initiation and progression of HF.

To further explore the biological functions of differentially expressed mRNAs in HF, we performed GO and KEGG pathway analysis of 65 differentially expressed mRNAs in the ceRNA

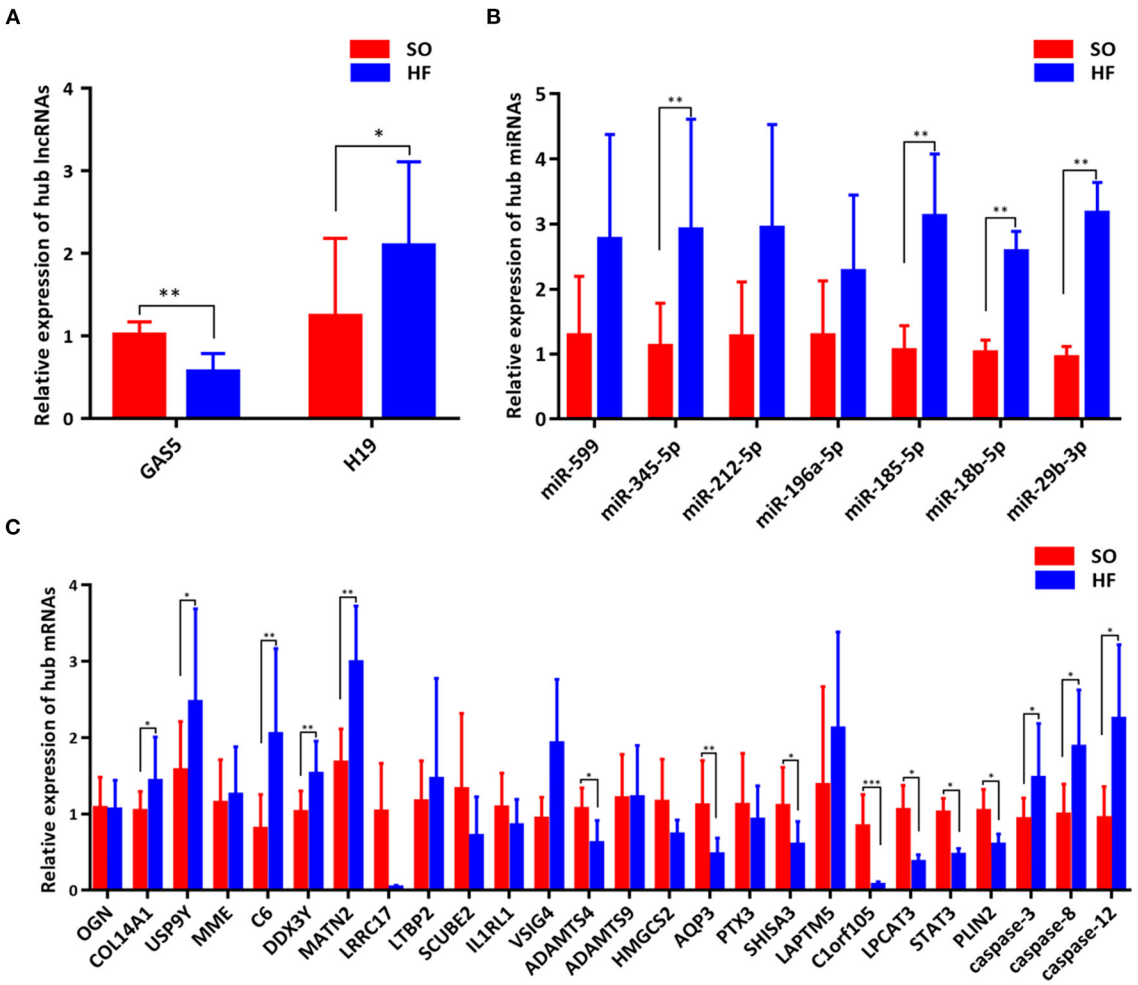

FIGURE 6 | Validation of genes in the programmed cell death regulatory pathways. **(A)** Expression of hub lncRNAs in ceRNA networks; **(B)** Expression of hub miRNAs in ceRNA networks; **(C)** Expression of hub mRNAs in ceRNA networks. *$P < 0.05$; **$P < 0.01$; ***$P < 0.001$.

network. We found these mRNAs were significantly enriched in the "extracellular matrix organization" and "collagen–containing extracellular matrix." This is consistent with previous points of view that cardiac remodeling is accompanied by several cellular changes, such as cardiomyocyte hypertrophy, myocyte apoptosis and necrosis, fibroblast proliferation, accumulation of proinflammatory mediators, and extracellular matrix reorganization characterized by fibrosis induction (31). Tanshinone IIA, traditional Chinese medicine to protect against organ injuries, reversed the increased expression of collagen I, collagen III, MMP-2 and MMP-9 in HF rat model and improved cardiac dysfunction and fibrosis (32). An observational, prospective, longitudinal study of outpatients with HF found collagen turnover biomarkers (e.g., MMP-2) combined with clinical, biochemical and echocardiographic characteristics can improve the predictive precision of cardiovascular prognosis at the time of diagnosis (33). In addition, mRNAs in our ceRNA networks were significantly enriched in the "complement and coagulation cascade." In patients with stable systolic HF, increased C3c levels were associated with less adverse cardiac remodeling and improved survival rate (34). Therefore, it was reasonable to hypothesize that our newly constructed ceRNA networks may play a role in the previously reported dysregulated alternative pathway of complement activation in patients with chronic HF. The combined effect of alternative pathways mediated by the ceRNA network in inflammation and fibrogenesis may be the underlying mechanisms of the development of diastolic dysfunction (35).

Apart from the above biological functions extracted from GO and KEGG pathway analysis, it is believed that featured programmed cell death is essential in the regulation of cardiomyocyte death in HF (36–38). Programmed cell death represents the primary means through which the organism coordinates the elimination of damaged cells at risk of neoplastic transformation or those hijacked by microbes for pathogen replication, including apoptosis, ferroptosis, and pyroptosis (38). Here, we interacted the significantly differentially expressed mRNAs in our ceRNA networks with genes related to

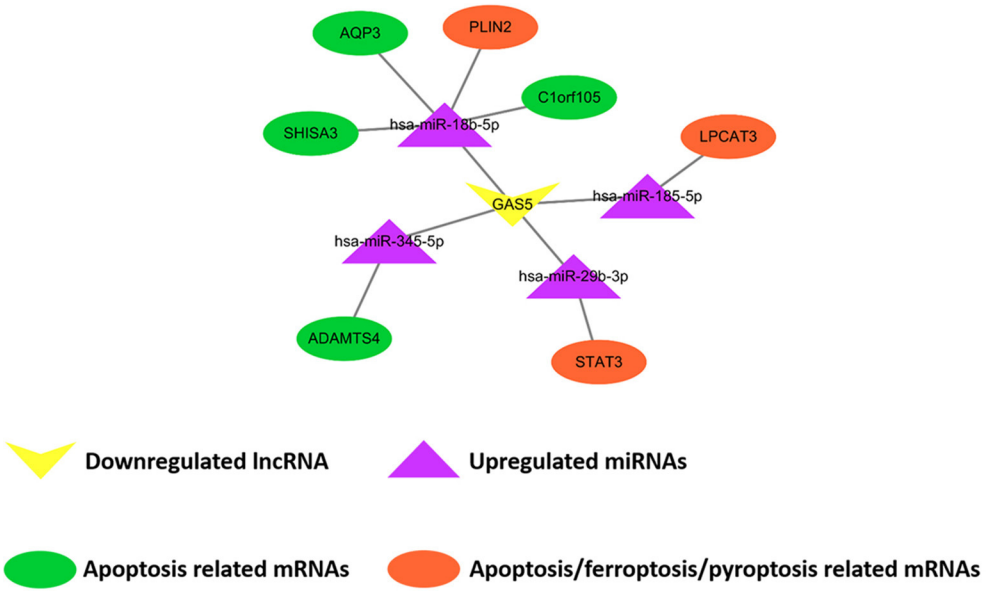

FIGURE 7 | Demonstration of proposed lncRNA GAS5-mediated ceRNA regulatory networks on programmed cell death. The rectangle, triangles, and circles represent lncRNAs, miRNAs and mRNAs, respectively. The circles highlighted in orange and green indicate apoptosis related mRNAs, the circles highlighted in orange indicate ferroptosis related mRNAs, and the circle highlighted in orange (STAT3) indicates pyroptosis related mRNAs.

programmed cell death. In our networks, we obtained 57 mRNAs related to these three sub-types of programmed cell death. Seven ceRNA regulatory pathways were finally validated with qRT-PCR testing.

Among the above ceRNA regulatory pathways, several hub nodes have been demonstrated to play crucial roles in cardiovascular diseases. For example, ADAMTS4, known as a secreted proteinase involved in inflammation and matrix degradation, was reported to translocated to the nucleus in smooth muscle cell (SMCs), through cleaving and degrading poly ADP ribose polymerase-1, leading to SMC apoptosis (39). STAT3 signaling was demonstrated to be activated by IL-35, followed by inhibited cytochrome C release and reduced apoptosis signaling, and finally protected cardiomyocytes against mtROS-induced apoptosis (40). Celastrol, an anti-inflammatory and anti-apoptotic agent, could antagonize high glucose-induced cardiomyocyte apoptosis and inflammation through restraining miR-345-5p (41). Overexpression or knockdown of miR-29b-3p showed its crucial roles on regulation of apoptosis and production of pro-inflammatory cytokines in rat cardiac myocytes (42). However, the impact of dynamic regulatory crosstalk networks involving the above hub nodes on these downstream functional changes in HF has not been well-studied. Our newly detected ceRNA networks were very likely to exert regulatory functions not only for apoptosis but potentially for all sub-types of programmed cell death, and in turn impact the pathophysiological process of HF. Even though, the detailed mechanisms for each step need further validation.

The other sub-type of programmed cell death, ferroptosis, has gained attention recently (43–45). It is an iron-dependent form of regulated cell death that is characterized by the accumulation of lipid hydroperoxides to lethal levels, resulting in oxidative damage to cell membranes. Recent studies have preliminarily uncovered the links between ferroptosis and cardiovascular diseases (46). Previous studies found that ferroptosis was involved in HF, however few studies in depth explored the regulatory mechanisms of ferroptosis in HF (47, 48). In our analysis, GAS5/miR-18b-5p/PLIN2, GAS5/miR-185-5p/LPCAT3, and GAS5/miR-29b-3p/STAT3 were potentially linked to ferroptosis. Unfortunately, the ferroptosis related hub nodes detected in our study were only explored in non-HF diseases. For example, RNA-seq analysis indicated PLIN2 was an indispensable gene in the suppression of ferroptosis caused by abnormal lipometabolism in gastric carcinoma (49). Another study demonstrated that LPCAT3 triggered the process of Arachidonoyl (AA)-CoA converted to AA-phosphatidylethanolamine (PE), the latter promoted esterification and ultimately led to ferroptosis (43). In addition, phosphorylated STAT3 could upregulate the expression of SLC7A11 and reduce ferroptosis, thereby improving the pathological processes associated with acute lung injury (50). As the most focused mRNA, while considering the crosstalk between ceRNA network mediated STAT3 regulation and ferroptosis, evidence was only reported in cancers but not in HF (51–54). Nonetheless, our promising results provided potential research spots and information for linking ferroptosis and ceRNA regulatory networks in HF, the functional changes and specific interactions between ferroptosis and ceRNA regulatory networks are warranted to be further explored. With the clarification of the role lncRNA GAS5 plays in the pathophysiological process

of HF, it may serve as biomedical target for the treatment of HF. In addition, clinical measurement of lncRNA GAS5 may benefit diagnostic process and contribute to prognostic prediction of HF.

This study also has several limitations. Firstly, our study was conducted according to genetic information downloaded from GEO database while sequencing analysis (e.g., DNA-seq, RNA-seq) of samples obtained from human or animal is recommended. Nonetheless, enlarged human cohort validating the observations or well-designed animal studies exploring the comprehensive mechanisms cannot be ruled out. Secondly, our hypothesized potential binding affinity between lncRNAs, miRNAs, and mRNAs should be further experimentally investigated. Last but not the least, should any of our newly proposed seven lncRNA GAS5-mediated ceRNA regulatory networks on programmed cell death to be validated, it would step forward the clinical diagnosis and treatment of HF to some extent.

CONCLUSIONS

In conclusion, we newly found two ceRNA regulatory networks in HF including two lncRNAs, eight miRNAs and 65 mRNAs based on the bioinformatic analysis. Their potential target mRNAs were validated and suggested to mainly impact extracellular matrix. Apart from the biological functions extracted from GO and KEGG enrichment analysis, seven newly discovered lncRNA GAS5-mediated ceRNA regulatory pathways, were hypothesized and validated to impact programmed cell death including seven for apoptosis (lncRNA GAS5/miR-345-5p/ADAMTS4, lncRNA GAS5/miR-18b-5p/AQP3, lncRNA GAS5/miR-18b-5p/SHISA3, lncRNA GAS5/miR-18b-5p/C1orf105, lncRNA GAS5/miR-18b-5p/PLIN2, lncRNA GAS5/miR-185-5p/LPCAT3, and lncRNA GAS5/miR-29b-3p/STAT3), three for ferroptosis (lncRNA GAS5/miR-18b-5p/PLIN2, lncRNA GAS5/miR-185-5p/LPCAT3, and lncRNA GAS5/miR-29b-3p/STAT3), and one for pyroptosis (lncRNA GAS5/miR-29b-3p/STAT3). Based on these results, we provided novel insights and potential research plots for bridging programmed cell death and ceRNA regulatory networks in HF.

DATA AVAILABILITY STATEMENT

The datasets presented in this study can be found in online repositories. The names of the repository/repositories and accession number(s) can be found in the article **Supplementary Material**.

ETHICS STATEMENT

The animal study was reviewed and approved by the Ethics Committees of the Nanjing Medical University, Jiangsu Province, China.

AUTHOR CONTRIBUTIONS

XL, YZhe, and YD conceived of and designed the research plans. XZ and YZha completed data processing and bioinformatics analyses. YZha, XZ, YC, WH, MT, SW, and XZ established the HF rat model and YZha isolated RNA samples from myocardial tissues and performed qRT-PCR testing. YZhe, XZ, and YZha drafted the manuscript with contributions from all the authors. YZhe and YD supervised and modified the drafting process. All authors contributed to the article and approved the submitted version.

FUNDING

This study was funded by the National Natural Science Foundation of China (Grant number: 81772441, 81902288, and 82072546).

ACKNOWLEDGMENTS

We would like to express our gratitude to several people who participated in this study or supported us. We especially acknowledge Min Zhang and Zihao Kong from the Department of Gastroenterology of the First Affiliated Hospital of Nanjing Medical University for their support on data processing and bioinformatics analyses. Deep appreciation is also extended to Qiuyu Yu and Aimei Yin, from the Department of Rehabilitation Medicine of the First Affiliated Hospital of Nanjing Medical University, for their contribution to the animal sample collection.

SUPPLEMENTARY MATERIAL

The Supplementary Material for this article can be found online at: https://www.frontiersin.org/articles/10.3389/fcvm.2021.747449/full#supplementary-material

REFERENCES

1. Dobre D, Borer J, Fox K, Swedberg K, Adams K, Cleland J, et al. Heart rate: a prognostic factor and therapeutic target in chronic heart failure. The distinct roles of drugs with heart rate-lowering properties. *Eur J Heart Fail.* (2014) 16:76–85. doi: 10.1093/eurjhf/hft129
2. Shah SJ, Feldman T, Ricciardi MJ, Kahwash R, Lilly S, Litwin S, et al. One-year safety and clinical outcomes of a transcatheter interatrial shunt device for the treatment of heart failure with preserved ejection fraction in the reduce elevated left atrial pressure in patients with heart failure (REDUCE LAP-HF I) trial: a randomized clinical trial. *JAMA Cardiol.* (2018) 3:968–77. doi: 10.1001/jamacardio.2018.2936
3. Fico A, Fiorenzano A, Pascale E, Patriarca E, Minchiotti G. Long non-coding RNA in stem cell pluripotency and lineage commitment: functions and evolutionary conservation. *Cell Mol Life Sci.* (2019) 76:1459–71. doi: 10.1007/s00018-018-3000-z
4. Gomes C, Schroen B, Kuster G, Robinson E, Ford K, Squire I, et al. Regulatory RNAs in heart failure. *Circulation.* (2020) 141:313–28. doi: 10.1161/CIRCULATIONAHA.119.042474

5. Jiang X, Ning Q. The emerging roles of long noncoding RNAs in common cardiovascular diseases. *Hypert Res.* (2015) 38:375–9. doi: 10.1038/hr.2015.26
6. Bär C, Chatterjee S, Thum T. Long noncoding RNAs in cardiovascular pathology, diagnosis, and therapy. *Circulation.* (2016) 134:1484–99. doi: 10.1161/CIRCULATIONAHA.116.023686
7. Kowara M, Borodzicz-Jazdzyk S, Rybak K, Kubik M, Cudnoch-Jedrzejewska A. Therapies targeted at non-coding rnas in prevention and limitation of myocardial infarction and subsequent cardiac remodeling-current experience and perspectives. *Int J Mol Sci.* (2021) 22. doi: 10.3390/ijms22115718
8. Zhu L, Li N, Sun L, Zheng D, Shao G. Non-coding RNAs: the key detectors and regulators in cardiovascular disease. *Genomics.* (2021) 113:1233–46. doi: 10.1016/j.ygeno.2020.10.024
9. Xuan L, Sun L, Zhang Y, Huang Y, Hou Y, Li Q, et al. Circulating long non-coding RNAs NRON and MHRT as novel predictive biomarkers of heart failure. *J Cell Mol Med.* (2017) 21:1803–14. doi: 10.1111/jcmm.13101
10. Leung C, Wang L, Nielsen J, Tropak M, Fu Y, Kato H, et al. Remote cardioprotection by transfer of coronary effluent from ischemic preconditioned rabbit heart preserves mitochondrial integrity and function via adenosine receptor activation. *Cardiovasc Drugs Ther.* (2014) 28:7–17. doi: 10.1007/s10557-013-6489-2
11. Tay Y, Rinn J, Pandolfi P. The multilayered complexity of ceRNA crosstalk and competition. *Nature.* (2014) 505:344–52. doi: 10.1038/nature12986
12. Sen R, Ghosal S, Das S, Balti S, Chakrabarti J. Competing endogenous RNA: the key to posttranscriptional regulation. *Sci World J.* (2014) 2014:896206. doi: 10.1155/2014/896206
13. Wang K, Liu C, Zhou L, Wang J, Wang M, Zhao B, et al. APF lncRNA regulates autophagy and myocardial infarction by targeting miR-188-3p. *Nat Commun.* (2015) 6:6779. doi: 10.1038/ncomms7779
14. Yu XH, Deng WY, Chen JJ, Xu XD, Liu XX, Chen L, et al. LncRNA kcnq1ot1 promotes lipid accumulation and accelerates atherosclerosis via functioning as a ceRNA through the miR-452-3p/HDAC3/ABCA1 axis. *Cell Death Dis.* (2020) 11:1043. doi: 10.1038/s41419-020-03263-6
15. Zheng H, Shi L, Tong C, Liu Y, Hou M. circSnx12 is involved in ferroptosis during heart failure by targeting miR-224-5p. *Front Cardiovasc Med.* (2021) 8:656093. doi: 10.3389/fcvm.2021.656093
16. Zou J, Chai H, Zhang X, Guo D, Tai J, Wang Y, et al. Reconstruction of the lncRNA-miRNA-mRNA network based on competitive endogenous RNA reveal functional lncRNAs in cerebral infarction. *Sci Rep.* (2019) 9:12176. doi: 10.1038/s41598-019-48435-3
17. Vejnar C, Zdobnov E. MiRmap: comprehensive prediction of microRNA target repression strength. *Nucl Acids Res.* (2012) 40:11673–83. doi: 10.1093/nar/gks901
18. Betel D, Wilson M, Gabow A, Marks D, Sander C. The microRNA.org resource: targets and expression. *Nucl Acids Res.* (2008) 36:D149–53. doi: 10.1093/nar/gkm995
19. Wong N, Wang X. miRDB: an online resource for microRNA target prediction and functional annotations. *Nucl Acids Res.* (2015) 43:D146–52. doi: 10.1093/nar/gku1104
20. Agarwal V, Bell G, Nam J, Bartel D. Predicting effective microRNA target sites in mammalian mRNAs. *eLife.* (2015) 4. doi: 10.7554/eLife.05005.028
21. Chou C, Shrestha S, Yang C, Chang N, Lin Y, Liao K, et al. miRTarBase update 2018: a resource for experimentally validated microRNA-target interactions. *Nucl Acids Res.* (2018) 46:D296–302. doi: 10.1093/nar/gkx1067
22. Li J, Liu S, Zhou H, Qu L, Yang J. starBase v2.0: decoding miRNA-ceRNA, miRNA-ncRNA and protein-RNA interaction networks from large-scale CLIP-Seq data. *Nucl Acids Res.* (2014) 42:D92–7. doi: 10.1093/nar/gkt1248
23. Shannon P, Markiel A, Ozier O, Baliga N, Wang J, Ramage D, et al. Cytoscape: a software environment for integrated models of biomolecular interaction networks. *Gen Res.* (2003) 13:2498–504. doi: 10.1101/gr.1239303
24. Yu G, Wang L, Han Y, He Q. clusterProfiler: an R package for comparing biological themes among gene clusters. *OMICS.* (2012) 16:284–7. doi: 10.1089/omi.2011.0118
25. Mircoli L, Fedele L, Benetti M, Bolla GB, Radaelli A, Perlini S, et al. Preservation of the baroreceptor heart rate reflex by chemical sympathectomy in experimental heart failure. *Circulation.* (2002) 106:866–72. doi: 10.1161/01.CIR.0000024981.48160.6D
26. Xing Y, Liu C, Wang H, Zhang X, Wang Y, Yue X, et al. Protective effects of nicorandil on cardiac function and left ventricular remodeling in a rat model of ischemic heart failure. *Arch Med Res.* (2018) 49:583–7. doi: 10.1016/j.arcmed.2018.12.006
27. Gao G, Chen W, Yan M, Liu J, Luo H, Wang C, et al. Rapamycin regulates the balance between cardiomyocyte apoptosis and autophagy in chronic heart failure by inhibiting mTOR signaling. *Int J Mol Med.* (2020) 45:195–209. doi: 10.3892/ijmm.2019.4407
28. Meng XD, Yao HH, Wang LM, Yu M, Shi S, Yuan ZX, et al. Knockdown of GAS5 inhibits atherosclerosis progression via reducing EZH2-mediated ABCA1 transcription in ApoE(-/-) mice. *Mol Ther Nucleic Acids.* (2020) 19:84–96. doi: 10.1016/j.omtn.2019.10.034
29. Li G, Du P, Qiang X, Jin D, Liu H, Li B, et al. Low-expressed GAS5 injure myocardial cells and progression of chronic heart failure via regulation of miR-223-3P. *Exp Mol Pathol.* (2020) 117:104529. doi: 10.1016/j.yexmp.2020.104529
30. Liu L, An X, Li Z, Song Y, Li L, Zuo S, et al. The H19 long noncoding RNA is a novel negative regulator of cardiomyocyte hypertrophy. *Cardiovasc Res.* (2016) 111:56–65. doi: 10.1093/cvr/cvw078
31. Tanai E, Frantz S. Pathophysiology of heart failure. *Comprehen Physiol.* (2015) 6:187–214. doi: 10.1002/cphy.c140055
32. Chen R, Chen W, Huang X, Rui Q. Tanshinone IIA attenuates heart failure via inhibiting oxidative stress in myocardial infarction rats. *Mol Med Rep.* (2021) 23. doi: 10.3892/mmr.2021.12043
33. Sanchis L, Andrea R, Falces C, Llopis J, Morales-Ruiz M, López-Sobrino T, et al. Prognosis of new-onset heart failure outpatients and collagen biomarkers. *Eur J Clin Invest.* (2015) 45:842–9. doi: 10.1111/eci.12479
34. Frey A, Ertl G, Angermann C, Hofmann U, Störk S, Frantz S. Complement C3c as a biomarker in heart failure. *Med Inflam.* (2013) 2013:716902. doi: 10.1155/2013/716902
35. Shahini N, Michelsen A, Nilsson P, Ekholt K, Gullestad L, Broch K, et al. The alternative complement pathway is dysregulated in patients with chronic heart failure. *Sci Rep.* (2017) 7:42532. doi: 10.1038/srep42532
36. Yussman MG, Toyokawa T, Odley A, Lynch RA, Wu G, Colbert MC, et al. Mitochondrial death protein Nix is induced in cardiac hypertrophy and triggers apoptotic cardiomyopathy. *Nat Med.* (2002) 8:725–30. doi: 10.1038/nm719
37. Wencker D, Chandra M, Nguyen K, Miao W, Garantziotis S, Factor SM, et al. A mechanistic role for cardiac myocyte apoptosis in heart failure. *J Clin Invest.* (2003) 111:1497–504. doi: 10.1172/JCI17664
38. Bedoui S, Herold M, Strasser A. Emerging connectivity of programmed cell death pathways and its physiological implications. *Nat Rev Mol Cell Biol.* (2020) 21:678–95. doi: 10.1038/s41580-020-0270-8
39. Ren P, Hughes M, Krishnamoorthy S, Zou S, Zhang L, Wu D, et al. Critical role of ADAMTS-4 in the development of sporadic aortic aneurysm and dissection in mice. *Sci Rep.* (2017) 7:12351. doi: 10.1038/s41598-017-12248-z
40. Zhou F, Feng T, Lu X, Wang H, Chen Y, Zhang Q, et al. Interleukin 35 protects cardiomyocytes following ischemia/reperfusion-induced apoptosis via activation of mitochondrial STAT3. *Acta Biochim Biophys Sin.* (2021) 53:410–8. doi: 10.1093/abbs/gmab007
41. Ma L, Cao Y, Zhang L, Li K, Yan L, Pan Y, et al. Celastrol mitigates high glucose-induced inflammation and apoptosis in rat H9c2 cardiomyocytes via miR-345-5p/growth arrest-specific 6. *J Gene Med.* (2020) 22:e3201. doi: 10.1002/jgm.3201
42. Li Z, Yi N, Chen R, Meng Y, Wang Y, Liu H, et al. miR-29b-3p protects cardiomyocytes against endotoxin-induced apoptosis and inflammatory response through targeting FOXO3A. *Cell Sign.* (2020) 74:109716. doi: 10.1016/j.cellsig.2020.109716
43. Wang H, Lin D, Yu Q, Li Z, Lenahan C, Dong Y, et al. A promising future of ferroptosis in tumor therapy. *Front Cell Dev Biol.* (2021) 9:629150. doi: 10.3389/fcell.2021.629150
44. Sharma A, Flora SJS. Positive and negative regulation of ferroptosis and its role in maintaining metabolic and redox homeostasis. *Oxid Med Cell Longev.* (2021) 2021:9074206. doi: 10.1155/2021/9074206
45. Wang H, Cheng Y, Mao C, Liu S, Xiao D, Huang J, et al. Emerging mechanisms and targeted therapy of ferroptosis in cancer. *Mol Ther.* (2021) 29:2185–208. doi: 10.1016/j.ymthe.2021.03.022
46. Wu X, Li Y, Zhang S, Zhou X. Ferroptosis as a novel therapeutic target for cardiovascular disease. *Theranostics.* (2021) 11:3052–59. doi: 10.7150/thno.54113

47. Chen X, Xu S, Zhao C, Liu B. Role of TLR4/NADPH oxidase 4 pathway in promoting cell death through autophagy and ferroptosis during heart failure. *Biochem Biophys Res Commun.* (2019) 516:37–43. doi: 10.1016/j.bbrc.2019.06.015
48. Liu B, Zhao C, Li H, Chen X, Ding Y, Xu S. Puerarin protects against heart failure induced by pressure overload through mitigation of ferroptosis. *Biochem Biophys Res Commun.* (2018) 497:233–40. doi: 10.1016/j.bbrc.2018.02.061
49. Sun X, Yang S, Feng X, Zheng Y, Zhou J, Wang H, et al. The modification of ferroptosis and abnormal lipometabolism through overexpression and knockdown of potential prognostic biomarker perilipin2 in gastric carcinoma. *Gastric Cancer*. (2020) 23:241–59. doi: 10.1007/s10120-019-01004-z
50. Qiang Z, Dong H, Xia Y, Chai D, Hu R, Jiang H. Nrf2 and STAT3 alleviates ferroptosis-mediated IIR-ALI by regulating SLC7A11. *Oxid Med Cell Longev*. (2020) 2020:5146982. doi: 10.1155/2020/5146982
51. Ji W, Jiao J, Cheng C, Xiao Y, Shao J, Liu H. A positive feedback loop of LINC00662 and STAT3 promotes malignant phenotype of glioma. *Pathol Res Pract.* (2021) 224:153539. doi: 10.1016/j.prp.2021.153539
52. Hua K, Deng X, Hu J, Ji C, Yu Y, Li J, et al. Long noncoding RNA HOST2, working as a competitive endogenous RNA, promotes STAT3-mediated cell proliferation and migration via decoying of let-7b in triple-negative breast cancer. *J Exp Clin Cancer Res.* (2020) 39:58. doi: 10.1186/s13046-020-01561-7
53. Sun X, Shen H, Liu S, Gao J, Zhang S. Long noncoding RNA SNHG14 promotes the aggressiveness of retinoblastoma by sponging microRNA-124 and thereby upregulating STAT3. *Int J Mol Med.* (2020) 45:1685–96. doi: 10.3892/ijmm.2020.4547
54. Zhao X, Li X, Zhou L, Ni J, Yan W, Ma R, et al. LncRNA HOXA11-AS drives cisplatin resistance of human LUAD cells via modulating miR-454-3p/Stat3. *Cancer Sci.* (2018) 109:3068–79. doi: 10.1111/cas.13764
55. Hu L, Chen Y, Chen T, Huang D, Li S, Cui S. A systematic study of mechanism of sargentodoxa cuneata and patrinia scabiosifolia against pelvic inflammatory disease with dampness-heat stasis syndrome via network pharmacology approach. *Front Pharmacol.* (2020) 11:582520. doi: 10.3389/fphar.2020.582520

Conflict of Interest: The authors declare that the research was conducted in the absence of any commercial or financial relationships that could be construed as a potential conflict of interest.

Publisher's Note: All claims expressed in this article are solely those of the authors and do not necessarily represent those of their affiliated organizations, or those of the publisher, the editors and the reviewers. Any product that may be evaluated in this article, or claim that may be made by its manufacturer, is not guaranteed or endorsed by the publisher.

Frontiers in
Cardiovascular Medicine

Innovations and improvements in cardiovascular treatment and practice

Focuses on research that challenges the status quo of cardiovascular care, or facilitates the translation of advances into new therapies and diagnostic tools.

Discover the latest Research Topics

See more →

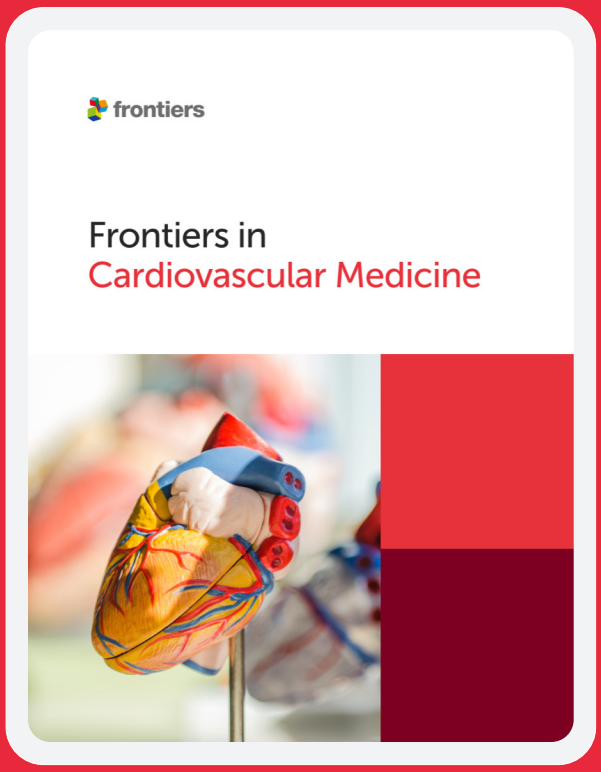

Frontiers

Avenue du Tribunal-Fédéral 34
1005 Lausanne, Switzerland
frontiersin.org

Contact us

+41 (0)21 510 17 00
frontiersin.org/about/contact